Investigating the Relationship between *Listeria monocytogenes* and Leaf Vegetables and the Use of Volatile Organic Compounds for Detecting Contamination

Thesis presented by:

Nicolaas Dominique Bruyniks

A thesis submitted for the degree of
Doctor of Philosophy

School of Biosciences

Cardiff University

February 2025

Acknowledgements

Firstly, I would like to thank my beautiful and caring girlfriend. Your support and companionship were critical to successfully reaching this point. I love you, Teresa, and I am truly blessed to have you in my life.

I want to thank my family. My (step) parents for their unwavering support, for always pushing me to achieve the most in life and for believing in me even when I doubted myself. My sisters, who are my longest and dearest friends and their partners, for being supportive during my PhD and hyping me up. I am so lucky to have you all in my life!

Thank you to all my friends who have been there throughout this journey. A PhD can be isolating, and while I didn't get to see many of you as often as I would have liked, you all showed me the support and understanding I could wish for from friendship.

I would like to thank my supervisors for their patience and guidance. Thank you to Dr Carsten Müller for supporting me through technical and administrative challenges and for our scintillating conversations. Dr Cedric Berger for sharing your technical expertise, putting my mind at ease and making the lab a comfortable environment where I could be myself. Prof Hilary Rogers for challenging me and giving me the tools to be a better scientist. I've learned so much from all of you and feel privileged to have had you as my mentors.

I want to thank everyone in the lab and across other departments who contributed to this journey. To those in the Tuesday, Friday and MMI meetings, thank you for listening to me talk about salads, *Listeria* and the scientific challenges I encountered while providing valuable input and encouragement. Thank you to Dr Laura Rushton for encouraging me to pursue a PhD. Thanks also to Dr Gordon Webster and Dr Sarah Christophides for always being willing to lend a helping hand and sharing your technical expertise. Sam Vaughan and the team at the greenhouses for your professionalism and for taking such excellent care of my plants. Dr Richard Ludlow for assisting with the plant growing and technical challenges with GC-MS and data analysis. The staff at the Bioimaging Research Hub for assisting me in the microscopy work and providing advice

on technical challenges. And to all the MMI lab members for creating an inclusive and supportive environment, showing an interest in my research and being understanding during my write-up period.

Finally, I would like to thank UKRI, SWBio and Cardiff University for providing me with this opportunity and ensuring that the financial, administrative and logistical aspects during my project were taken care of, allowing me to reach this point.

To all of you, I hope I have made you proud!

Summary

Listeria monocytogenes (*Lm*) is considered a high-risk foodborne pathogen due to its high mortality rate. *Lm* has predominantly been associated with ready-to-eat (RTE) animal products but is increasingly detected in RTE salads. However, the factors contributing to *Lm* contamination of salad have not been well investigated. With the growing demand for healthy, nutritious RTE foods and the increasing association of *Lm* with salads, the risk of foodborne infections rises. Conventional detection methods for *Lm* in salad take too long to identify contamination within a suitable timeframe. Analysis of volatile organic compounds (VOCs) released from foods has been proposed as a faster alternative to identify bacterial contamination. This study aims to improve understanding of *Lm*'s interaction with salad leaves and develop a VOC-based detection method for *Lm* to improve food safety. In this study, 15 *Lm* strains isolated from the produce supply chain, along with 2 reference strains, were examined for genetic and phenotypic characteristics linked to vegetable contamination. NLmo8 and NLmo15 exhibited phenotypic characteristics suggesting a capacity for contaminating leafy vegetables and were examined for their attachment to salad leaves, alongside phylogenetically related strains. Strain-specific differences in attachment were observed. Microscopy and a novel assay were employed to determine whether these differences were due to variations in preferential attachment sites. NLmo8 exhibited the greatest attachment to various plant surfaces. Therefore, NLmo8 was used to determine whether VOC profiles from inoculated rocket leaves could be differentiated from uninoculated leaves. Retail-ready rocket leaves from different years and seasons were sampled, and inoculated leaves could be differentiated from uninoculated ones in 3 of 4 batches. The VOC analysis method demonstrated specificity, as VOC profiles from rocket leaves inoculated with *L. innocua* could be differentiated from those inoculated with *Lm*. Analysis of 25 VOCs consistently identified across the 4 batches enhanced the differentiation of *Lm*-inoculated leaves.

Table of Contents

List of Figures

List of Tables

Abbreviations

ANI – Average Nucleotide Identity
BHI – Brain Heart Infusion
BLAST – Basic Local Alignment Search Tool
BLASTP – Protein BLAST
BSA – Bovine Serum Album
CBD – Cellulose Binding Domain
CC – Clonal Complex
CDS – Coding Sequences
CFU – Colony Forming Units
CFU/cm^2 – Colony Forming Units per square centimetre
CFU/g – Colony Forming Units per gram
CFU/mL – Colony Forming Units per millilitre
cgMLST – core genome Multi-Locus Sequence Typing
CLIMB – Cloud Infrastructure for Microbial Bioinformatics
CNS – Central Nervous System
cv. – cultivar
dH_2O – Ultrapure deionised water
diam. – Diameter
DNA – Deoxyribonucleic acid
EFSA – European Food Safety Authority
EU – European Union
Exp. – Experiment
FA – Formaldehyde
FA-PBS – Formaldehyde (4%) in Phosphate Buffered Saline
FDA – Food and Drug Administration
FERG – Foodborne Disease Burden Epidemiology Reference Group
GC-MS – Gas Chromatography Mass Spectrometry
GC-TOF-MS – Gas Chromatography–Time-of-Flight–Mass Spectrometry
GFP – Green Fluorescent Protein
GTR – General Time Reversible
ISO – International Organization for Standardization
kbp – kilobase pairs
LB – Luria Bertani
LCP – *Listeria* Cellulose-Binding Protein
LEA – *Listeria* Enrichment Agar
Lm – *L. monocytogenes*
MAP – Modified Atmosphere Packaging
Mbp – Mega base pairs
m/z – mass-to-charge (ratio)

MLEE – Multi-Locus Enzyme Electrophoresis
MLST – Multi-Locus Sequence Typing
NIST – National Institute of Standards and Technology
OD – Optical Density
PALCAM – Polymyxin Acriflavine Lithium-chloride Ceftazidime Esculin Mannitol
PBS – Phosphate Buffered Saline
PCR – Polymerase Chain Reaction
QAC – Quaternary Ammonium Compounds
QUAST – Quality Assessment Tool for Genome Assemblies
RT – Room Temperature
RTE – Ready-To-Eat
rpm – revolutions per minute
SEM – Scanning Electron Microscopy
ser. – serovar
SPME – Solid Phase Micro Extraction
ST – Sequence Type
TBLASTN – Translated Nucleotide BLAST
TD – Thermal Desorption
TD-GC-TOF-MS – Thermal Desorption Gas Chromatography Time-Of-Flight Mass Spectrometry
TEM – Transmission Electron Microscopy
TSB – Tryptic Soy Broth
UV – Ultraviolet
VOC – volatile organic compound
VPB – Vegetable Peptone Broth
v/v – volume to volume
w/v – weight to volume
WGS – Whole Genome Sequencing
WHO – World Health Organisation
Wt – Wild type

Chapter 1 – General introduction

1.1 Microbial contaminants are responsible for the majority of foodborne diseases

Ensuring food safety is paramount to safeguarding human health. Unfortunately, food is susceptible to biological, chemical, or physical contamination, jeopardising consumer safety. A foodborne disease, also known as foodborne illness, is an illness resulting from the consumption of contaminated food. Microbial contaminants, such as bacteria, fungi, parasites and viruses, are among the leading causes of foodborne diseases. In severe cases, infection or exposure to the toxins produced by these organisms can result in hospitalisation, long-term health complications, and even death.

Beyond the individual health impacts, foodborne diseases have major public health and economic implications. They diminish productivity, disrupt trade and tourism and strain healthcare systems. The World Health Organisation (WHO) Foodborne Disease Burden Epidemiology Reference Group (FERG) published a report in 2015 with estimates of the incidence, mortality, and disease burden of 31 foodborne hazards for the year 2010 (Havelaar *et al.*, 2015). This report highlighted the significant global impact of foodborne illnesses, revealing that annually, 1 out of 10 people fall ill due to microbial or chemical contaminants in food. For the year 2010, the WHO estimated there were 600 million cases of foodborne illness globally, leading to ~420,000 deaths and the loss of 33 million healthy years of life.

Microorganisms were identified as the greatest threat to food safety, with foodborne bacteria being the leading cause of mortality, responsible for an estimated 315,000 deaths. Non-typhoidal *Salmonella enterica* was reported as the leading cause of death due to the consumption of contaminated food (~59,000 deaths). While non-typhoidal *S. enterica* posed a significant burden across all 14 regions studied, the FERG report highlighted notable regional variations in the most impactful microbial pathogens (Havelaar *et al.*, 2015).

1.2 *L. monocytogenes*: leading cause of death among foodborne pathogens

A recent report by the European Food Safety Authority (EFSA) and the European Centre for Disease Prevention and Control on zoonotic diseases in Europe identified *Listeria monocytogenes* (*Lm*) as the leading cause of death amongst foodborne disease outbreaks in 2022 (EFSA, 2023). Foodborne disease outbreaks are defined as the occurrence of two or more cases of illness resulting from the consumption of the same food. In the EU, *Salmonella*, *Campylobacter*, and Norovirus are the most common pathogens responsible for such outbreaks (Figure 1.1) (EFSA, 2023). Nevertheless, reports compiled by EFSA each year from 2018 to 2022 confirm that *Lm* has consistently been the leading cause of foodborne disease-related deaths (Figure 1.2) (EFSA, 2019,2021a,b,2022,2023).

Although *Lm* related foodborne outbreaks are less frequent than those caused by other common food borne pathogens, such as *Campylobacter* spp., *Escherichia coli* and *Salmonella* spp. (Figure 1.1), Listeriosis has a significantly higher mortality rate (Jordan *et al.*, 2018; EFSA, 2023). For instance, Campylobacteriosis was the most commonly reported foodborne illness in the EU, with 137,107 confirmed cases in 2022 and a case fatality rate of just 0.04% (EFSA, 2023). In contrast, *Lm* had a fatality rate of 18.1% from 2,738 confirmed cases of Listeriosis in the same year (EFSA, 2023). In addition to its high mortality rate, Listeriosis also has a high hospitalisation rate, with 81.8% of reported cases in Europe in 2022 requiring hospitalisation (EFSA, 2023). In fact, hospitalisation rates for Listeriosis frequently exceed 90%, underscoring the disease's severity, particularly among high-risk groups (WHO, 2015; Scallan Walter *et al.*, 2025). Consequently, the EFSA considers *Lm* one of the most serious foodborne diseases under European Union surveillance.

The long-term health effects of Listeriosis can have a considerable emotional and financial cost for individuals. In addition to the individual health impacts, *Lm* outbreaks can result in significant financial losses for producers and retailers, as well as reputational damage. Foodborne outbreaks often lead to costly product recalls, generation of food waste, loss of consumer confidence and sales, the implementation

of costly sanitation procedures and even potential business closures (Olanya *et al.*, 2019). Thus, foodborne *Lm* presents a serious threat to public health and has significant economic and social impacts, demanding ongoing food safety monitoring.

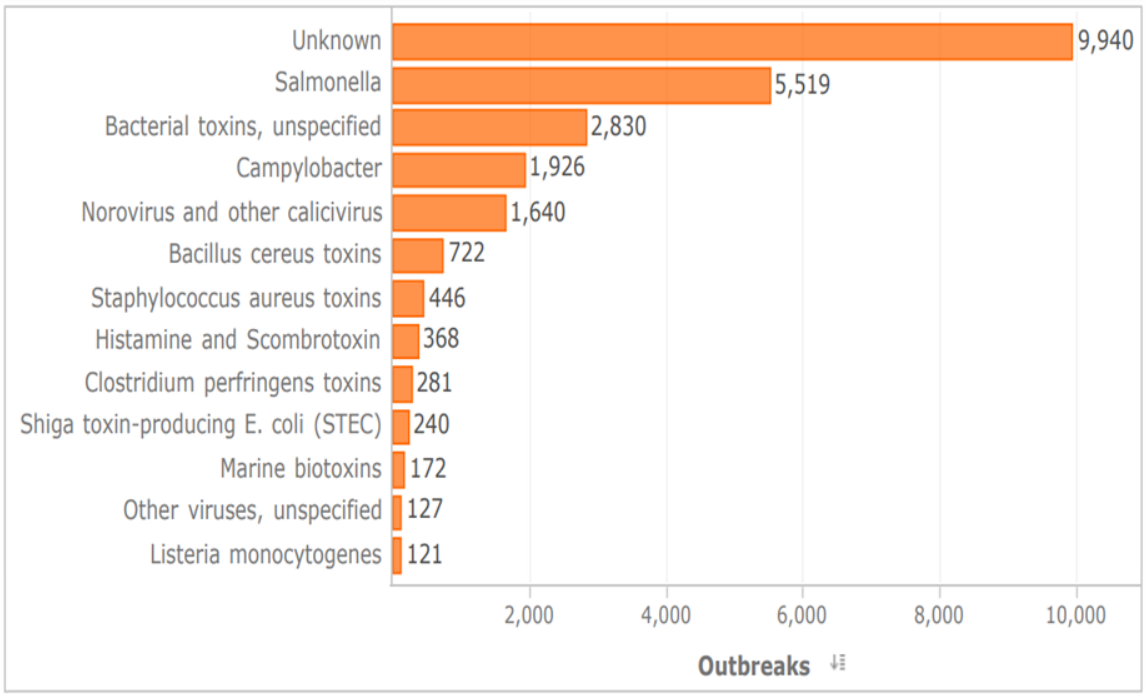

Figure 1.1 Number of foodborne outbreaks in Europe by causative agent from 2018 to 2022.
Adapted from: https://www.efsa.europa.eu/en/microstrategy/FBO-dashboard

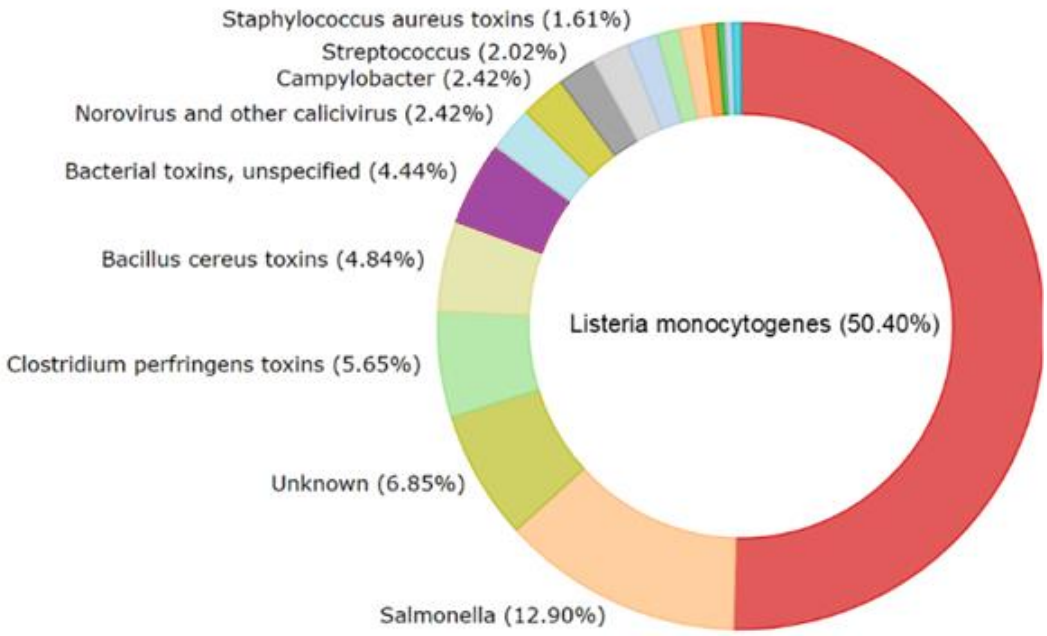

Figure 1.2 Distribution of foodborne related deaths in the Europe by causative agent from 2018 to 2022.
Adapted from: https://www.efsa.europa.eu/en/microstrategy/FBO-dashboard

1.3 History of *L. monocytogenes*

Lm is a Gram-positive, rod-shaped, facultative anaerobic bacterium. The bacterium is ubiquitous in the natural environment where it has been isolated from soil, waterways, plants and animals (Félix *et al.*, 2022). In nature, it lives as a saprophyte but is capable of infecting humans and animals, with transmission occurring mainly through the ingestion of contaminated food.

The bacterium was first described by Murray *et al.* (1926) during an investigation into an outbreak of disease among laboratory rabbits and guinea pigs. The animals exhibited symptoms such as fever, liver abscesses, and septicaemia. Another notable characteristic of the disease was monocytosis, an abnormal increase in monocytes in the blood of the infected animals. The authors identified a Gram-positive, rod-shaped bacterium as the causative agent, which they named *Bacterium monocytogenes* to reflect this distinctive pathological effect.

The following year, J. H. H. Pirie identified a bacterium responsible for causing disease in wild gerbils (Pirie, 1927). He named it *Listerella hepatolytica* in recognition of its ability to cause severe liver necrosis in gerbils and to pay tribute to British surgeon Lord Joseph Lister, a pioneer of antiseptic surgery. It was later determined that the infections investigated by Murray and Pirie were caused by the same bacterium, leading to the combined name *Listerella monocytogenes* (Gibbons, 1972). However, the name *Listerella* had already been assigned to a slime mould. Consequently, in 1940, Pirie proposed the name *Listeria monocytogenes*, which ultimately became the bacterium's official name, with *Listeria* designated as the official genus name (Pirie, 1940).

1.4 The *Listeria* genus

The *Listeria* genus, at the time of writing, has 28 recognised species, including 6 subspecies, validly published under the International Code of Nomenclature of Prokaryotes (https://lpsn.dsmz.de/genus/listeria). Orsi and Wiedmann (2016) proposed that the *Listeria* genus could be subdivided into two distinct groups, *Listeria sensu lato* and *Listeria sensu stricto*, based on genotypic and phenotypic characteristics. *Listeria sensu stricto* ("in a strict sense") currently includes 10 species (Table 1.1) (Orsi *et al.*,

2024). The term '*sensu lato*' ("in a broad sense") originally referred to all species in the genus, but it is now more commonly used to denote those less phylogenetically related to *Lm* than the *sensu stricto* species. The *Listeria sensu lato* group currently comprises 18 species (Table 1.1) (Orsi *et al.*, 2024). *Listeria sensu lato* shares a most recent common ancestor with the *sensu stricto* group. However, the *sensu lato* group is paraphyletic, forming three major clades, while the *sensu stricto* group is monophyletic, consisting of a single clade that includes the ten described species. Within the clades formed by the *sensu lato* group, the species are more distantly related to each other than those within the *sensu stricto* clade (Orsi *et al.*, 2024).

Table 1.1 Division of *Listeria* species into *sensu stricto* and *sensu lato* group according to Orsi and Wiedmann (2016); Orsi *et al.* (2024).

Sensu stricto	***Sensu lato***
L. monocytogenes	*L. grayi,*
L. seeligeri	*L. fleischmannii*
L. welshimeri	*L. floridensis*
L. innocua	*L. aquatic*
L. ivanovii	*L. valentina*
L. marthii	*L. thailandensis*
L. farberi	*L. goaensis*
L. immobilis	*L. ilorinensis*
L. cossartiae	*L. costaricensis*
L. swaminathanii	*L. rustica*
	L. portnoyi
	L. cornellensis
	L. newyorkensis
	L. rocourtiae
	L. weihenstephanensis
	L. grandensis
	L. booriae
	L. riparia

Publications concerning the discovery and description of each strain can be accessed at: **https://lpsn.dsmz.de/genus/listeria**

In addition to their phylogenetic differences, species in the *sensu stricto* group share most of the phenotypic traits typical for *Lm*. In contrast, several species in the *sensu lato* group lack those characteristics common amongst *sensu stricto* species such as the ability to grow at low temperatures, reduce nitrate, produce acetoin, and exhibit motility (Carlin *et al.*, 2022). Another key difference is that the *sensu stricto* group includes the only known pathogenic species (Guillet *et al.*, 2010). Overall, *Listeria sensu lato* species are more genetically diverse, lack some of the phenotypic traits typical of the *sensu stricto* group and are not considered pathogenic to humans or animals.

The two strains considered pathogenic are *Lm* and *L. ivanovii*, however, *L. ivanovii* is rarely associated with human disease and more commonly with disease in ruminant animals (Guillet *et al.*, 2010). Although other species are generally considered non-pathogenic there have been isolated cases of *L. innocua* (Perrin *et al.*, 2003), *L. seeligeri* (Rocourt *et al.*, 1986) and *L. grayi* (Rapose *et al.*, 2008) causing disease in humans, predominantly in individuals with a compromised immune system. Nevertheless, *Lm* is the most significant species in terms of pathogenicity and responsible for the majority of Listeriosis cases in humans.

1.5 Listeriosis transmission and disease progression

Lm is an opportunistic pathogen and the causative agent of Listeriosis, a serious bacterial infection that poses significant risks to vulnerable groups such as pregnant women, newborns, the elderly (typically 60 years and older) and immunocompromised individuals (Vázquez-Boland *et al.*, 2001). The first report of *Lm* as a human pathogen came from Denmark in 1929, when it was identified as the causative agent of a mononucleosis-like illness in three patients (Nyfeldt, 1929). Interestingly, *Lm* was not recognised as a foodborne pathogen until much later.

The first conclusive evidence of foodborne transmission emerged from an outbreak in Canada between 1980 and 1981 which was linked to the consumption of contaminated coleslaw (Schlech *et al.*, 1983). Since then, it has become evident that human Listeriosis is predominantly transmitted through the consumption of contaminated food, with an estimated 99% of cases attributed to this route (Scallan *et al.*, 2011). Due to a high mortality rate of 20 – 30% (WHO, 2015) as well as a high hospitalisation rate

(94%) (Scallan *et al.*, 2011), *Lm* is considered as a priority pathogen for national surveillance in many countries (Moura *et al.*, 2016). Notably, it is a notifiable disease with mandatory reporting required in all EU member states (EU Directive 2003/99/EC).

Listeriosis can manifest as either a non-invasive or invasive form. In most healthy adults, Listeriosis is typically non-invasive causing some mild flu-like symptoms and self-limiting febrile gastroenteritis (Matereke and Okoh, 2020). While this form is generally less severe, it can progress to invasive Listeriosis in individuals with a compromised immune system and the elderly. This invasive form can lead to sepsis, meningitis, encephalitis and ultimately death. Additionally, in pregnant women, Listeriosis can also cause neonatal infections, preterm delivery, miscarriages, and stillbirth (Vázquez-Boland *et al.*, 2001).

The infectious dose, that is, the exact minimum number of bacteria required to cause Listeriosis, has not been conclusively established. While bacterial counts of 10^6 CFU/g (colony-forming units per gram) have been found in foods linked to sporadic or epidemic Listeriosis cases, contamination levels as low as 10^2 – 10^4 CFU/g have also been associated with human infection (Farber and Peterkin, 1991; Vázquez-Boland *et al.*, 2001). The infectious dose depends on the type of food ingested, host risk factors as well as the pathogenicity and virulence of the strain involved. Overall, it has been estimated that ingestion of 10^7 – 10^9 CFU is required to cause infection in healthy individuals, whereas just 10^5 – 10^7 CFU may be sufficient to cause disease in vulnerable individuals (Quereda *et al.*, 2021).

After ingestion, *Lm* travels from the mouth to the stomach, where it encounters an extremely acidic pH (1–2) and a rapid change in temperature. If the bacterium survives the stomach and continues through the GI tract, it must further resist high osmolality, bile and competing microbiota (Quereda *et al.*, 2021). Various stress response pathways are triggered by the harsh conditions *Lm* encounters in the gut lumen. These pathways allow *Lm* to resist acidic environments, adapt to changing temperatures, and respond to high osmolality, bile, and competing microbiota (Gahan and Hill, 2014). These same stress adaptation mechanisms also contribute to its persistence in food processing environments, where, for example, acids and salt are often used for disinfection and preservation (Wiktorczyk-Kapischke *et al.*, 2021).

The next phase of *Lm* infectious lifecycle involves crossing the gut epithelial barrier. Within the gut, it invades phagocytic and non-phagocytic epithelial cells via receptor-mediated endocytosis or phagocytosis (Matereke and Okoh, 2020). Once inside, *Lm* expresses virulence factors that enable it to escape from the endosome or phagosome, proliferate in the cytosol and spread to adjacent cells (Quereda *et al.*, 2021).

In invasive Listeriosis, *Lm* crosses the epithelial barrier into the lamina propria, where it disseminates via the lymphatic system and blood to the rest of the body. From the blood, *Lm* can invade the central nervous system (CNS) by crossing the blood-brain barrier and the blood-cerebrospinal fluid barrier, which is likely the most common route of CNS invasion (Quereda *et al.*, 2021). In pregnant women, *Lm* can cross the maternal-foetal barrier, leading to major foetal or neonatal complications (Quereda *et al.*, 2021). Although *Lm* can infect a wide range of host tissues, it primarily targets and infects the CNS, placenta, liver and spleen tissue (Vázquez-Boland *et al.*, 2001).

The incubation period for invasive Listeriosis is often cited as ranging from 3 to 70 days following ingestion of contaminated food, with a median of approximately 3 weeks. This estimate is largely based on data from a 1985 Listeriosis outbreak and case reports of sporadic infections (Linnan *et al.*, 1988; Angelo *et al.*, 2016). However, more recent studies have provided slightly different estimates. For instance, Goulet *et al.* (2013) found that the incubation period for invasive Listeriosis can vary from 1 to 67 days, with a median of 8 days, based on an analysis of 37 cases. Contrastingly, their research indicates that pregnancy-associated cases typically have longer incubation periods than other types (median: 27.5 days; range: 17–67 days). Another study by Angelo *et al.* (2016), using simulation modelling, estimated a median incubation period of 11 days, with 90% of Listeriosis cases occurring within 28 days. Collectively, these studies indicate that when investigating Listeriosis outbreaks, an initial 2-week window should be considered when reviewing the food history of those infected, with an even longer period warranted for pregnancy-associated cases.

Given the variability and potential length of the incubation period for Listeriosis, source identification during outbreak investigations can be particularly challenging, delaying the detection of the contamination source and potentially extending the outbreak. To

prevent such outcomes, it is crucial to identify *Lm*-contaminated food before it reaches consumers. When contaminated food does reach consumers, effective tracing of the origins of foodborne outbreaks is essential to facilitate product recalls and inform the public. Extensive efforts have been made to characterise *Lm* strains based on their genotypic and phenotypic traits, which has been vital in developing detection methods, identifying outbreak sources, studying the epidemiology of *Lm* and identifying problematic strains.

1.6 *L. monocytogenes* subtyping and whole-genome sequencing for strain identification and genetic characterisation

1.6.1 Subtyping methods for *L. monocytogenes*

Listeria spp. are a group of closely related bacteria that exhibit many similar morphological and biochemical traits. These common biochemical characteristics have been effectively used to differentiate *Listeria* spp. from other bacteria. Additionally, *Listeria* spp. also possess distinct biochemical features which have been exploited to differentiate between different species (Gasanov *et al.*, 2005). While biochemical characteristics can be used to identify *Lm*, they have limited utility in distinguishing between different isolates.

Not long after the discovery of *Lm* as an etiological agent, it became evident that the species does not constitute a homogeneous group with regards to infection outcomes and physiological characteristics (Paterson, 1940). To improve understanding of *Lm* ecological distribution, epidemiology, and virulence, efforts were directed towards developing more precise methods for strain differentiation (Paterson, 1940; Liu, 2006). Various phenotypic and molecular subtyping techniques have since been employed to differentiate and classify *Lm* strains. Phenotypic methods for subtyping *Lm* include serotyping, phage typing, multi-locus enzyme electrophoresis (MLEE), and esterase typing. In contrast, molecular subtyping techniques analyse the genetic material of *Lm* to differentiate and group strains. Molecular techniques used to subtype *Lm* include pulsed-field gel electrophoresis, ribotyping, PCR-based-, and DNA sequencing-based methods (Liu, 2006).

The following section provides a brief overview of the key subtyping methods employed in the classification of *Lm* strains. It further examines how these strains have been phylogenetically grouped using different subtyping approaches, offering insights into the associations between these groupings and specific strain characteristics, including virulence, geographical distribution and isolation sources.

1.6.2 Serotyping as a method for *L. monocytogenes* subtyping

The first subtyping method for *Lm* was introduced by Paterson (1940), focusing on the differentiation of strains based on flagellar and somatic antigens. *Listeria* spp. possess two types of group-specific surface proteins: somatic (O) and flagellar (H) antigens. These antigens became the target for serological detection using monoclonal and polyclonal antibodies, with serotypes of individual *Listeria* strains determined by unique combinations of their O and H antigens. Paterson's method was later refined to improve strain differentiation (Seeliger and Höhne, 1979; Seeliger and Jones, 1986). Eventually, the serotyping scheme developed by Seeliger and Höhne (1979) became the most widely adopted.

Presently, at least 14 serotypes for *Lm* (1/2a, 1/2b, 1/2c, 3a, 3b, 3c, 4a, 4ab, 4b, 4c, 4d, 4e, 4h and 7) have been defined (Orsi *et al.*, 2011; Feng *et al.*, 2020). Despite its widespread use, the value of serotyping for epidemiological purposes is somewhat limited. This is primarily because the majority of human Listeriosis (95%) cases have been associated with only four serotypes (1/2a, 1/2b, 1/2c, and 4b) (Doumith *et al.*, 2004a; Ragon *et al.*, 2008). Consequently, serotyping has largely been superseded by molecular methods, which offer greater specificity and sensitivity for the identification and differentiation of *Listeria* spp..

1.6.3 Genomic lineages in *L. monocytogenes*

Both phenotypic and molecular subtyping methods have been utilised to delineate *Lm* strains into four distinct phylogenetic lineages. Piffaretti *et al.* (1989) were the first to propose *Lm* could be divided into two lineages according to MLEE analysis of 175 *Lm* isolates. A third lineage was subsequently identified by Rasmussen *et al.* (1995) through partial sequence analysis of virulence-associated genes, including flagellin (*flaA*), invasion-associated protein (*iap*), and listeriolysin O (*hly*), from 77 *Lm* isolates. A further

subdivision of lineage III into three subgroups, IIIA, IIIB, and IIIC, was proposed by Roberts *et al.* (2006) based on the analysis of partial *sigB* (stress response regulator) and *actA* (actin assembly protein) sequences. Ward *et al.* (2008) later proposed that the isolates classified as lineage IIIB by Roberts *et al.* (2006) should be renamed lineage IV. These four lineages are now widely accepted, with numerous phylogenetic studies confirming this subdivision (Orsi *et al.*, 2011; Haase *et al.*, 2014; Zamudio *et al.*, 2020). The classification of *Lm* into lineages has been valuable for researchers, as each lineage has been linked to specific traits, enabling the prediction of characteristics such as virulence, ecological niches, and genetic features based on lineage (Orsi *et al.*, 2011).

1.6.4 Multi-locus sequence typing as a comprehensive tool for *L. monocytogenes* strain classification

Phenotypic subtyping methods for *Lm* often lack the discriminatory power and reproducibility provided by molecular subtyping methods. Among these, DNA sequence analysis has gained immense popularity for species classification due to the steadily decreasing cost of sequencing, high resolution it provides, and reliable reproducibility. One effective approach for differentiating *Lm* strains is through the sequence analysis of several conserved core genes, a method known as multi-locus sequence typing (MLST) (Haase *et al.*, 2014).

MLST schemes have been widely employed for various bacterial genera and species to investigate epidemiology, population biology, pathogenicity and evolutionary patterns (Maiden, 2006). The first MLST scheme for *Lm* was developed by Salcedo *et al.* (2003), based on the sequence analysis of seven housekeeping genes [*acbZ* (ABC transporter), *bglA* (beta-glucosidase), *cat* (catalase), *dapE* (succinyl diaminopimelate desuccinylase), *dat* (D-amino acid aminotransferase), *ldh* (lactate dehydrogenase), and *lhkA* (histidine kinase)]. Ragon *et al.* (2008) further refined this scheme, which has since become widely adopted for differentiating *Lm* strains, examining their evolutionary relationships, and tracking the species' epidemiology (Orsi *et al.*, 2011; Haase *et al.*, 2014).

The MLST scheme developed by Ragon *et al.* (2008) assigns allele numbers to each of the seven genes (loci) based on unique sequence variants. An MLST profile refers to the specific combination of allele numbers across these seven loci for a given isolate. Each unique MLST profile is assigned a distinct sequence type (ST) number, which acts as a shorthand identifier for that specific profile. Profiles differing by no more than one gene are assigned to the same clonal complex (CC). Using MLST, Ragon *et al.* (2008) confirmed that *Lm* could be divided into four distinct evolutionary lineages.

A key advantage of the scheme developed by Ragon *et al.* (2008) was the creation of a publicly accessible database (https://bigsdb.pasteur.fr/listeria/) that stores the sequence information of these seven genes from *Lm* isolates characterised using this method. As of the time of writing, the database contains sequence data from 7,942 isolates and 3,602 MLST profiles. Overall, the database provides a consistent language for population groupings making it a valuable resource for evaluating uncharacterised strains, tracking epidemiology and assessing the genetic diversity of *Lm*.

1.6.5 Whole-genome sequencing: a key tool for *Listeria* epidemiology and genetic characterisation

MLST has been successfully used to categorise *Lm* into subtypes, such as sequence types and clonal complexes (CC; also referred to as clonal groups), and has been widely applied to study its epidemiology, pathogenicity, isolation sources and stress resistance (Ragon *et al.*, 2008; Maury *et al.*, 2016; Lakicevic *et al.*, 2022). However, MLST lacks the resolution needed to distinguish between outbreak-related and unrelated isolates within the same clonal group, limiting its utility in epidemiological investigations (Chen *et al.*, 2016).

Advances in high-throughput whole genome sequencing (WGS) and bioinformatics have significantly improved the affordability and speed of genome sequencing and analysis. As a result, publicly available sequence databases have become inundated with microbial genomes, which can be exploited for comprehensive microbial genome comparisons. Furthermore, WGS has proven particularly valuable in epidemiology by offering superior strain resolution and more robust genetic evidence, which allows for

more precise case definitions and clearer differentiation of outbreak cases (Jackson *et al.*, 2016).

Due to the unmatched resolution WGS analysis offers compared to other subtyping methods, it is increasingly being adopted for Listeriosis outbreak surveillance (Jackson *et al.*, 2016; Painset *et al.*, 2019). In fact, WGS has been applied in numerous national studies for outbreak detection and investigation including Australia (Kwong *et al.*, 2016), the USA (Jackson *et al.*, 2016) and France (Moura *et al.*, 2017) as well as others (Painset *et al.*, 2019). In the US, WGS is now routinely used for Listeriosis outbreak surveillance and response. Since its introduction into routine practice, WGS has identified outbreak clusters earlier and pinpointed food sources more rapidly than traditional methods, leading to quicker resolution of outbreaks (Jackson *et al.*, 2016).

Additionally, WGS enables researchers to identify the pan-, core-, and accessory genomes within an *Lm* dataset. The pan-genome represents the complete set of genes in a group of organisms, while the core genome comprises genes shared by all organisms in the group. The accessory genome includes genes present only in some strains. Sequence similarity within the core genome is regarded as a highly effective measure for comparing microbial genomes (Chen *et al.*, 2016). Efforts have been made to define the core genome of the entire *Lm* species and develop a core genome multi-locus sequence typing (cgMLST) scheme (Ruppitsch *et al.*, 2015; Chen *et al.*, 2016; Moura *et al.*, 2016). This approach expands on MLST by incorporating a larger set of loci (core genes) which improves resolution at the strain level.

Several cgMLST schemes have been developed for *Lm*, each utilising different sets of core genes (Ruppitsch *et al.*, 2015; Chen *et al.*, 2016; Moura *et al.*, 2016). While cgMLST improves strain differentiation and species subgrouping, there is no consensus on which genes definitively constitute the *Lm* core genome. As more genomes are sequenced, these schemes may need to be revised to account for changes in the genes considered part of the core genome. Defining the *Lm* core genome may also help uncover traits that are inherent to the species, particularly those relevant to food safety and pathogenicity, which could be leveraged to prevent Listeriosis outbreaks. Ultimately, a cgMLST scheme that reliably captures all genes consistently shared

across *Lm* strains would provide a valuable inter-laboratory standard for strain classification.

In addition to improving the differentiation of *Lm* isolates, WGS provides comprehensive genetic insights, enabling the identification of key genes related to stress response, antimicrobial resistance, disinfectant tolerance and virulence (Maury *et al.*, 2016; Lakicevic *et al.*, 2022). This has made WGS invaluable for understanding the genetic factors that contribute to *Lm* contamination of food, its persistence in food-processing environments and pathogenicity. Overall, WGS plays a crucial role in epidemiological investigations and understanding its pathogenicity and association with foodborne outbreaks.

1.7 *L. monocytogenes* an emerging threat in fresh produce

The foods considered high risk for *Lm* contamination include fish and fishery products, meat and meat products and milk and milk products (Quereda *et al.*, 2021). Furthermore, across all food categories ready-to-eat (RTE) food products are most often implicated in *Lm* outbreaks (EFSA, 2021a). Although *Lm* outbreaks have predominantly been linked to RTE animal-based products, RTE products made from fruit and/or vegetables are also increasingly being associated with *Lm* outbreaks (EFSA, 2021a).

In fact, one of the most severe foodborne outbreaks in US history occurred in 2011 due to contaminated cantaloupe, leading to 147 cases of Listeriosis and 33 deaths (McCollum *et al.*, 2013). More recently, in 2021, contaminated packaged leafy vegetables caused a multistate Listeriosis outbreak in the US, affecting 18 people across 13 states (FDA, 2021). A variety of other fruits and vegetables have also been implicated in Listeriosis outbreaks in recent years (Table 1.2).

Table 1.2 Foodborne Listeriosis outbreaks associated with fruit and vegetables with known outcomes.

Location of Listeriosis cases	Year	Food source	Death/ Cases	Reference
U.S. – Texas	2010	Cut celery	5/10	(Gaul *et al.*, 2013)
U.S. – 22 states	2011	Cantaloupe melons	33/147	(McCollum *et al.*, 2013)
U.S. – 4 states	2014	Stone fruits	0/2	(Jackson *et al.*, 2015)
U.S. – 2 states	2014	Mung bean sprouts	2/5	(CDC, 2015)
Australia and Europe – 5 countries	2015 to 2018	Frozen vegetables	10/53	(EFSA *et al.*, 2020)
Australia	2018	Cantaloupe melons	8/22[a]	(NSW Food Authority, 2018)
U.S. – 13 states	2021	Packaged leafy greens	3/18	(FDA, 2021)
U.S. – 6 states	2022	Peaches, Nectarines, and Plums	1/11	(FDA, 2023)

[a] 1 miscarriage recorded as a death

1.8 The persistence of *L. monocytogenes* in RTE foods: from processing to storage

The RTE products commonly associated with foodborne Listeriosis are those that support the growth of *Lm*, are consumed without inactivation treatments (e.g. heat treatment) and have an extended refrigerated shelf life (Quereda *et al.*, 2021).

A variety of processing methods such as heating, curing, smoking, fermentation, and drying have been shown to effectively reduce and eliminate pathogens in RTE meat, fish, and dairy products (Ricci *et al.*, 2018; Gómez *et al.*, 2020). Although contamination of these food products can occur following processing, appropriate sanitation of the processing area and handling of these products should prevent contamination from occurring. In contrast, RTE fruits and vegetables receive only minimal processing, such as washing with acids or chlorine-based sanitisers, which can reduce microbial numbers but may not fully eliminate pathogens (Ricci *et al.*, 2018). For instance, Hellström *et al.* (2006) demonstrated that washing pre-cut iceberg lettuce inoculated with *Lm* using water, chlorinated water (100 ppm), peracetic acid (0.05%) or a

commercial citric acid-based wash (0.25%) reduced but did not completely eliminate *Lm*. In fact, following washing and cold storage at 6 °C for 6 days, *Lm* counts returned to pre-washing levels. Thus, although fresh produce generally has a shorter shelf life compared to foods treated with heat or preservatives, if *Lm* is not eliminated or sufficiently reduced during processing, it may grow to harmful levels during a product's shelf life (Chan and Wiedmann, 2008).

In addition to processing methods aimed at eliminating, inactivating, or suppressing microorganisms in food, several other strategies are employed to prevent microbial growth throughout a product's shelf life (Ricci *et al.*, 2018). Cold storage of food products is a commonly used strategy for food safety and quality management as it can effectively suppress growth of spoilage organisms (Cai *et al.*, 2019). However, *Lm* is considered a psychrotolerant bacterium, meaning it thrives at 30 – 37 °C but is also capable of growing at temperatures below 15 °C (Chan and Wiedmann, 2008). In fact, *Lm* has been observed to grow at temperatures as low as -1.5 °C and as high as 45 °C (Saldivar *et al.*, 2018).

Several types of fruit and vegetables have been shown to support growth of *Lm* during their shelf life, even under refrigerated conditions (Cai *et al.*, 2019; Culliney and Schmalenberger, 2020; Marik *et al.*, 2020). Culliney and Schmalenberger (2020) demonstrated that spinach, rocket, and iceberg lettuce, inoculated with 100 CFU/g of *Lm*, reached median cell counts of 4 $\log_{10}$, 3 $\log_{10}$, and 3 $\log_{10}$ CFU/g, respectively, after 7 days of storage at 8 °C. These contamination levels are comparable to those found in foods linked to Listeriosis outbreaks (Farber and Peterkin, 1991; Vázquez-Boland *et al.*, 2001). Thus, *Lm* ability to grow on fresh produce during refrigerated storage suggests that even low-level contamination can escalate to pathogen levels capable of causing infection over the course of a product's shelf life (Chan and Wiedmann, 2008).

Additional measures, such as modified atmosphere packaging (MAP), are also commonly applied to processed foods like packaged salads to further inhibit spoilage organisms and extend shelf life (Francis *et al.*, 2012). MAP works by replacing oxygen with gases like nitrogen, carbon dioxide or argon to inhibit microbial growth and slow decay. However, *Lm* is a facultative anaerobic organism meaning it can grow in both

oxygenated and low-oxygen environments (Chan and Wiedmann, 2008). Culliney and Schmalenberger (2020) reports that *Lm* can grow on rocket and spinach even under MAP and cold storage conditions (Culliney and Schmalenberger, 2020). In fact, several studies have shown that the survival and growth of *Lm* on produce is unaffected by MAP (Francis *et al.*, 2012; Cai *et al.*, 2019).

RTE foods often consist of multiple components, which can increase the risk of *Lm* contamination and proliferation. Interestingly, a study examining the contribution of different food sources to Listeriosis cases recorded from 2004 to 2007 in England and Wales found that most infections were linked to multi-component foods, such as sandwiches and pre-packed mixed salads (Little et al., 2010). These multi-component foods have a more complex nutritional profile, potentially supporting *Lm* growth while providing additional niches for colonisation. Notably, Alegbeleye and Sant'Ana (2022) showed that a salad mix comprised of Iceberg lettuce, Romaine lettuce, purple curly lettuce, and green curly lettuce was able to support the growth of *Lm* at 4 °C, while single-component foods like Iceberg lettuce, curly lettuce, and butterhead lettuce did not. Furthermore, contamination can occur at various stages in the supply chain. In multi-component foods, the risk of contamination is higher because ingredients sourced from different locations and processed in various environments are combined into a single product. As a result, the complexity of multi-component foods, coupled with the potential for cross-contamination, significantly increases the likelihood of *Lm* contamination.

In conclusion, *Lm* ability to survive and even thrive under conditions typically used to prevent spoilage poses a significant risk for pathogen transmission. For fresh produce, washing methods intended to reduce pathogen numbers often prove ineffective at completely eliminating *Lm*. *Lm* contamination in fruit and vegetables is particularly concerning, as they are often consumed raw, meaning no "killing step" is introduced during processing or before consumption. Furthermore, strategies such as cold storage and MAP, used to suppress spoilage organisms, are often ineffective at preventing the growth of *Lm*. As a result, low-level contamination that goes undetected during sampling can grow to harmful levels during storage. This highlights the critical need to prevent contamination from occurring in the first place. However, each stage of the

supply chain, from production to packaging and distribution, presents opportunities for *Lm* to be introduced or spread.

1.9 Sources of *L. monocytogenes* contamination

Understanding the natural reservoirs of *Lm* is vital to determining how it enters the food supply chain and developing effective strategies to mitigate contamination. This section focuses specifically on the sources of contamination for fruits and vegetables, exploring how *Lm* moves from its environmental reservoirs into food production, and the challenges this poses for ensuring food safety.

Early theories regarding the natural reservoir of *Lm* proposed that the bacterium primarily existed in soil as a saprophytic organism (Weis and Seeliger, 1975; Vidovic *et al.*, 2024). While soil is recognised as an important environmental niche for *Lm*, it is now well-established that the bacterium occupies a broad range of environments and is not restricted to soil alone (Vivant *et al.*, 2013; Vidovic *et al.*, 2024). Indeed, *Lm* has been isolated from various sources, including soil, water, wild and farm animals and plants (Félix *et al.*, 2022).

In animals, *Lm* has been isolated from over 40 species of wild and domestic mammals, 22 species of birds as well as fish, crustaceans and insects (Quereda *et al.*, 2021). These organisms all function as vehicles for the transmission of *Lm* into the farming and processing environment. Notably, farm animals are considered to play a crucial in the farm environment, acting as key reservoirs and aiding its circulation through faecal shedding (Hurtado *et al.*, 2017).

A study by Locatelli *et al.* (2013) investigating the occurrence of *Lm* in different soil types in France revealed the bacterium was frequently isolated from cow pasture soils but not from cultivated soils, meadows or forest soils. Similarly, Chapin *et al.* (2014) found that *Lm* prevalence was significantly higher in farm samples compared to those from the natural environment in New York, with proximity to pasture identified as a key factor contributing to these higher rates. These findings suggest that anthropogenic activities, particularly farming practices such as livestock management, play a significant role in the persistence and spread of *Lm*.

Although *Lm* is widespread in the natural environment, its prevalence is strongly influenced by human activity. In farming environments, *Lm* has been detected in manure (Denis *et al.*, 2022), soil (Vivant *et al.*, 2013), animals (Lyautey *et al.*, 2007) and irrigation water (Gartley *et al.*, 2022), all of which act as vehicles for its dissemination. Consequently, fresh produce can become contaminated through various routes in the growing environment, including contaminated irrigation water, soil splash, roaming animals and farming equipment (Smith *et al.*, 2018).

An investigation into a 2021 Listeriosis outbreak linked to packaged salad (Table 1.2) traced the contamination source to equipment used for harvesting iceberg lettuce (FDA, 2021). In theory, any lettuce harvested with this equipment could have been contaminated, potentially spreading *Lm* to multiple processing locations and causing cross-contamination of other equipment and food. In fact, Magdovitz *et al.* (2021) examined 290 raw vegetable samples upon arrival at food processing facilities, prior to any cleaning or preprocessing, and detected *Lm* in 17 samples. This highlights how produce contaminated in the growing environment can serve as a vehicle for transmitting *Lm* into the processing environment.

There are several other routes through which *Lm* can enter food processing environments, including cross-contamination by workers, contaminated materials and equipment (Smith *et al.*, 2018). The fresh produce processing environment is typically inhospitable to *Lm* due to the abundance of nutritionally poor abiotic surfaces, regular cleaning with detergents and the common practice of operating at refrigeration temperatures. Nevertheless, once inside the facility, *Lm* may settle in areas known as harbourage sites (Gil *et al.*, 2024).

Harbourage sites provide an ecological niche for *Lm* and can include areas such as drains, cracks in surfaces, crevices in machinery and other hard-to-reach areas (Carpentier and Cerf, 2011). Harbourage sites are typically difficult to clean, as disinfectants and sanitisers often cannot effectively reach them. Additionally, nutrients may be available in those areas such as organic matter from soil, product debris and factory run off (Smith *et al.*, 2018). Since *Lm* requires moisture to grow, moisture-retentive areas which are hard to clean are typical harbourage sites for the pathogen (Carpentier and Cerf, 2011).

Once established inside the processing facility, *Lm* can contaminate other fruits and vegetables through direct contact with contaminated surfaces, aerosols, or improper handling and storage practices. Indeed, routine sampling frequently detects *Lm* in fresh produce processing areas, highlighting the ongoing risk of cross-contamination throughout the food production process (Jordan *et al.*, 2018).

The persistence of *Lm* in food processing environments is well documented, with various strains reported to survive for years, or even decades, in these settings (Tompkin, 2002). This long-term persistence drives the ongoing transmission of *Lm* through the food supply chain by enabling repeated contamination of surfaces, equipment, and food products during processing, handling, and packaging. Given that fresh produce is often processed raw without antimicrobial treatments (e.g. heat inactivation), any contamination acquired during harvesting or processing can be passed directly to the consumer. Indeed, numerous studies have identified *Lm* in fruits and vegetables during processing or at retail, underscoring the importance of stringent hygiene and monitoring practices to mitigate contamination risks (Zhu *et al.*, 2017; Ricci *et al.*, 2018; Willis *et al.*, 2020).

The persistence of *Lm* in both farm and food processing environments is a key factor in its transmission to foodstuffs. *Lm* ubiquity and ability to survive in a wide range of environments are attributed to its exceptional capacity to sense and respond to various physicochemical stresses (Quereda *et al.*, 2021).

1.10 Stress tolerance and genetic adaptation in *L. monocytogenes* for environmental persistence

In order for *Lm* to persist in the wide range of environments it inhabits, the bacterium needs to be able to withstand the various environmental pressures it encounters. Stress tolerance mechanisms enable survival under these harsh conditions and contribute to *Lm* persistence in food and farm and food processing settings.

Lm has a high tolerance to osmotic, pH and thermal stresses, with certain strains possessing higher levels of tolerance than others (Wagner and McLauchlin, 2008; Saldivar *et al.*, 2018). It can grow across a wide temperature range, with growth observed at temperatures as low as -1.5 °C and as high as 45 °C (Saldivar *et al.*, 2018).

Tienungoon *et al.* (2000) reports growth of *Lm* at salt concentrations as high as 10% NaCl. The bacterium can also resist extended periods of desiccation, an uncommon trait among major foodborne bacteria (Hingston *et al.*, 2017; Vidovic *et al.*, 2024). Additionally, *Lm* can grow in acidic environments as low as pH 4.3 and in alkaline conditions up to pH 9.5 (Giotis *et al.*, 2008). These characteristics enable *Lm* to persist throughout the food supply chain and proliferate in foods subjected to treatments meant to inhibit microbial growth, such as drying, salting, acid and alkaline washes, and refrigeration.

In addition to these stress tolerance mechanisms, *Lm* possesses other survival strategies that further enhance its persistence in food processing environments. One such strategy is the formation of biofilms which can increase resistance to disinfectants and prolonged periods of desiccation (Smith *et al.*, 2018). *Lm* can also enter a protective, viable non-culturable state (VNS) which may protect it from environmental stresses and assist in avoiding detection by routine laboratory culture (Ayrapetyan and Oliver, 2016). Another contributing factor to its persistence in food processing environments is its ability to adhere to abiotic surfaces such as stainless steel and polystyrene (Lee *et al.*, 2017).

Furthermore, exposure to one stress may make *Lm* more resistant to other unrelated stressors. For instance, Lou and Yousef (1997) showed that adaptation to pH 4.5 – 5.0 or 5% ethanol significantly increased the resistance of *Lm* to typically lethal doses of acid, ethanol, and hydrogen peroxide. Additionally, heat shock significantly increased the resistance to ethanol and NaCl. Stress adaptation may also increase virulence in some strains; Alves *et al.* (2020) reported that exposure to cold stress improved the invasion of Caco-2 cells in five out of eight *Lm* strains tested.

Thus, the selective pressures *Lm* encounters can lead to the selection of more resistant phenotypes in a particular environment. Selective pressures also drive the acquisition of resistance genes and favourable mutations that contribute to *Lm* persistence in the environment (Orsi *et al.*, 2011). For example, several plasmids acquired by *Lm* have been shown to confer resistance to quaternary ammonium compounds (QAC) which are widely used as disinfectants in the food industry (Hingston *et al.*, 2017). In fact, QAC

resistance is frequently detected in *Lm* isolates recovered from food samples (Cooper *et al.*, 2021).

Additionally, other plasmids acquired by *Lm* have been shown to confer resistance to cadmium and antibiotics including chloramphenicol, clindamycin, erythromycin, streptomycin, and tetracycline (Hingston *et al.*, 2017). Other mobile genetic elements in *Lm* strains have also been reported. For example, Müller *et al.* (2013) reports certain *Lm* strains with ST 121 harbour the transposon Tn*6188*, which confers tolerance to the QAC benzalkonium chloride. Overall, these mobile genetic elements may confer resistance to environmental stresses, toxic metals, sanitisers and possibly other compounds that *Lm* may encounter in the environment.

Evolutionary mechanisms such as horizontal gene transfer and mutations enable strains to acquire stress resistant mechanisms, while selective pressures in farm and processing environments drive the evolution of more resistant phenotypes (Vidovic *et al.*, 2024). Some characteristics required for survival in specific ecological niches have been shown to correlate with lineage, while certain stress response mechanisms are closely linked to specific clonal groups (Orsi *et al.*, 2011; Lakicevic *et al.*, 2022). Nevertheless, some characteristics may be strain-specific, shaped by the selective pressures of the environment the strain inhabits (Hingston *et al.*, 2017). Overall, a strain's association with a particular food likely arises from traits that not only help it survive in environments where contamination occurs but also enable attachment, survival, and growth within the food itself.

1.11 Leaf and bacterial characteristics in *L. monocytogenes* salad contamination

Amongst the RTE fruit and vegetables category, RTE salads have been identified as “high risk” in terms of bacterial contaminations. Notably, the EFSA reported that in 2017, *Lm* was most frequently detected in RTE salads, second only to fish and fishery products (EFSA, 2018). The RTE salad market is a growing segment of the fresh food industry, driven by increasingly health-conscious consumers, as RTE salads offer an easily accessible source of vitamins, minerals, and other phytonutrients with minimal processing (Gullino *et al.*, 2019). However, there is a high risk of microbiological

contamination associated with fresh leafy salads due to their close association with soil microbes. Furthermore, RTE salad mixes can contain a variety of salad species which vary in their physical characteristics and nutritional composition, providing a diverse range of ecological niches which can be colonised by *Lm* (Kyere *et al.*, 2019b).

Previous research efforts have mainly focussed on the interaction of *Lm* with lettuce, whereas other leafy vegetable components of RTE salads have not been well investigated (Kyere *et al.*, 2019b). Spinach is a common component of RTE salads and previous research has shown *Lm* can grow on spinach during normal storage and processing conditions, which could lead to consumers eating contaminated food and subsequent infections (Culliney and Schmalenberger, 2020).

Salad leaves can become contaminated through contact with contaminated soil, water, wild animals and fertiliser in the growing environment or through contact with contaminated food contact surfaces in the processing environment (Smith *et al.*, 2018). Upon contact the bacterium may colonise the leaf surface where it can grow and multiply to harmful levels. Successful colonisation of leaves is dependent on the ability of the bacteria to attach to the leaf surface. Plant leaf characteristics such as leaf roughness, stomatal density, surface hydrophobicity and cuticular wax composition have all been reported to influence the attachment of bacteria to leaves (Lima *et al.*, 2013; Macarisin *et al.*, 2013; Hunter *et al.*, 2015). These characteristics have been reported to vary with leaf age. In fact, Hunter *et al.* (2015) reported the differential attachment of *Salmonella enterica* serovar Senftenberg to lettuce leaves of different ages could be associated with differences in leaf vein and stomatal densities, leaf surface hydrophobicity and leaf surface soluble protein concentrations.

Understanding the interaction of *Lm* with salad vegetables is vital in identifying plant traits and growing practices linked to a higher risk of *Lm* contamination. For example, Lima *et al.* (2013) reported *Salmonella* Enteritidis attachment to lettuce leaves was significantly higher ($P<0.05$) to lettuces grown hydroponically than conventional systems. Understanding which plant leaf characteristics influence bacterial attachment, and how these vary with growing practices, can aid in promoting better growing practices. Furthermore, differences in bacterial attachment between cultivars has also been reported. Macarisin *et al.* (2013) investigated the attachment of *E. coli*

O157:H7 to different spinach cultivars and demonstrated that variations in leaf blade roughness and stomatal density influenced the differential attachment of *E. coli* O157:H7. In addition, Jacob and Melotto (2020) reported there was significant variation in attachment of *Salmonella enterica* serovar Typhimurium 14028s and *E. coli* O157:H7 amongst 11 different lettuce cultivars. However, the researchers were unable to identify a correlation between plant leaf characteristics, such as stomatal density, stomatal aperture width and stomatal pore area. These results highlight the complexity in identifying intraspecific and interspecific differences in leaf characteristics which influence bacterial attachment.

In addition to plant leaf characteristics, bacterial attachment may be strain specific. Identifying strain specific differences can facilitate the identification of cell surface characteristics which influence bacterial attachment. Cell surface characteristics such as flagella, surface proteins and extracellular polysaccharides have been reported to play a role in attachment of *Lm* (Gorski *et al.*, 2009; Bae *et al.*, 2013; Tan *et al.*, 2016). However, establishing strain to strain variability remains challenging. For example, Gorski *et al.* (2021) did not detect significant differences in bacterial attachment to lettuce by a collection of 23 *Lm* strains. These results indicate that surface characteristics involved in salad leaf attachment may be widespread in *Lm* and highlights the importance of food safety testing and monitoring of the growing and processing environment.

1.12 Detection methods for *L. monocytogenes* in food

Both MAP and cold storage suppresses the growth of spoilage organisms that typically alter the appearance and smell of food. However, *Lm* ability to grow under cold and restricted oxygen conditions allows it to reach harmful levels while spoilage bacteria remain suppressed (Cai *et al.*, 2019). Consequently, these quality changes are not reliable indicators of *Lm* contamination, as it can proliferate to dangerous levels before any visual deterioration or unpleasant odours become apparent (Cai *et al.*, 2019).

This ability of *Lm* to grow without noticeable signs of contamination poses significant challenges for food safety management, as traditional signs of spoilage may not be present to alert producers or consumers. Therefore, proactive measures are crucial to

mitigate the risk. To prevent bacterial contamination of produce, food business owners in the fresh produce supply chain are responsible for monitoring food processing areas for the presence of *Lm* (Jordan *et al.*, 2018). Sampling schemes aim to detect and eliminate persistent strains or, if elimination is impossible, to implement appropriate actions to avoid food contamination by *Lm*.

The detection limits of *Lm* in processing areas and end of product testing can vary between countries (Jordan *et al.*, 2018). Current EU Regulation (EC) 2073/2005 mandates that in RTE foods able to support the growth of *Lm,* the bacterium must be absent in 5x25 g samples at the time of leaving the production plant or does not exceed 100 CFU/g throughout the product's shelf-life (5 × 25 g samples) (European Commission, 2021). Current detection methods involve a two-step broth-based enrichment followed by plating on selective differential agar and phenotypic tests, which can take 4-7 days to get a conclusive result (Law *et al.*, 2015).

More rapid detection methods have been developed utilising DNA or protein-based assays, but these methods fail to recover bacterial isolates for further characterisation, require specialist equipment and training, include complex processing steps and can lack the sensitivity afforded with culture-based methods (Law *et al.*, 2015). Unfortunately, the time taken to confirm a contamination using standard detection methods can exceed the average shelf-life of 5-7 days for RTE salads, which puts customers at risk of consuming contaminated food (Arienzo *et al.*, 2020).

1.13 Volatile organic compound-based detection of *L. monocytogenes* in fresh produce

New detection methods are being developed to overcome challenges with detecting *Lm* in a suitable time frame. Analysis of volatile organic compounds (VOCs) released from fresh produce has been proposed as an alternative strategy for detecting bacterial contaminants (Tait *et al.*, 2014b). VOCs are low-molecular-weight compounds with high vapor pressures that are easily volatilized. Gas chromatography (GC) coupled with mass spectrometry (MS) is a rapid and highly sensitive analytical technique which can separate, identify and quantify compounds in a complex mixture of VOCs. Changes in

the VOCs released by fresh produce during their shelf-life have been used to assess product quality (Spadafora *et al.*, 2018; Spadafora *et al.*, 2019).

Indeed, the profile of VOCs released by fresh produce is in part due to spoilage bacteria (Paramithiotis *et al.*, 2018). Bacteria produce a range of VOCs which have been implicated in signalling, defence or growth-promoting mechanisms (Kanchiswamy *et al.*, 2015). Some bacteria produce specific VOCs such as indole which is associated with *E. coli* (Kai *et al.*, 2009) or 2-aminoacetophenone which is associated with *Pseudomonas aeruginosa* (Cox and Parker, 1979). Although specific compounds can be associated with specific bacteria, because of the complexity of VOC profiles generated by food samples, determining the presence of bacteria based on the analysis of a set of VOCs might be more suitable than single markers.

Multivariate statistical analyses of large datasets can be used to analyse changes in whole VOC profiles or identify a common set of VOCs to determine the presence of bacteria. Bianchi *et al.* (2009) identified approximately 100 VOCs from canned tomatoes contaminated with *E. coli, Saccharomyces cerevisiae* and *Aspergillus carbonarius* and could differentiate between contaminated and uncontaminated cans using a selection of VOC markers (ethanol, β-myrcene, o-methyl styrene, 6-methyl-5-hepten-2-ol and 1-octanol). *Lm* is not considered a spoilage bacterium but can multiply on the surface of fresh produce producing its own sets of VOCs including alcohols, amines esters, hydrocarbons, and ketones (Doyle, 2007).

Spadafora *et al.* (2016b) reports being able to discriminate between melon slices inoculated with 6 log CFU/g of *Lm* and uninoculated controls. The researchers used thermal desorption (TD) tubes with analysis on a gas chromatography time-of-flight mass spectrometry (GC-TOF-MS) system as this combines rapid, simple and stable sampling of VOCs on site, with greater detection sensitivity than other forms of mass spectrometry (Paramithiotis *et al.*, 2018). Using multivariate statistical analyses Spadafora *et al.* (2016b) identified a unique set of VOCs for discriminating between inoculated and uninoculated samples. Furthermore, *Lm* at <100 CFU/g could be detected after an equilibration step for 6 h at 37°C following 7 days of storage at a commercially relevant temperature of 4°C (Spadafora *et al.*, 2016b). These levels (<100 CFU/g) are considered a low contamination as defined by EU guidance

documents and highlights the sensitivity and applicability of VOC analysis for detecting *Lm* on fresh produce (European Commission, 2021).

1.14 Project overview

The overall aim of this project was:

Improving food safety of leafy salad vegetables by (i) advancing our understanding of *L. monocytogenes* interaction with leaf surfaces and (ii) developing VOC-based detection methods.

To address the overall aim of this project, the following hypotheses were proposed to investigate the factors contributing to *L. monocytogenes* contamination risk in leafy salad vegetables and to develop more rapid detection methods:

- Genetic characteristics of *L. monocytogenes* strains may be associated with their potential for contaminating leafy salad vegetables.
- Specific phenotypic characteristics can determine a strain's ability to contaminate leafy salad vegetables.
- *L. monocytogenes* interacts with specific structural features on leaf surfaces, which mediate the differential attachment of strains across various leaf surfaces.
- Analysis of volatile organic compounds can be used to detect *L. monocytogenes* contamination in salad leaves.

To address the hypotheses outlined above, the following methodology was employed to investigate the genetic, phenotypic, and attachment characteristics of *L. monocytogenes* strains, and to develop VOC-based detection methods.

Whole genome sequence analysis was performed on 15 *L. monocytogenes* strains isolated from the fresh produce supply chain, along with 2 widely used reference strains, to characterise their genetic profiles, assess genetic diversity and determine subtypes. Genetic features previously associated with contamination of fruit and vegetables were examined across the collection and their relationship to subtype or phylogenetic grouping was analysed. Phenotypic characteristics, including those

previously associated with fruit and vegetable contamination and growth characteristics, were examined across the collection.

Strains exhibiting traits which suggest an enhanced capacity for fruit and vegetable contamination were selected for further investigation of their attachment potential to leaf surfaces. Additionally, strains phylogenetically closely related to these strains were also included. Attachment potential of this set of strains was evaluated across various leaf surfaces. The influence of external factors, such as exposure time to the leaf and inoculum preparation temperature, were considered for their impact on attachment. Microscopy techniques and a novel assay were employed to investigate the specific leaf surface structures targeted by *L. monocytogenes*.

To investigate whether VOC analysis could be used for contamination detection, a strain with high attachment capacity to leaf surfaces was selected for VOC analysis. This strain was used to assess whether VOC analysis could differentiate between rocket leaves inoculated with this strain and uninoculated leaves. The sensitivity of the VOC detection method was evaluated by testing rocket batches from different years and seasons to account for variability in VOC production. The method's efficacy in detecting *L. monocytogenes* was further tested by evaluating its ability to differentiate *L. monocytogenes* inoculated samples from *L. innocua* inoculated samples. A subset of VOCs consistently identified across all experiments was used to assess whether this subset offered higher sensitivity for contamination detection than the total VOC profile.

Chapter 2 – Materials and methods

2.1 Strain collection, materials and bacteria enumeration

2.1.1 Chemicals

All chemicals were purchased from Merck (UK), Fisher Scientific (UK), VWR (UK) or Scientific Laboratory Supplies (UK), unless otherwise stated. All aqueous solutions of chemicals were prepared using ultrapure deionised water ≥18MΩ cm (dH_2O). Solutions requiring heat sterilisation were autoclaved at 121 °C for 15 min. For small volumes requiring filter sterilisation, Minisart® syringe filters (pore size 0.2 µm; Sartorius Stedim Biotech, UK) were used. Large volumes requiring filter sterilisation were processed with Fisherbrand™ PES Filter Units (pore size 0.2 µm; Fisher Scientific, UK). Phosphate-buffered saline (PBS) (Merck, UK) was prepared in dH_2O (0.01 M Na_2HPO_4/NaH_2PO_4, 0.0027 M KCl, 0.137 M NaCl) and sterilised by autoclaving, resulting in pH 7.4 at 25 °C.

2.1.2 Media

All media were prepared in dH_2O and sterilised by autoclaving for 15 min at 121 °C, except for Vegetable Peptone Broth (VPB; Thermo Scientific, US), which was sterilised by filtration. Media were prepared according to the manufacturer's instructions unless otherwise stated. Brain Heart Infusion (BHI) broth and agar (Merck, Germany) were used for the routine cultivation of *L. monocytogenes* (*Lm*) as well as for preparing inoculum for the protocols outlined in this chapter, unless otherwise specified. VPB was used for growth curve experiments and prepared on the day of the experiments. Tryptic Soy Broth (TSB; Thermo Scientific, US) was used for growth curve experiments, leaf adhesion assays and cellulose adhesion assays. Polymyxin Acriflavine Lithium-chloride Ceftazidime Esculin Mannitol (PALCAM; VWR, UK) agar was always supplemented with the associated supplement (PALCAM agar base (ISO) Cat. No. 84625.0500; VWR, UK) and used as a selective and differential medium for enumerating *Lm* in mixed microbial suspensions. *Listeria* Motility Medium NutriSelect Plus (Merck, Germany) was used to evaluate the swimming motility of *Lm* strains. *Listeria* Enrichment Agar (LEA) was prepared by supplementing *Listeria* Enrichment Broth (VWR, UK) with 0.8% (w/v) bacteriological agar (VWR, UK) and used for the leaf overlay experiments. Luria Bertani

broth (LB; Thermo Scientific, US) was used for the cultivation of *E. coli*. Where applicable, media were supplemented with selective agents as stated.

2.1.3 Enumeration of viable bacteria

Viable bacteria were enumerated using a standard drop plate method unless otherwise stated. Briefly, a dilution series was prepared in PBS and dilutions plated in triplicate (3 x 25 µL) on BHI for enumerating *Lm* from pure cultures, or on PALCAM for enumerating *Lm* in mixed microbial suspensions. The plates were allowed to dry before being incubated at 37 °C for 24 to 48 h, after which the colonies were counted.

2.1.4 *Listeria* strain collection

The *Lm* strains NLmo 2-10, 13-16, 18 and 20 (NLmo collection) were supplied by Prof. I. Singleton from Edinburgh Napier University, UK (Table 2.1). The strains were obtained from a commercial food testing laboratory following routine sampling of produce and food contact surfaces from UK based food production and processing companies (Smith *et al.*, 2019a). Prof. I. Singleton also supplied strain EGD-e (ATCC BAA-679) which is a lab reference strain, and a derivative of strain EGD which was originally isolated from rabbits in 1926 (Murray *et al.*, 1926). The *Lm* strain F2365 was supplied by Dr Des Field from APC Microbiome, Ireland and was originally isolated from soft cheese following an outbreak in 1985 in California, US (Nelson *et al.*, 2004). The *L. innocua* strain BUG499 (CLIP 11262) was supplied by Prof. P. Cossart from the Pasteur institute, Paris however the source of isolation is unknown (Glaser *et al.*, 2001).

For long term storage, bacteria were grown overnight at 37 °C under agitation (150 rpm) on Brain Heart Infusion (BHI) broth (Merck, Germany) and 500 µL of overnight culture added to Microbank™ cryovials (Pro-Lab Diagnostics, Spain) before freezing at -80 °C.

Table 2.1 Characteristics and sample information for one *L. innocua* and 16 *L. monocytogenes* isolates from the Cardiff University collection.

Internal Reference[a,b]	Species	Source	Sample location	Stage in supply chain	Reference
EGD-e[b]	*L. monocytogenes*	Rabbit	Cambridgeshire, UK	N/A	(Murray *et al.*, 1926)
NLmo2	*L. monocytogenes*	Spinach	West Sussex, UK	Raw Product, Unwashed	(Smith *et al.*, 2019a)
NLmo3[b]	*L. monocytogenes*	Spinach	West Sussex, UK	Raw Product, Unwashed	(Smith *et al.*, 2019a)
NLmo4[b]	*L. monocytogenes*	Drain	West Sussex, UK	Tray cleaning facility	(Smith *et al.*, 2019a)
NLmo5	*L. monocytogenes*	Spinach	West Sussex, UK	Raw Product, Unwashed	(Smith *et al.*, 2019a)
NLmo6	*L. monocytogenes*	Red leaf lettuce	Norfolk, UK	Raw Product, Unwashed	(Smith *et al.*, 2019a)
NLmo7	*L. monocytogenes*	Spinach	West Sussex, UK	Post Cooling, Unwashed	(Smith *et al.*, 2019a)
NLmo8[b]	*L. monocytogenes*	Spinach	Cambridgeshire, UK	Final Product, Unwashed	(Smith *et al.*, 2019a)
NLmo9[b]	*L. monocytogenes*	Spinach	Cambridgeshire, UK	Final Product, Unwashed	(Smith *et al.*, 2019a)
NLmo10[b]	*L. monocytogenes*	Spinach	Cambridgeshire, UK	Post Cooling, Unwashed	(Smith *et al.*, 2019a)
NLmo13[b]	*L. monocytogenes*	Spinach	Cambridgeshire, UK	Final Product, Unwashed	(Smith *et al.*, 2019a)
NLmo14	*L. monocytogenes*	Beetroot	Cambridgeshire, UK	Final Product, Washed	(Smith *et al.*, 2019a)
NLmo15[b]	*L. monocytogenes*	Pea shoots	Cambridgeshire, UK	Final Product, Unwashed	(Smith *et al.*, 2019a)
NLmo16	*L. monocytogenes*	Spinach	Cambridgeshire, UK	Final Product, Unwashed	(Smith *et al.*, 2019a)
NLmo18[b]	*L. monocytogenes*	Baby salad kale	Cambridgeshire, UK	Post Cooling, Unwashed	(Smith *et al.*, 2019a)
NLmo20	*L. monocytogenes*	Baby salad kale	Cambridgeshire, UK	Final Product, Unwashed	(Smith *et al.*, 2019a)
F2365	*L. monocytogenes*	Soft cheese	California, US	Unknown	(Nelson *et al.*, 2004)
BUG499	*L. innocua*	Cheese	Rabat, Morocco	Unknown	(Glaser *et al.*, 2001)

[a] Strain identification code for the Cardiff University Collection
[b] Strains selected for analysis of growth dynamics at 25 °C in BHI, TSB and VPB

2.2 Whole-genome sequencing and comparative genomic analyses of *Listeria* strain collection

2.2.1 DNA extraction and quantification

Bacterial cultures were grown in 5 mL BHI broth for ~16 h at 37 °C under agitation. DNA was extracted from a 2 mL aliquot of the cultures with either the Monarch® Genomic DNA Purification Kit (New England Biolabs, US) or PureLink™ Microbiome DNA Purification Kit (Invitrogen, US) according to the manufacturer's instructions. The DNA was eluted with 200 µL of elution buffer from the DNA extraction kit utilised, or 200 µL molecular grade water (Severn Biotech, UK). DNA concentrations were quantified using the Nanodrop 1000 spectrophotometer (Thermo Scientific, US) and the Qubit dsDNA BR (broad range, 100 pg/µL – 1 µg/µL) Assay Kit (Invitrogen, US) with the Qubit 3.0 fluorometer (Invitrogen, US) according to the manufacturer's protocols; a sample volume of 1 µl was added to 199 µl of a Qubit working solution. DNA samples were stored at -20 °C post-extraction until further use.

2.2.2 Genome sequencing and assembly

2.2.2.1 Cloud infrastructure for remote computing

Bioinformatics analysis was conducted using the MRC-funded Cloud Infrastructure for Microbial Bioinformatics (CLIMB) (Connor *et al.*, 2016) and *iago*, a high-performance computing (HPC) service provided by the School of Biosciences at Cardiff University. Both CLIMB and *iago* services were accessed via Secure Shell (SSH) connections over the internet, with MobaXterm (v21.5; Mobatek, France) serving as a secure command-line terminal for remotely connecting to and managing bioinformatics tasks.

On CLIMB, terminal commands were executed on a preconfigured virtual machine equipped with software and predefined pipelines or tools, including the Genomics Virtual Laboratory. Bash scripts were parallelised using the shell tool GNU parallel (Tange, 2018).

On the *iago* HPC cluster, installed software and environment variables are managed using the Environment Modules package (v5.4.0; available from: https://modules.sourceforge.net/). Applications, libraries, and tools are installed within

Module environments and loaded as needed. The *iago* cluster consists of several partitions, each offering varying computational resources and task management capabilities. All jobs submitted to the *iago* cluster are managed by the Slurm Workload Manager (v24.05; SchedMD, US).

Tasks were submitted to *iago* via bash scripts specifying the required partition, necessary modules, and the command for the desired programme. Once submitted, tasks were queued and executed as soon as the required resources became available.

2.2.2.2 Genome sequencing of *Listeria* strain collection

The genomes of the entire NLmo collection were sequenced by Smith *et al.* (2019a) and this sequence data was supplied along with the strains. DNA extraction, quantification, library preparation and whole genome sequencing was conducted at MicrobesNG (University of Birmingham, UK). Libraries were sequenced with the Illumina HiSeq system using a 250 base-pair paired-end protocol, with a target 30-fold depth of coverage. Illumina reads were adapter trimmed using Trimmomatic (v0.30)(Bolger *et al.*, 2014), with a sliding window quality cut-off of Q15, prior to receiving the sequence data from Edinburgh Napier University, UK.

The genomes of *L. innocua* strain BUG499 and *Lm* strains EGD-e and F2365 were sequenced at Novogene, UK. DNA was extracted as described in Section 2.2.1. Before submitting samples to Novogene, DNA concentrations were quantified using the Qubit dsDNA BR Assay Kit (Invitrogen, US) with the Qubit 3.0 fluorometer (Invitrogen, US) according to the manufacturer's instructions. Genomes were sequenced with the Illumina NovaSeq X Plus system generating 150-nucleotide paired-end reads with a 30-fold depth of coverage for each sample.

2.2.2.3 Genome assembly and quality control

For *Listeria* strains BUG499, EGD-e, and F2365, the wrapper script Trim Galore (v0.6.10)(Krueger *et al.*, 2023) was used to automate adapter and quality trimming, as well as quality control of the sequence data. Trim Galore integrates the programmes Cutadapt (v4.1) (Martin, 2011) and FastQC (v0.11.9) (Andrews, 2010). Cutadapt removes adapter sequences, primers, poly-A tails and other unwanted sequences from

sequencing reads. FastQC analyses raw sequence data, generating summary graphs and tables for quality control assessment.

Trimmed Illumina reads of the entire *Listeria* collection (Table 2.1) were checked for quality using Fast QC (v0.11.9) (Andrews, 2010) and subsequently assembled using the Unicycler (v0.5.0) (Wick *et al.*, 2017) pipeline, which assembles genomes using SPAdes (v3.15.5) (Bankevich *et al.*, 2012). Genome assemblies were analysed using Quast (v5.2.0) (Gurevich *et al.*, 2013), which computes various metrics presented in summary reports, graphs, and tables for assessing quality and comparing genome assemblies. Metrics such as the N50 values, GC content and other statistics have been reported for the genome assemblies.

2.2.3 Multi-locus sequence typing

2.2.3.1 PCR amplification of multi-locus sequence typing genes

The MLST scheme used to characterize *Listeria* strains as reported by Ragon *et al.* (2008) is based on the sequence analysis of seven housekeeping genes. The 7 housekeeping genes include *acbZ* (ABC transporter), *bglA* (beta-glucosidase), *cat* (catalase), *dapE* (succinyl diaminopimelate desuccinylase), *dat* (D-amino acid aminotransferase), *ldh* (lactate dehydrogenase), and *lhkA* (histidine kinase). The genes were amplified using primers with a sequence specific region and a universal sequencing tail (Table 2.2) as reported by Ragon *et al.* (2008).

The primer specific thermocycler (MJ Research, Canada) settings are shown in Table 2.3 and PCR mixture components in Table 2.4. PCR products were analysed using gel electrophoresis on a 1.2% agarose gel containing SYBR™ Safe DNA Gel Stain at a 1:10,000 dilution of the stock (Thermo Scientific, US). Gels were run at 120 V for 30 min and visualised using a UV transilluminator (Bio Rad, US). The size of fragments was determined using a 1 kb DNA Ladder (New England Biolabs, US). PCR products were purified using the Monarch® PCR & DNA Cleanup Kit (New England Biolabs, US) and sequenced by Eurofins Genomics (UK).

To determine sequence types, the sequences of the MLST genes for each strain were concatenated into individual FASTA files, which were then collectively searched against

the *L. monocytogenes* database (https://bigsdb.pasteur.fr/listeria/) using the "Batch sequence query" function.

Table 2.2 PCR primers used in this study.

Gene	Direction	Primer Sequence[a]
abcZ	*abcZoF*:	**GTTTTCCCAGTCACGACGTTGTA**TCGCTGCTGCCACTTTTATCCA
	abcZoR:	**TTGTGAGCGGATAACAATTT**CTCAAGGTCGCCGTTTAGAG
bglA	*bglAoF*:	**GTTTTCCCAGTCACGACGTTGTA**GCCGACTTTTTATGGGGTGGAG
	bglAoR:	**TTGTGAGCGGATAACAATTT**CCGATTAAATACGGTGCGGACATA
cat	*catoF*:	**GTTTTCCCAGTCACGACGTTGTA**ATTGGCGCATTTTGATAGAGA
	catoR:	**TTGTGAGCGGATAACAATTT**CAGATTGACGATTCCTGCTTTTG
dapE	*dapEoF*:	**GTTTTCCCAGTCACGACGTTGTA**CGACTAATGGGCATGAAGAACAAG
	dapEoR:	**TTGTGAGCGGATAACAATTT**CATCGAACTATGGGCATTTTTACC
dat	*datoF*:	**GTTTTCCCAGTCACGACGTTGTA**GAAAGAGAAGATGCCACAGTTGA
	datoR:	**TTGTGAGCGGATAACAATTT**CTGCGTCCATAATACACCATCTTT
ldh	*ldhoF*:	**GTTTTCCCAGTCACGACGTTGTA**GTATGATTGACATAGATAAAGA
	ldhoR:	**TTGTGAGCGGATAACAATTT**TATAAATGTCGTTCATACCAT
lhkA	*lhkAoF*:	**GTTTTCCCAGTCACGACGTTGTA**AGAATGCCAACGACGAAACC
	lhkAoR:	**TTGTGAGCGGATAACAATTT**CTGGGAAACATCAGCAATAAAC

[a] Universal sequencing tail is shown in bold

Table 2.3 Thermocycler conditions for amplification of the MLST genes.

PCR step	Temperature (°C)	Time (s)	Number of cycles
Initial denaturation	94	240	1
Denaturation	94	30	35
Primer annealing[a]	52	30	35
Primer extension	72	120	35
Final extension	72	600	1

[a] PCR amplification is performed at an annealing temperature of 52 °C for all genes except for *bglA* (45 °C).

Table 2.4 Components of a 25 µL PCR reaction using Taq polymerase.

Components	Final Volume (µL)	Final Concentration
New England Biolabs OneTaq® 2X Master Mix with Standard Buffer	12.5	1X
10 µM Forward Primer	0.5	0.2 µM
10 µM Reverse Primer	0.5	0.2 µM
Template	1	Variable
Nuclease-Free Water	10.5	/

2.2.3.2 Sequence typing using published MLST scheme

The assembled genomes of the entire *Lm* collection were scanned for sequence types using the MLST software application (v2.19.0) (Seemann, 2020). The programme identifies the genes from the multi-locus sequence typing scheme described by Ragon *et al.* (2008) and compares the sequences against a database of *Lm* MLST profiles hosted at https://bigsdb.pasteur.fr/listeria/. To corroborate the identity of each strain and ensure the correct genome sequence was associated with each, the sequence types derived from the genome sequences were compared to those from the PCR-amplified sequences.

2.2.4 Comparative genomic analysis and strain characterisation

2.2.4.1 Gene prediction, sequence annotation and pan-genomics

Non-scaffolded contigs were annotated using Prokka (v1.14.6) (Seemann, 2014) with the default annotation mode ('Bacteria'). Prokka is a genome annotation pipeline that integrates multiple feature prediction tools to identify genomic feature coordinates and provide feature descriptors.

The core, accessory and pan-genomes of the entire *Lm* collection were predicted using Panaroo (v.1.3.2) (Tonkin-Hill *et al.*, 2020). Panaroo is a bioinformatics tool that combines multiple tools and algorithms to identify all genes within a collection of genomes (pan-genome), genes shared among all the bacterial genomes analysed (core genome), and those unique to specific strains (accessory genome).

Additionally, reference genomes of *Lm* strains belonging to lineage 3 (HCC23; GCF_000021185.1) (Steele *et al.*, 2011) and 4 (FSL J1-208; GCF_014843315.1) (Cardenas-Alvarez *et al.*, 2022) were downloaded from RefSeq (NCBI). Panaroo was used to predict the core, accessory and pan-genomes for the entire *Listeria monocytogenes* collection, *L. innocua* strain BUG499, and representative strains from *Lm* lineages 3 and 4. Additionally, Panaroo was also utilised to predict the core, accessory and pan-genomes of the *Lm* strains NLmo8, NLmo9, NLmo15 and EGD-e used for the leaf adhesion experiments.

For each dataset, the core, accessory and pan-genomes were predicted with a 'strict' stringency mode, requiring genes to be present in at least 5% of genomes to avoid being

considered contaminant genes. A minimum of 95% identity in BLASTP comparisons was applied to each dataset, and a core genome threshold of 99% was set, meaning that genes must be present in 99% of strains to qualify as core genes.

The script roary_plot.py (Available at: https://sanger-pathogens.github.io/Roary/) was used to reproduce a pie chart of the pan genome, breaking down the core, soft core, shell and cloud for the *Lm* collection (Table 2.1).

2.2.4.2 Core-genome phylogenies

Core gene alignments were generated using Panaroo (v.1.3.2) (Tonkin-Hill *et al.*, 2020) with the MAFFT (Katoh and Standley, 2013) alignment algorithm. The bioinformatic tool RaxML-NG (v1.2.0) (Kozlov *et al.*, 2019) was employed to generate to generate high-accuracy phylogenies using a maximum-likelihood with General Time Reversible (GTR) substitution and a GAMMA model of rate heterogeneity supported by 200 bootstraps. Phylogenies constructed with RAxML-NG were visualised and edited with MEGA X (v10.1.8) (Kumar *et al.*, 2018) and PowerPoint (v2407; Microsoft, US).

2.2.4.3 Average nucleotide identity for evaluating genetic relatedness

To evaluate the genetic relatedness between strains of the *Lm* collection, the Python-based software package PYANI (v0.2.11) (Pritchard *et al.*, 2016) was used to calculate alignment-based pairwise average nucleotide identity (ANI) values. PYANI was run with the MUMmer software option (Kurtz *et al.*, 2004), which aligns genome sequences and identifies homologous regions. After alignment by MUMmer, PYANI calculates ANI and other related metrics and presents them in summary graphs. All nucleotide similarity values are reported to three significant figures.

2.2.4.4 *In silico* serogroup prediction of *L. monocytogenes* strains

In silico serogroup prediction was conducted for the *Lm* strain collection using the bioinformatics tool LisSero (v0.4.6) (available from: https://github.com/MDU-PHL/LisSero). LisSero predicts the serogroup of *Lm* strains by analysing their genomic sequences and determining the presence or absence of five genes (*lmo1118, lmo0737, ORF2110, ORF2819*, and *prs*). LisSero is based on the multiplex PCR method described by Doumith *et al.* (2004a), which utilizes these five genes for predicting *Lm* serogroups.

2.2.4.5 Identification and sequence analysis of *Listeria* cellulose binding protein homologues

Bae *et al.* (2013) report an association between a *Listeria* cell surface protein (*Listeria* cellulose binding protein; LCP) and attachment of *Lm* to fruit and vegetables. To determine which *Lm* strains encoded LCP homologues, a translated nucleotide BLAST (v2.5.0) search was conducted (Camacho *et al.*, 2009).

A local nucleotide BLAST database of the *Lm* genomes was generated using the makeblastdb command with parse-seqids option. The local databases were queried with the LPC amino acid sequence (accession number Q721X5) published by Bae *et al.* (2013) using the TBLASTN command with default parameters.

Homologous sequences showing the highest percentage of sequence identity were extracted from each genome and compiled into a FASTA file. The amino acid sequence of the putative cellulose-binding domain of LCP, as described by Bae *et al.* (2013), was then used as a query in a TBLASTN search against the sequences in the FASTA file.

Additionally, homologous sequences of the LCP were aligned using the Clustal Omega tool (https://www.ebi.ac.uk/jdispatcher/msa/clustalo), applying the ClustalW algorithm with default parameters (Madeira *et al.*, 2024) to generate a pairwise identity matrix. This matrix which was imported into R (v4.3.1) (R Core Team, 2024) and processed with the ggplot2 (version 3.5.1) (Wickham, 2016) and reshape2 (version 1.4.4) (Wickham, 2007) packages to generate a heatmap.

2.3 Phenotypic characterisation of *L. monocytogenes* collection

2.3.1 Analysis of growth dynamics

2.3.1.1 Investigating growth dynamics of *L. monocytogenes* with the Bioscreen C instrument

The growth dynamics of the entire NLmo collection (Table 2.1) and strain EGD-e in BHI and TSB at 37 °C, as well as a subset of NLmo strains and EGD-e in BHI, TSB, and VPB at 25 °C (Table 2.1), were investigated using a Bioscreen C Microbiological Growth Analyzer (Labsystems, Finland).

Overnight cultures were prepared by picking a single colony from a fresh BHI plate and inoculating 5 mL of VPB, BHI or TSB. For analysis at 25 °C, overnight cultures were grown at 30 °C. For analysis at 37 °C, overnight cultures were grown at 37 °C. BHI and TSB were freshly prepared the day before the experiment by heat sterilisation, whereas VPB was prepared on the day of the experiment by filter sterilisation.

Following overnight incubation, bacterial cultures were standardised to 0.1 OD_{600nm} and subsequently diluted in fresh media at a 1:100 ratio, corresponding to approximately 10^6 CFU/mL. A 200 µL aliquot from diluted overnight cultures was added in quadruplicate to wells of the Bioscreen honeycomb plates (Labsystems, Finland) for analysis. Growth at 37 °C was monitored for 24 h, whereas growth at 25 °C was monitored for 48 h and 45 min. Turbidity measurements were taken at 15 min intervals using a wide-band filter (420 to 580 nm) after shaking the microplates for 10 s at an intermediate intensity. Each experiment was repeated independently to obtain three biological replicates.

Viable bacteria in the standardised cultures were enumerated using the drop plate method, as described in Section 2.1.3. At the end of each monitoring period, the bacterial suspensions from the wells of each strain were combined, and the bacteria were enumerated using the drop plate method.

2.3.1.2 Processing and analysis of Bioscreen C data for the estimation of growth metrics

The data from the Bioscreen C were exported to Microsoft Excel 365 for inspection and processing. The standard deviation at each time point, for four wells of broth only and the four wells of each technical replicate, was inspected to ensure that the optical density did not vary outside of acceptable parameters (<1 SD, Z score ±2). To determine if the broth-only wells changed significantly over the course of the experiment, a one-way ANOVA was used.

For each technical replicate, the mean value of the broth-only wells was subtracted from the measurements at each time point. Subsequently, the mean value at each time point for each biological replicate was calculated and used to plot logistic growth curves and determine the growth metrics of the population.

Growth metrics were obtained using the R package 'Growthcurver' (v0.3.1) (Sprouffske and Wagner, 2016) in R (v4.3.1) (R Core Team, 2024). The analysis was performed in RStudio (v2024.4.2.764) (Posit team, 2024), which provides an integrated development environment for R. GraphPad Prism (v10.2.3) for Windows (GraphPad Software, US) was used to carry out further statistical analyses, visualise growth curves and compare growth metrics.

2.3.1.3 Investigation of growth dynamics of *L. monocytogenes* strains under inoculum preparation conditions for leaf adhesion assay

The growth dynamics of various *Lm* strains were investigated under conditions emulating those used to prepare the inoculum for the leaf adhesion assay. Specifically, strains NLmo8 and EGD-e were analysed at 37 °C, while strains NLmo8, NLmo9, NLmo10, NLmo15, and EGD-e were evaluated at 30 °C. The experiment at 37 °C was repeated three times, whereas the experiment at 30 °C was performed only once.

Overnight cultures were prepared by picking a single colony from a fresh BHI plate and inoculating 5 mL BHI broth. All strains were cultured overnight (~16 h) at either 30 °C or 37 °C with agitation (200 rpm). The following day, tubes containing 4.5 mL BHI broth, pre-warmed to 30 °C or 37 °C, were inoculated with 0.5 mL of the overnight culture. Identical tubes with a maximum capacity of 30 mL were used throughout the experiment.

To investigate growth dynamics at 37 °C, OD_{600nm} measurements were taken at 0 min, 30 min, and hourly intervals up to 7 h. For the third experiment, the 30 min measurement was omitted. For the experiment at 30 °C, OD_{600nm} measurements were taken at 0, 1, 2, 3, 4, and 7 h. All tubes were incubated under agitation at 200 rpm. Each strain had its own series of tubes, and a new tube was used for each time point to ensure identical culture conditions.

Following optical density measurements, viable bacteria were enumerated for each time point using the drop plate method described in Section 2.1.3, with PALCAM agar plates including supplement (Merck, Germany). Plates were incubated for 24 to 48 h at 37 °C before colonies were counted. GraphPad Prism (v10.2.3; GraphPad Software, US) was utilized for generating graphs and performing statistical analyses.

2.3.2 Assessment of *L. monocytogenes* swimming motility using a modified semi-solid agar plate assay

Listeria monocytogenes motility in extracellular environments is facilitated by the movement of peritrichous flagella on its surface. These flagella enable *Lm* to move in different directions, a process characterized as swimming motility (Wright *et al.*, 2014).

Swimming motility of *Lm* strains was assessed using a semi-solid agar plate assay as described by Partridge and Harshey (2020) with the following modifications (Figure 2.1). A single colony from a freshly streaked BHI agar plate was used to inoculate 5 mL of fresh BHI broth and incubated overnight (~18 h) at 30 °C under agitation (200 rpm). The following day, 0.5 mL of the overnight culture was transferred to 4.5 mL of fresh BHI broth. The mixture was then incubated at 30 °C with agitation (200 rpm) for 2 h until it reached early to mid-logarithmic phase (OD_{600nm} 0.4 – 0.6).

The exponential phase culture was used to inoculate *Listeria* Motility Medium NutriSelect Plus (Merck, Germany), a low percentage agar (0.35% w/v) growth medium specifically designed to assess motility of *Lm* strains. The agar plates were prepared by pouring 25 mL of heat sterilised agar (autoclaved at 121 °C for 15 min) into petri-dishes which were dried under laminar flow at room temperature (~21 °C) before inoculation. Plates were inoculated by piercing the surface of the agar in the centre, without passing through the agar, with a sterile pipette tip loaded with 6 µL exponential phase culture and gently expelling the contents.

Following inoculation, plates were incubated upright at 22 °C, 30 °C, and 37 °C for 44 and 65 h in sealed bags to prevent drying. Strains were assayed in triplicate at each temperature. The experiment was repeated three times to obtain biological replicates for each temperature, except for 22 °C, where only two biological replicates were collected. Photographic images were taken at each time interval to measure the surface area of the corona, which forms around the point of inoculation, using ImageJ (version 2.14.0/1.54i) (Schindelin *et al.*, 2012). GraphPad Prism (v10.2.3; GraphPad Software, US) was utilized for generating graphs and performing statistical analyses.

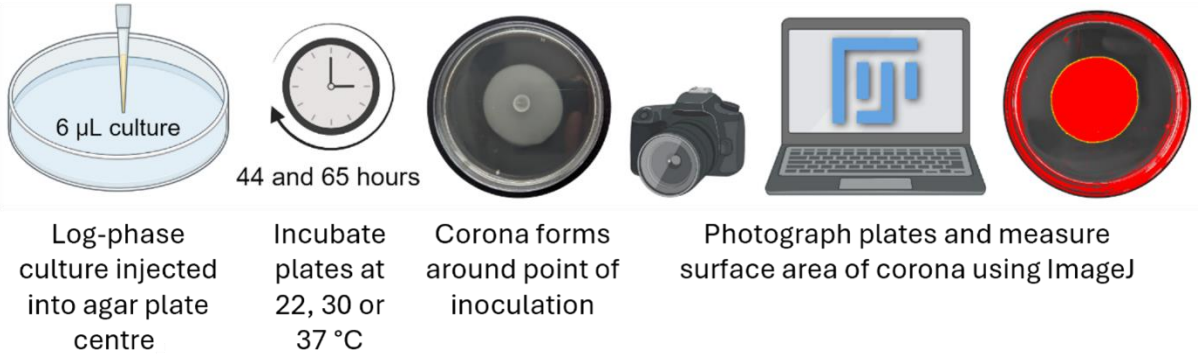

Figure 2.1 Graphical representation of the modified agar plate assay used to assess swimming motility in *L. monocytogenes*.
Created with BioRender.com

2.3.3 Evaluating bacterial adhesion to cellulose-coated wells

The following protocol was adapted from the cellulose binding assay described by (Bae *et al.*, 2013). Cellulose acetate (Merck, Germany) was dissolved in glacial acetic acid (≥99%) (Thermo Scientific, US) at a concentration of 1% (w/v). A volume of 300 µL of this solution was added to wells of a 96-well plate (Greiner Bio-One, Austria). The plate was covered with a lid and placed in a fume hood to allow the acetic acid to evaporate slowly over several days. Once the acetic acid had evaporated completely, the cellulose-acetate-coated wells were washed twice with PBS using an orbital shaker.

After washing, 100 µL bacterial suspensions were added to the cellulose acetate-coated wells and incubated for approximately 16 h at room temperature (~21 °C). The bacterial suspensions were prepared according to the method described by Bae *et al.* (2013). Briefly, *Lm* strains were grown overnight (~16 h) in 5 mL BHI at 37 °C with agitation. The following day, overnight cultures were washed twice with PBS and standardised to a concentration of 1 x 10^7 CFU/mL. Bacterial enumeration in the suspensions was performed using the drop plate method as previously described (Section 2.1.3).

After incubating for 21 h in the cellulose acetate-coated wells, the bacterial suspensions were removed. The wells were then washed three times with PBS and allowed to air dry for 45 min. The bacteria attached to the wells were stained by adding 150 µL of 0.5% w/v crystal violet solution (Merck, Germany) in dH_2O, incubating for 5

min at room temperature and then washing three times with PBS. The stained bacteria were subsequently de-stained with 150 µL of 33% v/v glacial acetic acid. The de-staining solution was then transferred to a fresh 96-well microtiter plate, and the optical density was measured at 590 nm using a Tecan Infinite 200m Pro microplate reader (Tecan, Switzerland). The results were blank corrected by subtracting the average absorbance of control wells (PBS only) from the absorbance measured for the test wells.

2.4 Investigating *L. monocytogenes* interaction with leaf surfaces

2.4.1 Leaf disc assay

2.4.1.1 Cultivation of spinach for leaf attachment assays using leaf discs

Seeds of spinach (*Spinacia oleracea* L.) cultivars 'Lazio' (Wilko, UK) and 'Samish' (Mr. Fothergill's, UK) were purchased from local retailers. Seeds were sown in moistened Levington Advance Pot & Bedding M2 Compost (ICL, Israel) and kept in the dark at 15-17 °C for 3 to 4 days until germination.

Seedlings were then grown in a temperature- and humidity-regulated plant growth chamber (Conviron CMP5090, Conviron, Canada) with a photoperiod of 16 h of light and 8 h of darkness. The ambient temperature was maintained at 21 ± 0.5 °C during the light period and 18 ± 0.5 °C during the dark period, with the relative humidity fixed at 55%. Water was added to trays every two days to keep the soil moist but not saturated.

2.4.1.2 Quantifying *L. monocytogenes* attachment to plant leaves using leaf discs

The following protocol (Figure 2.2) was adapted from the attachment assay described by Salazar *et al.* (2013). *Lm* strains were grown overnight (~16 h) in 5 mL of TSB or BHI at 37 °C under agitation (Table 2.5). Following overnight growth, cultures were diluted 1:10 in pre-warmed BHI or TSB (37 °C) to a total volume of 5 mL. Diluted cultures were incubated at 37 °C with agitation until reaching the early- to mid-exponential phase (OD_{600nm} = 0.4 – 0.5). Once the desired OD_{600nm} was reached, viable bacteria in the inoculum were enumerated using the drop plate method as previously described (Section 2.1.3).

Inoculum (10^7 CFU/mL) for the leaves was prepared by diluting the exponential phase cultures 1:50 in sterile PBS. Leaves were immersed in 25 mL of inoculum in 50 mL Falcon tubes which were placed on a rocking platform for 10 min. After 10 min, leaves were removed from the tubes and dried at room temperature (~21 °C) for 1 h. To remove unattached bacteria the leaves were washed 3 times by placing leaves in 50 mL Falcon tubes containing 10 mL of sterile PBS and gently inverting the tubes several times.

Following washing, discs (diam. = 0.5 cm) were cut from the leaves using a sterilised cork borer and macerated in Eppendorf tubes containing 500 µL PBS using sterilised pestles. Bacteria in the macerate were enumerated on PALCAM plates with supplement (Merck, Germany) using either the drop plate method as previously described (Section 2.1.3) or the spread plate method. In brief, 200 µL of undiluted macerate and a 10^{-1} dilution were spread on PALCAM plates and the plates left to dry. Dry plates were incubated for 48 h at 37 °C after which the colonies were counted.

The number of attached cells was calculated as colony forming units per unit of surface area (CFU/cm^2). GraphPad Prism (v9.1.0) (GraphPad Software, US) was used to generate graphs and carry out statistical analyses.

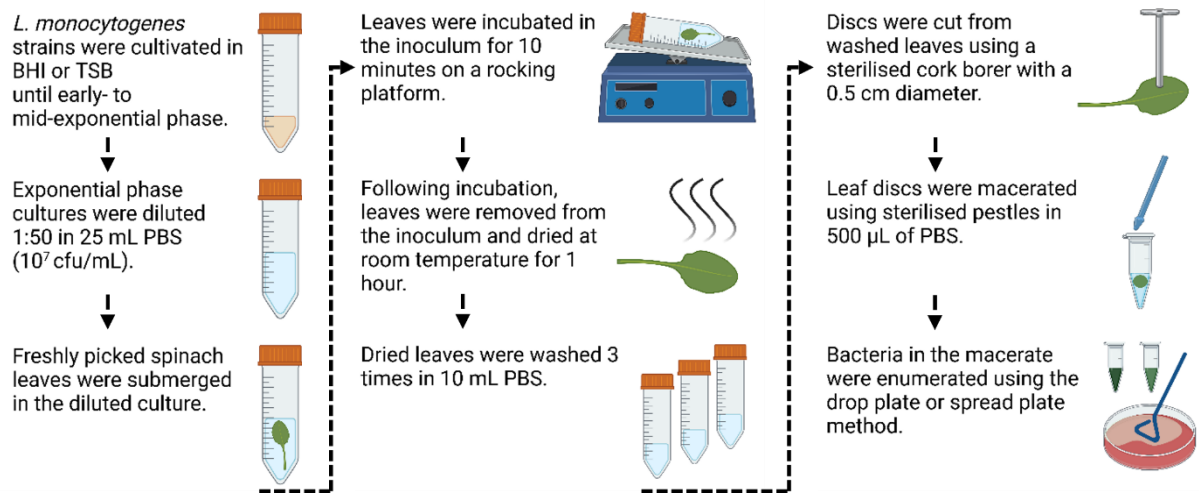

Figure 2.2 Graphical representation of the leaf disc assay used to inoculate spinach leaves with *L. monocytogenes* and quantify attached bacteria following washing.
Created with BioRender.com

2.4.2 Whole leaf assay

2.4.2.1 Cultivation of wild rocket and spinach for whole leaf attachment assays

Seeds of wild rocket (*Diplotaxis tenuifolia* (L.) DC) cultivar 'Monza' were purchased from a commercial seed company (CN Seeds, UK). Spinach seeds of the cultivar 'Nandu RZ' were supplied by collaborators at Vitacress (UK), an agricultural company specializing in leafy salad vegetables, and were purchased from a commercial seed company (Rijk Zwaan, The Netherlands).

Plants were cultivated in a custom-formulated growing medium consisting of 4 parts Levington Advance Seed & Modular F2 Compost (ICL, Israel), 1 part Sinclair Vermiculite Fine Grade (Fargro, UK), 1 part Sinclair Perlite Standard Grade (Fargro, UK), and 1/2 part Melcourt Sharp Sand (Fargro, UK). Additionally, 7-7-7 Growmore fertilizer was incorporated at a rate of 5 g/L (Fargro, UK). For wild rocket, fine vermiculite was substituted with Sinclair Vermiculite Medium Grade (Fargro, UK) to improve drainage.

Plants were grown in a temperature-controlled greenhouse with a baseline temperature of 22 °C, with forced-air ventilation cooling the greenhouse when temperatures rose above 26 °C. Kroptek Sunstream LED grow lights (Kroptek, UK) with a KP04 light spectrum were employed when the natural photoperiod was below 16 h. Two weeks post-germination, thinning of seedlings was performed to optimize light exposure and growing space. Plants were irrigated as needed, approximately every two days, ensuring the medium remained moist but not saturated.

After 4 to 5 weeks in the greenhouse, plants were transferred to a temperature-, humidity- and photoperiod-regulated plant growth chamber (Fitotron SGC097.CFX.F, SANYO Gallenkamp, UK) equipped with Kroptek LED grow lights (iTube0600-12-S33-KP04, Kroptek, UK) emitting a KP04 light spectrum. The chamber maintained a 12 h light/12 h dark photoperiod, with temperatures set at 22 ± 0.5 °C during the dark period and 24 ± 0.5 °C during the light period. Relative humidity was consistently held at 50% ± 5%.

2.4.2.2 Whole leaf assay for quantifying *L. monocytogenes* attachment on rocket and spinach leaves

The following protocol was used to quantify bacterial attachment of strains NLmo8, NLmo8::cGFP, NLmo9, NLmo15, and EGD-e to rocket leaves and of NLmo8, NLmo8::cGFP and EGD-e to spinach leaves (Table 2.5).

Overnight cultures were prepared by picking a single colony from a BHI plate and inoculating 5 mL BHI broth. All strains were cultured overnight (~16 h) at 30 °C under agitation at 200 rpm. Following overnight incubation, 0.5 mL of this culture was added to 4.5 mL BHI broth pre-warmed to 30 °C. This culture was then incubated at 30 °C for up to 2 h under agitation until it reached the early- to mid-exponential phase (OD_{600nm} = 0.4 – 0.5). The number of viable bacteria in the exponential phase culture were enumerated using the drop plate method as previously described (Section 2.1.3). Once the culture reached the desired OD the inoculum was prepared by diluting the culture 1:500 in sterile PBS to achieve a final concentration of 10^6 CFU/mL.

Leaves were inoculated by placing a freshly picked leaf in a sterile container with 100 mL of inoculum. A negative control was included in each experiment by replacing the bacterial suspension with PBS but treating the leaf in the same manner throughout. For each replicate, the second mature leaf was picked, ensuring that each leaf was taken from plants growing in separate pots. The container was placed on a rocking platform for 10 min to ensure continuous coverage of the leaf surface by the inoculum. Following inoculation, leaves were washed three times by placing them in 100 mL PBS in a sterile container on a rocking platform for 1 min. In addition, to assess the effect of drying on bacterial attachment, spinach leaves inoculated with strains NLmo8 and EGD-e were either dried for 1 h after 10 min in the inoculum or washed immediately.

After washing, leaves were placed in 25 mL of sterile PBS and macerated using an Ultra-Turrax T25 homogenizer (IKA, UK) with a separate sterilized disperser tool for each leaf. The number of viable bacteria in the macerate was then enumerated using the spread plate method. For each leaf, 200 µL of the undiluted macerate was spread onto three PALCAM plates (i.e. 200 µL per plate). Additionally, for each leaf, three separate dilution series (10^{-1} and 10^{-2}) were prepared, and 200 µL from each dilution was spread

onto PALCAM plates. The plates were subsequently dried and incubated at 37 °C for 48 h before colony counting.

Prior to inoculation, leaves were photographed alongside a ruler to measure their surface area using ImageJ (version 2.14.0/1.54i) (Schindelin *et al.*, 2012). The number of attached cells for each leaf was calculated as colony-forming units per unit of surface area (CFU/cm^2). GraphPad Prism (v10.2.3) (GraphPad Software, US) was used for generating graphs and performing statistical analyses.

Table 2.5 *L. monocytogenes* strains investigated for attachment to rocket and spinach.

	Internal Reference	Protocol used	Cultivars tested	Source of isolation	Reference
Spinach	EGD-e	Section 2.4.1; 2.4.2	Nandu RZ, Lazio, Samish	Rabbit	(Murray *et al.*, 1926)
	NLmo8	Section 2.4.1; 2.4.2	Nandu RZ, Lazio, Samish	Spinach	(Smith *et al.*, 2019a)
	NLmo8::cGFP[a]	Section 2.4.2	Nandu RZ	Spinach	(Balestrino *et al.*, 2010; Smith *et al.*, 2019a)
Rocket	EGD-e	Section 2.4.2	Monza	Rabbit	(Murray *et al.*, 1926)
	NLmo8	Section 2.4.2	Monza	Spinach	(Smith *et al.*, 2019a)
	NLmo8::cGFP[a]	Section 2.4.2	Monza	Spinach	(Balestrino *et al.*, 2010; Smith *et al.*, 2019a)
	NLmo9	Section 2.4.2	Monza	Spinach	(Smith *et al.*, 2019a)
	NLmo15	Section 2.4.2	Monza	Pea shoots	(Smith *et al.*, 2019a)

[a] Strain genetically modified to constitutively express green fluorescent protein

2.4.3 Imaging of *L. monocytogenes* on leaf surfaces

2.4.3.1 Indirect immunofluorescence labelling for microscopic imaging of *Listeria* on leaf surfaces

A rabbit anti-*Listeria* polyclonal antibody (ab35132, Abcam, UK) was used as the primary antibody to label *Lm* (Table 2.6). This antibody is reported to be specific for *Lm* strains, although the immunogen used to generate the ab35132 antibody has not been disclosed (Bastounis *et al.*, 2018). For labelling the rocket cell wall, a monoclonal rat anti-pectic polysaccharide antibody (LM19, PlantProbes, UK) was utilized (Table 2.6). The LM19 antibody targets the homogalacturonan domain of pectin in plant cell walls

(Verhertbruggen *et al.*, 2009). Additionally, samples were treated with Hoechst 33342 (Fisher Scientific, UK) which is a DNA-specific fluorescent stain.

Rocket (cv. 'Monza') leaves were inoculated with *Lm* strains NLmo8, NLmo10, and EGD-e as detailed in Section 2.4.2.2. Following inoculation, the leaves were cut into 1x1 cm sections and fixed in 4% (w/v) formaldehyde (FA) (Thermo Scientific, US) dissolved in PBS (FA-PBS). The samples were stored in FA-PBS for one week prior to further processing. Additionally, to assess the specificity of ab35132, 10 µL droplets of overnight cultures from strains NLmo8, NLmo9, and EGD-e were dried on coverslips for antibody labelling. Overnight cultures were prepared by inoculating 5 mL BHI broth with a single colony and incubating at 37 °C for approximately 16 h with agitation at 200 rpm. Following drying, the overnight cultures were fixed for 15 min in FA-PBS and subsequently processed as follows.

Leaf sections and coverslips were submerged in PBS with 50 mM ammonium chloride (NH_4Cl) (Fisher Scientific, UK) for 5 min, washed with PBS, submerged in 0.2% (v/v) Triton X-100 (Sigma-Aldrich, US) in PBS for 4 min and washed again with PBS. The samples were then treated with 0.2% (w/v) bovine serum albumin (BSA) (Sigma-Aldrich, US) dissolved in PBS (BSA-PBS) to minimize non-specific antibody binding. Following removal of the blocking agent, the samples were stained with primary antibodies. Primary antibodies, ab35132 and LM19, were mixed and diluted in BSA-PBS to working concentrations of 1:100 (40 – 50 µg/mL) and 1:200 (5 µg/mL), respectively. Samples were incubated in this antibody mixture for 1 h at room temperature (~21 °C). Following primary antibody labelling, the samples were washed with PBS and incubated in BSA-PBS for 5 min before applying the secondary antibodies.

Goat anti-rat conjugated with Alexa Fluor 594 (Jackson ImmunoResearch, US) was used for the rocket cell wall and donkey anti-rabbit conjugated with Alexa Fluor 488 (Jackson ImmunoResearch, US) for *Lm* (Table 2.6). Hoechst 33342 was also used for DNA staining. Secondary antibodies and Hoechst were mixed in BSA-PBS at working concentrations of 1:100 (15 µg/mL) and 1:500 (0.04 mM), respectively. Samples were incubated in this mixture for 45 min at room temperature (~21 °C). After incubation, the samples were washed with PBS and briefly dipped in molecular grade water (Severn

Biotech, UK). Leaf sections were mounted in a drop of ProLong Gold antifade reagent (Thermo Scientific, US) on a microscope slide and covered with a square coverslip. Sections were cut from the base, middle, and apex of each leaf, including features such as the central vein, lateral veins, and margins. For each region, sections were prepared to allow imaging from both the adaxial and abaxial sides. Coverslips with the overnight culture drop were also mounted on antifade reagent on microscope slides. Samples were stored in the dark for 2 h before imaging.

The samples were examined using a bScope fluorescent microscope (model BS.1153-PLi/4N; Euromex Microscopen, the Netherlands), and images were captured with a GXCAM HiChrome HR4 Lite camera (GT Vision, UK). Confocal images were obtained with a confocal microscope (LSM 880 with Airyscan; Carl Zeiss, Germany) with 40x (NA = 1.3) and 63x (NA = 1.4) oil immersion objectives. Images were acquired using the ZEN Black 2012 software (Carl Zeiss, Germany) and processed in ZEN Blue (version 3.7; Carl Zeiss, Germany) and ImageJ (version 2.14.0/1.54i) (Schindelin *et al.*, 2012).

Table 2.6 Antibodies used in this study.

Antibody	Isotype	Clonality	Host organism	Target	Supplier
ab35132[a]	IgG	Polyclonal	Rabbit	*L. monocytogenes*	Abcam, UK
LM19[a]	IgM	Monoclonal	Rat	Plant pectic polysaccharides	PlantProbes, UK
Alexa Fluor 488[b]	IgG	Polyclonal	Donkey	Rabbit	Jackson ImmunoResearch, US
Alexa Fluor 594[b]	IgG	Polyclonal	Goat	Rat	Jackson ImmunoResearch, US

[a] Primary antibody
[b] Secondary antibody

2.4.3.2 Transformation of *L. monocytogenes* strain NLmo8 to express green fluorescent protein

Strain NLmo8 was genetically modified using the site-specific integration vector pAD_1-cGFP, designed by Balestrino *et al.* (2010), which contains a genetic construct enabling the constitutive expression of GFP in *Lm*. The genetic construct within the pAD_1-cGFP vector was derived from the integrative plasmid pH-*hly gfp*-PL3 and includes several key elements: tandem copies of the *rrnB* T1 transcription terminator to prevent any residual transcription from upstream promoters, the Hyper-SPO1 (*Phyper*)

constitutive promoter, and the *hly* 5' UTR sequence, which enhances the expression of *cis*-associated genes (Figure 2.3) (Shen and Higgins, 2005). Additionally, the original *gfp* gene from pH-*hly gfp*-PL3 was replaced with the gene encoding GFPmut2, which provides greater fluorescence intensity (Cormack *et al.*, 1996). The pPL2 plasmid (Figure 2.3) also harbours a chloramphenicol resistance cassette, which is integrated into the *Lm* chromosome along with the GFP construct. The plasmid was supplied to us in *Escherichia coli* BUG 2479 by collaborators at the Pasteur Institute, Paris.

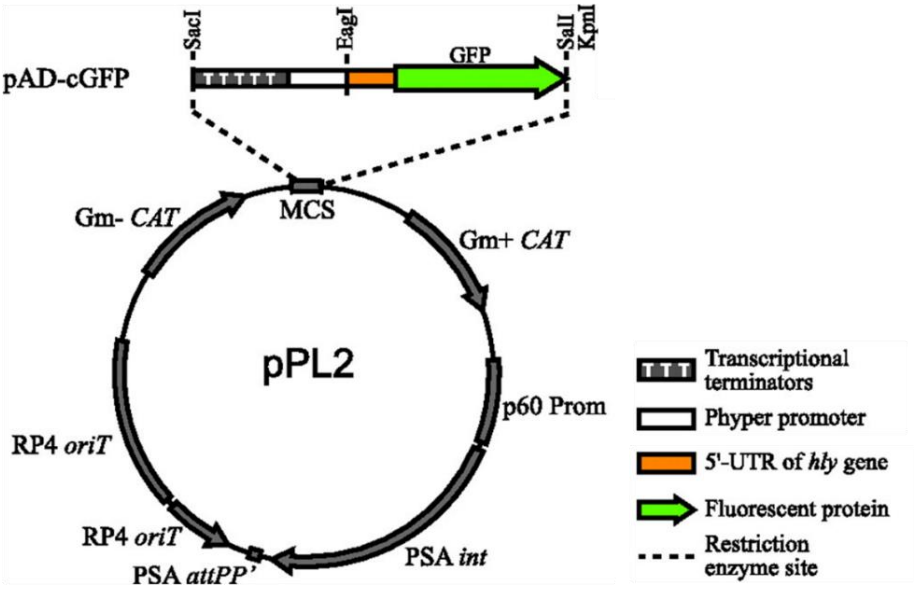

Figure 2.3 Schematic diagram of the pPL2 plasmid backbone and the genetic construct inserted into the vector to generate pAD$_1$-cGFP.
The key elements as indicated on the plasmid include chloramphenicol resistance genes for Gram-negative and Gram-positive bacteria (*Gm- CAT* and *Gm+ CAT*), multiple cloning site (MCS), origin of transfer (*RP4 oriT*), phage attachment site (*PSA attPP'*), integrase gene (*PSA int*), and the p60 promoter. The construct includes tandem copies of the *rrnB* T1 transcription terminator, Hyper-SPO1 (*Phyper*) constitutive promoter, the *hly* 5' UTR sequence and the gene encoding GFPmut2. Adapted from Balestrino *et al.* (2010).

Transformation of *Lm* strain NLmo8 was achieved by purifying the plasmid from *E. coli* BUG2479, generating electrocompetent cells and introducing the pAD$_1$-cGFP plasmid via electroporation. *E. coli* cultures were grown in LB media containing 35 µg/mL of chloramphenicol throughout. The pAD$_1$-cGFP plasmid was purified from *Escherichia coli* BUG 2479 using the QIAGEN Plasmid Maxi Kit (QIAGEN, Germany) according to the manufacturer's instructions. After purification, the DNA pellet was dissolved in 800 µL of molecular grade water (Severn Biotech, UK), and the concentration of the extracted

DNA quantified using a NanoDrop spectrophotometer (NanoDrop 1000; Thermo Scientific, US).

To generate electrocompetent *Listeria* cells, an overnight culture (~16 h) of *Lm* in BHI was diluted 1:100 in 100 mL of filter-sterilised BHI supplemented with 500 mM sucrose (Fisher Scientific, UK) (BHIS) prewarmed to 37 °C. The bacterial suspension was incubated at 37 °C with agitation at 200 rpm for approximately 4.5 h until the OD_{600nm} reached 0.23. Ampicillin was then added to a final concentration of 10 µg/mL, and the culture incubated for an additional 2 h at 37 °C with agitation at 200 rpm until the OD_{600nm} reached 0.47. The bacterial suspension was subsequently divided into two 50 mL Falcon tubes and cooled on ice for 10 min, followed by centrifugation at 5000 g for 10 min at 4 °C.

Bacterial pellets were resuspended in 50 mL of cold (< 4°C) filter-sterilised sucrose glycerol water buffer (SGWB) (500 mM sucrose, 10% (v/v) glycerol, pH adjusted to 7) and centrifuged again at 5000 g for 10 min at 4 °C. This resuspension and centrifugation process was repeated twice more with volumes of 15 mL and 5 mL cold SGWB, respectively. Filter-sterilised lysozyme was added to the 5 mL suspension at a final concentration of 10 µg/mL, and the mixture was incubated at 37 °C for 25 min in a water bath. The suspension was centrifuged at 3000 g for 10 min at 4°C, the pellet resuspended in 1.5 mL cold SGWB, centrifuged again (10 min, 3000 g, 4 °C), and finally resuspended in 0.5 mL cold SGWB. Aliquots of 50 µL were prepared for electroporation.

For electroporation, 1 µL of the purified plasmid preparation was added to a 50 µL aliquot of electrocompetent cells, and the mixture incubated on ice for 5 min. Electroporation was performed using a 0.1 cm cuvette and a Bio-Rad Gene Pulser (Bio-Rad, USA) set to 25 µF and 400 Ω, delivering a 10 msec pulse at 1 kV. Immediately after electroporation, 1 mL BHIS, prewarmed to 37 °C, was added to the cuvette and the mixture transferred to a 1.5 mL tube and incubated at 37 °C for 1.5 h.

The suspension was spread onto two BHI plates (500 µL/plate) containing 7 µg/mL of chloramphenicol (Cm7) and incubated at 37 °C for 48 h. Colonies were picked and used to inoculate 5 mL BHI with Cm7 and incubated overnight at 37 °C with agitation at 200 rpm. Freezer stocks were prepared as described in Section 2.1.4. Fluorescence of the

overnight culture was checked by spreading 100 µL on BHI Cm7 plates, incubating overnight at 37 °C, and inspecting the plates the following day using a blue-light (400–500 nm) transilluminator (DR-46B, Clare Chemical Research, USA).

2.4.3.3 Comparative growth dynamics of NLmo8::cGFP and wild-type NLmo8 strains under inoculum preparation conditions

The growth dynamics of NLmo8::cGFP were investigated under conditions emulating those used to prepare the inoculum for the leaf adhesion assay. A single colony of NLmo8::cGFP was selected from a freshly streaked BHI plate supplemented with Cm7 and used to inoculate 5 mL BHI Cm7 broth. The culture was incubated overnight (~16 h) at 30 °C with agitation at 200 rpm. The following day, tubes containing 4.5 mL BHI Cm7 broth, pre-warmed to 30 °C, were inoculated with 0.5 mL of the overnight culture. Tubes were subsequently incubated at 30 °C with agitation at 200 rpm. Measurements were taken after 0 min, 2 h, 3 h, and 7 h of incubation, with separate tubes prepared for each time point. This procedure was conducted in duplicate. In parallel, the NLmo8 Wt strain was grown overnight in BHI broth, and 0.5 mL of this overnight culture was dispensed into tubes with 4.5 mL pre-warmed (30 °C) BHI broth. As before, each time point had its own dedicated tube to ensure identical culture conditions. All tubes were incubated at 30 °C with agitation at 200 rpm. Optical density (600 nm) was measured at 0, 2, 3, and 7 h, and viable bacteria were estimated at each time point using the drop plate method described in Section 2.1.3. For NLmo8 Wt, cells were plated on BHI, while for NLmo8::cGFP, cells were plated on BHI Cm7. The plates were incubated for 24 to 48 h at 37 °C before colonies were counted. GraphPad Prism (v10.2.3, GraphPad Software, US) was used to generate graphs and perform statistical analyses.

2.4.3.4 Microscopic investigation of leaf surfaces inoculated with *L. monocytogenes* strain NLmo8::cGFP

Rocket (cv. 'Monza') and spinach (cv. 'Nandu RZ') leaves were inoculated with *Lm* strain NLmo8::cGFP as detailed in Section 2.4.2.2. Following inoculation, the leaves were cut into 1x1 cm sections and fixed in FA-PBS. Sections were taken from the base, middle, and apex of each leaf, including features such as the central vein, lateral veins, and margins. For each region, sections were prepared to allow imaging from both the adaxial

and abaxial sides. The samples were kept in FA-PBS for 20 min at room temperature (~21 °C) before further processing.

To evaluate the effect of FA-PBS on NLmo8::cGFP fluorescence, 10 µL of an exponential-phase culture was dried onto a coverslip and fixed in FA-PBS overnight. The exponential-phase culture was prepared by adding 0.5 mL of an overnight culture to 4.5 mL pre-warmed (30 °C) BHI Cm7 broth and incubating at 30 °C with agitation until it reached the early- to mid-exponential phase (up to 2 h). The overnight culture was prepared by inoculating 5 mL BHI Cm7 broth with a single colony from a freshly streaked plate, followed by overnight incubation (~16 h) at 30 °C with agitation.

Fixed leaf sections were washed three times with sterile PBS and once with dH_2O. Coverslips with the bacterial culture were washed following the same procedure. Each leaf section was then mounted on a microscope slide in a drop of Vectashield with DAPI (Vector Laboratories, US) and covered with a square coverslip. Coverslips with bacteria were also mounted on microscope slides using Vectashield containing DAPI.

Dried bacterial cultures were examined using an Olympus BX61 fluorescent microscope (Olympus Life Science, US) equipped with an ORCA-spark camera (Hamamatsu Photonics, Japan). Images were acquired using the Olympus cellSens Dimension software (version 2.3) (Olympus Life Science, US), exported as full-resolution TIF files and processed in ImageJ (version 2.14.0/1.54i) to adjust brightness and contrast (Schindelin *et al.*, 2012). Leaf sections were examined using a confocal microscope (LSM 880 with Airyscan; Carl Zeiss, Germany) with 40x (NA = 1.3) and 63x (NA = 1.4) oil immersion objectives.

2.4.3.5 Determining *L. monocytogenes* attachment sites on leaf surfaces using semi-soft agar

To identify *Lm* strain NLmo8 attachment sites on the leaf surface without microscopy, a novel overlay assay was developed. The overlay assay combines elements of the classical overlay assay for screening antimicrobial activity (Mahenthiralingam *et al.*, 2011) and the leaf imprint assay (Mensi *et al.*, 2017). Inoculated leaves are embedded in a selective media with a low agar concentration, enabling *Lm* attached to the leaf surface to form colonies, thereby revealing putative attachment sites.

Leaves of rocket (cv. 'Monza') and spinach (cv. 'Nandu RZ') were inoculated with *Lm* strain NLmo8, as described in Section 2.4.2.2. PBS was used as a negative control. After washing, the leaves were dried at 37 °C for 20 min to eliminate any visible droplets on the surface and subsequently submerged in *Listeria* enrichment agar (LEA).

LEA was prepared by combining *Listeria* enrichment broth (VWR, UK) with 0.8% w/v bacteriological agar (Fisher Scientific, UK). On the day of use, the medium was sterilized through autoclaving at 121 °C for 15 min and cooled to 42 °C in a water bath. The cooled LEA was poured into square petri dishes, and the dried leaves were gently pressed into the agar until fully submerged. The leaves were held in place until the agar solidified sufficiently to prevent them from floating. The agar, with the leaves embedded, was allowed to set completely before being incubated at 30 °C for 48 to 72 h. Following incubation, photographic images of the plates were taken using a mobile device (Google Pixel 6, Google, US). The images were exported as .jpeg files and processed in ImageJ (version 2.14.0/1.54i) to adjust brightness and contrast (Schindelin *et al.*, 2012).

2.5 Volatile organic compound based detection of *L. monocytogenes* in artificially inoculated rocket

2.5.1 Sampling and analysis of volatile organic compounds released from store bought rocket artificially inoculated with *L. monocytogenes*.

2.5.1.1 Preparing inoculum and enumerating bacteria

Overnight cultures for *Lm* strain NLmo8 and *L. innocua* strain BUG499 were initiated by picking a single colony from a freshly streaked BHI plate and inoculating 5 mL BHI broth. Cultures were incubated overnight (~16 h) at 37 °C with agitation at 200 rpm. Overnight cultures were centrifuged at 4000 rpm for 5 min and pellets resuspended in 5 mL PBS. This centrifugation and resuspension process was repeated three times, after which bacteria in the suspension were enumerated using the drop plate method as previously described (Section 2.1.3).

2.5.1.2 Plant material and sample preparation

Pre-washed wild rocket (*Diplotaxis tenuifolia*), with at least three days remaining before its 'use by' date, was purchased from a local supermarket in Wales (Sainsbury’s,

Cardiff). Approximately 1 g of leaf material was weighed and placed in a sterile square Petri dish and inoculated by spraying with approximately 100 µL bacterial suspension (≈2 x 10^9 CFU/mL) or 100 µL PBS (control) (Figure 2.4)

After spraying, 3 g of leaf material treated with either *Lm*, *L. innocua*, or PBS was combined and washed by immersing it in 200 mL PBS in a sterile container on a rocking platform for 10 min, followed by air drying for 1 h. The dried leaf material (3 g) was placed into an oven roasting bag (Wilkinson, Cardiff) constituting one biological replicate (Figure 2.4). Bags were sealed, placed in a large container, and incubated at 37 °C for up to 6 h. The experiment was repeated four times by three different operators to assess reproducibility. For the third and fourth experiments, 200 g of activated charcoal (Merck, US) was placed at the bottom of each container to absorb VOCs from the surrounding environment in order to reduce background noise.

Each experiment was conducted in a different year or season to account for both year-to-year and seasonal variability in rocket leaf composition. The rocket leaves were purchased and sampled during the following months and years: for Experiment 1, leaves were acquired in August 2019; for Experiment 2, in August 2020; for Experiment 3, in December 2020; and for Experiment 4, in November 2022.

2.5.1.3 Headspace collection with thermal desorption tubes

VOCs were collected onto thermal desorption tubes (TD tubes, Tenax TA and SulfiCarb, Markes International Ltd, Wales) after 3 h and 6 h of incubation from 1000 mL headspace in the bags using an EasyVOC™ manual pump (Markes International Ltd, Wales) (Figure 2.4). For experiment 1, three biological replicates were performed for both the uninoculated control and *Lm*. For experiment 3, four biological replicates were prepared for the uninoculated control, *Lm*, and *L. innocua*. In experiments 2 and 4, four biological replicates were prepared for the uninoculated control and *Lm*.

2.5.1.4 Thermal desorption gas chromatography time-of-flight mass spectrometry

A TD100 (Markes International Ltd, Wales) was used to desorb the tubes in the trap with the following conditions: desorption for 5 min at 100 °C followed by 5 min at 280 °C with a nitrogen flow of 40 mL/min. Desorption of trap at a rate of 20 °C/s to 300 °C for 6 min

with a split ratio of 4.3:1 into the GC (7890A; Agilent Technologies, US). VOCs were separated over 60 m, 0.32 mm ID, 0.5 µm film thickness Rxi-5ms (Restek, US) with 1.5 mL/min helium in constant flow mode using the following temperature program: 2 min at 40 °C initially, 5 °C/min to 240 °C followed by 20 °C/min to 300 °C and a final hold of 2 min (total run time 47 min). The BenchTOF-dx mass spectrometer (Almsco International, US) was operated at ion source temperature of 250 °C, transfer line temperature of 250 °C and mass spectra recorded in EI mode (70 eV) over a mass range of 30–450 m/z (1970 scans/scanset). A retention time standard (C8–C20; Sigma Aldrich, US) was prepared by injection of 1 µL of the standard mixture directly onto a collection tube (Tenax TA; Markes International, Wales) and analysed under the same conditions as the samples.

GC–MS data were processed using MSD ChemStation software (E.02.01.1177; Agilent Technologies, US) and deconvoluted and integrated with AMDIS (NIST 2011) after first constructing a retention-indexed custom MS library. MS spectra from deconvolution were searched against the National Institute of Standards and Technology (NIST) 2011 library (Software by Stein *et al.*, version 2.0 g, 2011) and only compounds scoring > 80% in forward and backward fit were included. Putative identifications were based on match of mass spectra (>80%) and retention index (RI ± 15) (Beaulieu and Grimm, 2001).

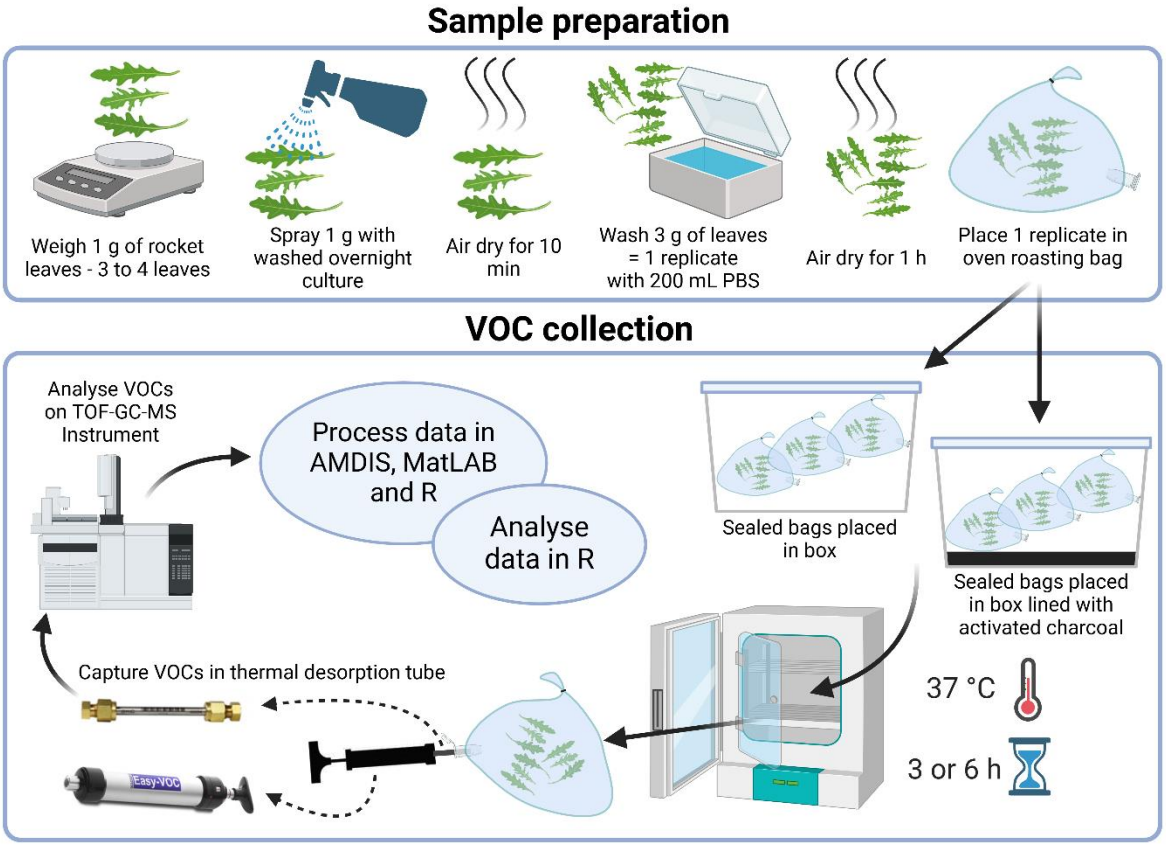

Figure 2.4 Graphic representation of the processing and preparation of rocket leaves and the volatile organic compound collection method.
Created with BioRender.com

2.5.1.5 Data processing for statistical analysis

Following compound identification, AMDIS output is further processed using the GC-MS Assignment Validator and Integrator 3 script (Gavin3) in the MATLAB software (v9.10.0)(The MathWorks Inc., 2021) (Behrends *et al.*, 2011). Gavin3 is employed to visually inspect chromatographic peaks corresponding to AMDIS-identified compounds and to manually adjust peak alignment and integration areas. Some compounds identified by AMDIS are not reliably detected in all samples. During inspection in Gavin3, compounds which were identified by AMDIS but fell below the detectable range were noted.

Following Gavin3, integrals for each compound are exported to an Excel file and further processed using the STAtistics for gC-ms Experimental analysis (Stacey) script (https://github.com/ecologysarah/lolium-rumen-voc/tree/main) in R (v3.6.3) (R Core Team, 2024). The integrals for compounds flagged as unreliable are retrieved from the Excel file and used to compute a baseline value, which is the mean of the

integrals for compounds that fell below the detectable range. This baseline serves as the inclusion threshold for further analysis. The Stacey script removes known contaminants and compounds falling below the baseline threshold. A compound is excluded from analysis if the peak integral falls below the baseline value in more than three replicates in every sample group. Sample groups include *Lm*-inoculated leaves incubated for 3 h, *Lm*-inoculated leaves incubated for 6 h, *L. innocua*-inoculated leaves incubated for 3 h, *L. innocua*-inoculated leaves incubated for 6 h, PBS-inoculated leaves incubated for 3 h, and PBS-inoculated leaves incubated for 6 h.

Following compound filtering, VOC peak integral areas were normalised using the total sum normalisation method before subsequent statistical analyses (Noonan *et al.*, 2018). VOC peak integrals for ethanol and butane were removed from the data prior to normalisation as these two compounds fell outside the linear range of detection.

2.5.1.6 Statistical analyses

Statistical analysis was carried out using R software (v3.6.3) (R Core Team, 2024). VOC profiles of rocket leaves with different inoculation status and incubation period were compared using permutational multivariate analysis of variance (PerMANOVA) (Anderson, 2001; Mcardle and Anderson, 2001) using 999 permutations. PerMANOVA assumes homogeneity of dispersion, meaning that the spread of VOC profiles within groups should be similar. To test this assumption, the Tukey's Honestly Significant Difference (HSD) test was used to evaluate whether there were significant differences in the dispersion of VOC profiles between sample groups.

Canonical Analysis of Principal coordinates (CAP) analysis (Anderson and Willis, 2003) using 99 permutations was used to further evaluate the data and determine differences in VOC profiles. Ordination plots from CAP with ellipses representing 95% confidence intervals (CI) were used to visualise differences between inoculation status and incubation period. PerMANOVA and CAP analysis were carried out using the ‘adonis2’ and ‘CAPdiscrim’ functions, respectively, in the package ‘vegan’ (Oksanen, 2011).

Chapter 3 – Examining genetic and phenotypic characteristics of *Listeria monocytogenes*

3.1 Introduction

3.1.1 Serotyping for strain differentiation

Serotyping has traditionally been used to differentiate *L. monocytogenes* (*Lm*) strains based on the unique combination of their O and H antigens. Presently, 13 serotypes for *Lm* (1/2a, 1/2b, 1/2c, 3a, 3b, 3c, 4a, 4ab, 4b, 4c, 4d, 4e and 7) have been defined (Orsi *et al.*, 2011). Despite its widespread use, the value of serotyping for epidemiological purposes is somewhat limited. This is primarily because the majority of human Listeriosis (95%) cases have been associated with only four serotypes (1/2a, 1/2b, 1/2c, and 4b) (Doumith *et al.*, 2004a; Ragon *et al.*, 2008). In fact, the majority of Listeriosis outbreaks worldwide are attributed to serotype 4b, however, some have also been caused by serotype 1/2b and serotype 1/2a isolates (Orsi *et al.*, 2011).

While serotyping provides broad differentiation, it does not offer the resolution required to identify strain-level variation and genetic relationships. To achieve more precise strain differentiation than serotyping, advanced subtyping methods such as MLST and WGS have been employed. These methods have confirmed that *Lm* can be divided into four distinct evolutionary lineages (Orsi *et al.*, 2011; Haase *et al.*, 2014; Zamudio *et al.*, 2020). Previous research has shown that serotypes can be associated with specific lineages. For example, lineage I strains encompass serotypes 1/2b, 3b, 4b, 4d, and 4e and lineage II strains includes serotypes 1/2a, 1/2c, 3a, and 3c. Interestingly, strains belonging to serotype 4b have also been grouped in lineage III and IV using molecular subtyping methods, highlighting the limited resolution provided by serotyping (Orsi *et al.*, 2011). Nevertheless, strain serotypes have historically been utilised in numerous studies to identify specific associations with phenotypic and genetic traits. As such, a strain's serotype can still provide valuable insights into its potential behaviour and risks.

3.1.2 Lineages and association with ecological and virulence traits

The classification of *Lm* into lineages has proven valuable for researchers, as each lineage has been linked to specific traits, allowing predictions of characteristics such as virulence, ecological niches, and genetic or phenotypic features based on lineage (Orsi *et al.*, 2011). For instance, lineage I strains are responsible for the majority of human Listeriosis outbreaks whereas lineage II have predominantly been isolated from cases of animal Listeriosis and sporadic human clinical cases (Nightingale *et al.*, 2005; Sauders *et al.*, 2006; Haase *et al.*, 2014). Additionally, lineage II strains are more frequently encountered in food processing environments, the natural environment and farm settings than other lineages (Orsi *et al.*, 2011). Although lineage II strains are generally considered less virulent due to the frequent detection of deleterious mutations in key virulence genes among these strains, they remain significant because of their high prevalence in food and food processing environments (Lakicevic *et al.*, 2022). In contrast, lineages III and IV have primarily been isolated from animal and environmental samples, with limited involvement in human infections (Roberts *et al.*, 2006; Tsai *et al.*, 2011).

3.1.3 Sequence typing and associating strain characteristics

While phylogenetic lineage may provide some insight into a strain's virulence potential and environmental habitat, lineage grouping alone is insufficient for reliably predicting specific characteristics. To facilitate more accurate predictions, researchers have utilised various subtyping methods, which offer greater resolution than lineage classifications, to investigate associations between specific traits and genetic subtypes. Using the MLST scheme developed by Ragon *et al.* (2008), researchers have identified associations between sequence types (STs) and epidemic outbreaks, environmental sources, geographical distribution, and genes linked to virulence and persistence. For example, specific STs have been linked to multiple Listeriosis outbreaks (ST382) (Chen *et al.*, 2017), specific isolation sources (ST121) (Orsi *et al.*, 2021) or Listeriosis cases with poor clinical outcomes (ST6) (Koopmans *et al.*, 2013).

3.1.4 Clonal grouping for examining broader genetic relationships

The MLST scheme by Ragon *et al.* (2008) assigns strains to a sequence type (ST) based on the unique allelic profiles of seven housekeeping genes. Sequence types differing by no more than one allele are assigned to the same clonal complex (CC), also referred to as clonal groups. Members of a CC display a high level of genetic similarity, enabling researchers to investigate broader genetic relationships among strains beyond the resolution of individual sequence types. For instance, some clonal complexes (CC1, CC2, CC4, and CC6) are strongly linked to human disease and are associated with specific virulence factors (Maury *et al.*, 2016). While other CCs (CC9 and CC121) are more prevalent in food production environments and have been associated with a higher prevalence of genes involved in stress resistance and tolerance to disinfectants (Maury *et al.*, 2019). Some clonal groups are associated with specific geographical regions, while others are globally distributed (Chenal-Francisque *et al.*, 2011; Chen *et al.*, 2016). Overall, specific clonal groups exhibit strong correlations with isolation sources, food types (Maury *et al.*, 2019), stress resistance genes (Lakicevic *et al.*, 2022), and virulence potential (Maury *et al.*, 2016), providing a foundation for strain characterisation through phylogenetic relationships.

3.1.5 Exploring the link between phenotype and genotype in *L. monocytogenes*

Examining the relation between genetic classifications and phenotypes can reveal why particular groupings are more commonly associated with virulence, persistence and isolation sources. For instance, Maury *et al.* (2019) found that CC121 and CC9 formed significantly stronger biofilms in the presence of sub-lethal doses of benzalkonium chloride compared to other clonal complexes. This likely explains their frequent isolation from food processing environments, as their robust biofilm production enhances their resistance to standard cleaning and disinfection measures. Bergholz *et al.* (2010) looked at how salt stress tolerance is distributed across lineages, showing lineage-specific adaptations to osmotic stress. These studies highlight that specific phenotypic characteristics can be associated with genetic classification.

3.1.6 Genetic and phenotypic factors contributing to plant contamination

Numerous genes in *Lm* related to stress tolerance, environmental persistence and virulence have been characterised, with many shown to be associated with specific genetic subtypes (Maury *et al.*, 2019; Lakicevic *et al.*, 2022). However, relatively few genes have been characterised that specifically mediate interactions with plants. Notably, prior research has implicated a putative cell surface protein, the *Listeria* cellulose-binding protein, and a Crp/Fnr family transcription factor in *Lm* attachment to fresh produce (Bae *et al.*, 2013; Salazar *et al.*, 2013). Identifying genetic determinants specifically associated with attachment to fresh produce remains a challenging endeavour. For instance, Palumbo *et al.* (2005) compared the expression profiles of *Lm* cells grown under standard laboratory conditions with those of cells attached to cabbage leaves after 16 h of inoculation. The study identified a substantial number of differentially expressed genes, including those related to cell surface characteristics. However, disruption of certain genes did not significantly affect attachment or colonisation of cabbage.

While specific genetic features have been linked to plant attachment and colonisation, inherent structural and functional traits of *Lm*, such as flagella, motility, and exopolysaccharides, have also been reported to contribute to the contamination of fresh produce (Gorski *et al.*, 2009; Fulano *et al.*, 2023). For instance, Gorski *et al.* (2009) suggested that flagella facilitate attachment to specific plant types, as the researchers showed mutants lacking flagella exhibited reduced attachment. Investigating the variation of these traits across strains will help determine whether certain phenotypic characteristics are specific to particular *Lm* subtypes. Additionally, assessing phenotypic variability under controlled conditions could provide insights into strain adaptability. Together, these findings, along with genetic traits linked to contamination, could help identify subtypes with increased contamination risk. Identifying traits associated with contamination in leafy vegetables and their correlation with specific genetic classifications can provide valuable insights into which strains pose a higher risk of contamination. This information could be used to improve sanitation practices and enhance food safety monitoring.

3.1.7 Aims and objectives

The genotypic and phenotypic traits associated with leafy vegetable contamination and whether these correlate with phylogenetic relationships of *Lm* remains underexplored. This chapter addresses this gap by investigating the genetic and phenotypic characteristics of 15 *Lm* strains isolated from the fresh produce supply chain, along with two reference strains. Whole-genome sequencing was conducted to determine genetic classifications, explore genetic diversity and identify traits associated with fruit and vegetable contamination. Additionally, the phenotypic variability of these strains was assessed under controlled conditions to evaluate their adaptability to diverse environments. The genetic and phenotypic traits examined, including those previously associated with produce contamination, were compared with the strains' genetic groupings to identify potential correlations. Strains which demonstrated a high degree of adaptability and propensity for contamination, based on phenotypic and genotypic profiles, were selected for further investigation.

This chapter investigates the phenotypic and genetic diversity of a collection of 15 *Lm* field isolates, and 2 *Lm* lab reference strains, and explores the potential relationship between genetic groupings and leafy vegetable contamination. To achieve this, the following objectives are addressed:

- Investigate the phylogenetic relationships within the *L. monocytogenes* collection and determine genetic classifications using whole-genome sequence analysis.
- Examine phenotypic and genetic traits previously associated with fruit and vegetable contamination across the *L. monocytogenes* strain collection.
- Assess whether specific phenotypic characteristics are associated with genetic subtypes or phylogenetic groupings.

3.2 Results

3.2.1 Genome statistics of the *Listeria* collection

To examine the genomic characteristics of the *Listeria* strains used for whole-genome analysis and to assess the quality of sequencing and assembly of the draft genomes, the Quast package was employed. Species identifications were confirmed by comparing the genome assemblies to the NCBI RefSeq database (https://www.ncbi.nlm.nih.gov/refseq/). A summary of genome statistics is provided in (Table 3.1).

Throughout this study, the 17 *Lm* strains are collectively referred to as the *Lm* collection. The *Lm* genome sizes ranged from 2.87 to 3.06 Mbp with a GC content spanning 37.73 to 37.94%. The number of coding sequences predicted using Prokka ranged from 2,792 to 3,071. N50 values ranged from 301034 (NLmo9) to 1495635 (NLmo13/NLmo16).

Table 3.1 *Listeria* collection genomic statistics.

Species ID	Strain	Total length (Mbp)	GC (%)	No. predicted CDS[a]	Total contigs	No. contigs >500 bp	N50 (bp)
L. monocytogenes	NLmo14	2.92	37.89	2867	23	9	595378
L. monocytogenes	NLmo7	2.92	37.89	2867	23	9	595378
L. monocytogenes	**F2365**	**2.87**	**37.92**	**2796**	**43**	**18**	**356808**
L. monocytogenes	NLmo10	2.91	37.89	2874	26	14	556900
L. monocytogenes	NLmo20	2.91	37.9	2868	38	14	555943
L. monocytogenes	NLmo9	2.91	37.92	2855	45	23	301034
L. monocytogenes	NLmo6	2.87	37.94	2792	43	22	476672
L. monocytogenes	NLmo8	2.92	37.92	2865	22	12	546873
L. monocytogenes	NLmo3	3.02	37.83	2974	38	18	553888
L. monocytogenes	NLmo2	3.02	37.83	2973	38	17	553888
L. monocytogenes	NLmo5	3.06	37.77	3065	37	17	506338
L. monocytogenes	NLmo4	3.06	37.78	3071	21	12	815154
L. monocytogenes	NLmo13	2.93	37.85	2918	24	13	1495635
L. monocytogenes	NLmo16	2.93	37.85	2919	26	14	1495635
L. monocytogenes	NLmo15	2.97	37.74	2892	31	17	463842
L. monocytogenes	**EGD-e**	**2.89**	**37.87**	**2848**	**30**	**14**	**583236**
L. monocytogenes	NLmo18	2.97	37.73	2907	30	18	540333
L. innocua	**BUG499**	**3.03**	**37.28**	**3062**	**75**	**39**	**454611**

Reference strains have been highlighted in bold.
[a] Coding sequences (CDS) predicted by Prokka

3.2.2 Pan, core and accessory genome analysis of the *L. monocytogenes* collection

To evaluate the genetic diversity of the *Lm* collection, the pan, core, and accessory genomes were predicted for the *Lm* collection using Panaroo (Figure 3.1). This analysis yielded a total of 3,938 genes, constituting the pan genome of the collection. Among these, 2,541 genes were shared by all 17 strains, forming the core genome. The accessory genome, comprising the soft-core, shell, and cloud genes, included 1,397 genes. More than half of the genes (701) in the accessory genome were strain-specific, each occurring in only one of the 17 strains. Strain NLmo4 has the largest accessory genome, comprising 520 genes, while strains NLmo6 and F2365 have the smallest accessory genomes, each with 245 genes.

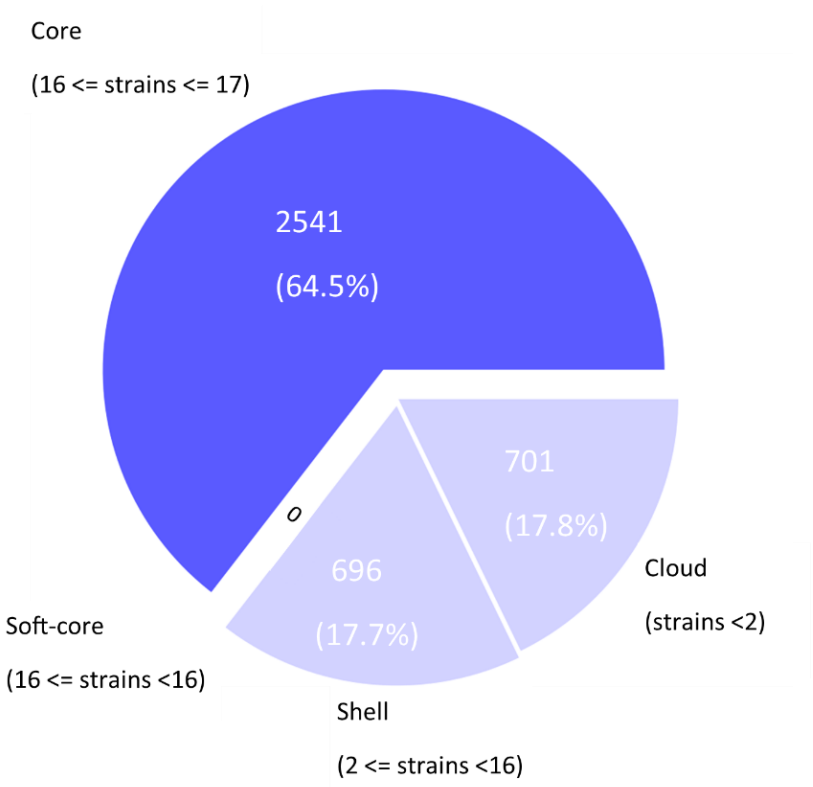

Figure 3.1 The number of pan, core and accessory genes identified for 17 *L. monocytogenes* strains.
The program Panaroo was used to predict the pan, core, soft-core, shell and cloud genomes of the *L. monocytogenes* strains collection. The total number of genes encoded by the collection constitutes the pan genome. The core genome encompasses the genes encoded by every member of the collection. All the genes not encoded by every member of the collection constitutes the accessory genome and includes the genes in the soft-core, shell and cloud genome.

3.2.3 Examining lineage grouping and strain-to-strain relatedness using core genome phylogeny

To examine the phylogenetic relationships and strain-to-strain relatedness of the *Lm* collection, a core genome phylogeny was constructed. Reference genomes for *Lm* strains from lineage III (HCC23) and lineage IV (FSL J1-208) were included to establish lineage groupings accurately. Additionally, the genome of *L. innocua* strain BUG499 was sequenced and used as an outgroup to root the phylogenetic tree (Figure 3.2). The core genome, consisting of 2,368 genes shared across the 19 *Lm* and 1 *L. innocua* strains, was predicted using Panaroo and aligned to construct a maximum likelihood phylogeny with RaxML-NG (Figure 3.2).

The *Lm* strains clustered into four distinct clades. Nine strains grouped with F2365, confirming their classification as lineage I, while six strains clustered with EGD-e, aligning with lineage II. Strains HCC23 and FSL J1-208 formed a separate clade but shared a common ancestor with both lineage I and lineage II clades. Lineage I strains exhibited shorter evolutionary branch lengths compared to lineage II, indicating closer relatedness among lineage I members. Notably, strains NLmo2 and NLmo3 were identical in their core genes, as determined by RaxML-NG. All nodes had bootstrap values of 100%, indicating strong support for each division.

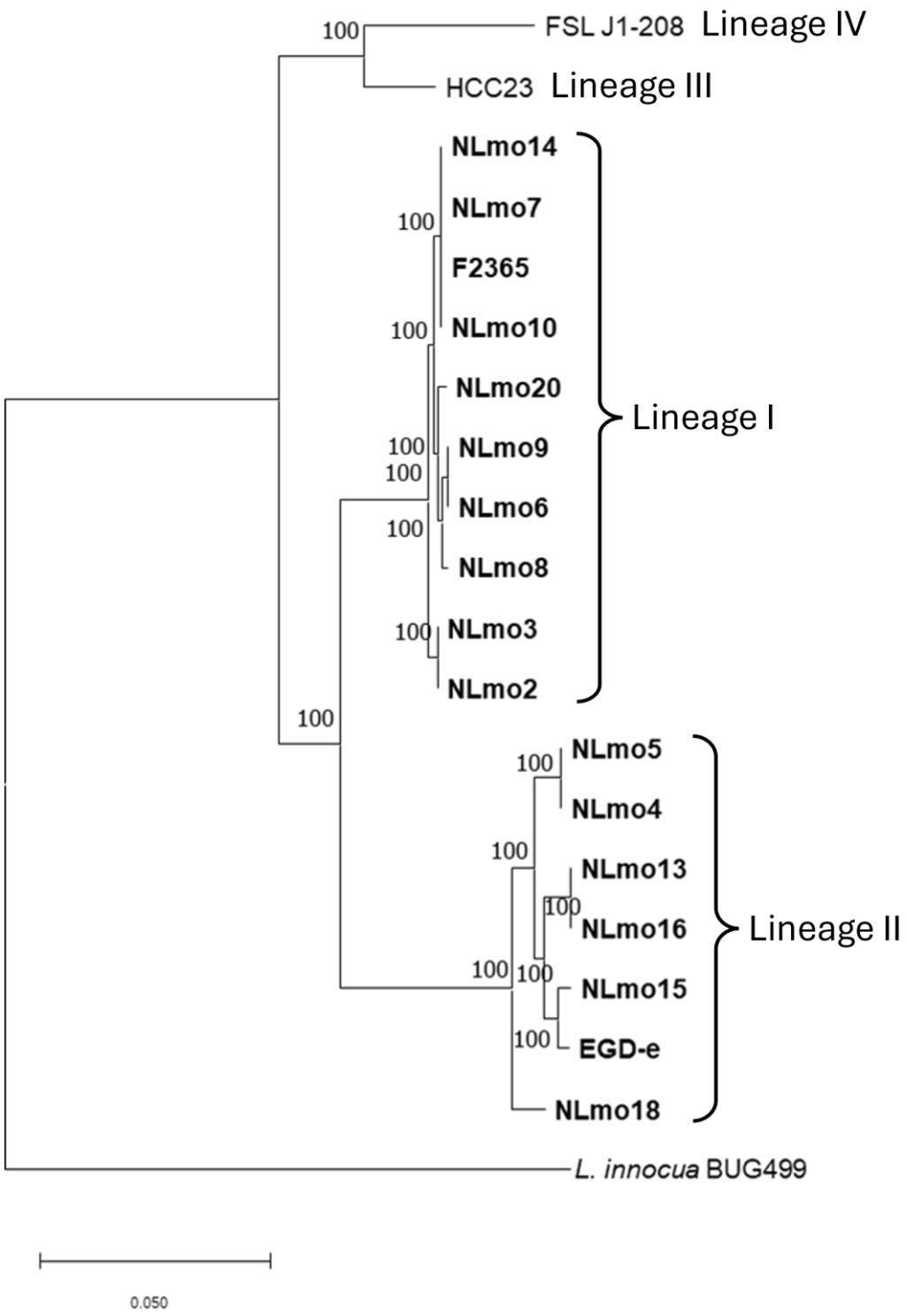

Figure 3.2 Core-gene phylogeny of 19 *L. monocytogenes* strains and 1 *L. innocua* strain.

A core-gene alignment of 2,368 genes was generated using Panaroo and utilized to construct a maximum likelihood phylogeny with RaxML-NG (200 bootstraps). *L. monocytogenes* strains whose draft genomes were assembled in this study are indicated in bold. The draft genome of *L. innocua* strain BUG499, also assembled in this study, was included as an outgroup to root the tree. All nodes had bootstrap values of 100%, including those not annotated on the figure. The scale bar represents the number of substitutions per base position.

3.2.4 Average nucleotide identity analysis to examine genetic relatedness

To confirm lineage groupings and examine the genetic relatedness of the *Lm* strains ANI analysis was conducted. The 17 *Lm* strains exhibited ANI values ranging from 98.4% to 100%. Strains from lineage I (Figure 3.3; green rectangle) and lineage II (Figure 3.3; blue rectangle) clustered into two distinct groups, confirming their respective lineage classifications. Within lineage II, ANI values ranged from 98.4% to 100%, while lineage I strains showed higher relatedness, with ANI values ranging from 99.4% to 100%, indicating that lineage I strains were more closely related to each other than those in lineage II.

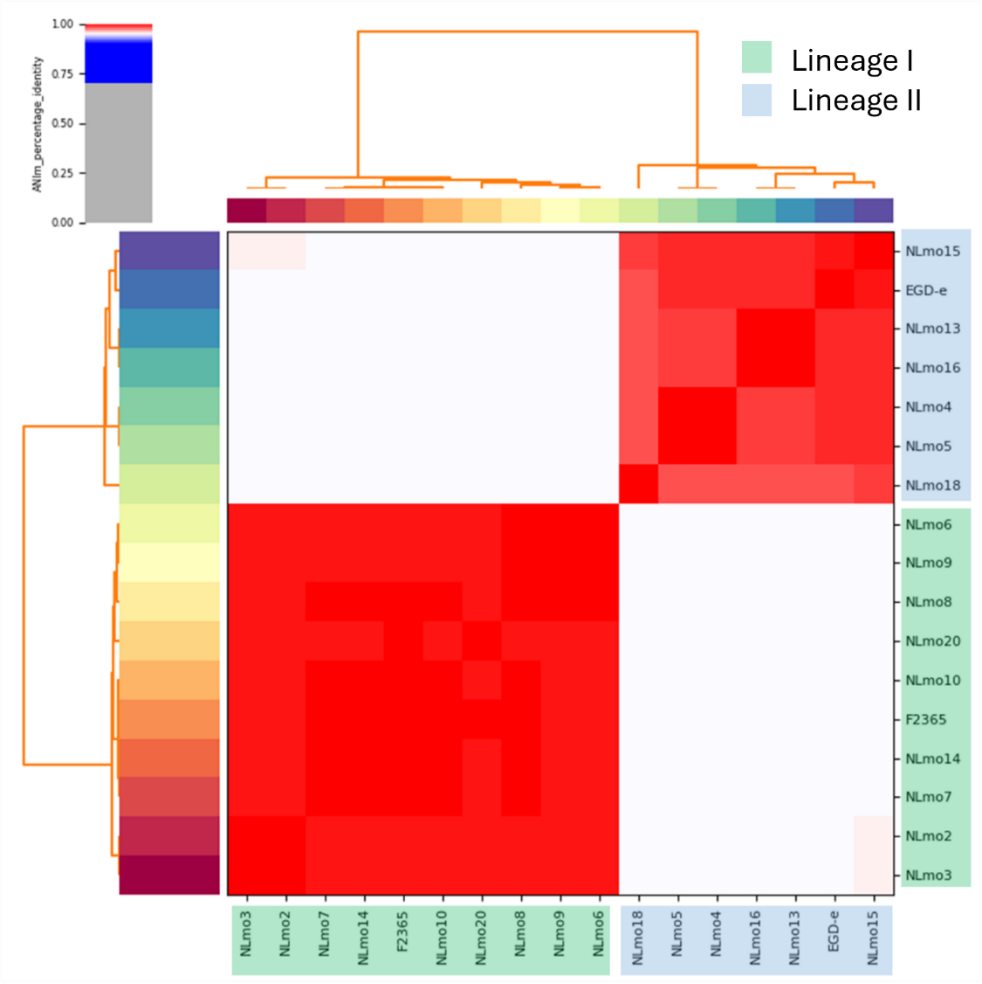

Figure 3.3 Heatmap of ANI values illustrating genetic relatedness among 17 *L. monocytogenes* strains.
Graphical representation of ANI analysis generated using the PYANI script. Red shading denotes >95% nucleotide similarity, with darker red indicating higher similarity. Rows and columns are ordered by dendrograms based on nucleotide similarity values. Strains from lineage I are highlighted in green, and strains from lineage II in blue.

3.2.5 Comparison of accessory genes, multi-locus sequence typing, clonal groups and serogroups using whole genome sequencing

The MLST profiles of the *Lm* strains were determined by querying PCR amplicons of MLST genes against the Institut Pasteur database (https://bigsdb.pasteur.fr/listeria/). These profiles were cross-referenced with MLST profiles derived from genome sequence data to verify strain identities and establish accurate associations between each strain and its genome data. All isolates belonged to either phylogenetic lineage I or II, encompassing 10 distinct sequence types organised into 9 clonal groups (Figure 3.4). Lineage II strains were predominantly associated with a higher number of accessory genes. Among these, EGD-e had the fewest accessory genes within lineage II. In fact, only two other strains (F2365 and NLmo6) in the entire collection possessed fewer accessory genes than EGD-e (Figure 3.4).

Due to the limited research on *Lm* interaction with leafy vegetables, historical reliance on serotyping for strain differentiation, and unavailability of commercial agglutination assays, *in silico* serogrouping was used to compare the strains in this study with previous *Lm* research. The collection consisted of four serogroups, with each lineage represented by two distinct serogroups (Figure 3.4).

Several strain pairs could not be differentiated using MLST analysis, serogrouping or accessory gene counts. These include NLmo2 and NLmo3, NLmo7 and NLmo14, and NLmo13 and NLmo16. The genomes of each strain pair were compared using Panaroo to assess the presence or absence of homologous genes and to identify any variations in gene content. Strains NLmo2 and NLmo3 were found to encode homologues for every gene annotated using Prokka. Similarly, NLmo7 and NLmo14 encoded homologues for all annotated genes. For NLmo13 and NLmo16, Panaroo identified a single gene in NLmo13 that was absent in NLmo16; however, this discrepancy may be due to differences in assembly quality or annotation accuracy, as the gene identified in NLmo13 was only a partial sequence.

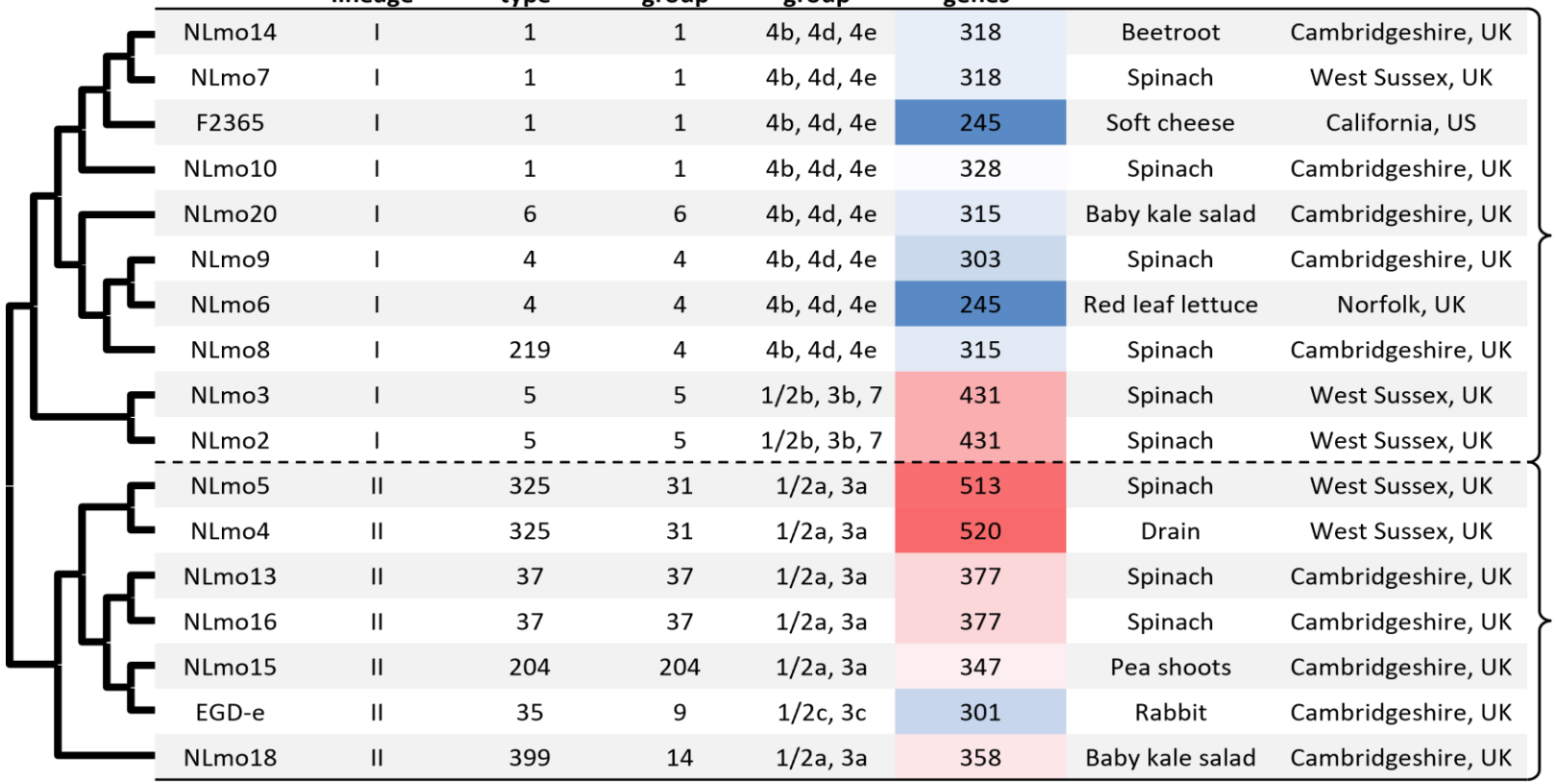

Strain ID	Genomic lineage[a]	Sequence type[a]	Clonal group[a]	Serotype group[b]	Accessory genes[c]	Isolation source	Sample location
NLmo14	I	1	1	4b, 4d, 4e	318	Beetroot	Cambridgeshire, UK
NLmo7	I	1	1	4b, 4d, 4e	318	Spinach	West Sussex, UK
F2365	I	1	1	4b, 4d, 4e	245	Soft cheese	California, US
NLmo10	I	1	1	4b, 4d, 4e	328	Spinach	Cambridgeshire, UK
NLmo20	I	6	6	4b, 4d, 4e	315	Baby kale salad	Cambridgeshire, UK
NLmo9	I	4	4	4b, 4d, 4e	303	Spinach	Cambridgeshire, UK
NLmo6	I	4	4	4b, 4d, 4e	245	Red leaf lettuce	Norfolk, UK
NLmo8	I	219	4	4b, 4d, 4e	315	Spinach	Cambridgeshire, UK
NLmo3	I	5	5	1/2b, 3b, 7	431	Spinach	West Sussex, UK
NLmo2	I	5	5	1/2b, 3b, 7	431	Spinach	West Sussex, UK
NLmo5	II	325	31	1/2a, 3a	513	Spinach	West Sussex, UK
NLmo4	II	325	31	1/2a, 3a	520	Drain	West Sussex, UK
NLmo13	II	37	37	1/2a, 3a	377	Spinach	Cambridgeshire, UK
NLmo16	II	37	37	1/2a, 3a	377	Spinach	Cambridgeshire, UK
NLmo15	II	204	204	1/2a, 3a	347	Pea shoots	Cambridgeshire, UK
EGD-e	II	35	9	1/2c, 3c	301	Rabbit	Cambridgeshire, UK
NLmo18	II	399	14	1/2a, 3a	358	Baby kale salad	Cambridgeshire, UK

[a] Determined using MLST database hosted at: https://bigsdb.pasteur.fr/listeria/ with genomic lineages written in roman numerals according to convention.

[b] *In silico* prediction using LisSero

[c] Predicted with Panaroo (v.1.3.2)

Figure 3.4 Tabular summary of serogroups, MLST profiles, clonal groups and number of accessory genes for 17 *L. monocytogenes* strains, ordered by core-genome phylogeny.
A phylogenetic tree was constructed using RAxML-NG based on a core-gene alignment of 2,541 genes generated with Panaroo. Average nucleotide identity (ANI) values were calculated with PYANI, with the ANI range for each lineage reported.

3.2.6 Screening *L. monocytogenes* for cellulose binding protein and *in vitro* cellulose attachment

The *Lm* collection was screened for genes encoding protein homologous to the *Listeria* cellulose-binding protein (LCP) described by Bae *et al.* (2013). Additionally, the strains were tested for their ability to adhere to cellulose-coated wells, as cellulose is a key component of plant cell walls. This was done to assess their potential for attachment to leaf surfaces. Attempts to replicate the cellulose-adhesion assay described by Bae *et al.* (2013) were unsuccessful, with OD readings from the de-stained solution measuring 100-fold lower than those reported by Bae *et al.* (2013), even for the same strain used in their study, rendering these values effectively negligible.

A TBLASTN search using the LCP amino acid sequence reported by Bae *et al.* (2013) revealed that all strains encoded homologous proteins, with amino acid sequence identities ranging from 84.5% to 100% (Table 3.2). For each strain, the gene with the highest sequence homology encoded a LPXTG cell-wall sorting signal near the C-terminus. Three strains (NLmo7, NLmo10 and NLmo14) encoded proteins identical to LCP and clustered with strain F2365, where the LCP gene was initially identified (Bae *et al.*, 2013), in the core-genome phylogeny (Figure 3.2).

The genes encoding proteins homologous to LCP were highly conserved among strains within the same lineage (lineage I) as F2365, with all strains displaying 100% amino acid sequence identity in the cellulose-binding domain (CBD). In these homologous genes, the CBD was located at the same amino acid positions (20 to 144) as in the LCP characterised by Bae *et al.* (2013). Although the gene was less conserved among lineage II strains, with some variability observed in the CBD region, it remained well-conserved across all strains, with the CBD retained in the same position as in the original LCP.

To assess the conservation of the LCP gene and identify patterns of sequence variability across the *Lm* collection, pairwise sequence identities were calculated from a multiple sequence alignment of homologous sequences (Figure 3.5). These values were visualised as a heatmap to highlight sequence similarity among strains. The analysis revealed that the LCP gene is highly conserved among lineage I strains, with sequence

identities ranging from 99.7% to 100%, while lineage II strains showed greater variability, with sequence identities ranging from 91.2% to 100%.

Table 3.2 TBLASTN results for *Listeria* cellulose-binding protein and cellulose-binding domain across 17 *L. monocytogenes* genomes.

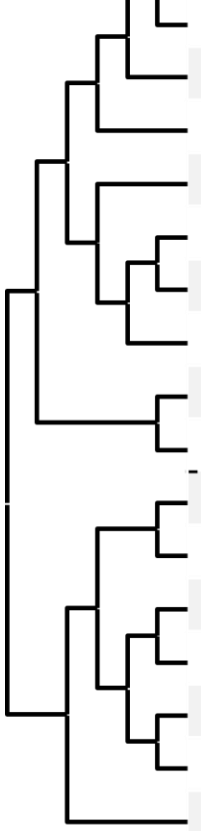

	Listeria cellulose binding protein[a]			Cellulose binding domain[b]		
	Strain ID[c]	Identity (%)	LPXTG motif aa position[d]	Identity (%)	Query cover (%)	Aa position[d]
	NLmo14	100	1990 to 1994	100	100	20 to 144
	NLmo7	100	1990 to 1994	100	100	20 to 144
	F2365	100	1990 to 1994	100	100	20 to 144
	NLmo10	100	1990 to 1994	100	100	20 to 144
	NLmo20	99.951	1990 to 1994	100	100	20 to 144
	NLmo9	99.557	1993 to 1997	100	100	20 to 144
	NLmo6	99.557	1993 to 1997	100	100	20 to 144
	NLmo8	99.41	1996 to 2000	100	100	20 to 144
	NLmo3	99.165	1999 to 2003	100	100	20 to 144
	NLmo2	99.165	1999 to 2003	100	100	20 to 144
	NLmo5	85.042	2001 to 2005	88.8	100	20 to 144
	NLmo4	85.042	2001 to 2005	88.8	100	20 to 144
	NLmo13	85.281	2007 to 2011	88.8	100	20 to 144
	NLmo16	85.281	2007 to 2011	88.8	100	20 to 144
	NLmo15	85.118	1998 to 2002	90.4	100	20 to 144
	EGD-e	85.281	2007 to 2011	88.8	100	20 to 144
	NLmo18	84.521	1994 to 1998	92.8	100	20 to 144

[a] LCP amino acid sequence searched against genome data using *tblastn*.
[b] Nucleotide sequences of homologous genes were queried with the CBD amino acid sequence using *tblastn*.
[c] Ordered according to core-genome phylogeny
[d] Aa = amino acids

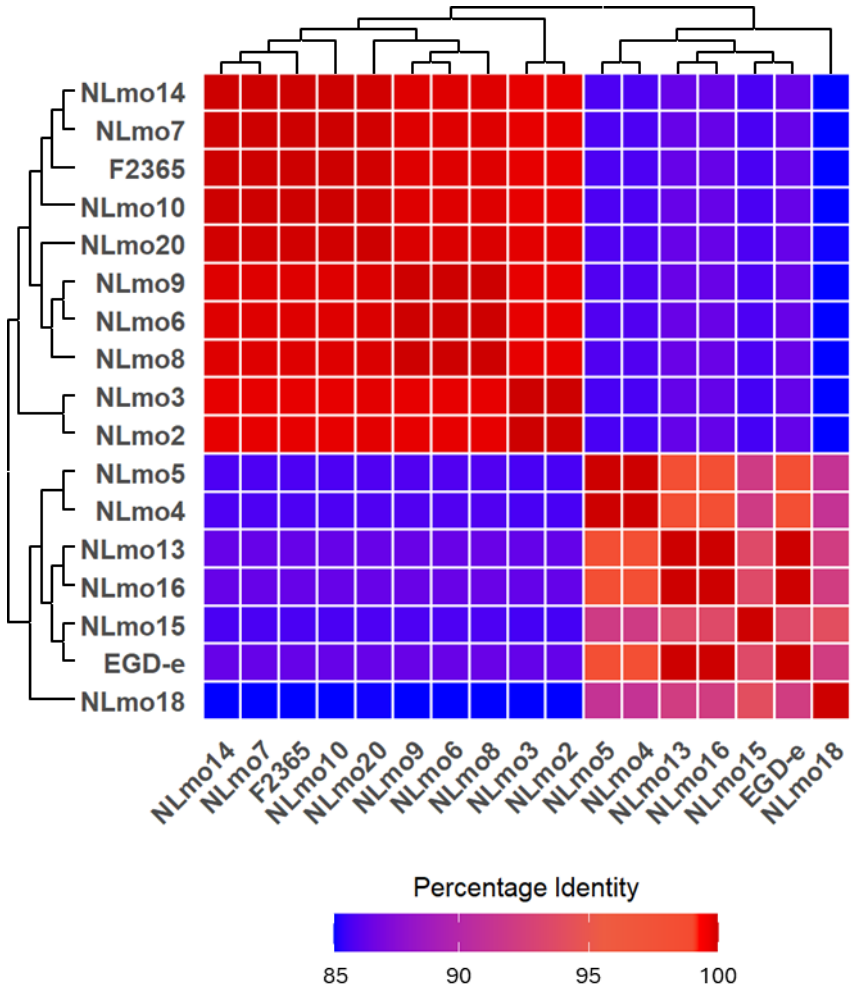

Figure 3.5 Heatmap illustrating the conservation of the amino acid sequence of the *Listeria* cellulose-binding protein (LCP) across the *L. monocytogenes* collection. Homologous sequences of the LCP protein were aligned using the ClustalW algorithm to generate a multiple sequence alignment. A pairwise sequence identity matrix was calculated from this alignment and visualised as a heatmap in R. To contextualise conservation patterns, a topology-only phylogenetic tree was constructed using RAxML-NG, based on a core-gene alignment of 2,541 genes generated with Panaroo, and aligned alongside the heatmap.

3.2.7 Modified swimming motility assay

Swimming motility was assessed for four strains to determine whether motility varied between closely related strains and across different phylogenetic lineages (Figure 3.6). Two strains from each phylogenetic lineage were selected: NLmo8 and NLmo9, which belong to the same clonal group, and EGD-e and NLmo15, which cluster together in the core-genome phylogeny but belong to different clonal groups (Figure 3.4). This selection allowed for a comparison of motility within a clonal group, between closely related strains that are not in the same clonal group, and across distinct phylogenetic lineages. Additionally, the effect of different incubation temperatures on motility was investigated to examine how temperature influences motility in *Lm (*Figure 3.6*)*.

At 22 °C, the surface area of the corona for each strain was the smallest compared to all other temperatures, a pattern that persisted after both 44 and 65 h of incubation. The largest coronas were observed at 30 °C after 65 h, although no significant differences between strains were detected. At 37 °C, after 44 h of incubation, the surface area of the corona for NLmo8 was significantly larger than that of NLmo9 and NLmo15. After 65 h of incubation, NLmo8's corona was significantly larger than those of all other strains examined. Interestingly, the average surface area of the corona for NLmo8 at 37 °C after 65 h was 23 cm^2, while at 30 °C it was only slightly larger at 23.8 cm^2.

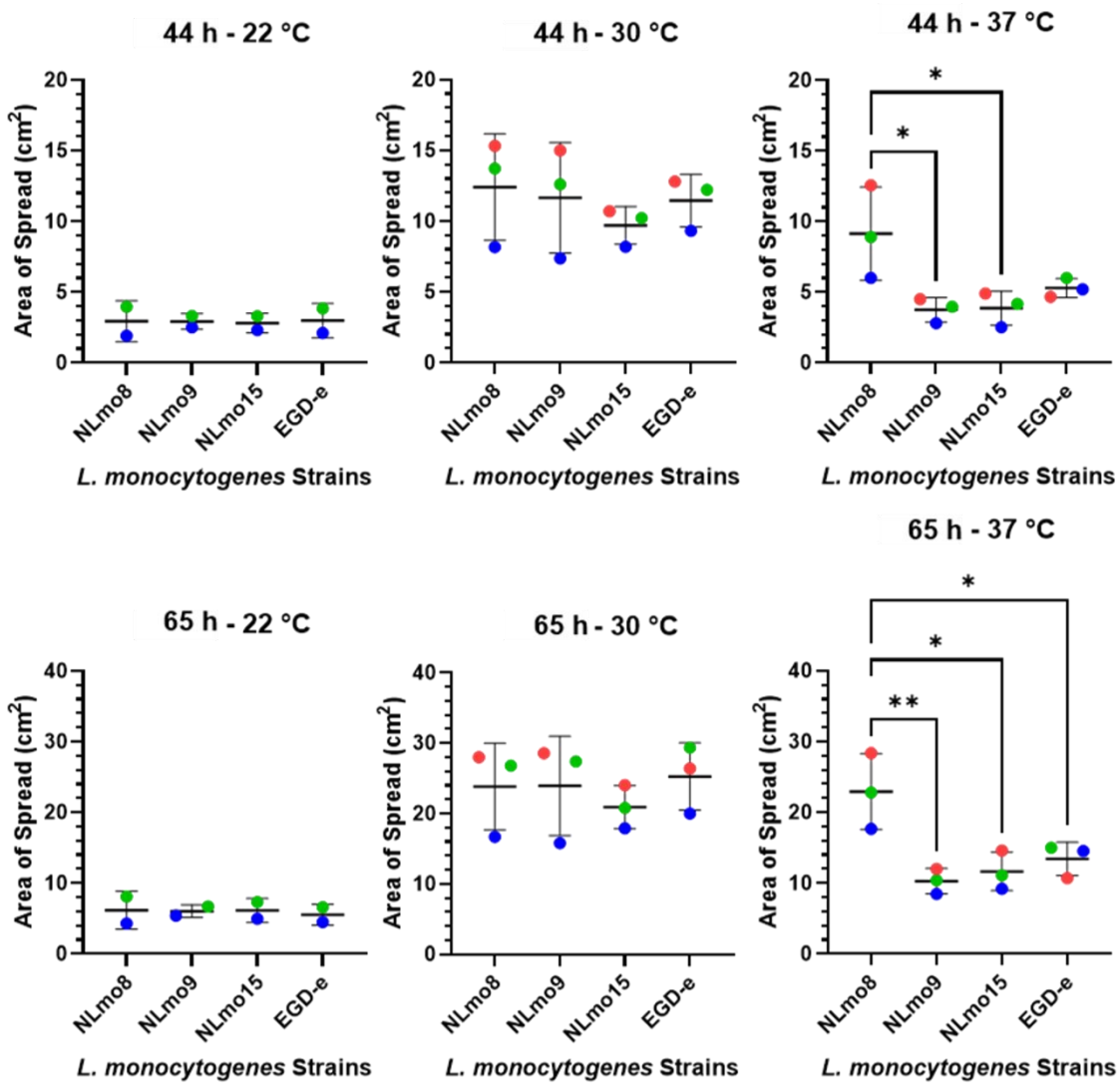

Figure 3.6 Motility assay results for four *L. monocytogenes* strains.
Exponential phase cultures were spot inoculated onto *Listeria* motility media agar plates, which were incubated at three different temperatures. The surface area of the corona around the inoculation spot was measured after 44 and 65 h (mean ± SD). Each experiment was performed in triplicate, with three technical replicates, except at 22 °C, where experiments were conducted twice. Significant differences ($P < 0.05$) between strains at each temperature were determined using one-way ANOVA followed by Tukey's post-hoc test, with significant differences indicated by asterisks (*).

3.2.8 Examining growth dynamics of *L. monocytogenes* strains at 37 °C

Intrinsic growth rates, representing the maximum rate of population increase under optimal conditions, were compared across media types. These rates reflect each strain's natural reproductive potential, determined by the efficiency of its cellular machinery and metabolic capacity.

In BHI, lineage II strains exhibited relatively uniform growth rates, with no significant variability observed (Figure 3.7). In contrast, lineage I strains showed greater variability in growth rates. Notably, strain NLmo20 displayed a significantly lower growth rate compared to all other strains in the collection. Similarly, strain NLmo8 exhibited significantly lower growth rate compared to most strains, differing significantly from all but three strains (NLmo2, NLmo6, and NLmo10). Although these three strains belonged to the same lineage, they varied in sequence type, clonal grouping and isolation source (Table 3.1).

In TSB, growth rates across the collection did not differ significantly, except for strains NLmo20 and EGD-e (Figure 3.7). EGD-e exhibited a significantly lower growth rate compared to all other strains except NLmo20. While NLmo20 had a lower average growth rate than all strains except EGD-e, this difference was only statistically significant when compared to four strains (NLmo5, NLmo7, NLmo9, and NLmo13). However, NLmo20's growth rate did not differ significantly from strains with the same sequence type or clonal grouping as these four strains. Overall, in TSB, NLmo20 remained among the slowest-growing strains, second only to EGD-e.

No significant differences in growth rates were observed between strains within the same clonal group in either BHI or TSB. Most strains exhibited higher average growth rates in TSB than in BHI, with the exception of EGD-e. In BHI, lineage II strains appeared to exhibit more consistent growth rates. NLmo20, the only strain in the collection representative of sequence type 6 (ST6) and clonal group 6, consistently demonstrated poor growth relative to other strains in both media types.

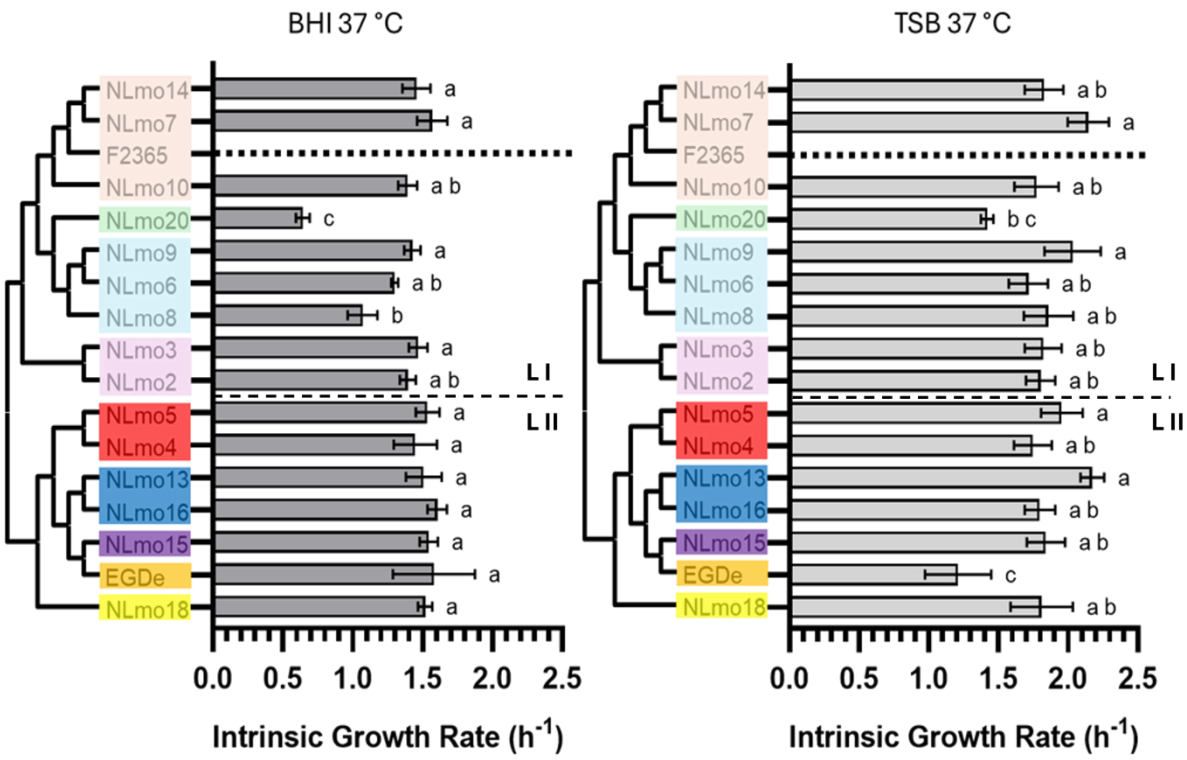

Figure 3.7 Comparative growth rates of *L. monocytogenes* strains in TSB and BHI at 37 °C.

Growth dynamics were monitored for 24 h using a Bioscreen C instrument, and intrinsic growth rates (mean ± SD) were calculated using the R package *Growthcurver*. Experiments were performed in triplicate, with three technical replicates per strain. Bar charts were generated using Prism, with strains ordered according to their phylogenetic relationships, illustrated by a phylogenetic tree constructed in RAxML-NG from a core gene alignment of 2,541 genes generated with Panaroo. Clonal groupings are indicated by distinct colours. Statistical analysis using a one-way ANOVA revealed significant differences in growth rates between strains ($P < 0.05$), with pairwise comparisons performed using Tukey's post-hoc test. In the compact letter display, strains sharing a letter are not statistically significantly different.

3.2.9 Optical density and viable cell counts of EGD-e and NLmo8 during growth in BHI under continuous agitation at 37 °C.

Growth of NLmo8 and EGD-e was investigated under conditions used to prepare the inoculum for the leaf adhesion assay in Chapter 4. This was done to determine when strains reached the exponential phase and whether the relationship between optical density and viable cell counts is consistent across *Lm* strains. Following 1:10 dilution of the overnight culture the optical density at 600 nm and bacterial concentrations (mean ± SD) for NLmo8 were 0.15 ± 0.02 and (2.3 ± 0.5) × 10^8 CFU/mL CFU/mL, respectively. The optical density at 600 nm of the diluted overnight culture for EGD-e was 0.16 ± 0.2 and the viable cell count (1.9 ± 0.6) × 10^8 CFU/mL. Optical density of the cultures suggested exponential growth occurred between 1 and 6 h (Figure 3.8; panel A) whereas the viable cell count indicated exponential growth occurred between 1 and 4 h (Figure 3.8; Panel B). A multiple comparison t-test with Welch correction was conducted to determine at which time point there were significant differences ($P < 0.05$) in viable cell counts between NLmo8 and EGD-e. Significant differences in viable cell count between NLmo8 and EGD-e were observed at 3 h and after 5 h (Figure 3.8; Panel B). After 1 h the total viable cells averaged 2.7 x 10^8 (SD = 7.2 x 10^7) for NLmo8 and 2.3 x 10^8 (SD = 7.2 x 10^7) for EGD-e. At 4 h the total viable cells for NLmo8 averaged 1.9 x 10^9 (SD = 2.1 x 10^8) and 1.5 x 10^9 (SD = 1.5 x 10^8) for EGD-e. Generation doubling time for NLmo8 was roughly 86 min and 89 min for EGD-e.

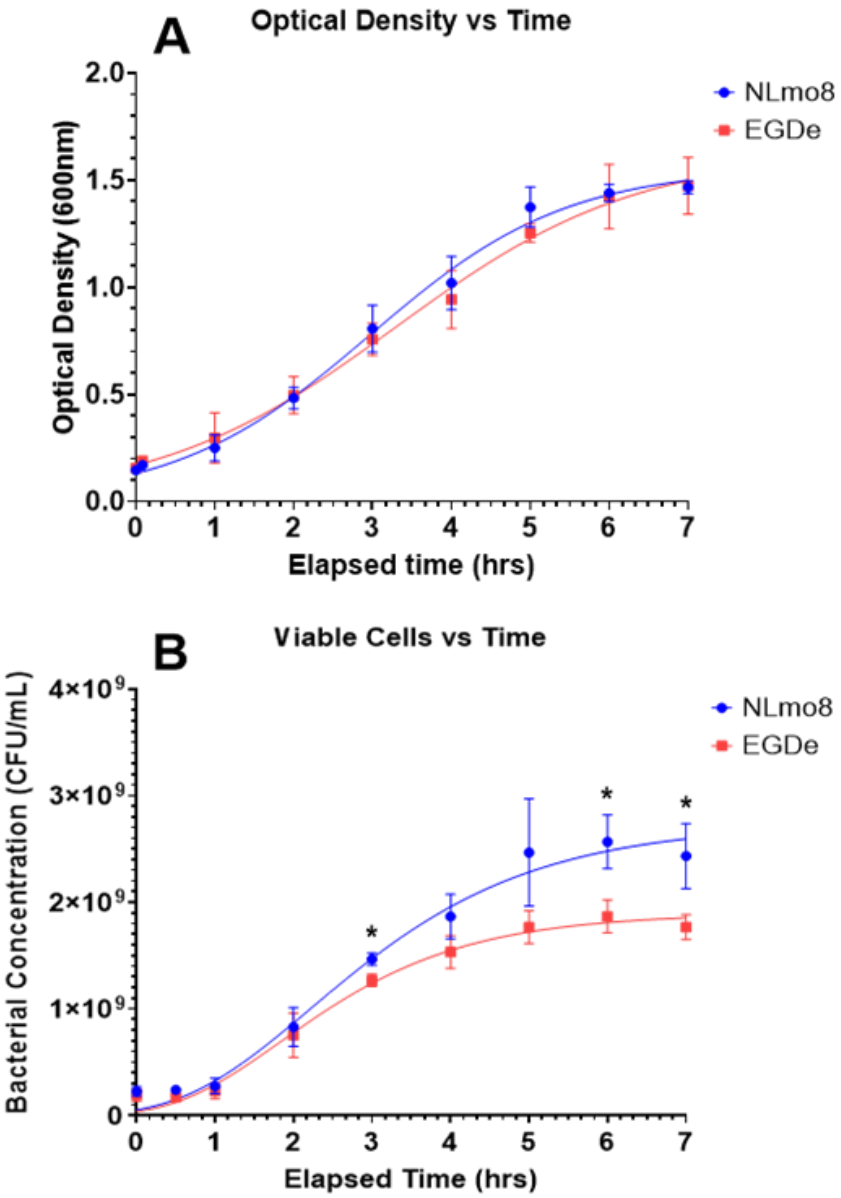

Figure 3.8 Growth curves for *L. monocytogenes* strains NLmo8 and EGD-e.
Overnight cultures grown in BHI were diluted 1:10 in fresh BHI and subsequently incubated at 37°C under agitation. Optical density (A) at 600nm (mean, ± 1 SD) and bacterial concentrations (B) (mean, ± 1 SD) were measured at hourly intervals. Whereas no difference in optical density was observed overtime between the two strains, a reduction in viable cells for EGD-e (CFU/mL) was observed during the late phase (>5h) compared to NLmo8. N=3 with 3 technical replicates. The astrisks (*) represent significant differences (Unpaired t-test with Welch correction, $P<0.05$) in colony-forming units at specific time points.

3.2.10 Examining growth dynamics of *L. monocytogenes* strains at 25 °C

The intrinsic growth rates of nine strains from the *Lm* collection were assessed at 25 °C in VPB, BHI, and TSB (Figure 3.9). A single representative strain was selected for each sequence type, with the exception of NLmo20 (ST6), which was excluded from the analysis. This approach aimed to establish potential associations with phylogenetic lineages and growth dynamics and identify strains that consistently exhibited high growth rates across different media types.

Average growth rates in BHI were nearly half of those observed in TSB and VPB for the same strains. Significant differences in growth rates were observed among strains belonging to the same phylogenetic lineage in both BHI and TSB. In contrast, no significant differences were detected between strains from the same lineage in VPB. Notably, only NLmo10 (lineage I) and NLmo18 (lineage II) exhibited significant differences in growth rates in VPB, with NLmo18 (ST399) achieving a significantly higher growth rate. Interestingly, NLmo18 displayed the highest average growth rate in VPB but ranked third lowest in TSB and second lowest in BHI.

In TSB and BHI, strain NLmo4 (ST325) consistently exhibited the lowest average growth rate. In BHI, its growth rate was significantly lower than all other strains, whereas in TSB, only NLmo9 did not differ significantly from NLmo4. Conversely, strains NLmo13 (ST37) and NLmo15 (ST204) consistently showed high average growth rates across all media types. NLmo13 ranked third in BHI, first in TSB, and second in VPB, while NLmo15 ranked second in both BHI and TSB and fifth in VPB. Notably, all three strains belonged to lineage II, indicating that growth rate at 25 °C in the media investigated does not correlate with phylogenetic lineage.

Overall, growth rates varied significantly among strains in BHI and TSB, while less variability was observed in VPB. Statistical analysis revealed that the relationships among strains in one medium were not consistently maintained in another.

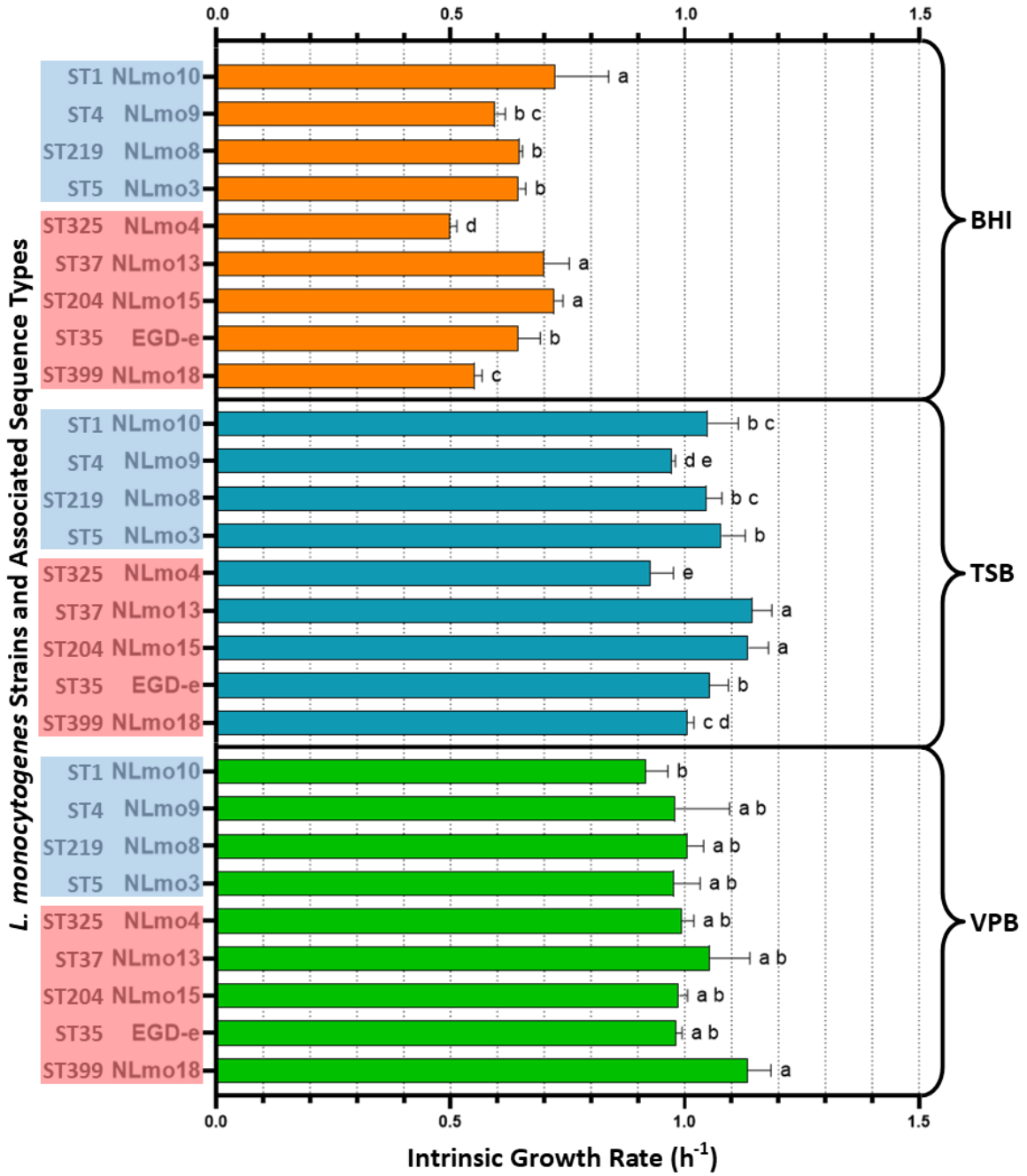

Figure 3.9 Growth rate comparison between *L. monocytogenes* strains representing nine distinct sequence types in BHI, TSB and VPB at 25 °C.
Growth dynamics were monitored for 48 h and 15 min using a Bioscreen C instrument, with intrinsic growth rates (mean ± SD) calculated using the R package *Growthcurver*. Experiments were conducted in triplicate, with three technical replicates per strain. Bar charts were generated using Prism, with lineage groupings distinguished by colour: red for lineage II and blue for lineage I. Statistical analysis via one-way ANOVA revealed significant differences in growth rates between strains ($P < 0.05$), with pairwise comparisons performed using Tukey's post-hoc test. In the compact letter display, strains sharing a letter are not statistically significantly different.

3.3 Discussion

3.3.1 Genomic characteristics and subtypes of the *L. monocytogenes* collection

The core-genome phylogeny revealed greater genetic variability among lineage II strains compared to lineage I strains, as evidenced by longer branch lengths (Figure 3.2). This was further supported by average nucleotide identity (ANI) analysis, which showed considerably more variability in ANI values among lineage II strains than lineage I strains (Figure 3.3). These findings align with previous reports suggesting that lineage I strains generally exhibit a more clonal structure (Orsi *et al.*, 2011). This has been attributed to higher recombination rates in lineage II, which drive greater genetic diversity, whereas the lower rates in lineage I result in its more clonal structure (den Bakker *et al.*, 2008; Ragon *et al.*, 2008).

Besides exhibiting greater variability in core genes, lineage II strains in the collection harboured significantly more accessory genes than lineage I strains (Figure 3.4). This may be due to the greater abundance of mobile genetic elements observed in lineage II strains. In fact, a whole-genome study by Chen *et al.* (2020) of 49 lineage I and 51 lineage II food isolates found plasmids to be more common in lineage II strains (72.5%) than in lineage I strains (24.5%). Furthermore, a microarray study by Doumith *et al.* (2004b) analysing 39 lineage II and 49 lineage I strains identified a transposase-encoding gene (*lmo0172*) in all lineage II strains exclusively. These findings suggest that mobile genetic elements are more prevalent in lineage II strains, potentially explaining their higher number of accessory genes. However, whether the accessory genes in the lineage II strains from the collection possess features of mobile genetic elements remains to be determined.

Interestingly, EGD-e contained significantly fewer accessory genes relative to other lineage II strains (Figure 3.4). Reports indicate that this strain has been frequently passaged through mice to maintain virulence (Bécavin *et al.*, 2014). This process likely drove positive selection for virulence-associated genes while reducing selective pressure on genes with redundant functions. Consequently, this may have led to gene loss through host adaptation, potentially explaining the reduced number of accessory genes.

In silico serogrouping was performed to assess whether any of the strains belonged to serogroups encompassing serotypes commonly associated with fruit and vegetable contamination (Figure 3.4). To our knowledge, no consistent trend has been reported between specific serotypes and fruit and vegetables, and no such association could be established in the literature. Furthermore, the presence of multiple serotypes in certain fresh produce outbreaks, coupled with the genetic diversity observed within serotypes, suggests that serotyping is not a reliable method for establishing such associations (Martinez *et al.*, 2016).

Although certain STs are common among food isolates, there is limited evidence linking specific STs predominantly to fruit and vegetables (Chen *et al.*, 2017; Wang *et al.*, 2019). A search of the BIGSdb database using 'fruit', 'vegetable', 'lettuce', 'salad', or 'leaf' as source descriptor, food type, sample type, or other source information revealed that only 2 STs (ST1 with 5 submissions and ST6 with 1 submission) from the collection had been deposited in the database under these identifiers (https://bigsdb.pasteur.fr/listeria/). One strain, NLmo20, was identified as belonging to ST6 (Figure 3.4), which has been frequently associated with Listeriosis outbreaks, including a multi-country outbreak in Europe linked to frozen vegetables (Nüesch-Inderbinen *et al.*, 2021). However, outbreaks involving ST6 have been associated with various food sources and not just fruit or vegetables (Smith *et al.*, 2019b).

In contrast, a link between clonal groups and certain food groups has been previously reported. For instance, Maury *et al.* (2019) showed that CC1 was commonly associated with dairy products, whereas CC9 and CC121 were commonly associated with meat and fish products. However, no specific association between clonal groups and fruit and vegetables has been reported.

In addition, Sévellec *et al.* (2022) reports that soil survival, an attribute potentially contributing to the association of *L. monocytogenes* (*Lm*) with plants, amongst a collection of 216 *Lm* strains did not correlate with phylogenetic position. Overall, these findings indicate that subtype or phylogenetic relationships are not reliable indicators of a strain's ability to contaminate fruits and vegetables.

The isolation sources of the *Lm* strains examined in this study, excluding EGD-e and F2356, suggest a prior relationship with plants. However, due to the lack of prior evidence linking fruit and vegetables to specific subtypes, there is insufficient evidence to support this food group as a preferential niche for any of the strains in the *Lm* collection. Ultimately, no specific association between genomic subtypes and fruit and vegetables may exist and *Lm* may instead possess an innate ability to contaminate these food types. To investigate this further, the prevalence of features previously linked to fruit and vegetable contamination was examined across the collection.

3.3.2 Genetic factors associated with fruit and vegetable contamination

Bae *et al.* (2013) characterised a cell surface protein with a putative cellulose-binding domain (CBD) in *Lm* strain F2365, showing its involvement in attachment to fresh produce. The deletion mutant of the gene encoding this protein, designated *Listeria* cellulose-binding protein (LCP), showed reduced attachment to iceberg lettuce, spinach, and cantaloupe compared to the wild type.

The original LCP sequence was highly conserved among lineage I strains in the collection, with all strains encoding an identical CBD sequence (Table 3.2)**.** In contrast, both the LCP and CBD were less conserved among lineage II strains, with considerable sequence variability observed across strains within this lineage (Figure 3.5). This variability may lead to structural variants that either enhance or reduce attachment capacity.

Bae *et al.* (2013) suggested that the CBD contributes to LCP's role in attachment to plant surfaces, as cellulose is a major plant cell wall component, and the LCP deletion mutant exhibited reduced attachment capacity to cellulose-coated plates. The *Lm* collection was examined using the cellulose adhesion assay described by Bae *et al.* (2013) to assess whether sequence variations in the LCP influenced attachment. However, the results reported for strain F2365 could not be replicated. This may be due to unaccounted variations in the methodology. For instance, different 96-well plates were used in this study, which may have been unable to support the cellulose layer, leading to its detachment during processing.

Homologs of the LCP described by Bae *et al.* (2013) were identified in all strains of the *Lm* collection, featuring a conserved C-terminal LPXTG domain and a well-conserved CBD (Table 3.2). The LPXTG motif facilitates anchoring of proteins to the cell wall, suggesting that these homologs are likely cell surface proteins. Bae *et al.* (2013) also reported well conserved homologs of the LCP in several other *Lm* strains, suggesting it is a core gene of the species. This supports the hypothesis that *Lm* has an innate ability to contaminate fresh produce.

A Crp/Fnr family transcription factor in *Lm* which in deletion mutants reduced attachment to lettuce leaves and cantaloupe rind was highly conserved across the collection (96.9 – 100% sequence identity) (Salazar *et al.*, 2013). This gene may regulate functions contributing to leaf attachment, potentially including the expression of LCP. However, further research is required to verify this relationship.

3.3.3 Phenotypic characteristics associated with fruit and vegetable contamination

Lm is motile due to the presence of four to six peritrichous flagella (Schirm *et al.*, 2004). Gorski *et al.* (2009) demonstrated that flagella and motility contribute to the colonisation of alfalfa, radish and broccoli sprouts in certain strains of *Lm*. Four *Lm* strains were tested for motility at three temperatures, with the area of spread used as a measure of movement efficiency (Figure 3.6). Motility was significantly reduced at 22 °C compared to higher temperatures. Although the presence of flagella at temperatures below 22 °C has been previously observed (Peel *et al.*, 1988), the diminished motility at this temperature is likely due to reduced metabolic activity.

At 30 °C, all *Lm* strains examined exhibited comparable motility, with similar areas of spread observed across the strains (Figure 3.6). In contrast, motility was significantly reduced at 37 °C for all strains except NLmo8, consistent with reports that motility is generally repressed at this temperature (Kathariou *et al.*, 1995). Flagellar expression in *Lm* has been shown to be regulated in a temperature-dependent manner, with expression generally halted at 37 °C (Cho *et al.*, 2022). However, some studies have reported the expression of flagellin, the primary structural component of flagella, and

the retention of motility at 37 °C amongst some *Lm* strains (Kathariou *et al.*, 1995; Way *et al.*, 2004). Nevertheless, this is considered a rare trait within the species.

Strain NLmo8 (ST219, CC4) exhibited comparable motility at both 30 °C and 37 °C. In contrast, NLmo9 (ST4, CC4), a closely related strain in the collection, showed significantly reduced motility at 37 °C (Figure 3.6). In the context of fruit and vegetable contamination, NLmo8's ability to maintain motility at 37 °C may provide a competitive advantage in colonising plant surfaces, particularly during periods of elevated temperatures. The genetic and regulatory mechanisms underlying this phenotype in NLmo8 remain to be elucidated. Determining its prevalence among fruit and vegetable isolates could offer critical insights into its significance as a contamination factor.

3.3.4 Growth dynamics of *L. monocytogenes* collection at 37 °C

The growth dynamics of the *Lm* collection were assessed at 37 °C in BHI and TSB to determine whether sequence type, clonal grouping, or phylogenetic relationships could be associated with phenotypic characteristics (Figure 3.7). The analysis also aimed to evaluate the metabolic flexibility of each strain, providing insights into their adaptability to diverse environments.

In BHI, Lineage II strains had more consistent growth rates than lineage I and this may be attributed to the strains in this lineage having more genes in their accessory genome (Figure 3.4). According to den Bakker *et al.* (2013), the *Lm* accessory genome is enriched with genes related to cell surface structures and phosphotransferase systems. Thus, lineage II strains are more likely to possess genes that enhance nutrient uptake, potentially explaining their more consistent growth rates compared to Lineage I strains.

In contrast, no clear association between phylogenetic relationships or genetic subtypes and growth rates was observed in TSB. Average growth rates were lower in BHI than in TSB, likely due to differences in composition. BHI, composed of beef heart and calf brain infusions, likely contains complex proteins requiring enzymatic hydrolysis to release nutrients. In contrast, TSB contains enzymatic digests of soybean and casein peptones, which provide readily accessible nutrients and therefore supporting faster growth.

While no specific correlation between subtypes and growth rates was identified, strain NLmo20 was consistently the worst performer in both BHI and TSB (Figure 3.7). NLmo20 belongs to a sequence type (ST6) considered a hypervirulent clone, associated with numerous foodborne outbreaks and poor clinical outcomes (Koopmans *et al.*, 2013; Nüesch-Inderbinen *et al.*, 2021). Slow growing or dormant bacteria are less susceptible to sanitizers that require active growth for killing (Levin-Reisman *et al.*, 2017). This slow-growth phenotype may contribute to its persistence in food processing environments, and combined with its pathogenicity, could explain the prevalence of ST6 in foodborne outbreaks.

3.3.5 Comparative growth analysis of NLmo8 and EGD-e under inoculum preparation conditions

NLmo8's motility at 37 °C suggests an enhanced capacity to contaminate fruit and vegetables (Figure 3.6). Additionally, EGD-e, widely used for studying *Lm* biology, may offer valuable insights into mechanisms involved in plant contamination. This prompted further investigation into the interactions of both strains with leafy salad vegetables. To optimise experimental design, their growth was first examined under conditions used to prepare inoculum for the leaf adhesion assay (Figure 3.8).

A suitable culture for inoculation has balanced growth during which bacterial cells have uniform properties i.e., gene expression and protein synthesis are constant. Bacterial cultures are said to have balanced growth when cells are growing exponentially (Cooper, 1991). The growth kinetics of *Lm* NLmo8 and EGD-e were investigated to determine the period of exponential growth during the preparation of inoculum for the leaf adhesion assays.

OD measurements revealed similar time dependencies for both strains, but the relationship between OD and viable cell counts differed. Notably, OD is an unreliable measure of cell count, as it is only linearly related to CFU within a limited range (Stevenson *et al.*, 2016). Neither the cell size of NLmo8 or EGD-e, or their ability to form aggregates in BHI, was investigated which can affect OD measurements and could explain the variability.

Overall, viable cell counts indicated exponential growth occurred between 1 and 4 h, and inocula should be prepared within this period. The observed discrepancy in cell counts despite similar OD readings between the two strains highlights the importance of assessing each strain's growth characteristics prior to experimentation to ensure consistent and comparable results.

3.3.6 Growth dynamics of *L. monocytogenes* collection at 25 °C

Since 37 °C is not typically encountered during salad cultivation, growth was assessed at 25 °C to better reflect the conditions in which *Lm* might proliferate during crop production. By examining growth at 25 °C across multiple media, this study aimed to explore variations in growth dynamics across the strain collection and correlations with phylogenetic relationships.

Growth rates in BHI were consistently lower than in the other media types (Figure 3.7), mirroring trends observed at 37 °C (Figure 3.9). The more consistent growth rates in VPB compared to TSB and BHI may reflect adaptation to plant-derived nutrients, as most strains were isolated from plant sources. However, the similar performance of EGD-e and NLmo4, which are not plant-derived, challenges this assumption.

TSB and BHI both contain glucose as their primary carbon source, whereas VPB contains dextrose. Glucose has been shown to repress genes regulated by the positive regulatory factor *prfA*, a key protein controlling the expression of virulence determinants in *Lm* (Aké *et al.*, 2011). Glaser *et al.* (2001) reported that the genome of *Lm* contains a notably high proportion of regulatory genes (>7% of total genes) compared to other bacteria with similar genome sizes. If the regulatory targets of these genes are similarly repressed by glucose, this could explain the less consistent growth rates observed between strains in TSB and BHI (Figure 3.9).

At 37 °C, EGD-e exhibited the lowest growth rate in TSB compared to all other strains (Figure 3.7); however, this trend was not observed at 25 °C (Figure 3.9). Previous studies have shown that numerous genes in *Lm* are regulated in a temperature-dependent manner (Saldivar *et al.*, 2018). The differential regulation of genes at 25 °C likely contributed to the observed differences in growth dynamics between temperatures.

Overall, these findings indicate that *Lm* exhibits strain-specific metabolic and regulatory responses, resulting in variable growth dynamics. Notably, NLmo13 (ST37) and NLmo15 (ST204) consistently demonstrated high growth rates across all media. Both sequence types (STs) have been associated with a wide range of environmental sources, food products, and cases of animal and human Listeriosis (Fox *et al.*, 2016; Voronina *et al.*, 2023). This suggests that these STs pose a significant risk to food safety as they are highly adaptable to varied environments. Both strains belong to lineage II, further supporting the idea that strains from this lineage exhibit greater metabolic flexibility compared to those from lineage I. This adaptability may account for the broader range of environmental sources from which lineage II strains have been isolated compared to lineage I strains (Orsi *et al.*, 2011).

3.3.7 Conclusion

Lineage II strains in the collection exhibited greater genetic variability and larger accessory genomes. These features may enhance their adaptability to diverse environments and likely explain their more frequent isolation from food and food processing environments compared to other lineages. Despite the more frequent isolation of lineage II strains from food, no consistent association between *Lm* subtypes and fruit or vegetable contamination has been reported.

The increasing incidence of *Lm* outbreaks linked to fresh produce highlights the need for a deeper understanding of the factors driving this relationship. Although a few genetic factors associated with fruit and vegetable contamination have been described, these appear widespread across the species, suggesting an innate capacity to contaminate such food sources. Overall, this study included a limited number of strains, representing only a small subset of the clonal groups identified within the species. Expanding the collection to include more isolates from fruit and vegetables is essential to determine the prevalence of contamination factors and assess whether these can be linked to specific subtypes.

Specific phenotypic traits, such as metabolic flexibility (Section 3.2.8 and 3.2.10) and motility (Section: 3.2.7), may play a role in fruit and vegetable contamination but appear to be strain specific. Future studies should explore these traits across a larger collection

of *Lm* strains isolated from fresh produce to elucidate the factors driving the increased incidence of produce-associated Listeriosis outbreaks. Strains exhibiting phenotypic traits potentially facilitating fruit and vegetable contamination, such as metabolic flexibility and motility, will be prioritised for further analyses to enhance our understanding of *Lm* interactions with fruit and vegetables.

Chapter 4 – Investigating *Listeria monocytogenes* attachment to salad leaves

4.1 Introduction

4.1.1 Preharvest contamination of salad vegetables by *L. monocytogenes*

Leafy salad vegetables can become contaminated through exposure to *L. monocytogenes (Lm)* in the rhizosphere, which includes the roots and the surrounding environment influenced by them, or the phyllosphere, the plant's above-ground parts. Numerous studies have reported the isolation of *Lm* from faecal, soil, water and fertiliser samples at fresh produce farming sites, highlighting its widespread occurrence in these environments (Strawn *et al.*, 2013; Weller *et al.*, 2015; Zhu *et al.*, 2017). In fact, preharvest contamination has been reported in salad vegetables such as spinach (Weller *et al.*, 2015), lettuce and rocket (Aytac *et al.*, 2010), indicating the transfer of *Lm* to plants in the growing environment.

4.1.2 From the rhizosphere to edible plant parts

Soil is a common environmental reservoir for *Lm*, and since plants co-inhabit this environment with microbes, they may encounter the bacterium (Vivant *et al.*, 2013). In fact, the edible parts of leafy vegetables can become contaminated through the translocation of *Lm* from the soil or other growing media. Shenoy *et al.* (2017) reported detecting fluorescently labelled *Lm* strains in all major plant tissues of 20-day-old romaine lettuce plants, inoculated at the seed stage and grown in commercial potting mix. Similarly, Standing *et al.* (2013) reported *Lm* internalisation in the leaves and roots of butterhead lettuce irrigated with *Lm* in a hydroponic system. In contrast, Jablasone *et al.* (2005) did not detect *Lm* in the internal tissues of lettuce and spinach after seed inoculation and cultivation in solidified hydroponic solution, although *Lm* was recovered from leaf surfaces after 49 days. These findings suggest that *Lm* can translocate from the rhizosphere to edible plant parts, where it may proliferate to harmful levels or go on to contaminate other food products, thereby posing a food safety risk.

4.1.3 Persistence and survival on leaf surfaces

In addition to translocation of *Lm* from the rhizosphere, leaves may become contaminated through contact with contaminated soil, irrigation water, animals and farming equipment (Smith *et al.*, 2018). Once on the leaf surface, *Lm* can adhere, colonise and persist. Studies have demonstrated *Lm* is able to survive on salad leaves following contamination during cultivation, highlighting the potential for transmission from the growing environment to consumers (Jablasone *et al.*, 2005; Honjoh *et al.*, 2018). Honjoh *et al.* (2018) showed that *Lm* could survive for up to 7 days on leaf lettuce during cultivation when artificially contaminated with ≥1600 CFU/plant using spray inoculation to simulate contaminated irrigation water.

In addition to surviving on salad leaves during cultivation, various studies report the survival and even growth of *Lm* on leafy salad vegetables post-harvest (Marik *et al.*, 2020). Culliney and Schmalenberger (2020) demonstrated that spinach, lettuce and rocket supported growth of *Lm* over 7 days at 8 °C under modified atmosphere conditions. This suggests that contamination during cultivation can result in the accumulation of harmful bacterial levels by the time of consumption.

4.1.4 *L. monocytogenes* attaches rapidly to leafy vegetables

The leaf surface is considered a hostile environment for microorganisms due to low nutrient availability, competing microflora, direct UV radiation, and temperature and humidity fluctuations (Leveau, 2019). Ultimately, in order to colonise the leaf surface *Lm* must be able to attach, survive those stresses and access and utilize available nutrients (Truong *et al.*, 2021). Despite these challenges, attachment remains the critical first step in *Lm* contamination of leafy salads.

Studies on *Lm* have shown that the bacterium rapidly attaches to leaf surfaces, possibly establishing strong interactions from the onset (Ells and Truelstrup Hansen, 2006; Milillo *et al.*, 2008; Kyere *et al.*, 2019a). For instance, Kyere *et al.* (2019a) investigated the attachment of three *Lm* strains to hydroponically and soil-grown butterhead lettuce using exposure times of 1 s, 10 s, 30 s, 60 s, 2 min, and 5 min. They found no significant differences in attachment between exposure times or growing conditions, suggesting even brief contact is sufficient for *Lm* to attach firmly. However, strain O8A08 showed

significantly higher attachment to hydroponically grown lettuce after 2- and 5-min exposure compared to the other strains. These findings suggest that bacterial attachment to leafy vegetables may be strain-specific but also influenced by leaf characteristics, which can differ between soil- and hydroponically-grown plants (Lima *et al.*, 2013). Understanding which leaf characteristics influence bacterial attachment could inform strategies to reduce contamination by promoting better cultivation practices or selecting plant varieties with surface traits less conducive to attachment.

4.1.5 Bacterial characteristics influencing attachment

Bacterial attachment is thought to begin with a stochastic, non-specific phase, where bacteria form a weak, reversible attachment to the leaf surface. This involves a combination of intermolecular forces, including van der Waals forces, hydrogen bonding and electrostatic and hydrophobic interactions. This is followed by irreversible attachment, driven by specific adhesins or the production of exopolysaccharides (Romantschuk, 1992). For *Lm*, cell wall-anchored proteins (Bae *et al.*, 2013), flagella (Gorski *et al.*, 2009) and exopolysaccharides (Fulano *et al.*, 2023) have been implicated in facilitating the bacterium's attachment to leaf surfaces.

The cell surface charge and hydrophobicity of *Lm* have been reported to play a role in attachment to plant surfaces (Ukuku and Fett, 2002). Leaf surfaces are coated with a hydrophobic cuticle, and it has been suggested that hydrophobic bacteria more readily attach to these surfaces than less hydrophobic bacteria (Tan *et al.*, 2016; Fuchs *et al.*, 2020). While attachment is essential for colonisation, bacterial proliferation depends on water and nutrient availability, making hydrophilic regions potentially more favourable for attachment. Research indicates that *Lm* is generally weakly hydrophobic, although this characteristic is strain-dependent and can be influenced by culture conditions (Dabrowski *et al.*, 2001; Tan *et al.*, 2016). Whether *Lm* preferentially attaches to hydrophobic or hydrophilic regions on leaf surfaces, and how this attachment varies across different strains, remains to be investigated.

Further research is needed to better understand the roles of hydrophobicity and cell surface charge in attachment, as well as the specific adhesins that contribute to *Lm* attachment to salad leaves. Understanding these mechanisms could help identify high-

risk strains and environmental conditions that promote attachment, aiding the development of strategies to reduce contamination. Notably, identifying specific attachment sites on leaf surfaces may offer insights into the mechanisms driving *Lm* adherence to plants.

4.1.6 Identifying attachment sites

To investigate where *Lm* attaches to leaf surfaces numerous studies have employed microscopy techniques including confocal (Takeuchi *et al.*, 2000; Milillo *et al.*, 2008; Gorski *et al.*, 2021), scanning electron (Ells and Truelstrup Hansen, 2006; Guan *et al.*, 2023), transmission electron (Standing *et al.*, 2013), fluorescent (Bae *et al.*, 2013) and brightfield microscopy (Standing *et al.*, 2013). Each method has its own advantages and drawbacks, and researchers must decide which technique is most suitable for the target application.

Brightfield microscopy is a simple and accessible technique, but its low contrast and resolution limit its ability to capture detailed images of bacterial attachment sites. Scanning (SEM) and transmission electron microscopy (TEM) offer high resolution, providing greater detail of surface structures, though both require labour-intensive sample preparation. Additionally, TEM necessitates the preparation of thin sections, complicating the examination of multiple replicates or large tissue areas (Wilson and Bacic, 2012). Although SEM does not require extensive sectioning, distortion of surface topology and fixation artifacts are inherent to the technique complicating the interpretation of observations (Edwards, 2001). While using brightfield and electron microscopy, differentiating between a leaf's natural microflora and *Lm* can be challenging. Sterilising leaves before inoculation can mitigate this, but it may alter surface features, raising uncertainty about whether the findings reflect natural attachment behaviour (Saldierna Guzmán *et al.*, 2020).

To distinguish *Lm* from other bacteria or enhance its detectability, researchers can employ marker technologies such as staining, labelling, or genetically modifying the bacteria to express detectable marker genes (Edwards, 2001). Confocal and fluorescent microscopy are particularly useful for examining samples that make use of fluorescent labels or gene products. Gorski *et al.* (2021) and Jablasone *et al.* (2005) used plasmids

encoding constitutively expressed GFP to label *Lm*; however, these plasmids require antibiotic pressure to be maintained during culturing. As a result, studies focusing on long-term plant-bacteria interactions cannot utilise such plasmid vectors. To overcome this limitation researchers can utilise a suicide vector, which does not require antibiotic pressure during culturing to maintain the plasmid (Milillo *et al.*, 2008; Balestrino *et al.*, 2010). However, the applicability of suicide vectors depends on the successful transformation of the host organism and the efficient integration of the relevant construct.

One important consideration when preparing samples for fluorescent and confocal microscopy is the use of preservative or fixative solutions, which may lead to the loss of GFP fluorescence (Shenoy *et al.*, 2017). Antibody labelling post-fixation can permit researchers to overcome loss of fluorescence due to fixation. Shenoy *et al.* (2017) reported using a fluorophore-conjugated antibody to label *Lm* to mitigate the loss of GFP fluorescence caused by fixation, allowing for the assessment of bacterial internalisation in romaine lettuce inoculated at the seed stage. However, antibodies require specific antigens and may need to be designed specifically for the target application. Moreover, chemical fixation can alter plant cell antigenicity, potentially preventing antibody binding (Wilson and Bacic, 2012). Observing fresh tissue avoids these issues but requires stringent safety protocols to manage the risks associated with *Lm*.

Attachment sites can potentially be identified on fresh tissue without microscopic techniques. For example, Fulano *et al.* (2023) transformed *Lm* strains to express the red fluorescent protein mScarlet which turns bacterial biomass pink. This allowed the researchers to visually identify attachment sites on cantaloupe rind and celery. However, this approach is limited by the need for bacterial access to nutrients for growth, revealing only attachment sites where the bacterium can proliferate.

Overall, a strain with an integrated GFP plasmid offers a robust solution to the challenges of plasmid maintenance and antibody labelling. Combined with the high resolution of confocal microscopy, this approach enables detailed examination of bacterial attachment sites without labour-intensive sample preparation and offers the potential for fresh tissue analysis.

4.1.7 Aims and objectives

Salad leaves can become contaminated with *Lm* at any stage of the food supply chain. Once on the leaf, the bacterium can survive and proliferate during both cultivation and storage, posing a significant food safety risk. Understanding the plant and bacterial characteristics, along with the environmental conditions influencing attachment to leafy salad vegetables, is essential for identifying key contributors to contamination risk. Previous research has primarily focussed on the interaction of *Lm* with lettuce, whereas other leafy salad vegetables have not been well investigated (Kyere *et al.*, 2019b).

This chapter investigates the attachment of *Lm* to rocket and spinach, two commonly consumed leafy vegetables. *Lm* attachment is quantified using two assays to assess the impact of plant species, variety, bacterial strain and inoculation conditions. Fluorescent and confocal microscopy, combined with antibody labelling and a suicide vector, are used to investigate whether *Lm* preferentially attaches to specific sites on intact leaf surfaces. Additionally, a novel assay is employed to identify attachment sites without the need for microscopy.

The following objectives will be addressed in this chapter to elucidate the factors contributing to *Lm* attachment to leafy salad vegetables:

- Determine whether strain-specific differences exist in the attachment of *L. monocytogenes* to salad leaves.
- Assess the impact of leaf characteristics, including variety and plant species, on the attachment of *L. monocytogenes*.
- Explore additional factors, aside from bacterial strain and leaf characteristics, that may influence *L. monocytogenes* attachment to salad leaves.
- Identify preferential attachment sites for *L. monocytogenes* on the surfaces of salad leaves.

4.2 Results

4.2.1 Quantifying attachment of *L. monocytogenes* to spinach using leaf disc assay

4.2.1.1 Strain specific differences in spinach leaf attachment

The attachment of *Lm* strains NLmo8 and EGD-e to spinach (cv. 'Samish') leaves was investigated to assess strain-specific differences in bacterial attachment (Figure 4.1). Bacterial attachment for EGD-e ranged from 2 to 36 CFU/cm^2 and for NLmo8 from 40 to 357 CFU/cm^2. Highly significant differences (Mann-Whitney U test, $P = 0.002$) in bacterial attachment were observed between NLmo8 (median = 207, mean = 210, SD = 128) and EGD-e (median = 7, mean = 13, SD = 14). No significant differences ($P > 0.05$) in bacterial attachment (Mann-Whitney U test) were observed between leaves from young and mature plants for either strain (data not shown).

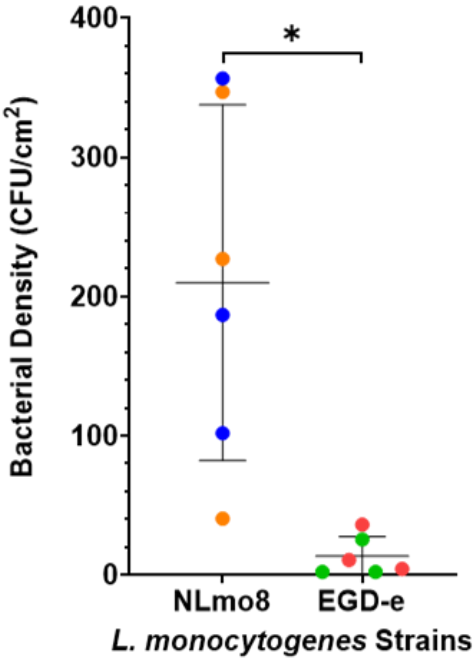

Figure 4.1 Comparison of *L. monocytogenes* strains NLmo8 and EGD-e attachment to spinach leaves of the Samish variety.
Leaves were immersed in PBS containing 10^7 CFU/mL of *L. monocytogenes*, dried, washed, and 0.5 cm diameter discs were taken from the leaves for maceration. Bacterial attachment (CFU/cm^2, mean ± SD) was calculated by dividing the total bacteria in the macerate by the leaf disc surface area. Orange and blue represent densities of attached NLmo8 on leaves from 20-day and 35-day old plants, respectively. Red and green represent the densities of attached EGD-e on leaves from 21-day and 36-day old plants, respectively. N = 6, with 3 technical replicates. (*) denotes a significant difference (Mann-Whitney, U = 0, $P = 0.002$).

4.2.1.2 Comparative analysis of *L. monocytogenes* attachment to different spinach varieties

To determine if *Lm* exhibits differential attachment to different spinach varieties, leaves from the 'Samish' and 'Lazio' varieties were inoculated with *Lm* strain NLmo8. Bacterial attachment ranged from 99 to 971 CFU/cm^2 for Samish and 30 to 510 CFU/cm^2 for Lazio (Figure 4.2). No statistically significant difference ($P > 0.05$) was observed between the Samish (mean = 512, median = 489, SD = 399) and Lazio (mean = 230, median = 191, SD = 202) varieties (Mann-Whitney U test, $P = 0.34$).

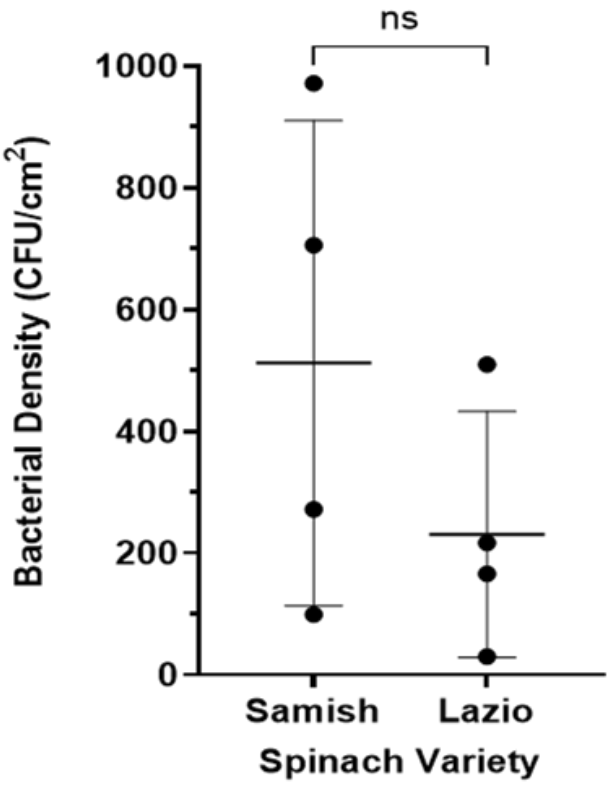

Figure 4.2 Comparison of *L. monocytogenes* strain NLmo8 attachment to leaves from different spinach varieties (Lazio and Samish).
Leaves were immersed in PBS containing 10^7 CFU/mL of *L. monocytogenes*, dried, washed, and 0.5 cm diameter discs were taken from the leaves for maceration. Bacterial attachment (CFU/cm^2, mean ± SD) was calculated by dividing the total bacteria in the macerate by the leaf disc surface area. Leaves from a 30-day old Samish plant (N = 4, 3 technical replicates) and a 33-day old Lazio plant (N = 4, 2 technical replicates) were sampled. "ns" denotes a non-significant difference in attached bacteria between the two varieties (Mann-Whitney, U = 4, $P = 0.34$).

4.2.2 Quantifying attachment of *L. monocytogenes* to spinach using whole leaf assay

4.2.2.1 Exposure time increases *L. monocytogenes* attachment

Spinach leaves (cv. 'Nandu RZ') inoculated with either *Lm* strain NLmo8 or EGD-e were either dried for 1 h or washed immediately following inoculation to determine how prolonged exposure affects bacterial attachment and whether it enhances attachment relative to initial adhesion. The attachment of *Lm* strains NLmo8 and EGD-e to spinach (cv. 'Nandu RZ') leaves was then compared within each condition to assess strain-specific differences in bacterial attachment (Figure 4.3).

No significant difference in bacterial attachment between the two strains was observed under either drying condition (unpaired two-tailed t-test). However, attachment significantly increased after drying for 1 h for both EGD-e ($P = 0.0068$) and NLmo8 ($P = 0.0013$) (unpaired two-tailed t-test).

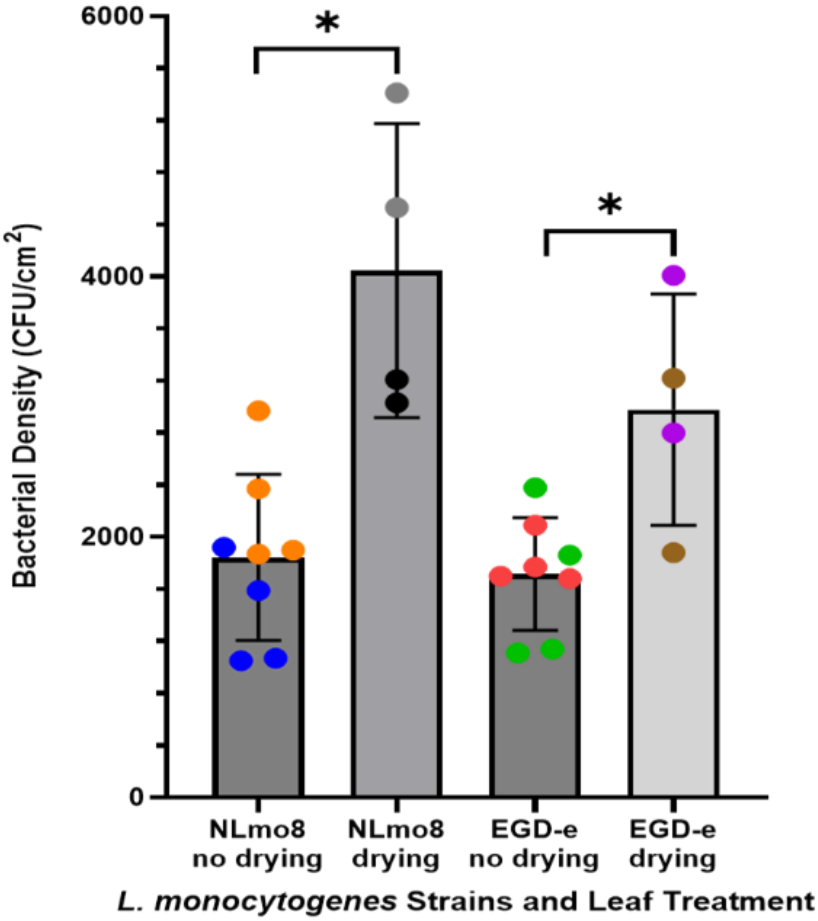

Figure 4.3 Comparison of bacterial attachment to spinach leaves under different inoculation conditions.
Spinach leaves (cv. 'Nandu RZ') were submerged in PBS containing 10^6 CFU/mL, followed by either drying or no drying, then washing and maceration. Bacterial attachment (CFU/cm^2, mean ± SD) was calculated by dividing the total number of bacteria in the macerate by the leaf surface area. Data points with the same colour represent measurements from the same experiment. Bacterial attachment was compared between leaves dried for 1 h (N = 4) and those washed immediately (N = 8). Leaves that were not subjected to drying post-inoculation were collected from plants 27–33 days after sowing, whereas leaves that underwent drying were collected from plants 30–38 days after sowing. Asterisks (*) indicate significant differences ($P < 0.05$) between drying conditions (NLmo8: $P = 0.0013$; EGD-e: $P = 0.0068$; unpaired two-tailed t-test). No significant differences ($P > 0.05$) were observed between strains under either condition (NLmo8 vs EGD-e; unpaired two-tailed t-test).

4.2.3 Quantifying attachment of *L. monocytogenes* to rocket using whole leaf assay

4.2.3.1 Strain specific differences in attachment to rocket

The attachment of *Lm* strains NLmo8, NLmo9, NLmo15, and EGD-e to rocket leaves (cv. 'Monza') was investigated to assess strain-specific differences in bacterial attachment (Figure 4.4). Phylogenetic analysis of the *Lm* collection indicated that NLmo9 is most closely related to NLmo8, while NLmo15 is most closely related to EGD-e. These strains were selected to investigate whether attachment ability is strain-specific or correlated with phylogenetic relationships.

A decreasing trend in mean bacterial attachment was observed from NLmo8 to EGD-e. A one-way ANOVA revealed significant differences in attachment between strains ($P = 0.0045$). Post hoc analysis using Tukey's test revealed a significant difference between NLmo8 and EGD-e ($P = 0.0037$, mean difference = 825), with NLmo8 exhibiting nearly 2-fold higher average attachment compared to EGD-e. No significant differences were detected between other strain comparisons, suggesting that the pronounced difference between NLmo8 and EGD-e is likely the primary contributor to the overall statistical differences in attachment observed across strains.

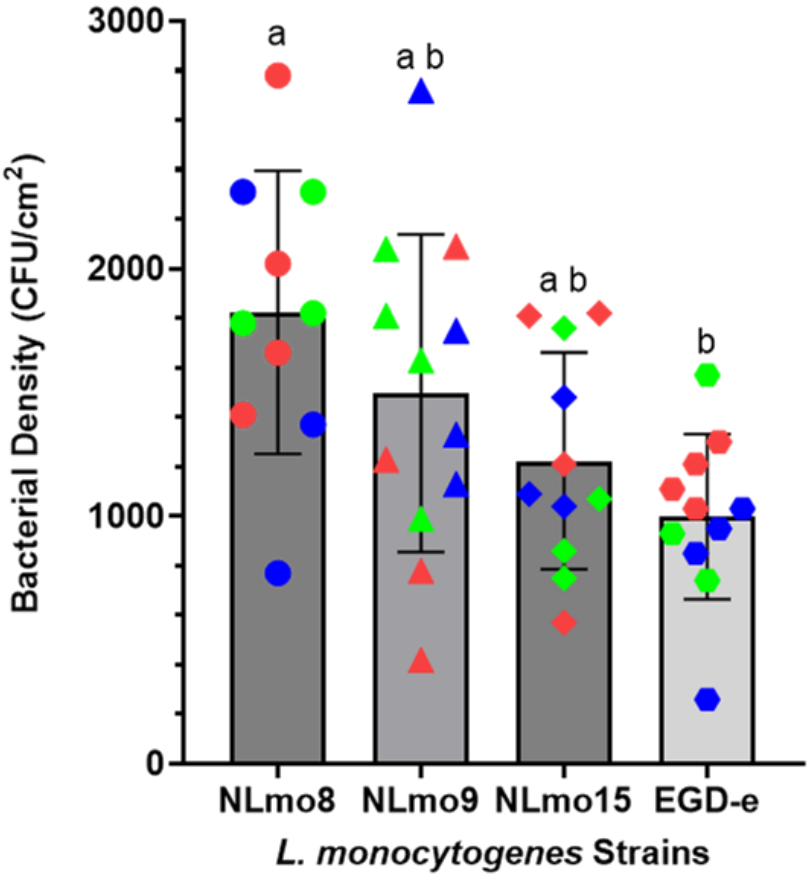

Figure 4.4 Comparison of *L. monocytogenes* strains attachment to rocket leaves. Rocket leaves (cv. 'Monza') were submerged in PBS containing 10^6 CFU/mL of either *L. monocytogenes* strain NLmo8 (N = 10), NLmo9 (N = 12), NLmo15 (N = 11), or EGD-e (N = 11), washed and macerated. Plants were sampled 36–43 days after sowing. Bacterial attachment (CFU/cm^2, mean ± SD) was calculated by dividing the total number of bacteria in the macerate by the leaf surface area. A one-way ANOVA revealed statistically significant differences ($P < 0.05$) in attachment between strains ($P = 0.0045$), with a Tukey's test showing a significant difference between NLmo8 and EGD-e ($P = 0.0037$). In the compact letter display, strains sharing a letter are not statistically significantly different. Data points with the same colour and shape represent measurements from the same experiment.

4.2.3.2 Evaluating the effect of plant species on *L. monocytogenes* attachment

To determine whether *Lm* exhibits differential attachment to different plant species, leaves from spinach (cv. 'Samish') and rocket (cv. 'Monza') were inoculated with either strain NLmo8 or EGD-e (Figure 4.5).

For strain NLmo8, bacterial attachment was similar between spinach (1843 CFU/cm^2, SD = 637.9) and rocket (1823 CFU/cm^2, SD = 571.7). In contrast, strain EGD-e showed a 1.7-fold higher attachment to spinach (1716 CFU/cm^2, SD = 431.8) compared to rocket (998.2 CFU/cm^2, SD = 334.4). No significant difference was observed for NLmo8 between the two plant species (P = 0.95), while a significant difference was found for EGD-e (P = 0.0008) (unpaired two-tailed t-test).

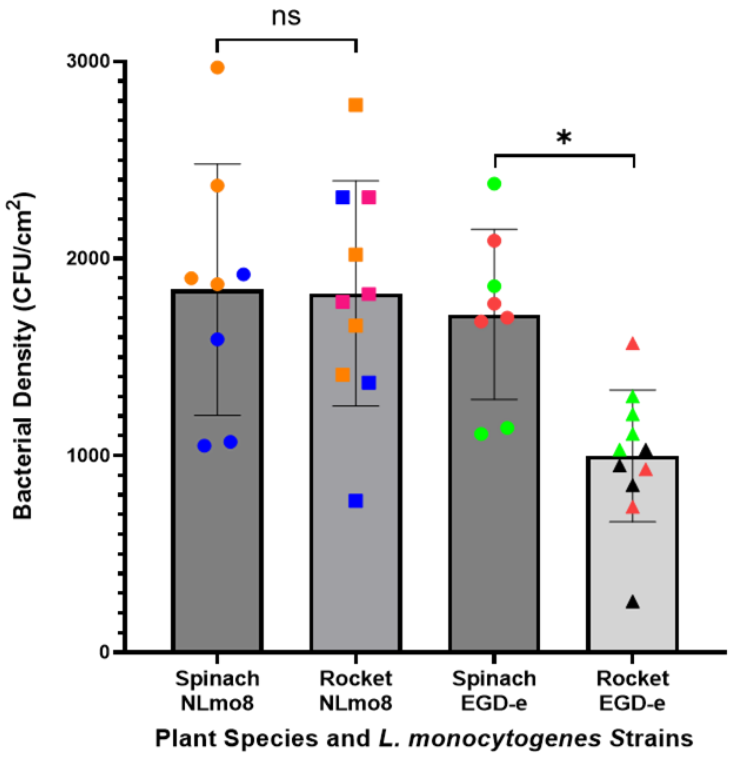

Figure 4.5 Comparison of *L. monocytogenes* attachment to rocket and spinach leaves for strains NLmo8 and EGD-e.
Spinach (cv. 'Nandu RZ') and rocket (cv. 'Monza') leaves were submerged in PBS containing 10^6 CFU/mL, washed and macerated. Rocket plants were sampled 36–43 days after sowing, and spinach 27–33 days after sowing. Bacterial attachment (CFU/cm^2, mean ± SD) was calculated by dividing the total number of bacteria in the macerate by the leaf surface area. Data points with the same colour and shape represent measurements from the same experiment. For spinach, N = 8; for rocket, N = 10 (NLmo8) and N = 11 (EGD-e). An asterisk (*) indicates statistically significant differences ($P < 0.05$), while "ns" denotes non-significant differences ($P > 0.05$) (unpaired two-tailed t-test).

4.2.4 Identifying preferential attachment sites of *L. monocytogenes* on leaf surfaces

4.2.4.1 Immunofluorescent staining of *L. monocytogenes*

To assess antibody specificity, strains NLmo8, NLmo9 and EGD-e were stained with antibodies and Hoechst, then examined using fluorescent microscopy. Microscopy analysis revealed that only EGD-e was successfully stained with antibodies and Hoechst (Figure 4.6; Panel A and B). Strains NLmo8 and NLmo9 showed no green fluorescence from the antibody fluorophore but were successfully stained with Hoechst, confirming the presence of bacterial DNA (data not shown).

To determine where EGD-e attaches to rocket leaves (cv. 'Monza'), inoculated leaves were stained and examined using confocal microscopy (Figure 4.6; Panel C and D). Based on the highest and lowest recorded attachment densities (Section 4.2.3.1), the estimated number of observable cells per field of view ranged from 0.12 to 0.47 at 40x magnification and 0.01 to 0.05 at 63x magnification, assuming a uniform distribution. Despite the low probability of detection at these concentrations, some cells were visible in the analysed leaf sections (Figure 4.6; Panel C and D, white arrow).

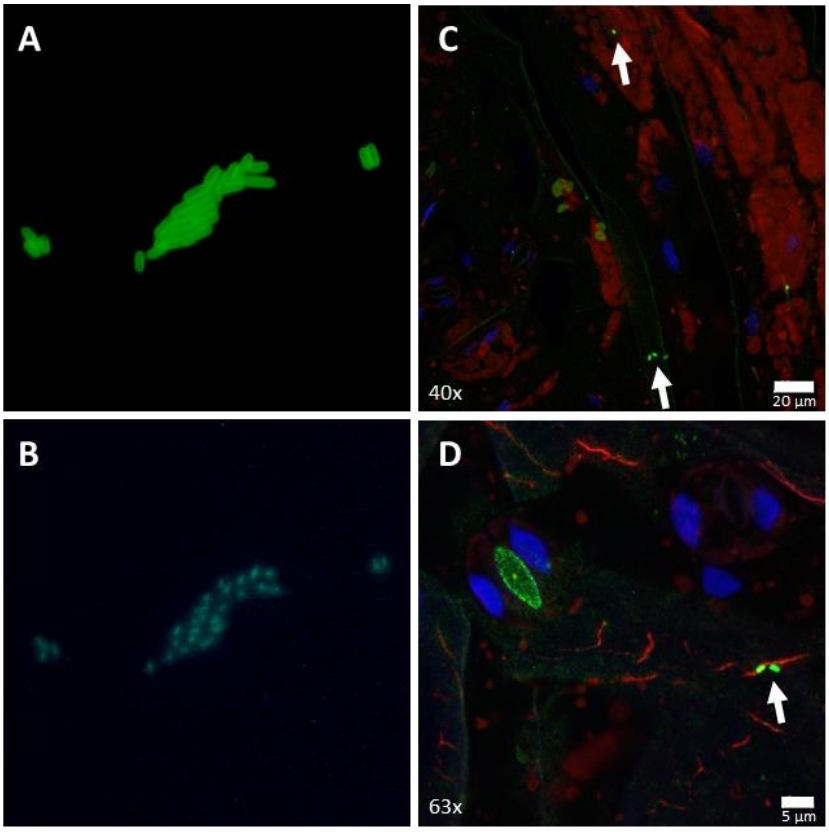

Figure 4.6 Fluorescent and confocal microscopy images of *L. monocytogenes* strain EGD-e labelled with specific antibodies.
(A) *L. monocytogenes* EGD-e from an overnight culture, fixed on a coverslip and labelled with a primary antibody specific to *L. monocytogenes*, followed by a secondary antibody conjugated to Alexa Fluor 488 (green) **(B)** The same sample as (A), viewed under UV light to detect Hoechst 33342 staining (blue). Images (A) and (B) were captured with a bScope fluorescent microscope. **(C)** Rocket leaf (cv. 'Monza') section inoculated with *L. monocytogenes* EGD-e, stained with primary antibodies targeting *L. monocytogenes* and plant pectin, followed by secondary antibodies conjugated to Alexa Fluor 488 for *L. monocytogenes* (green) and Alexa Fluor 594 for plant pectin (red). DNA was counterstained with Hoechst 33342 (blue). The section was obtained from the leaf apex, and imaging was performed on the abaxial surface. Field of view: 212.55 x 212.55 µm. **(D)** A rocket leaf (cv. 'Monza') section inoculated with *L. monocytogenes* EGD-e and stained the same way as (C). The section was obtained from the leaf apex, and imaging was performed on the adaxial surface. Field of view: 67.48 x 67.48 µm. Images (C) and (D) were captured using a Zeiss LSM 880 confocal microscope. White arrows indicate *L. monocytogenes* cells which measured approximately 1.5 – 1.8 µm in length and 0.8 – 0.9 µm in width.

4.2.4.2 Transformation of strain NLmo8 for detecting attachment sites of *L. monocytogenes* on leaf surfaces

Since NLmo8 could not be stained with antibodies (Section 4.2.4.1), it was genetically modified to constitutively express GFP to enable visualisation of its attachment to leaf surfaces without the need for antibody staining. To confirm successful transformation and GFP expression, exponential phase cultures of NLmo8 Wt and NLmo8::cGFP were analysed using fluorescent microscopy. Both strains showed blue fluorescence from DAPI staining, confirming bacterial DNA, while only NLmo8::cGFP emitted green fluorescence, indicating successful transformation (Figure 4.7)

To determine where NLmo8 attaches to the leaf surface, sections from spinach and rocket leaves inoculated with NLmo8::cGFP were analysed using confocal microscopy. Notably, no green fluorescent bacterial cells were detected on any of the leaf sections analysed. To assess the probability of observing bacterial cells, Table 4.1 presents the estimated number of NLmo8 Wt cells per field of view at 40x and 63x magnification, based on attachment data (Figure 4.5) and assuming uniform distribution.

Table 4.1 Estimated number of *L. monocytogenes* cells per field of view based on NLmo8 Wt attachment data.

Plant Species	Magnifi-cation	Size Field of View (µm)	Lowest Cell Counts (CFU/cm²)	Highest Cell Counts (CFU/cm²)	Average Cell Counts (CFU/cm²)	Cells per Field of View		
						min	max	avg
Rocket	40x	212.55 x 212.55	7.7×10^2	2.78×10^3	1823	0.35	1.26	0.82
Rocket	63x	67.48 x 67.48	7.7×10^2	2.78×10^3	1823	0.04	0.13	0.08
Spinach	40x	212.55 x 212.55	1.05×10^3	2.97×10^3	1843	0.47	1.34	0.83
Spinach	63x	67.48 x 67.48	1.05×10^3	2.97×10^3	1843	0.05	0.14	0.08

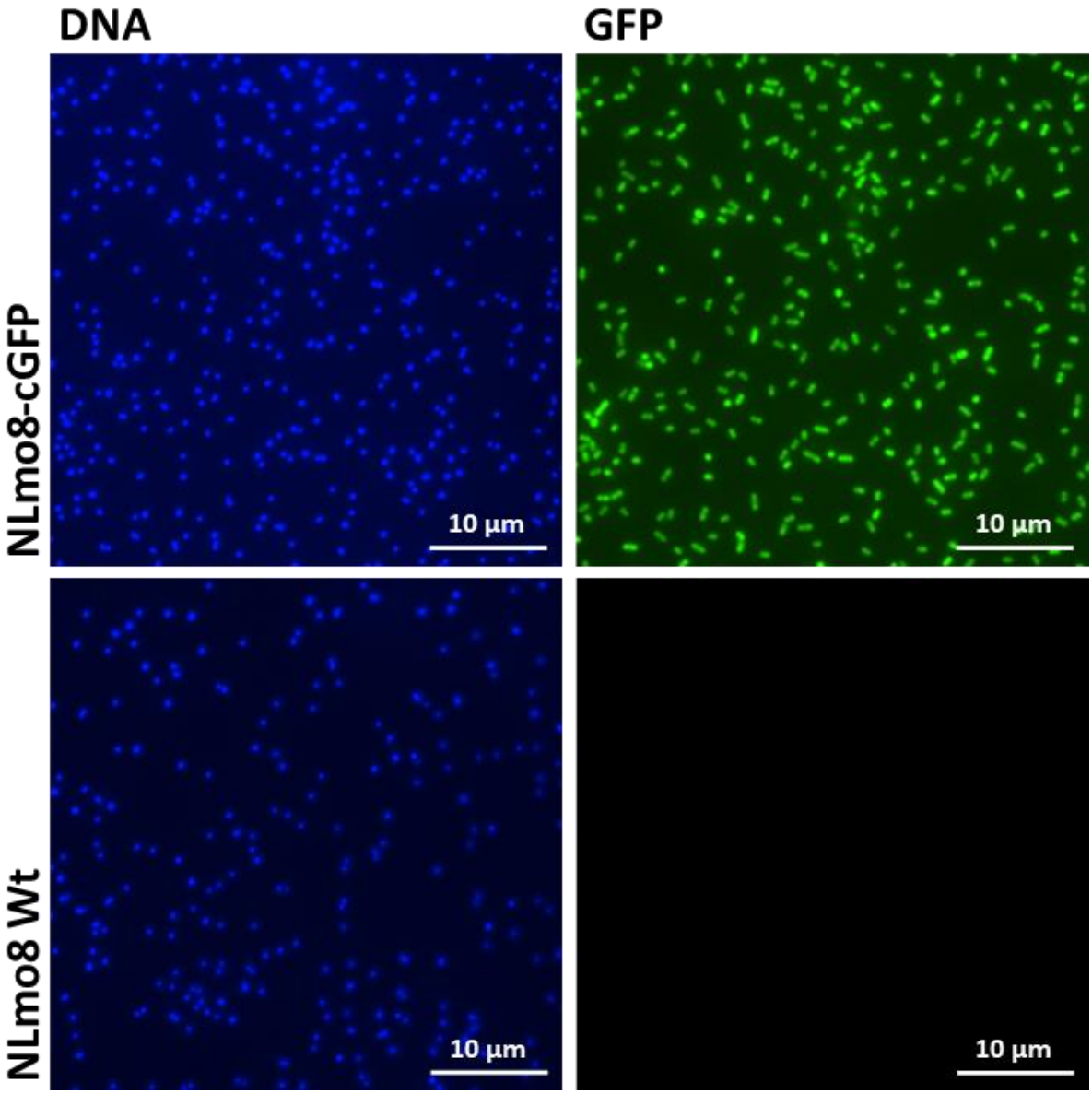

Figure 4.7 Fluorescent microscopy images of *L. monocytogenes* strains NLmo8 Wt and NLmo8::cGFP.
A volume of 10 µL of exponential phase cultures was applied to a coverslip, air-dried, fixed, and stained with DAPI. DAPI was excited by UV light and emits blue light. In strain NLmo8::cGFP, green fluorescent protein (GFP) was excited by blue light and emits green light. Images were captured using an Olympus BX61 fluorescent microscope equipped with a 100x oil immersion objective.

4.2.4.3 Quantifying attachment of NLmo8::cGFP to rocket and spinach

To determine if genetic modification of NLmo8 had altered the growth dynamics of relative to the wild-type, NLmo8::cGFP was examined under the conditions simulating those used for preparing the inoculum in the leaf adhesion assay. Results indicated that NLmo8::cGFP's growth was comparable to the NLmo8 Wt strain (data not shown). To further assess whether NLmo8::cGFP behaved similarly to NLmo8 Wt under experimental conditions, its attachment to rocket leaves (cv. 'Monza', Figure 4.8A) and spinach leaves (cv. 'Nandu RZ', Figure 4.8B) was investigated.

No significant difference in attachment between the wild-type and mutant strain was found for spinach (P = 0.2930) or rocket (P = 0.0601) (unpaired two-tailed t-test). Despite this, NLmo8::cGFP showed 1.2-fold higher average attachment to spinach compared to NLmo8 Wt, while attachment to rocket was 1.6-fold lower than the wild type (Figure 4.8)

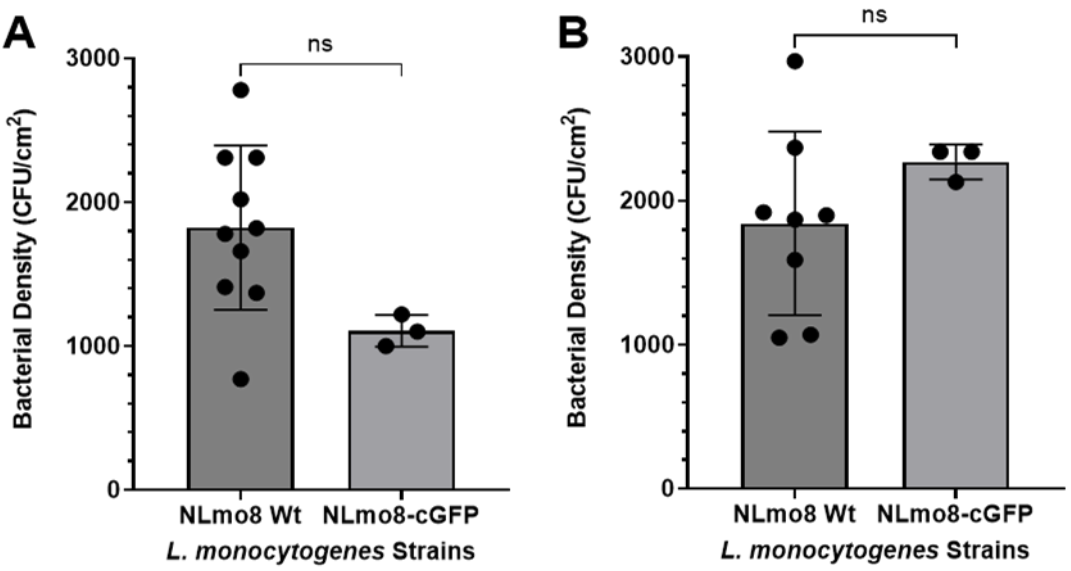

Figure 4.8 Comparison of *L. monocytogenes* strains NLmo8 Wt and NLmo8::cGFP attachment to rocket and spinach leaves.
Leaves were submerged in PBS containing 10^6 CFU/mL, washed and macerated. Bacterial attachment (CFU/cm^2, mean ± SD) was calculated by dividing the total number of bacteria in the macerate by the leaf surface area. For NLmo8::cGFP, rocket and spinach leaves were sampled 37 and 30 days after sowing, respectively, For NLmo8 Wt, rocket was sampled 36–43 days after sowing, and spinach 27–33 days. **(A)** Comparison of NLmo8 Wt (N = 10) and NLmo8::cGFP (N = 3) attachment to **rocket** leaves (cv. 'Monza'). **(B)** Comparison of NLmo8 Wt (N = 8) and NLmo8::cGFP (N = 3) attachment to **spinach** leaves (cv. 'Nandu RZ'). "ns" indicates a non-significant difference ($P > 0.05$, unpaired two-tailed t-test).

4.2.4.4 Identifying *L. monocytogenes* attachment sites on spinach using a novel overlay assay

To identify preferential attachment sites for *Lm* strain NLmo8 to spinach leaves, a novel overlay assay was developed. Inoculated leaves were submerged in selective growth medium, which was allowed to set, and then incubated at 30 °C. Colonies formed where *Lm* had attached to the leaf surface, indicating putative attachment sites (Figure 4.9).

Bacterial colonies were predominantly observed on the adaxial side, with fewer on the abaxial side. As shown in Figure 4.9; panel A, colonies can be seen dispersed across the adaxial surface, with larger ones primarily along the central vein. In Figure 4.9; panels B and C, colonies can be seen mainly near or on veins on the adaxial side. On the abaxial side, colonies were much sparser and can primarily be seen around the veins and along the leaf edge (Figure 4.9; panels A and B). An opaque yellow mass can be seen along the leaf edge, possibly representing *Lm* attached to that region (Figure 4.9; panel C).

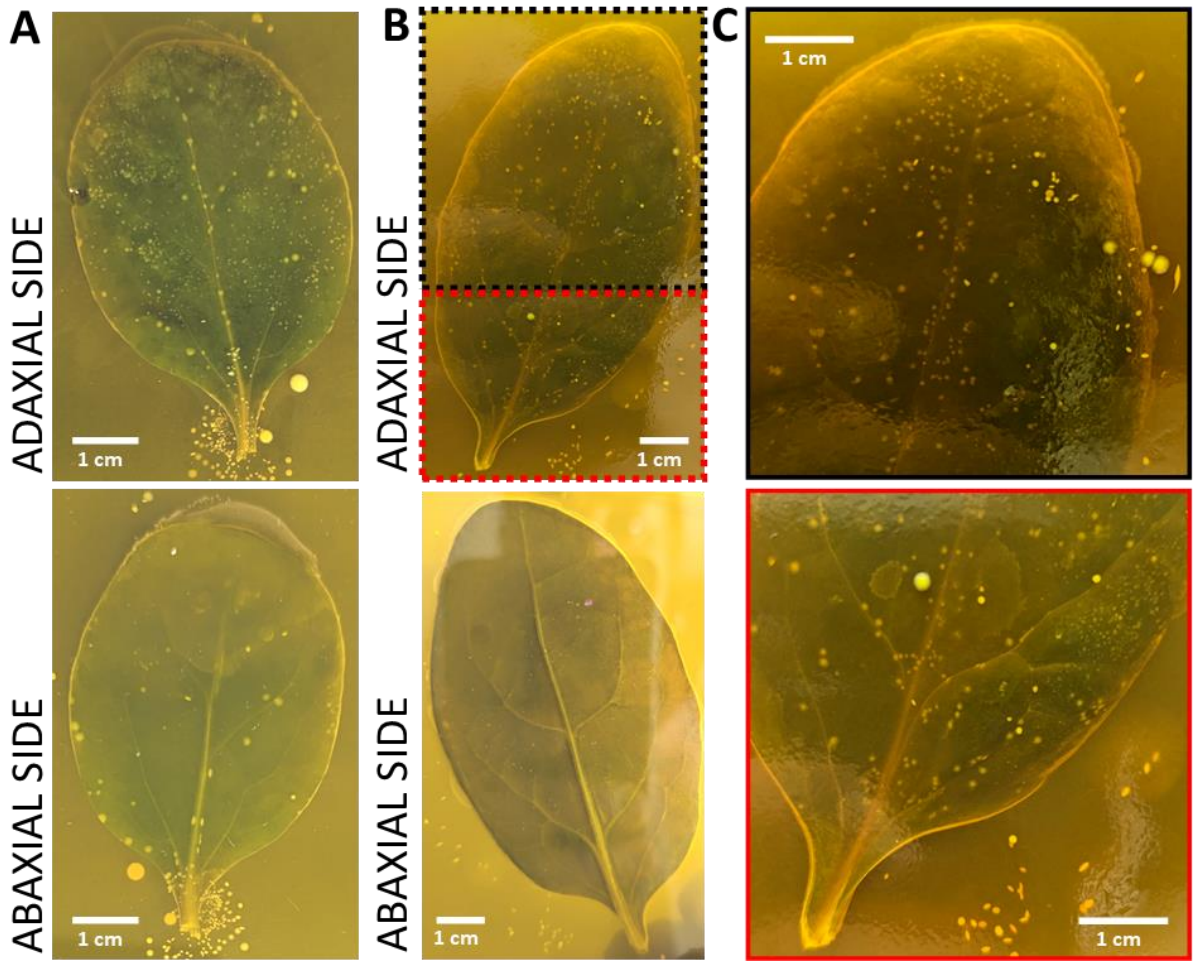

Figure 4.9 Photographs of spinach leaves inoculated with *L. monocytogenes* strain NLmo8 set in semi-soft agar.

Spinach leaves (cv. 'Nandu RZ') were submerged in PBS with 10^6 CFU/mL of bacteria, washed, embedded in *Listeria* enrichment agar, incubated at 30 °C, and photographed. Bacterial colonies, visible as opaque yellow spots, indicate the attachment sites of NLmo8 on the leaf surface. **(A)** Adaxial and abaxial sides of the same leaf. **(B)** Adaxial and abaxial sides of the same leaf. Red and black marked areas on the adaxial side are magnified in panel **(C)**.

4.3 Discussion

Different strains of *Lm* were investigated for their attachment to spinach and rocket, two commonly consumed salad vegetables. Strain EGD-e was selected as it has been widely used to study the biology of *Lm* (Bécavin *et al.*, 2014). Although limited information exists on EGD-e's interaction with plants, the extensive data available on other aspects of its biology could still provide valuable insights into potential mechanisms of leaf attachment. Strains NLmo8 and NLmo9 were originally isolated from spinach, and NLmo15 from pea shoots, indicating a prior association with salad vegetables, which suggests they may possess traits that facilitate attachment to plant surfaces.

4.3.1 Leaf disc assay to examine *L. monocytogenes* attachment to spinach leaves

Stomatal density, trichome presence, and moisture retention vary along the leaf axis and are known to affect bacterial attachment (Esmael *et al.*, 2023). Kroupitski *et al.* (2011) demonstrated that *S. enterica* ser. Typhimurium attachment to romaine lettuce varies across the leaf, reporting significant differences in bacterial attachment between the apex, centre, and base. To control for surface variability and solely compare the attachment capacity of different *Lm* strains, the lamina from the middle of the leaf was sampled in the disc assay to ensure consistent surface characteristics.

The leaf disc assay revealed a significant difference in attachment to spinach between strains NLmo8 and EGD-e (Figure 4.1). However, no significant difference was observed between EGD-e and NLmo8 when using the whole leaf assay (Figure 4.3). This disparity may be attributed to the significant variation between the two assays in terms of inoculum preparation, inoculation, and sampling methods.

Nevertheless, differences between the two strains in the disc assay may allude to strain-specific interactions with the leaf surface. Gorski *et al.* (2021) demonstrated that *Lm* attaches to leaf veins on romaine lettuce, while Ells and Truelstrup Hansen (2006) showed attachment to intact leaf surfaces but found no obvious affinity for specialised surface structures. These findings suggest that *Lm* can attach to various locations on the leaf surface. The difference observed between NLmo8 and EGD-e in the leaf disc

assay may reflect variations in their preferred attachment sites on the leaf surface. Further research is needed to determine whether specific strains exhibit distinct attachment patterns across different areas of the leaf.

4.3.2 Examining attachment to different cultivars using disc assay

Jacob and Melotto (2020) reported significant variation in the attachment of *S. enterica* ser. Typhimurium and *E. coli* among 11 lettuce cultivars. However, no significant difference in the attachment of NLmo8 to the 'Lazio' and 'Samish' spinach varieties was observed (Figure 4.2), which may be attributed to the disc assay's limitations in capturing variations in spinach surface topography that influence bacterial attachment (Lopez-Velasco *et al.*, 2011). For instance, the disc assay does not account for features such as vein density, which has been linked to cultivar-specific differences in *S. enterica* adherence to iceberg and Batavia lettuces (Hunter *et al.*, 2015). To address the limitations of the leaf disc assay in capturing the full range of surface features influencing bacterial attachment, the whole leaf assay developed. Overall, the findings by Hunter *et al.* (2015); Jacob and Melotto (2020) indicate that bacterial attachment may be cultivar dependent. The limited number of cultivars examined here likely underrepresents the variability in leaf surface characteristics across spinach varieties. Further investigation into *Lm* attachment across a broader range of cultivars is needed to assess potential cultivar-specific differences.

4.3.3 Role of inoculum exposure time in *L. monocytogenes* attachment to leaf surfaces

To assess how prolonged inoculum exposure affects attachment, spinach leaves inoculated with *Lm* strains NLmo8 or EGD-e were either dried for 1 h before washing or washed immediately after inoculation. Results showed that attachment significantly increased after the 1 h drying period for both strains (Figure 4.3). This trend aligns with findings by Ells and Truelstrup Hansen (2006), who quantified *Lm* strain Scott A attachment on cabbage leaves after 5 and 60 min of inoculum exposure. They reported increased attachment by 0.61, 0.74, and 0.51 log CFU/cm^2 for cells grown at 10 °C, 22 °C, and 37 °C, respectively. In the current study, attachment increased from non-

dried to dried spinach leaves by 0.34 log CFU/cm^2 for NLmo8 and 0.24 log CFU/cm^2 for EGD-e. Although this increase was smaller than that reported by Ells and Truelstrup Hansen (2006), differences between strains, inoculum preparation, and leaf surface characteristics may account for the variation. Nevertheless, these findings highlight the importance of considering inoculum exposure times in comparative studies, as they significantly impact bacterial recovery from leaf surfaces.

4.3.4 Investigating strain-specific attachment to salad leaves

Research on foodborne pathogens, such as *E. coli* and *Salmonella*, has demonstrated that attachment can differ significantly among strains on identical plant surfaces (Berger *et al.*, 2009b; Patel and Sharma, 2010; Wong *et al.*, 2019). Only a few studies have compared the attachment of multiple *Lm* strains on plant leaves of the same cultivar, highlighting a critical knowledge gap in understanding *Lm* interactions with plant leaf surfaces (Ells and Truelstrup Hansen, 2006; Kyere *et al.*, 2019a; Gorski *et al.*, 2021).

To assess variation in *Lm* attachment across strains on leaf surfaces, strains NLmo8 and EGD-e were tested on spinach (Figure 4.3), and NLmo8, NLmo9, NLmo15, and EGD-e on rocket leaves (Figure 4.4). No significant difference in attachment between strains NLmo8 and EGD-e on spinach was found (Figure 4.3). Similarly, Kyere *et al.* (2019a) reported no significant differences in attachment across three *Lm* strains on soil-grown buttercrunch lettuce. However, a significant difference was observed on hydroponically grown lettuce, with one strain attaching in significantly higher numbers than the other two after 2 and 5 min of exposure to the inoculum. These results highlight the multifactorial nature of attachment, where cultivation conditions, inoculum exposure time and strain-specific traits all contribute to variability in attachment outcomes.

Conversely, ANOVA analysis revealed significant differences in attachment among *Lm* strains NLmo8, NLmo9, NLmo15, and EGD-e on rocket leaves (Figure 4.4). However, post-hoc analysis showed that only EGD-e had significantly lower attachment to rocket leaves compared to NLmo8, with no significant differences observed among the other strains. Similar findings were reported by Ells and Truelstrup Hansen (2006) who

investigated the attachment of 24 *Listeria* strains to intact and cut cabbage leaf surfaces, including 14 *Lm* strains and 10 non-pathogenic strains, comprising 7 *L. welshimeri* and 3 *L. innocua*. Significant differences in attachment were observed across all strains on both surfaces as well as amongst the *Lm* strains. These results suggest that *Lm* exhibits strain specific attachment to rocket and cabbage leaf surfaces.

Strains NLmo8, NLmo9, and NLmo15 were originally isolated from plant-based sources, potentially having acquired characteristics through environmental selection that promote their interaction with plant surfaces. In contrast, EGD-e was originally isolated from rabbits and has been repeatedly passaged through mice to maintain virulence, suggesting it may be better adapted for interactions with animal cells than with plant surfaces (Murray *et al.*, 1926; Bécavin *et al.*, 2014). Given that only four strains were examined, three of which are from plant sources, further research is warranted to assess whether the isolation source influences bacterial attachment to plant surfaces. Identifying sources associated with enhanced attachment and colonisation could help reveal the environmental factors driving this phenotype, offering valuable insights for food safety monitoring.

4.3.5 Variation in *L. monocytogenes* attachment across salad species

Plant species exhibit considerable variation in surface characteristics, which can influence the attachment of *Lm* strains. For instance, Bae *et al.* (2013) found that *Lm* strain F2365 attached most efficiently to cantaloupe skin, followed by spinach, with the least attachment observed on lettuce. While these findings suggest variability in attachment across plant surfaces for the same strain, limited research exists on how attachment varies among *Lm strains* across various plant surfaces. To explore this further, the attachment of two *Lm* strains was assessed on spinach and rocket to determine if attachment varies by plant species and strain.

No significant difference was observed in the attachment of NLmo8 to spinach and rocket (Figure 4.5). In fact, the range and mean number of attached cells were similar for rocket (mean = 1823) and spinach (mean = 1843) (Figure 4.5). In contrast, EGD-e showed significantly higher attachment to spinach than to rocket (Figure 4.5). This variation in EGD-e attachment may be attributed to physicochemical differences

between the two plants and strain-specific attachment mechanisms. Notably, rocket leaves typically have fewer stomata and glandular trichomes than spinach, features that have been shown to influence bacterial attachment (Culliney and Schmalenberger, 2022; Esmael *et al.*, 2023). If EGD-e preferentially attaches to these features, it may explain the lower attachment observed on rocket. Identifying the preferential attachment sites for *Lm* could reveal which leaf features mediate attachment. Interestingly, no significant difference was found between NLmo8 and EGD-e on spinach (Figure 4.3). In fact, both strains attached in similar numbers after 1 h of drying. These results indicate that spinach may have a higher risk of contamination, as it supports attachment from a broader range of strains. Culliney and Schmalenberger (2022) reported that *Lm* has greater growth potential on spinach than on rocket. Together with the results from the present study, this suggests that *Lm* may be better adapted to colonising spinach than rocket, which should be considered when assessing *Lm* contamination risks in growing or processing environments. Identifying leafy vegetables that support attachment of fewer strains could help identify which salad species are at a lower risk of *Lm* contamination.

4.3.6 Exploring *L. monocytogenes* attachment preferences on leaf surfaces with immunofluorescent microscopy

To investigate where *Lm* strains NLmo8 and EGD-e attach to the leaf surface, immunofluorescent staining was used. Secondary antibody staining revealed that only EGD-e was successfully labelled with the *Lm*-specific antibody (Figure 4.6; Panel A and B), despite all strains (EGD-e, NLmo8, NLmo9) showing positive DNA staining (data not shown). This differential staining could suggest variability in surface epitopes among *Lm* strains, potentially influenced by structural or compositional differences in cell surface antigens. As details of the specific epitope targeted by the *Lm* antibody are proprietary, its conservation across strains could not be assessed. Additionally, the use of FA fixation may have compromised antigenicity, inhibiting antibody binding to NLmo8 and NLmo9 (Stanly *et al.*, 2016).

Confocal microscopy confirmed the attachment of EGD-e to the surface of rocket leaves (Figure 4.6; Panel C and D), though detection was limited to only a few sections

of leaf material, with a maximum of 2–3 cells observed in these sections. The sparse distribution of EGD-e made it difficult to assess attachment preference for specific leaf surfaces (e.g., abaxial vs. adaxial). EGD-e attachment was primarily observed in areas stained red by a plant-specific antibody (Figure 4.6; Panel C and D), which targets the homogalacturonan domain of pectin within plant cell walls. Pectins are primarily located beneath the cuticle, in the cell walls of epidermal cells (Domínguez *et al.*, 2011). In fact, previous research has shown that the cuticle restricts antibody access to pectin epitopes (Segado *et al.*, 2016). The localisation of EGD-e to pectin-stained areas suggests that the strain preferentially binds to sites where the cuticle is disrupted, exposing underlying pectin. This observation aligns with reports by Takeuchi *et al.* (2000), who, using confocal microscopy, observed *Lm* predominantly attaching to cut edges and cuticular cracks in lettuce, where pectin is more likely exposed. Similarly, Ells and Truelstrup Hansen (2006) observed *Lm* aggregation around tears and abrasions on cabbage leaves via SEM. Tan *et al.* (2016) reported that *Lm* can attach to pectin and xyloglucan, two major components of plant cell walls, in bacterial cellulose-based plant cell wall models. However, they found reduced attachment to these components compared to plain bacterial cellulose. Nonetheless, cracks in the cuticle and leaf edges likely expose cellulose in the plant cell walls. Notably, Bae *et al.* (2013) identified a gene in *Lm* encoding a cell surface protein with a cellulose-binding domain, demonstrating its role in cellulose attachment. Together, these studies suggest that structural damage to the leaf, exposing cellulose, may enhance *Lm* attachment. Overall, further research is needed to determine which plant cell wall components most effectively mediate *Lm* attachment.

4.3.7 Visualising *L. monocytogenes* attachment to leaf surfaces using GFP-expressing NLmo8

NLmo8 exhibited significantly higher attachment to rocket compared to EGD-e, which may improve its detection during microscopy analysis. As NLmo8 could not be stained with antibodies, it was genetically modified to constitutively express GFP for visualisation of its attachment to leaf surfaces (Figure 4.7). Growth dynamics did not differ significantly between NLmo8 Wt and NLmo8::cGFP, confirming that the integration of the GFP construct did not affect the strain's vigour (data not shown).

Despite successful transformation and comparable growth and attachment behaviour (Figure 4.8), no NLmo8::cGFP cells were detected on examined leaf sections.

The loss of fluorescence during fixation and autofluorescence from plant tissue, which obscures the GFP signal, may have hindered the detection of cells in this study. While exponential-phase cultures of NLmo8::cGFP fixed with FA retained GFP fluorescence (Figure 4.7), biochemical interactions between plant tissue and GFP during fixation may have compromised GFP stability and brightness. For example, Shenoy *et al.* (2017) investigated internalisation patterns in romaine lettuce using a *Lm* strain with an integrated GFP construct and reported GFP fluorescence loss during fixation. Therefore, fluorescence loss during fixation may have interfered with the detection of cells in this study.

Additionally, inoculated leaf tissue was fixed with formaldehyde, a weak cross-linker that can reverse during subsequent washes. Plant-specific features, such as the hydrophobic waxy cuticle and rigid cell wall, slow fixation, often leading to incomplete fixation (Wilson and Bacic, 2012). Consequently, many *Lm* cells may have been removed during subsequent processing, reducing detectable cell counts. Cell aggregation could further hinder detection by concentrating cells in specific regions of the leaf surface. For instance, Ells and Truelstrup Hansen (2006) observed *Lm* congregating around damaged tissue on cabbage leaves. Additionally, the limitations of confocal microscopy, particularly when examining thicker sections such as the central vein, made these regions difficult to analyse effectively.

Overall, factors such as low cell densities, clustering, autofluorescence, fluorescence quenching, cell removal during processing and imaging limitations with thicker sections may all have contributed to the lack of detectable cells. Milillo *et al.* (2008) successfully visualised GFP-expressing *Lm* bacteria on *Arabidopsis thaliana* leaves without using a fixative. This suggests it may be possible to view NLmo8::cGFP on the leaf surface if sections are prepared without fixation. Future work should explore alternative fixation protocols or non-fixative methods for the microscopic examination of *Lm* attachment to leaf surfaces.

4.3.8 Novel overlay assay to identify preferential attachment sites of *L. monocytogenes* on leaf surface

To identify *Lm* strain NLmo8 attachment sites on the leaf surface without microscopy, a novel overlay assay was developed. Inoculated leaves are embedded in a selective media with a low agar concentration, enabling *Lm* attached to the leaf surface to form colonies, thereby revealing putative attachment sites.

Following incubation, putative *Lm* colonies could be observed across the leaf surface, with distinct aggregation areas (Figure 4.9). Notably, colonies predominantly appeared on the adaxial side, which is the upper surface exposed to sunlight, on both leaves examined (Figure 4.9; Panel A and B). Preference for the adaxial side may be attributed to physicochemical differences between the adaxial and abaxial surfaces. Lopez-Velasco *et al.* (2011) demonstrated that three spinach cultivars exhibited greater stomatal density on the adaxial side, and two of these cultivars had more glandular trichomes on the adaxial surface. These factors have all been reported to facilitate bacterial attachment and may account for the observed preference for *Lm* attachment to the adaxial side of spinach leaves (Lopez-Velasco *et al.*, 2011; Esmael *et al.*, 2023).

Interestingly, the results from this study contrast with previous findings on bacterial attachment to leaf surfaces. For instance, Guan *et al.* (2023) reported significantly higher attachment of *Lm* on the abaxial side of lettuce, and Kroupitski *et al.* (2011) observed a similar preference in *Salmonella* on romaine lettuce. In contrast, Ells and Truelstrup Hansen (2006) observed no noticeable difference in *Lm* attachment between adaxial and abaxial sides on cabbage leaves, and Dong *et al.* (2024) reported no significant difference in *E. coli* attachment between these surfaces on various leafy greens, including spinach. Overall, these results suggest bacterial attachment may either occur equally on both sides of a leaf or preferentially to one side, depending on the specific bacterial and plant species involved.

In addition to the preferential attachment to adaxial surfaces observed here, bacterial colonies were predominantly concentrated along the leaf veins (Figure 4.9). Using confocal microscopy, Gorski *et al.* (2021) observed a similar trend, with *Lm* primarily attaching along the veins of romaine lettuce leaves. In the current study, large colonies

formed along the central vein, likely from cellular aggregation during growth (Figure 4.9; Panel A). Brandl and Mandrell (2002) similarly reported that *Salmonella* serovar Thompson developed microcolonies and aggregates along cilantro leaf veins 2 days post-inoculation, indicating that these regions are conducive to bacterial attachment and growth.

Several factors may account for the preferential attachment of bacteria to leaf veins. Vein cuticles are generally thinner and more prone to damage, providing additional attachment sites. Furthermore, bacteria frequently aggregate around leaf veins, potentially forming biofilms that can enhance *Lm* attachment (Beattie and Lindow, 1999). Additionally, in the present study, the grooves and crevices along veins likely shielded bacteria from washing, potentially contributing to the increased number of colonies observed in these areas.

Overall, *Lm* preferentially attached to the adaxial surface and leaf veins of the "Nandu RZ" spinach variety. Future research should examine the structural and biochemical differences between the adaxial and abaxial surfaces, which may provide insights into features that facilitate *Lm* attachment.

4.3.9 Conclusion

The attachment of different *Lm* strains was assessed on various spinach cultivars and rocket. Significant strain-specific differences in attachment were observed on the 'Samish' spinach cultivar using the leaf disc assay. However, no significant differences were found on the 'Nandu RZ' cultivar with the whole leaf assay. Differences in attachment between strains on the two cultivars may be attributed to variations in assay methodologies, strain-specific interactions and cultivar surface characteristics. Interestingly, no significant difference in attachment was found between two spinach cultivars or between rocket and spinach for NLmo8. In contrast, EGD-e exhibited a significant difference in attachment between rocket and spinach, suggesting that some plant species may support the attachment of a greater variety of strains. Furthermore, NLmo8 showed significantly higher attachment to rocket compared to EGD-e, indicating that certain strains, like NLmo8, have a greater capacity to attach to diverse plant surfaces. Prolonged exposure to an inoculum significantly increased attachment

for both NLmo8 and EGD-e, indicating that extended contact with a contamination source, such as a contaminated cutting surface, can lead to greater bacterial transfer.

While the preferential attachment sites for NLmo8 and EGD-e may explain strain specific attachment patterns, attempts to examine NLmo8's preferred attachment sites using antibody labelling or integrated GFP construct were unsuccessful. Microscopy analysis of EGD-e, labelled with a GFP antibody, revealed that the cells were predominantly attached to areas on rocket leaves stained red with a pectin antibody. This suggests that EGD-e preferentially attaches to regions where pectin is exposed. This result aligns with previous studies reporting that *Lm* preferentially attaches to damaged areas of the leaf, where pectin is likely exposed. The overlay assay used to identify preferential attachment sites for NLmo8 on spinach demonstrated a preference for the adaxial surface and along the leaf veins. Vein cuticles, being thinner, and more rigid vascular tissue, are more susceptible to damage, which may explain the higher attachment numbers in these areas. It remains to be determined whether this attachment to cut sites and damaged areas is due to an affinity for pectin or other exposed cell wall components.

Overall, the attachment of *Lm* to rocket and spinach leaves is a multifactorial process influenced by environmental conditions, as well as bacterial and leaf-specific characteristics. Further research is needed to elucidate the biochemical and structural differences between plant species that contribute to the observed variations in attachment. Understanding these factors could aid the development of strategies to reduce contamination risk, such as safer cultivation practices and the selection of salad varieties less prone to contamination. Nevertheless, the preference for damaged areas on the leaf underscores the importance of appropriate handling practices during cultivation and processing to minimise damage and reduce contamination risk.

Chapter 5 – Volatile organic compound analysis for detecting *Listeria monocytogenes* contamination in rocket

5.1 Introduction

5.1.1 *L. monocytogenes* a growing risk in RTE salad.

Listeriosis, the bacterial infection caused by *L. monocytogenes* (*Lm*), is primarily contracted through the consumption of contaminated food (Scallan *et al.*, 2011). Although Listeriosis outbreaks have predominantly been linked to RTE animal-based products, RTE fruit and vegetable products are also increasingly being associated with *Listeria* outbreaks (EFSA, 2021a). Amongst the RTE fruit and vegetables category, RTE salads is a growing segment of the fresh food industry due to a growing demand for convenient, nutritious foods that require minimal processing (Gullino *et al.*, 2019). *Lm* is frequently detected in the cultivation and processing environments of leafy salad vegetables, underscoring the risk of cross-contamination during the RTE salad production process (Smith *et al.*, 2018; Gil *et al.*, 2024). Given that RTE salads are generally consumed raw, with no "killing step" applied before consumption, they present an ongoing risk of Listeriosis transmission.

5.1.2 Rocket as a source of *L. monocytogenes*

Wild rocket (*Diplotaxis tenuifolia)*, known for its "peppery" and slightly bitter taste, contains various beneficial nutrients such as carotenoids, vitamin C, fibre, flavonoids and glucosinolates (Bell *et al.*, 2016; Spadafora *et al.*, 2016a). Valued for its distinct flavour and health benefits, fresh wild rocket is a popular vegetable in the UK, often consumed in salads or on its own, with year-round, steadily increasing demand (Bell *et al.*, 2017).

Rocket is typically grown in soil in open fields, polytunnels, or greenhouses, where it can become contaminated with *Lm* through contact with contaminated soil, irrigation water, fertilizer, animals or farming equipment (Bell *et al.*, 2017; Smith *et al.*, 2018). Besides the cultivation environment contamination can occur at various points throughout the supply chain. The British climate in not conducive to year around growth, therefore the

majority of rocket is imported from Italy, and occasionally from other countries (Bell *et al.*, 2020). The complexity of the supply chain, with multiple handling and transportation stages, increases the risk of contamination in rocket.

To retain product quality and ensure food safety, it is recommended that rocket is stored at 0 °C (Koukounaras *et al.*, 2007). However, in many cases leaves are processed, transported and stored at 5 °C. Breaks in cold-chain maintenance are common with reports of temperatures reaching +20 °C (Zhou *et al.*, 2022). Additionally, *Lm* can grow at refrigeration temperatures (Saldivar *et al.*, 2018). Culliney and Schmalenberger (2020) demonstrated that rocket inoculated with 100 CFU/g of *Lm*, reached median cell counts of 3 $\log_{10}$ CFU/g after 7 days of storage at 8 °C. These contamination levels are comparable to those found in foods linked to Listeriosis outbreaks (Farber and Peterkin, 1991; Vázquez-Boland *et al.*, 2001). While refrigeration can slow the growth of *Lm*, the temperatures typically used in the cold chain, along with disruptions in temperature maintenance, significantly increase the risk of contamination.

The shelf life of rocket ranges from 7 – 14 days, depending on environmental conditions, during which *Lm* can proliferate to harmful levels (Martínez-Sánchez *et al.*, 2008; Culliney and Schmalenberger, 2020). Consequently, it is essential to prevent contamination from occurring in the first place. While this may not always be possible, regular microbial testing of processing areas and food samples can help identify risks and prevent distribution of contaminated products.

5.1.3 Detection methods for *L. monocytogenes* in food

Most countries require the use of the International Organization for Standardization (ISO) method, or an adapted version, for the detection (ISO 11290-1:2017) and enumeration (ISO 11290-2:2017) of *Lm* in food and environmental samples (Jordan *et al.*, 2018). While the ISO method has a high degree of sensitivity and specificity it can take up to 5 – 7 days to confirm a contamination (Gnanou Besse *et al.*, 2019). Due to the highly perishable nature of leafy vegetables this time frame exceeds the shelf life of many fresh cut vegetables (Paramithiotis *et al.*, 2018). The farm-to-retail period should be as short as possible, typically 1 – 2 days, to maintain product quality, which may result in products reaching consumers before contamination is confirmed

(Paramithiotis *et al.*, 2018). A faster detection method could enhance food safety by enabling earlier identification of contamination in fresh-cut vegetables.

Due to the time-consuming nature of culture-based methods, various molecular and immunological techniques have been developed for faster detection. Most alternative methods certified for commercial use rely on nucleic acid sequences or protein epitopes to detect *Lm* (Chikhi *et al.*, 2024). Molecular methods typically use PCR for nucleic acid detection, which is highly sensitive but requires expensive equipment, consumables and specialised training. Immunological methods, based on antibody-antigen reactions, generally incur lower equipment costs. However, a major drawback of antibody-based tests is the potential for cross-reactivity with food samples or other bacteria, leading to false positives (Chikhi *et al.*, 2024). Additionally, both nucleic acid and antibody-based methods cannot distinguish between live and dead cells. Although faster than culture methods, both nucleic acid and antibody-based techniques require a pre-enrichment step, taking at least one day for presumptive positive identification (Rohde *et al.*, 2017).

The limitations of both conventional and alternative detection methods for *Lm* have driven ongoing research aimed at improving speed, sensitivity, specificity and throughput (Gupta and Adhikari, 2022). In this context, the analysis of volatile organic compounds (VOCs) released from fresh produce has been proposed as alternative strategy for detecting *Lm* in food samples.

5.1.4 VOC analysis for the detection of microorganisms in food

VOCs are low molecular weight compounds that readily volatilize at ambient pressure and are emitted by all organisms, including bacteria (Tait *et al.*, 2014b). Some VOCs can be associated with microbial growth, food spoilage or act as indicators of quality in RTE food products. For instance, elevated concentrations of dimethyl sulphide correlate with higher microbial counts (Spadafora *et al.*, 2016a; Luca *et al.*, 2017) and reduced sensorial quality of wild (Spadafora *et al.*, 2016a) and cultivated (Nielsen *et al.*, 2008) rocket. Certain VOCs are unique to specific organisms and can serve as biomarkers for a contamination or infection (Cox and Parker, 1979; Kai *et al.*, 2009; Żuchowska and Filipiak, 2024). Therefore, volatile organic compound (VOC) analysis can detect

microbial growth, food spoilage and potentially identify contamination (Fan *et al.*, 2023).

Technologies under development to detect microbial contaminants include sensor arrays and electronic noses (e-noses) (Fan *et al.*, 2023). Sensor arrays can detect specific compounds linked to particular contaminants (Perillo and Rodríguez, 2016). E-noses use multiple sensors to detect chemical signals or VOC patterns associated with specific organisms (Bonah *et al.*, 2020). While these methods can be effective for detecting microbial VOCs, they require appropriate detection systems and prior knowledge of the organism's VOC profile (Fan *et al.*, 2023).

Due to the complexity and variability of VOC profiles in food products, untargeted analysis of a wide range of VOCs typically involves gas chromatography coupled with mass spectrometry (GC-MS) (Żuchowska and Filipiak, 2024). Solid phase micro extraction (SPME) coupled with GC-MS has become a popular technique because it eliminates the need for solvents, reducing both cost and environmental impact (Fan *et al.*, 2023). SPME utilises a small fibre coated with an adsorbent material to capture VOCs from the sample environment, which are then desorbed and analysed by GC-MS. SPME can be used to detect and identify microorganisms in food (Wang *et al.*, 2016). However, the low stability of VOCs, which limits the long-term storage and transportation of the SPME fibres used for VOC collection, prevents off-site analysis (Żuchowska and Filipiak, 2024). Furthermore, the high cost of GC-MS equipment makes it economically unfeasible to store on-site at processing or farming facilities.

In contrast, a thermal desorption–gas chromatography–time-of-flight mass spectrometry (TD-GC-TOF-MS) platform allows for rapid and reliable on-site VOC collection, with subsequent off-site analysis. The platform employs thermal desorption tubes containing a porous polymer that efficiently traps VOCs, which are released through heating (Fan *et al.*, 2023). TD tubes have been shown to store VOCs from exhaled breath for up to 39 days without significant loss (Ahmed *et al.*, 2018). While GC-MS equipment is costly, TD tubes allow for analysis to be outsourced to external companies, eliminating the need to invest in and maintain expensive equipment and employ specialised in-house personnel.

The detection of *Lm* in cantaloupe melon through the analysis of VOCs using the TD-GC-TOF-MS platform has been previously reported by Spadafora *et al.* (2016b). The same group demonstrated that VOC analysis of rocket using this platform could differentiate between storage temperature and duration, with specific VOC changes correlating with shifts in nutritionally important compounds (Spadafora *et al.*, 2016a). VOC-based analysis can thus be used for microbial detection and coupled with quality assessment, providing insights into product quality, handling conditions, and potential hazards in the supply chain, offering additional benefits that other detection methods do not.

The increasing prevalence of *Lm* in RTE salads is a growing concern due to the rising demand for these products. Rocket is susceptible to *Lm* contamination and can support the growth of this pathogen. Due to the highly perishable nature of rocket, conventional detection methods take too long to detect contamination within a suitable timeframe. Analysis of VOCs using TD-GC-TOF-MS has shown potential in providing qualitative insights into rocket quality and detecting *Lm* in food samples. This study utilised TD-GC-TOF-MS to assess whether *Lm* can be detected in rocket, accounting for the seasonal and yearly variability in factors affecting VOC profiles. Sensitivity was further tested by examining VOC profiles of the non-pathogenic *L. innocua* strain. Further refinement of the method was achieved by analysing VOCs detected across all experiments.

The following aims and objectives are addressed in this chapter to evaluate the detection of *Lm* contamination in rocket through VOC analysis.

5.1.5 Aims and objectives

- Investigate whether *L. monocytogenes* contamination in rocket can be detected through the analysis of volatile organic compound profiles.
- Determine if specific volatile organic compounds can be associated with *L. monocytogenes* contamination, and whether a panel of these can be used to determine if rocket has become contaminated.
- Assess whether volatile organic compounds can be used to distinguish between *L. monocytogenes* and *L. innocua* contamination in rocket.

5.1.6 Review of the methodology

Four experiments were conducted using rocket leaves purchased in different years and seasons. This approach accounts for potential seasonal and annual variations in leaf composition, ensuring that any differences in VOCs between contaminated and uncontaminated samples are not confounded by these temporal factors.

Rocket leaves were spray-inoculated with *Lm* strain NLmo8 to simulate contamination from soil splash or irrigation water (Figure 2.4). As a control, leaves were sprayed with sterile PBS (uninoculated). After inoculation, the leaves were washed, dried, and placed in oven roasting bags, which were sealed and incubated at 37 °C. Headspace samples were collected at 3 and 6 h, with a separate bag used for each time point.

The experiments were performed sequentially. For Experiments 3 and 4, the bags were placed in storage boxes lined with activated carbon to absorb VOCs from the surrounding environment.

GC-MS data were processed to eliminate contaminants, compounds detected in blank samples and those outside the linear detection range. Compounds within the detectable range in all or all but one sample for each group (e.g. inoculated and incubated for 3 h) were included in the analysis.

5.2 Results

5.2.1 Compounds detected by TD-GC-TOF-MS across four experiments

A total of 101, 89, 60, and 70 compounds were detected in experiments 1, 2, 3 and 4 (Exp. 1–4), respectively (Table 5.1). Of these, 65, 65, 48, and 60 compounds, respectively, were putatively identified by matching mass spectra to the NIST library and retention index. For those without putative identification, 35, 22, 12, and 10 compounds, respectively, were assigned to a chemical class. Three compounds, one in Exp. 1 and two in Exp. 2 remained unknown. The number of compounds detected in each chemical class across the experiments is summarised in Table 5.1, with specific compounds listed and categorised by chemical class in Table 5.2.

Alkanes were the most prevalent class identified across all experiments. In Exp. 1 and 3, esters were the second most prevalent class, with 11 and 7 compounds identified, respectively. In Exp. 2, aldehydes (6), aromatic hydrocarbons (6), and esters (6) were the most frequently identified after alkanes. In Exp. 4, aldehydes (7) were the second most prevalent class. A total of 25 compounds were common to all four experiments, which are highlighted in bold in Table 5.2.

Table 5.1 Number of compounds detected in each chemical class across experiments with putative identifications and without putative identifications.

Chemical Class	Experiment [a]											
	1			2			3			4		
Alcohol	5	1	6	2	2	4	2	2	4	4	2	6
Aldehyde	7	0	7	6	0	6	4	0	4	7	0	7
Alkane	13	34	47	34	20	54	25	10	35	32	8	40
Alkene	5	0	5	3	0	3	1	0	1	1	0	1
Aromatic	7	0	7	6	0	6	2	0	2	4	0	4
Carboxylic acid	3	0	3	1	0	1	2	0	2	1	0	1
Cycloalkane	2	0	2	1	0	1			0			0
Ester	11	0	11	6	0	6	7	0	7	6	0	6
Ether	1	0	1			0	1	0	1			0
Heterocyclic	2	0	2			0			0			0
Ketone	5	0	5	1	0	1	2	0	2	0	0	3
Sulphur compound	2	0	2	2	0	2	2	0	2			0
Terpene	2	0	2	3	0	3			0	2	0	2
Unknown			1			2			0			0
Total	65	35	101	65	22	89	48	12	60	60	10	70

[a] The columns for each experiment, from left to right, represent: number of VOCs with putative ID, unidentified VOCs assigned to a chemical class and the total number of compounds detected for each chemical class.

Table 5.2 Volatile organic compounds detected from rocket leaves inoculated with *L. monocytogenes* and uninoculated leaves.

Compound Name	CAS No.	Molecular Formula	Experiment[a] 1	2	3	4
Alcohol						
1-Hexanol	111-27-3	$C_6H_{14}O$				
1-Octanol, 3,7-dimethyl-	106-21-8	$C_{10}H_{22}O$				
1-Octanol, 3,7-dimethyl-, (S)-	68680-98-8	$C_{10}H_{22}O$				
2-Ethyl-1-dodecanol	19780-33-7	$C_{14}H_{30}O$				
3-Hexen-1-ol, (Z)-	928-96-1	$C_6H_{12}O$				
Alcohol1	-	-				
Branched alcohol2	-	-				
Hexadecen-1-ol, trans-9-	64437-47-4	$C_{16}H_{32}O$				
Phenol	108-95-2	C_6H_6O				
Aldehyde						
2-Hexenal	505-57-7	$C_6H_{10}O$				
3-Hexenal	4440-65-7	$C_6H_{10}O$				
Acetaldehyde	75-07-0	C_2H_4O				
Benzaldehyde	100-52-7	C_7H_6O				
Decanal	112-31-2	$C_{10}H_{20}O$				
Dodecanal	112-54-9	$C_{12}H_{24}O$				
Nonanal	124-19-6	$C_9H_{18}O$				
Octanal	124-13-0	$C_8H_{16}O$				
Pentanal	110-62-3	$C_5H_{10}O$				
Tetradecanal	124-25-4	$C_{14}H_{28}O$				
Tridecanal	10486-19-8	$C_{13}H_{26}O$				
Undecanal	112-44-7	$C_{11}H_{22}O$				
Alkane						
2,6-Dimethyldecane	13150-81-7	$C_{12}H_{26}$				
Alkane2	-	-				
Branched alkane 2	-	-				
Branched alkane 21	-	-				
Branched alkane 3	-	-				
Branched alkane 5	-	-				
Branched alkane11	-	-				
Branched alkane16	-	-				
Branched alkane4	-	-				
Branched alkane9	-	-				
Branched alkane1	-	-				
Branched alkane3	-	-				
Branched alkane4	-	-				
Branched alkane5	-	-				
Branched alkaneG1	-	-				
Branched alkaneG12	-	-				
Branched alkaneG13	-	-				
Branched alkaneG14	-	-				
Branched alkaneG15	-	-				
Branched alkaneG16	-	-				
Branched alkaneG17	-	-				
Branched alkaneG2	-	-				
Branched alkaneG3	-	-				
Branched alkaneG4	-	-				
Branched alkaneG5	-	-				
Branched alkaneG6	-	-				
Branched alkaneG7	-	-				
Branched alkaneG8	-	-				
Butane, 2-methyl-	78-78-4	C_5H_{12}				
Decane	124-18-5	$C_{10}H_{22}$				
Decane, 2,4-dimethyl-	2801-84-5	$C_{12}H_{26}$				
Docosane	629-97-0	$C_{22}H_{46}$				
Dodecane	112-40-3	$C_{12}H_{26}$				
Dodecane, 2,6,10-trimethyl-	3891-98-3	$C_{15}H_{32}$				
Dodecane, 2,6,11-trimethyl-	31295-56-4	$C_{15}H_{32}$				
Dodecane, 2,7,10-trimethyl-	74645-98-0	$C_{15}H_{32}$				
Dodecane, 3-methyl-	17312-57-1	$C_{13}H_{28}$				
Dodecane, 4,6-dimethyl-	61141-72-8	$C_{14}H_{30}$				

Dodecane, 4-methyl-	6117-97-1	$C_{13}H_{28}$	
Eicosane	112-95-8	$C_{20}H_{42}$	
Heneicosane	629-94-7	$C_{21}H_{44}$	
Heptadecane	629-78-7	$C_{17}H_{36}$	
Heptane	142-82-5	C_7H_{16}	
Heptane, 2,2,4,6,6-pentamethyl-	13475-82-6	$C_{12}H_{26}$	
Heptane, 2,4-dimethyl-	2213-23-2	C_9H_{20}	
Heptane, 2,5,5-trimethyl-	1189-99-7	$C_{10}H_{22}$	
Heptane, 4-methyl-	589-53-7	C_8H_{18}	
Hexadecane	544-76-3	$C_{16}H_{34}$	
Hexadecane, 2-methyl-	1560-92-5	$C_{17}H_{36}$	
Hexadecane, 3-Methyl-	6418-43-5	$C_{17}H_{36}$	
Hexadecane, 7-methyl-	26730-20-1	$C_{17}H_{36}$	
Hexane	110-54-3	C_6H_{14}	
Nonadecane	629-92-5	$C_{19}H_{40}$	
Nonane	111-84-2	C_9H_{20}	
Nonane, 2,5-dimethyl-	17302-27-1	$C_{11}H_{24}$	
Nonane, 2,6-dimethyl-	17302-28-2	$C_{11}H_{24}$	
Nonane, 2-methyl-	871-83-0	$C_{10}H_{22}$	
Nonane, 4-methyl-	17301-94-9	$C_{10}H_{22}$	
Octadecane	593-45-3	$C_{18}H_{38}$	
Octane	111-65-9	C_8H_{18}	
Octane, 1,1'-oxybis-	629-82-3	$C_{16}H_{34}O$	
Octane, 2,4,6-trimethyl-	62016-37-9	$C_{11}H_{24}$	
Octane, 2,7-dimethyl-	1072-16-8	$C_{10}H_{22}$	
Octane, 4-methyl-	2216-34-4	C_9H_{20}	
Pentadecane	629-62-9	$C_{15}H_{32}$	
Pentadecane, 2-methyl-	1560-93-6	$C_{16}H_{34}$	
Pentadecane, 3-methyl-	2882-96-4	$C_{16}H_{34}$	
Pentadecane, 4-methyl-	2801-87-8	$C_{16}H_{34}$	
Pentane, 2-methyl-	107-83-5	C_6H_{14}	
Pentane, 3-methyl-	96-14-0	C_6H_{14}	

Tetradecane	629-59-4	$C_{14}H_{30}$	
Tetradecane, 2-methyl-	1560-95-8	$C_{15}H_{32}$	
Tetradecane, 3-methyl-	18435-22-8	$C_{15}H_{32}$	
Tetradecane, 5-methyl-	25117-32-2	$C_{15}H_{32}$	
Tridecane	629-50-5	$C_{13}H_{28}$	
Tridecane, 2-methyl-	1560-96-9	$C_{14}H_{30}$	
Tridecane, 3-methyl-	6418-41-3	$C_{14}H_{30}$	
Tridecane, 4,8-dimethyl-	55030-62-1	$C_{15}H_{32}$	
Undecane	1120-21-4	$C_{11}H_{24}$	
Undecane, 2,3-dimethyl-	17312-77-5	$C_{13}H_{28}$	
Undecane, 2-methyl-	7045-71-8	$C_{12}H_{26}$	
Undecane, 3,6-dimethyl-	17301-28-9	$C_{13}H_{28}$	
Undecane, 4,8-dimethyl-	17301-33-6	$C_{13}H_{28}$	
Undecane, 4-methyl-	2980-69-0	$C_{12}H_{26}$	
Undecane, 5,7-dimethyl-	17312-83-3	$C_{13}H_{28}$	
Undecane, 5-methyl-	1632-70-8	$C_{12}H_{26}$	
Alkene			
1-Nonene, 4,6,8-trimethyl-	54410-98-9	$C_{12}H_{24}$	
2,4-Dimethyl-1-heptene	19549-87-2	C_9H_{18}	
2-Decene, 5-methyl-, (Z)-	74645-86-6	$C_{11}H_{22}$	
5,9-Undecadien-2-one, 6,10-dimethyl-, (E)-	3796-70-1	$C_{13}H_{22}O$	
5-Ethyl-1-nonene	19780-74-6	$C_{11}H_{22}$	
Nonane, 2-methyl-3-methylene-	55499-08-6	$C_{11}H_{22}$	
Aromatic Hydrocarbon			
1H-Indene, 2,3-dihydro-1,1,3-trimethyl-3-phenyl-	3910-35-8	$C_{18}H_{20}$	
Benzene	71-43-2	C_6H_6	
Benzene, 1,2,3-trimethyl-	526-73-8	C_9H_{12}	
Ethylbenzene	100-41-4	C_8H_{10}	
o-Xylene	95-47-6	C_8H_{10}	
Styrene	100-42-5	C_8H_8	

Toluene	108-88-3	C_7H_8				
Carboxylic Acid						
Acetic acid	64-19-7	$C_2H_4O_2$				
Hexadecenoic acid, Z-11-	2416-20-8	$C_{16}H_{30}O_2$				
n-Hexadecanoic acid	57-10-3	$C_{16}H_{32}O_2$				
Cycloalkane						
Cyclohexane	110-82-7	C_6H_{12}				
Cyclohexane, hexyl-	4292-75-5	$C_{12}H_{24}$				
Cyclopropane, 1-ethyl-2-methyl-, cis-	19781-68-1	C_6H_{12}				
Ester						
1-Hexadecanol, acetate	629-70-9	$C_{18}H_{36}O_2$				
Butanoic acid, 2-methyl-, ethyl ester	7452-79-1	$C_7H_{14}O_2$				
Butanoic acid, 3-methyl-, ethyl ester	108-64-5	$C_7H_{14}O_2$				
Butanoic acid, ethyl ester	105-54-4	$C_6H_{12}O_2$				
Butanoic acid, methyl ester	623-42-7	$C_5H_{10}O_2$				
Dodecanoic acid, 1-methylethyl ester	10233-13-3	$C_{15}H_{30}O_2$				
Ethyl Acetate	141-78-6	$C_4H_8O_2$				
Isopropyl palmitate	142-91-6	$C_{19}H_{38}O_2$				
n-Propyl acetate	109-60-4	$C_5H_{10}O_2$				
Propanoic acid, 2-methyl-, ethyl ester	97-62-1	$C_6H_{12}O_2$				
Propanoic acid, ethyl ester	105-37-3	$C_5H_{10}O_2$				
Ether						
1,3-Dioxolane, 2-methyl-	497-26-7	$C_4H_8O_2$				
2-Propanol, 1-methoxy-	107-98-2	$C_4H_{10}O_2$				
Heterocyclic Compound						
Benzothiazole	95-16-9	C_7H_5NS				
Furan, 2-pentyl-	3777-69-3	$C_9H_{14}O$				
Ketone						
2-Butanone	78-93-3	C_4H_8O				
2-Hexanone	591-78-6	$C_6H_{12}O$				
2-Pentanone	107-87-9	$C_5H_{10}O$				
4-Heptanone, 2,6-dimethyl-	108-83-8	$C_9H_{18}O$				
5-Hepten-2-one, 6-methyl-	110-93-0	$C_8H_{14}O$				
Acetophenone	98-86-2	C_8H_8O				
Sulphur Compound						
Dimethyl sulfide	75-18-3	C_2H_6S				
Dimethyl sulfone	67-71-0	$C_2H_6O_2S$				
Diphenyl sulfone	127-63-9	$C_{12}H_{10}O_2S$				
Terpene						
β-Pinene	127-91-3	$C_{10}H_{16}$				
3-Carene	13466-78-9	$C_{10}H_{16}$				
α-Pinene	80-56-8	$C_{10}H_{16}$				
D-Limonene	5989-27-5	$C_{10}H_{16}$				
Limonene	138-86-3	$C_{10}H_{16}$				
Tricyclo[2.2.1.0(2,6)]heptane, 1,3,3-trimethyl-	488-97-1	$C_{10}H_{16}$				
Unknown						
Unknown1	-	-				
Unknown2	-	-				
Unknown3	-	-				
Total compounds			**101**	**89**	**60**	**70**

[a] Compounds detected in an experiment are indicated by blue cells.

5.2.2 Comparison of VOC profiles from rocket leaves inoculated with *L. monocytogenes* and uninoculated following incubation at 37 °C

Firstly, differences in VOC profiles between inoculated and uninoculated (control) leaves were tested using the complete data set (data from 3 h and 6 h incubation periods were combined for each group).

No significant difference ($P > 0.05$) was detected for Exp. 1, 2 and 4 (PerMANOVA, Table 5.3). In contrast, PerMANOVA revealed a significant difference ($P \leq 0.05$) between the VOC profiles of inoculated and uninoculated samples in Exp. 3 ($P = 0.005$, $R^2 = 0.38003$), with inoculation status accounting for 38% of the variance in the dataset (Table 5.3). A Tukey's HSD test showed a significant difference ($P \leq 0.05$) in dispersion between the VOC profiles of inoculated and uninoculated samples. This unequal dispersion should be considered a caveat, as it may affect the validity of the PerMANOVA results.

Linear discriminant (LD) plots from CAP showed significant discrimination between the total VOC profiles at a 95% confidence level between inoculated and uninoculated samples for Exp. 1, 2, and 3 (Figure 5.1). Overall, classification success exceeded 90% across the three experiments, with at least one sample group achieving 100% classification success per experiment, though the specific group varied between experiments.

In contrast, CAP analysis did not reveal significant differences in VOC profiles between inoculated and uninoculated samples at a 95% confidence level for Exp. 4 (Figure 5.1). Additionally, classification success for both groups in Exp. 4 was lower (71.43%) compared to the other experiments (Figure 5.1).

Table 5.3 PerMANOVA results examining differences between VOC profiles from rocket leaves inoculated with *L. monocytogenes* and uninoculated leaves.

Experiment	Source of Variation	Df [b]	R^2 [c]	F [d]	P-value[e]
1	Model (Inoculation Status) [a]	1	0.10101	1.1236	0.318
	Residual	10	0.89899		
	Total	11	1		
2	Model (Inoculation Status) [a]	1	0.0934	1.3393	0.234
	Residual	13	0.9066		
	Total	14	1		
3	Model (Inoculation Status) [a]	1	0.38003	8.5819	0.005 *
	Residual	14	0.61997		
	Total	15	1		
4	Model (Inoculation Status) [a]	1	0.04472	0.5617	0.717
	Residual	12	0.95528		
	Total	13	1		

[a] Model tested for differences in VOC profiles between inoculated and uninoculated samples, combining data from 3 and 6 h incubation periods for each condition.
[b] Df: Degrees of freedom
[c] R^2: Coefficient of determination, representing the proportion of variance explained by the factor.
[d] F: pseudo-F statistic, ratio of between-group to within-group variance.
[e] Differences between inoculated and uninoculated sample groups were considered statistically significant when $P \leq 0.05$, with significant results marked by an asterisk (*).

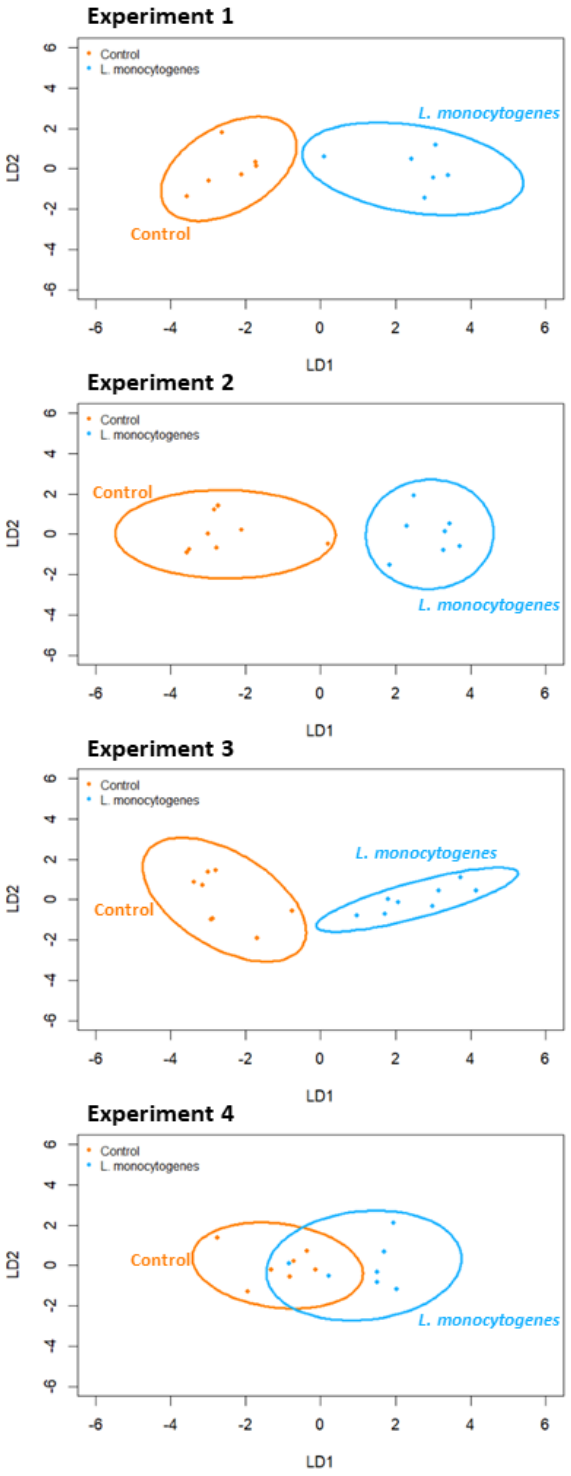

	Classification success (%)
Overall	91.67
Control (n=6)	100
L. monocytogenes (n=6)	83.33

	Classification success (%)
Overall	93.33
Control (n=8)	87.5
L. monocytogenes (n=7)	100

	Classification success (%)
Overall	93.75
Control (n=8)	87.5
L. monocytogenes (n=8)	100

	Classification success (%)
Overall	71.43
Control (n=7)	71.43
L. monocytogenes (n=7)	71.43

Figure 5.1 CAP analysis of VOC profiles from rocket leaves inoculated with *L. monocytogenes* and uninoculated leaves.
Ordination plots of LD 1 and LD 2 from CAP analysis are shown for each experiment. Rocket leaves were incubated for 3 or 6 h at 37 °C before headspace sampling. VOC profiles from inoculated leaves at both time points were combined and compared with combined VOC profiles from control (i.e. uninoculated) leaves. Ellipses represent 95% confidence intervals, and classification success for each group is indicated next to the ordination plots. Replicates for each condition are denoted by 'n'.

5.2.3 Analysis of VOC profiles from rocket leaves for differences caused by inoculation with *L. monocytogenes*, controlling for 3 and 6 h of incubation at 37 °C

The following analysis was conducted to assess the effect of inoculation on VOC profiles while accounting for potential temporal shifts in VOC production. PerMANOVA revealed that across all experiments, there was a significant ($P \leq 0.05$) effect of incubation period on VOC profiles (Table 5.4). The contribution of incubation period to the variability of the datasets varied across experiments, accounting for 30%, 37%, 17%, and 21% of the variability in Exp. 1, 2, 3, and 4, respectively. Only in Exp. 3 did inoculation status have a significant ($P \leq 0.05$) effect on VOC profiles, contributing 38% to the variability in the dataset. In all experiments, the interaction between incubation period and inoculation status was not significant ($P > 0.05$), indicating that the change in VOC profiles over time (from 3 to 6 h) followed a similar pattern for both inoculated and uninoculated samples.

Across experiments, LD plots from CAP, using incubation time and inoculation as combined variable, showed significant discrimination between VOC profiles of inoculated and uninoculated (control) leaves incubated for 6 h at the 95% confidence level. (Figure 5.2). Classification success for VOC profiles from inoculated leaves after 6 h of incubation was consistently among the highest across experiments (Exp. 1: 100%, Exp. 2: 100%, Exp. 3: 75%, Exp. 4: 66.67%) (Figure 5.2).

VOC profiles from all sample groups could be discriminated at the 95% confidence level in Exp. 2 and 3. In contrast, profiles from inoculated and uninoculated leaves in Exp. 1 and 4 could not be differentiated for the 3 h incubation period. For Exp. 4, VOC profiles for inoculated leaves after 6 h of incubation were distinct, whereas VOC profiles from the other sample groups could not be discriminated from each other. Notably, Exp. 4 had the lowest overall classification success, followed by Exp. 2, 1 and then 3 (Figure 5.2).

Across all experiments, correctly classified VOC profiles totalled 12/15 for uninoculated leaves after 3 h incubation, 9/14 for uninoculated leaves after 6 h, 9/14 for inoculated leaves after 3 h, and 12/14 for inoculated leaves after 6 h.

Table 5.4 PerMANOVA results testing the effect of incubation period and inoculation status on VOC profiles from rocket leaves.

Experiment	Source of Variation	Df [a]	R^2 [b]	F [c]	P-value[d]
1	Incubation Period	1	0.30807	4.1197	0.022 *
	Inoculation Status	1	0.12414	0.83	0.531
	Interaction	1	0.04433	0.5928	0.569
	Residuals	8	0.52346		
	Total	11	1		
2	Incubation Period	1	0.37058	7.8848	0.003 *
	Inoculation Status	1	0.07842	1.6685	0.187
	Interaction	1	0.034	0.7235	0.492
	Residuals	11	0.517		
	Total	14	1		
3	Incubation Period	1	0.17301	5.2401	0.034 *
	Inoculation Status	1	0.38003	11.5104	0.003 *
	Interaction	1	0.05076	1.5374	0.231
	Residuals	12	0.3962		
	Total	15	1		
4	Incubation Period	1	0.21448	3.2477	0.015 *
	Inoculation Status	1	0.04472	0.6771	0.607
	Interaction	1	0.0804	1.2174	0.282
	Residuals	10	0.6604		
	Total	13	1		

[a] Df: Degrees of freedom

[b] R^2: Coefficient of determination, representing the proportion of variance explained by the factor.

[c] F: pseudo-F statistic, ratio of between-group to within-group variance.

[d] Statistical significance at $P \leq 0.05$ is indicated by an asterisk (*).

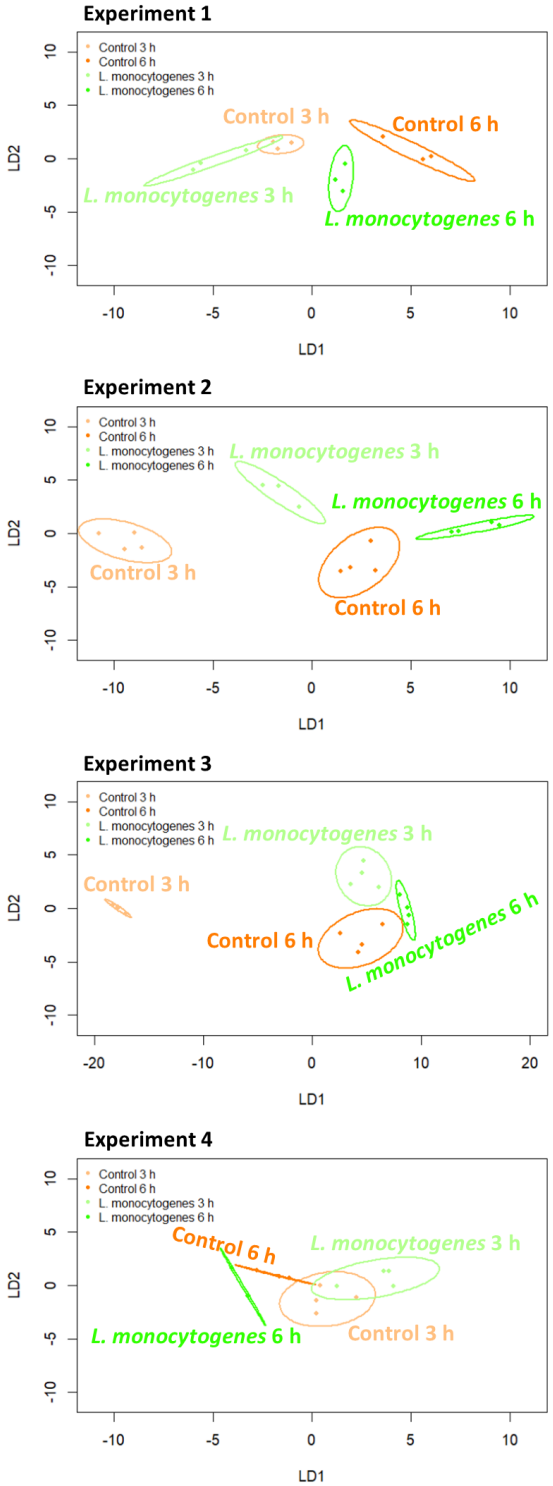

	Classification success (%)
Overall	83.33
Control 3 h (n=3)	100
Control 6 h (n=3)	66.67
L. monocytogenes 3 h (n=3)	66.67
L. monocytogenes 6 h (n=3)	100

	Classification success (%)
Overall	66.67
Control 3 h (n=4)	100
Control 6 h (n=4)	50
L. monocytogenes 3 h (n=3)	33.33
L. monocytogenes 6 h (n=4)	100

	Classification success (%)
Overall	87.5
Control 3 h (n=4)	100
Control 6 h (n=4)	75
L. monocytogenes 3 h (n=4)	100
L. monocytogenes 6 h (n=4)	75

	Classification success (%)
Overall	50
Control 3 h (n=4)	25
Control 6 h (n=3)	66.67
L. monocytogenes 3 h (n=4)	50
L. monocytogenes 6 h (n=3)	66.67

Figure 5.2 CAP analysis of VOC profiles from rocket leaves inoculated with *L. monocytogenes* and uninoculated leaves incubated for 3 or 6 h at 37 °C.
Ordination plots of LD 1 and LD 2 from CAP analysis are shown for each experiment. Rocket leaves were sprayed with *L. monocytogenes* (inoculated) or PBS (control i.e. uninoculated) and incubated for 3 or 6 h at 37 °C before headspace sampling. Ellipses represent the 95% confidence intervals, and classification success for each sample group is shown next to the ordination plots. Replicates for each condition are denoted by 'n'.

5.2.4 Analysis of VOC profiles from rocket leaves for differences caused by *L. monocytogenes* inoculation in data separated by incubation period

To examine how inoculation affects VOC profiles at each time point, samples incubated for 3 or 6 h were analysed separately using CAP and PerMANOVA.

PerMANOVA analysis revealed a significant ($P \leq 0.05$) difference between VOC profiles of inoculated and uninoculated samples following 3 h of incubation at 37 °C for Exp. 3 (Table 5.5). Inoculation status accounted for 65.6% of the variance in the dataset. However, for none of the experiments could PerMANOVA differentiate VOC profiles from inoculated and uninoculated samples following 6 h of incubation at 37 °C (Table 5.6).

As shown by LD plots (Figure 5.3), CAP differentiated VOC profiles for both sample groups after 3 h of incubation in Exp. 2 and 3 at the 95% confidence level, but not in the other two experiments. However, across experiments, VOC profiles of leaves incubated for 3 h were correctly classified for 12/15 uninoculated (control) and 11/14 inoculated samples. In contrast, after 6 h of incubation, classification success was lower for uninoculated samples (10/14) compared to inoculated samples (12/14) (Figure 5.4).

LD plots from CAP (Figure 5.4), showed differentiation of VOC profiles from inoculated and uninoculated samples for Exp. 1 after 6 h of incubation at the 95% confidence level, but not in the other three experiments. In two of the four experiments (Exp. 2 and 3), VOC profiles from inoculated samples after 6 h of incubation were misclassified for only a single replicate, with no misclassification in the remaining experiments. In contrast, uninoculated samples were misclassified more frequently across all experiments.

Table 5.5 PerMANOVA results testing for differences between VOC profiles of inoculated and uninoculated leaves following 3 h of incubation at 37 °C.

Experiment	Source of Variation	Df [a]	R^2 [b]	F [c]	P-value [d]
1	Inoculation status	1	0.22066	1.1325	0.3
	Residual	4	0.77934		
	Total	5	1		
2	Inoculation status	1	0.1729	1.0452	0.409
	Residual	5	0.8271		
	Total	6	1		
3	Inoculation status	1	0.65638	11.461	0.027 *
	Residual	6	0.34362		
	Total	7	1		
4	Inoculation status	1	0.16622	1.1962	0.365
	Residual	6	0.83378		
	Total	7	1		

[a] Df: Degrees of freedom

[b] R^2: Coefficient of determination, representing the proportion of variance explained by the factor.

[c] F: pseudo-F statistic, ratio of between-group to within-group variance.

[d] Statistical significance at P ≤ 0.05 is indicated by an asterisk (*).

Table 5.6 PerMANOVA results testing for differences between VOC profiles of inoculated and uninoculated leaves following 6 h of incubation at 37 °C.

Experiment	Source of Variation	Df [a]	R^2 [b]	F [c]	P-value[d]
1	Inoculation status	1	0.21368	1.087	0.4
	Residual	4	0.78632		
	Total	5	1		
2	Inoculation status	1	0.18715	1.3815	0.25
	Residual	6	0.81285		
	Total	7	1		
3	Inoculation status	1	0.29043	2.4558	0.127
	Residual	6	0.70957		
	Total	7	1		
4	Inoculation status	1	0.12425	0.5675	0.6
	Residual	4	0.87575		
	Total	5	1		

[a] Df: Degrees of freedom

[b] R^2: Coefficient of determination, representing the proportion of variance explained by the factor.

[c] F: pseudo-F statistic, ratio of between-group to within-group variance.

[d] Statistical significance at P ≤ 0.05 is indicated by an asterisk (*).

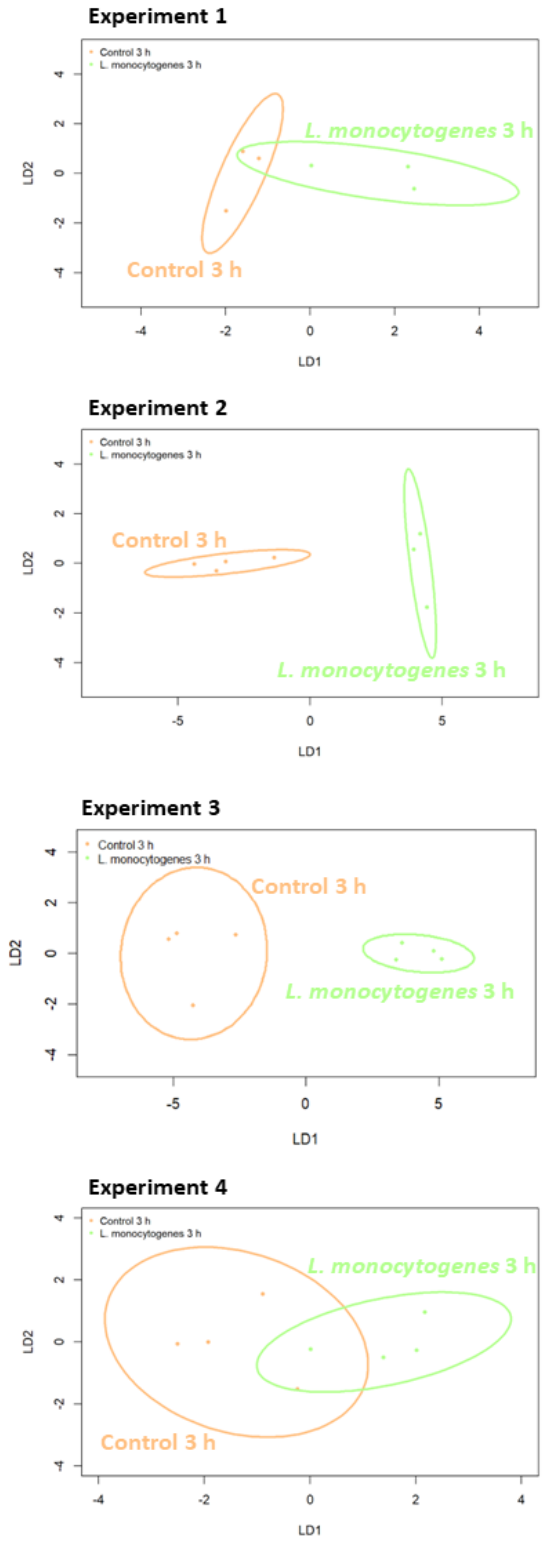

	Classification success (%)
Overall	83.33
Control 3 h (n=3)	100
L. monocytogenes 3 h (n=3)	66.67

	Classification success (%)
Overall	71.43
Control 3 h (n=4)	75
L. monocytogenes 3 h (n=3)	66.67

	Classification success (%)
Overall	87.5
Control 3 h (n=4)	75
L. monocytogenes 3 h (n=4)	100

	Classification success (%)
Overall	75
Control 3 h (n=4)	75
L. monocytogenes 3 h (n=4)	75

Figure 5.3 CAP analysis of VOC profiles from rocket leaves inoculated with *L. monocytogenes* and uninoculated leaves incubated for 3 h at 37 °C.
Ordination plots of LD 1 and LD 2 from CAP analysis are shown for each experiment. Rocket leaves were sprayed with *L. monocytogenes* (inoculated) or PBS (control i.e. uninoculated) and incubated for 3 h at 37 °C before headspace sampling. Ellipses represent the 95% confidence intervals, and classification success for each group is shown next to the ordination plots. Replicates for each condition are denoted by 'n'.

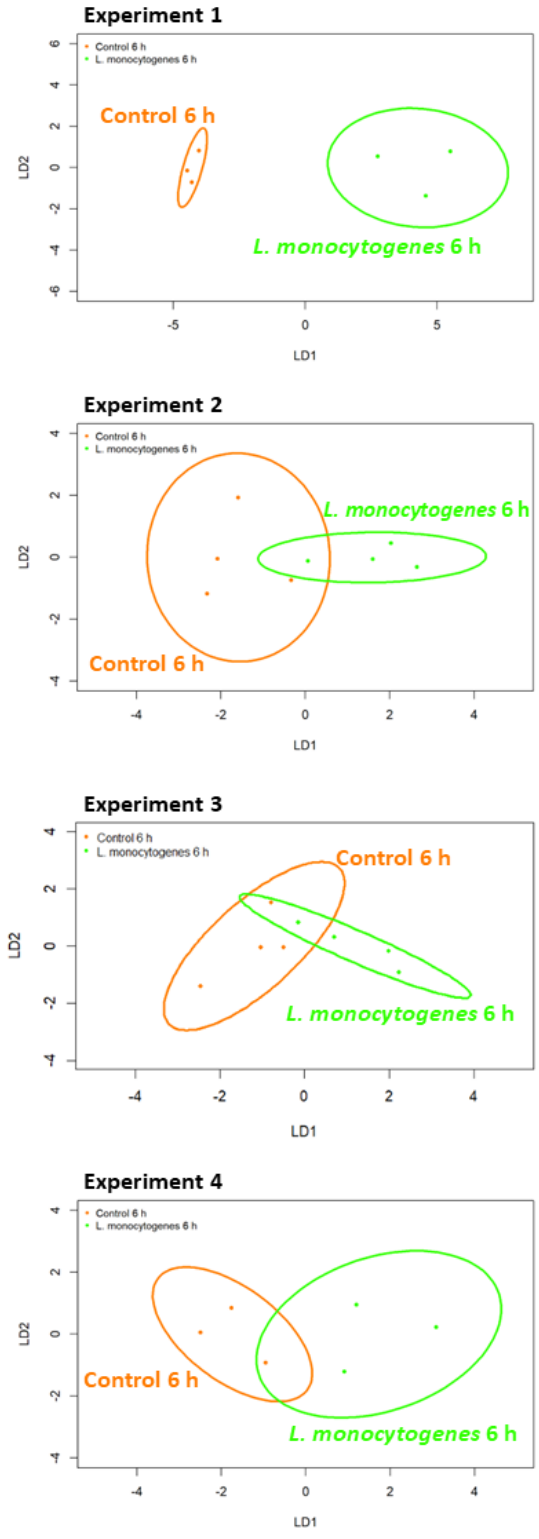

	Classification success (%)
Overall	100
Control 6 h (n=3)	100
L. monocytogenes 6 h (n=3)	100

	Classification success (%)
Overall	62.5
Control 6 h (n=4)	50
L. monocytogenes 6 h (n=4)	75

	Classification success (%)
Overall	75
Control 6 h (n=4)	75
L. monocytogenes 6 h (n=4)	75

	Classification success (%)
Overall	83.33
Control 6 h (n=3)	66.67
L. monocytogenes 6 h (n=3)	100

Figure 5.4 CAP analysis of VOC profiles from rocket leaves inoculated with *L. monocytogenes* and uninoculated leaves incubated for 6 h at 37 °C.
Ordination plots of LD 1 and LD 2 from CAP analysis are shown for each experiment. Rocket leaves were sprayed with *L. monocytogenes* (inoculated) or PBS (control i.e. uninoculated) and incubated for 6 h at 37 °C before headspace sampling. Ellipses represent the 95% confidence intervals, and classification success for each group is shown next to the ordination plots. Replicates for each condition are denoted by 'n'.

5.2.5 Analysis of a panel of VOCs, released from rocket leaves inoculated with *L. monocytogenes*, shared across all experiments.

A total of 25 VOCs were consistently identified across all four experiments (Table 5.2). CAP and PerMANOVA were used to evaluate whether this panel of VOCs could be used to distinguish between inoculated and uninoculated (control) samples.

Data from all four experiments were combined to test whether this panel of VOCs could differentiate between inoculated and uninoculated samples, irrespective of the incubation period. As shown by LD plots, CAP failed to differentiate between inoculated and uninoculated samples at the 95% confidence level when incubation periods and all four experiments were combined (Figure 5.5). Classification success was similar for both sample groups, with 21/29 (72.41%) for uninoculated samples and 21/28 (75%) for inoculated samples. To account for time-dependent variations in VOC production, the incubation periods were also analysed separately. When incubation periods were analysed separately in the combined dataset, LD plots revealed that CAP could not discriminate VOC profiles from inoculated and uninoculated samples at the 95% confidence level (Figure 5.5).

PerMANOVA did not reveal significant differences ($P > 0.05$) between VOC profiles of inoculated and uninoculated samples, whether incubation periods were combined or analysed separately. Specifically, for the combined incubation periods, $P = 0.96$; for the 3 h incubation period, $P = 0.95$; and for the 6 h incubation period, $P = 0.96$.

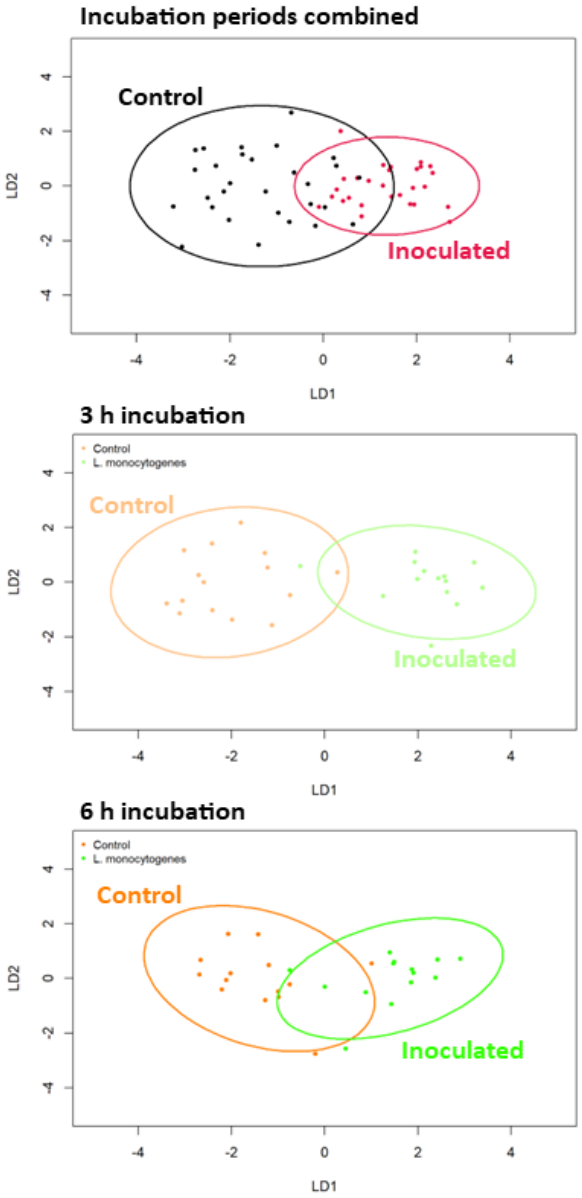

	Classification Success (%)
Overall	73.68
Control (n = 29)	72.41
Inoculated (n = 28)	75

	Classification Success (%)
Overall	75.86
Control (n = 15)	73.33
Inoculated (n = 14)	78.57

	Classification Success (%)
Overall	78.57
Control (n = 14)	78.57
Inoculated (n = 14)	78.57

Figure 5.5 Combined CAP analysis of a panel of VOCs shared across four experiments.

Ordination plots of LD 1 and LD 2 from CAP analysis testing for differences between inoculated and uninoculated rocket leaves. Leaves were sprayed with *L. monocytogenes* (inoculated) or PBS (control i.e. uninoculated) and incubated for 3 or 6 h at 37 °C before headspace sampling. This process was repeated in four separate experiments. VOCs collected from the headspace were separated and identified using GC-TOF-MS, and 25 compounds were consistently detected across all experiments. For this panel of VOCs, profiles from samples incubated for 3 and 6 h from all four experiments were combined and analysed by CAP. Additionally, the 3 and 6 h incubation periods were analysed separately. Ellipses represent 95% confidence intervals, and classification success for each group is indicated next to the ordination plots. Replicates for each condition are denoted by 'n'.

To account for differences in leaf composition due to year-to-year and seasonal variability, as well as differences in the VOC collection process between experiments, each experiment was analysed separately. This approach minimises confounding variability and allows for a clearer assessment of the effects of inoculation and incubation periods on VOC profiles from different batches of rocket leaves.

As shown by LD plots (Figure 5.6), CAP analysis successfully discriminated between all sample groups in Exp. 1, 2, and 3. Among these, Exp. 1 demonstrated the greatest separation between sample groups, as indicated by the largest dispersion along both the LD 1 and LD 2 axes. While LD plots for Exp. 2 and 3 showed comparable dispersion between groups, samples in Exp. 2 exhibited tighter clustering overall, suggesting lower within-group variability. Exp. 4 had the lowest overall classification success (50%), with ellipses representing the 95% confidence intervals overlapping for all groups, indicating that CAP could not discriminate the VOC profiles for any of the groups.

Across all experiments, uninoculated samples incubated for 3 h were most frequently correctly classified (11/15; 73.33%), followed by inoculated samples incubated for either 3 h or 6 h (10/14; 71.43%), and lastly uninoculated samples incubated for 6 h (8/14; 57.14%). However, classification success varied across experiments and was not consistently maintained for any group.

PerMANOVA revealed a significant ($P \leq 0.05$) effect of incubation period on VOC profiles across all experiments (Table 5.7). The contribution of incubation period to the variability of the datasets varied across experiments, accounting for 38%, 48%, 17%, and 25% of the variability in Exp. 1, 2, 3, and 4, respectively. In contrast, inoculation status significantly ($P \leq 0.05$) affected VOC profiles only in Exp. 1 and 3 accounting for 24% and 26% of the variability, respectively. The interaction between incubation period and inoculation status was not significant ($P > 0.05$) in any experiment, indicating that changes in VOC profiles over time (from 3 to 6 h) followed a similar pattern for both inoculated and uninoculated samples.

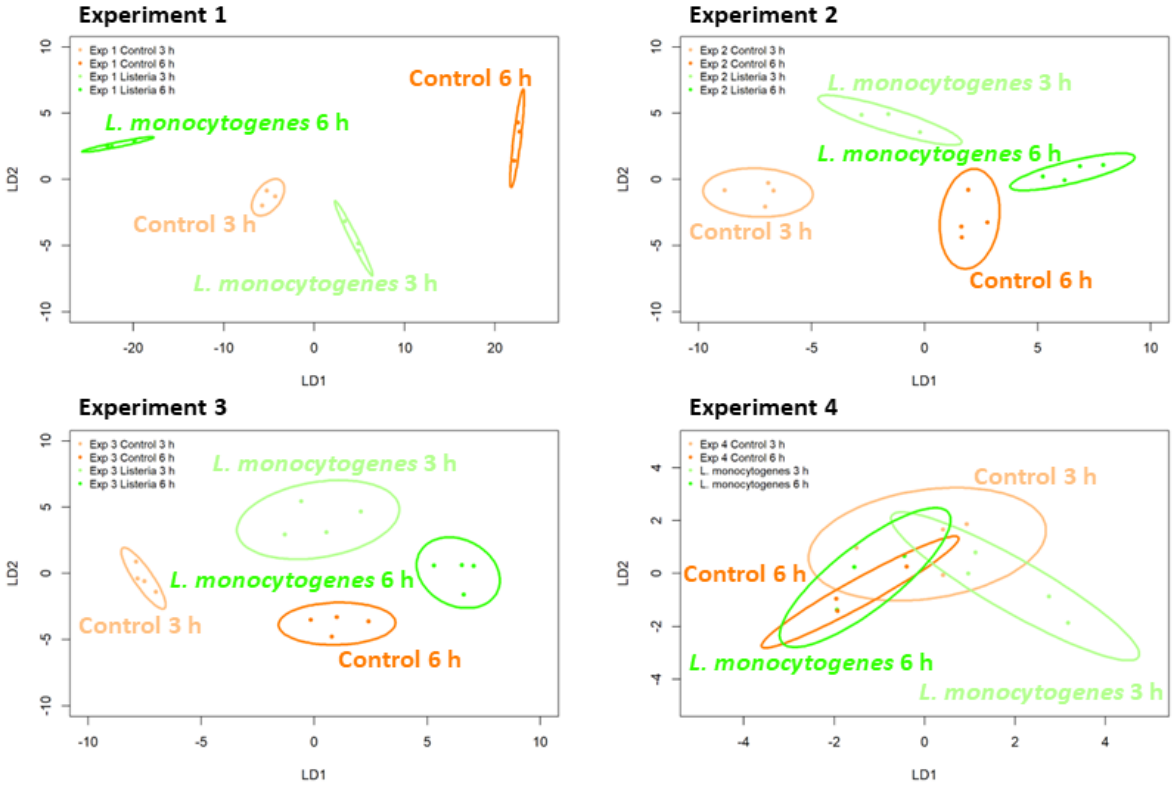

	Classification Success (%)			
	Experiment 1	Experiment 2	Experiment 3	Experiment 4
Overall	83.33	66.67	75	50
Control 3 h	66.67 (n=3)	100 (n=4)	75 (n=4)	50 (n=4)
Control 6 h	100 (n=3)	25 (n=4)	50 (n=4)	66.67 (n=3)
L. monocytogenes 3 h	66.67(n=3)	66.67 (n=3)	100 (n=4)	50 (n=4)
L. monocytogenes 6 h	100 (n=3)	75 (n=4)	75 (n=4)	33.33 (n=3)

Figure 5.6 CAP analysis of a panel of VOCs shared across four experiments, with each experiment analysed independently.

Ordination plots of LD1 and LD2 from CAP analysis testing for differences between inoculated and uninoculated rocket leaves are shown for each experiment. Leaves were sprayed with *L. monocytogenes* (inoculated) or PBS (control i.e. uninoculated) and incubated for 3 or 6 h at 37 °C before headspace sampling. This process was repeated across four separate experiments. VOCs collected from the headspace were separated and identified using GC-TOF-MS, and 25 compounds were consistently detected across all experiments. For this panel of VOCs, profiles for inoculated and uninoculated samples following 3 and 6 h of incubation were analysed by CAP. Ellipses represent 95% confidence intervals. Classification success for each sample group is summarised in a table below the ordination plots for all four experiments. Replicates for each condition are denoted by 'n'.

Table 5.7 PerMANOVA results testing the effect of inoculation status and incubation period on the composition of a panel of VOCs.

Experiment	Source of Variation	Df [a]	R^2 [b]	F [c]	P-value[d]
1	Time point	1	0.38275	9.3985	0.001 *
	Inoculation Status	1	0.24416	5.9952	0.005 *
	Interaction	1	0.04729	1.1612	0.314
	Residuals	8	0.3258		
	Total	11	1		
2	Time point	1	0.48485	12.356	0.001 *
	Inoculation Status	1	0.05946	1.5154	0.228
	Interaction	1	0.02405	0.6129	0.543
	Residuals	11	0.43164		
	Total	14	1		
3	Time point	1	0.16676	3.6959	0.042 *
	Inoculation Status	1	0.25651	5.685	0.029 *
	Interaction	1	0.03528	0.7818	0.392
	Residuals	12	0.54145		
	Total	15	1		
4	Time point	1	0.25015	3.892	0.02 *
	Inoculation Status	1	0.04127	0.6421	0.619
	Interaction	1	0.06586	1.0247	0.37
	Residuals	10	0.64272		
	Total	13	1		

[a] Df: Degrees of freedom

[b] R^2: Coefficient of determination, representing the proportion of variance explained by the factor.

[c] F: pseudo-F statistic, ratio of between-group to within-group variance.

[d] Statistical significance at $P \leq 0.05$ is indicated by an asterisk (*).

5.2.6 Analysis of VOC Profiles from rocket leaves to assess differences following inoculation with *L. monocytogenes* or *L. innocua* after 3 or 6 h of incubation at 37 °C

The VOC profiles released from rocket leaves inoculated with *L. innocua*, *L. monocytogenes* or PBS (control i.e. uninoculated) after 3 or 6 h of incubation at 37 °C were analysed using CAP and PerMANOVA (Figure 5.7; Table 5.8; Table 5.9). The analysis aimed to determine whether VOC profiles from *L. innocua* could be distinguished from *Lm* and whether VOC profiles from *L. innocua* obscured differences between *Lm* and uninoculated samples.

The datasets for *L. innocua* and *Lm* were processed independently before statistical analyses. In the *L. innocua* dataset, the peak integrals of *2-Hexanone, Toluene* and *Undecanal* were below the baseline value in two or more replicates for all sample groups (data not shown). However, these compounds were included in the analysis as they were above the baseline in three out of four replicates for at least one *Lm* sample group.

CAP analysis was first performed on the entire dataset to identify general separation patterns, then separately for each incubation period to minimise time-related confounding effects and identify the most discriminatory time point.

When VOC profiles from both the 3 h and 6 h incubation periods were analysed together, CAP could not differentiate profiles from *L. innocua*-inoculated samples and *Lm*-inoculated samples that were incubated for 3 h, at the 95% confidence level (Figure 5.7). However, CAP successfully distinguished VOC profiles from uninoculated samples from both bacterial inoculation groups at the 95% confidence level. For VOC profiles following 6 h of incubation, CAP could not differentiate *L. innocua*-inoculated samples from uninoculated samples at the 95% confidence level. Nevertheless, CAP distinguished profiles from *Lm*-inoculated samples from both *L. innocua*-inoculated and uninoculated samples at the 95% confidence level (Figure 5.7).

When VOC profiles from each incubation period were analysed independently, CAP successfully differentiated profiles from *L. innocua*, *Lm* and uninoculated samples following 3 h of incubation at the 95% confidence level (Figure 5.7). Additionally,

classification success for each group improved compared to the combined analysis of both incubation periods. These findings were further supported by PerMANOVA which revealed a significant difference ($P \leq 0.05$) between VOC profiles after 3 h of incubation, with inoculum type accounting for 71.3% of the variation in the model (Table 5.8). However, pairwise comparisons did not identify significant differences between individual sample groups, making it unclear which groups contributed to the observed variation.

In contrast, for VOC profiles following 6 h of incubation, CAP could not differentiate any sample group at the 95% confidence level (Figure 5.7). Classification success for *L. innocua*-inoculated samples also dropped significantly, from 75% in the combined analysis to 25% when the 6 h incubation period was analysed separately. Similarly, PerMANOVA did not reveal significant differences ($P > 0.05$) in VOC profiles between inoculum conditions after 6 h of incubation (Table 5.9).

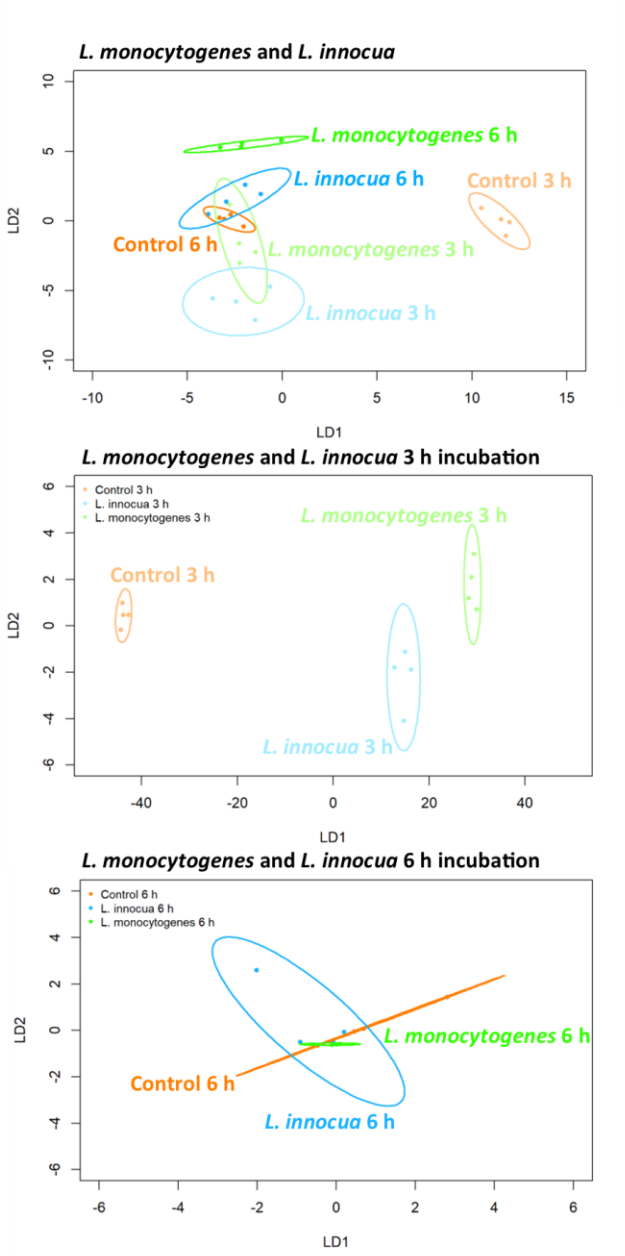

	Classification Success (%)
Overall	66.67
Control 3 h (n=4)	50
Control 6 h (n=4)	50
L. innocua 3 h (n=4)	75
L. innocua 6 h (n=4)	75
L. monocytogenes 3 h (n=4)	75
L. monocytogenes 6 h (n=4)	75

	Classification Success (%)
Overall	91.67
Control 3 h (n=4)	100
L. innocua 3 h (n=4)	100
L. monocytogenes 3 h (n=4)	75

	Classification Success (%)
Overall	66.67
Control 6 h (n=4)	75
L. innocua 6 h (n=4)	25
L. monocytogenes 6 h (n=4)	100

Figure 5.7 CAP analysis of VOC profiles from rocket leaves inoculated with *L. innocua*, *L. monocytogenes* and uninoculated leaves incubated at 37 °C.
Rocket leaves were sprayed with either *L. innocua, L. monocytogenes* or PBS (control i.e. uninoculated) and incubated for 3 or 6 h at 37 °C before headspace sampling. VOCs from the headspace were analysed using GC-TOF-MS. Ordination plots of LD 1 and LD 2 from CAP analysis are presented. VOC profiles from leaves inoculated with *L. innocua*, *L. monocytogenes* or PBS after 3 and 6 h of incubation were analysed together and for each incubation period separately. Ellipses represent 95% confidence intervals, and classification success for each group is shown next to the ordination plots. Replicates for each condition are denoted by 'n.

Table 5.8 Results from PerMANOVA testing for differences in VOC profiles from rocket leaves inoculated with *L. innocua*, *L. monocytogenes* or PBS after 3 h incubation at 37 °C.

Source of Variation	Df [a]	R^2 [b]	F [c]	P-value[d]
Inoculum	1	0.71325	24.873	0.002 *
Residuals	10	0.28675		
Total	11	1		
Pairwise comparison	**Df**	**R^2**	**F**	**Adjusted P-value[d e]**
L. monocytogenes – *L. innocua*	1	0.309962	2.69517	0.066
L. monocytogenes – Uninoculated	1	0.543769	7.15124	0.066
L. innocua – Uninoculated	1	0.555251	7.490757	0.066

[a] Df: Degrees of freedom

[b] R^2: Coefficient of determination, representing the proportion of variance explained by the factor.

[c] F: pseudo-F statistic, ratio of between-group to within-group variance.

[d] Statistical significance at P ≤ 0.05 is indicated by an asterisk (*).

[e] P-values were adjusted using the Benjamini-Hochberg method.

Table 5.9 Results from PerMANOVA testing for differences in VOC profiles from rocket leaves inoculated with *L. innocua*, *L. monocytogenes* or PBS after 6 h incubation at 37 °C.

Source of Variation	Df [a]	R^2 [b]	F [c]	P-value[d]
Inoculum	1	0.20179	2.528	0.071
Residuals	10	0.79821		
Total	11	1		
Pairwise comparison	**Df**	**R^2**	**F**	**Adjusted P-value[d e]**
Uninoculated – *L. monocytogenes*	1	0.3509984	3.244969	0.0585
Uninoculated – *L. innocua*	1	0.1783542	1.302416	0.2320
L. monocytogenes – *L. innocua*	1	0.3751308	3.602010	0.0585

[a] Df: Degrees of freedom

[b] R^2: Coefficient of determination, representing the proportion of variance explained by the factor.

[c] F: pseudo-F statistic, ratio of between-group to within-group variance.

[d] Statistical significance at P ≤ 0.05 is indicated by an asterisk (*).

[e] P-values were adjusted using the Benjamini-Hochberg method.

5.3 Discussion

Rocket leaves spray inoculated with *L. monocytogenes* (*Lm*) were estimated to have a bacterial load of 10^4 to 10^6 CFU/g of *Lm* prior to incubation. The ISO reference method (ISO 11290-1:2017) for the detection of *Lm* in food can detect *Lm* at concentrations of 10 to 100 CFU/g (Gnanou Besse *et al.*, 2019). While the bacterial load used in this study far exceeds these levels, it provides a suitable starting point for assessing whether the methodology employed in this study can be used to detect *Lm* contamination in rocket.

The VOC collection and analysis method employed in this study facilitated the detection and quantification of a total of 320 VOCs across the four experiments. Using a similar VOC collection and analysis method to that employed in this study, Spadafora *et al.* (2018) identified 41 distinct VOCs from store-bought rocket, of which only 6 (2-Hexenal, 3-Hexenal, 3-Hexen-1-ol, Eicosane, n-Propyl acetate, Dimethyl sulfide) were also detected in this study (Table 5.2). Interestingly, more than twice as many compounds were identified from rocket leaves in Exp. 1 and 2 (101 and 89 VOCs), and approximately 50% more compounds were identified in Exp. 3 and 4 (60 and 70 VOCs) compared to the Spadafora *et al.* (2018) study. Differences in sampling methodology between this study and that of Spadafora *et al.* (2018) likely contributed considerably to variability in VOC profiles.

Lm produces its own set of VOCs including alcohols, amines, esters, hydrocarbons and ketones (Lepe-Balsalobre *et al.*, 2022). The VOCs emitted by bacteria depend on the active metabolic pathways, which are influenced by culture conditions and available nutrients (Kai *et al.*, 2009). *Lm* has been reported to grow on rocket and may produce specific VOCs as a result of its interaction with this substrate (Culliney and Schmalenberger, 2020). In addition, plants release VOCs in response to microbial organisms, and rocket leaves may produce specific VOCs in response to *Lm* contamination (Hammerbacher *et al.*, 2019). Consequently, the VOCs produced by both *Lm* and rocket's response to *Lm* may have contributed to the differences in VOC profiles observed in this study, compared to previous research analysing VOCs from rocket leaves (Bell *et al.*, 2016; Spadafora *et al.*, 2016a; Spadafora *et al.*, 2018).

Since *Lm* produces its own set of VOCs and plants release VOCs in response to microbial organisms, the analysis of VOC profiles may be suitable for determining if fresh produce has become contaminated (Tait *et al.*, 2014b; Hammerbacher *et al.*, 2019; Lepe-Balsalobre *et al.*, 2022). In fact, Spadafora *et al.* (2016b) reports being able to discriminate between melon slices inoculated with 6 log CFU/g of *Lm* and uninoculated controls through the analysis of VOC profiles. Additionally, Spadafora *et al.* (2016b) report that samples with <100 CFU/g of *Lm* could be differentiated after an "enrichment" step for 6 h at 37 °C following 7 days of storage at 4 °C. The present study followed this protocol, with leaves incubated for 3 or 6 h at 37 °C to stimulate VOC production by promoting the metabolism of *Lm,* which grows optimally between 30 and 37 °C (Chan and Wiedmann, 2008). VOC profiles from inoculated and uninoculated leaves could be differentiated in 3 out of 4 experiments using CAP when incubation period was not considered a factor (Figure 5.1). While this analysis does not account for the effect of incubation period, the results suggest that measurable differences in VOC profiles exist between inoculated and uninoculated rocket leaves.

When accounting for incubation period, CAP analysis successfully differentiated VOC profiles from samples incubated for 3 h from those incubated for 6 h in all but Exp. 4 (Figure 5.2). PerMANOVA also identified a significant effect of incubation period on VOC profiles across all four experiments (Table 5.4). This finding aligns with previous research indicating that VOC profiles from rocket leaves can be used to distinguish between different storage durations (Spadafora *et al.*, 2016a; Luca *et al.*, 2017; Spadafora *et al.*, 2018). While the conditions in these studies, including lower temperatures (0, 5, and 10 °C) and longer storage periods, differed from those in the present study, the higher temperature used here likely increased metabolic activity and respiration rates, causing distinct VOC profiles between the 3 and 6 h incubation periods (Koukounaras *et al.*, 2007).

Across all experiments, CAP successfully differentiated VOC profiles between uninoculated and inoculated leaves for at least one incubation period, though the most effective incubation period varied between experiments (Figure 5.3; Figure 5.4). This suggests a more optimal incubation period may lie between 3 and 6 h, though this requires further investigation. Differences in the most effective incubation period

between experiments could be attributed to various factors, including rocket leaf composition, developmental stage, time since harvest, resident microbiota, and pre- and post-harvest stresses (Bell *et al.*, 2016; Tiwari *et al.*, 2020). These factors can influence both the VOCs produced by rocket leaves and *Lm.* Although the rocket leaves used in this study were sourced from the same retailer and had at least three days remaining before the "use by" date, there was likely significant variability in the factors influencing VOC production across the experiments. In fact, rocket leaf composition can fluctuate significantly on an annual and seasonal basis, even within the same cultivar (Bell *et al.*, 2020).

In Exp. 2 and 3, VOC profiles from inoculated and uninoculated leaves could not be discriminated by CAP after 6 h of incubation (Figure 5.4). After this longer incubation period, VOCs produced by both rocket leaves and the background microbiota may have obscured differences between inoculated and uninoculated samples. In contrast, VOC profiles for Exp. 1 could only be discriminated after 6 h of incubation (Figure 5.4). Interestingly, 3-hexen-1-ol, (Z), which is emitted from the leaves of plants in response to mechanical damage, was only detected in Exp. 1 (Table 5.2) (Ruther and Kleier, 2005). This suggests that a portion of the leaves in Exp. 1 may have been more damaged than those in the other experiments. The VOCs produced by bacteria depend on nutrient availability, which can be influenced by leaf composition, cultivar, leaf age and damage (Tait *et al.*, 2014b; Cai *et al.*, 2019). Additionally, plants emit specific VOCs when damaged (Tiwari *et al.*, 2020). In Exp. 1, after 3 h of incubation, VOCs from the background microbiota, feeding on available nutrients, as well as VOCs produced by rocket due to damage, may have obscured differences between inoculated and uninoculated samples. However, after 6 h, VOC profiles between inoculated and uninoculated samples may have become more distinct as *Lm* was more actively proliferating and contributing to the VOC profile.

VOC profiles after 3 h of incubation were only discriminated by both PerMANOVA and CAP in Exp. 3 (Table 5.5; Figure 5.3). This may be due to the incorporation of activated charcoal during incubation (see page 55). While bags were checked to ensure they were sealed from the ambient air, some VOCs may have infiltrated during incubation. To mitigate this, activated charcoal was included in Exp. 3 and 4, as it is a well-established

adsorbent for VOC removal (Gil *et al.*, 2014), reducing the likelihood of VOC infiltration at detectable levels. Notably, fewer VOCs were identified in Exp. 3 and 4 compared to Exp. 1 and 2, which may be partly due to the presence of activated charcoal (Table 5.2). This likely improved the discrimination of VOC profiles in Exp. 3, as the activated charcoal reduced noise in the VOC profiles. Despite the inclusion of activated charcoal in Exp. 4, CAP and PerMANOVA were unable to discriminate VOC profiles for inoculated and uninoculated leaves for either incubation period (Figure 5.3; Figure 5.4). This lack of discrimination may be attributed to differences in the pre- and post-harvest stresses the leaves were exposed to, relative to the other experiments.

Spadafora *et al.* (2016a) and Spadafora *et al.* (2018) reported a decrease in the relative abundance of seven aldehyde VOCs, including 2-Hexenal and 3-Hexenal, with increased storage time in rocket. In contrast, longer storage periods were associated with an increase in three sulphuric VOCs: dimethyl sulfoxide, dimethyl sulphide, and dimethyl disulphide. In this study, 2-Hexenal and 3-Hexenal were detected in Exp. 4 but not in the others, while dimethyl sulphide was present in Exp. 1, 2, and 3 but absent in Exp. 4 (Table 5.2). These results suggest that the time between harvesting and retail for the rocket leaves in Exp. 1, 2 and 3 was likely longer compared to those in Exp. 4. Extended storage of rocket leaves leads to product degradation, with microbial counts typically increasing over time (Spadafora *et al.*, 2016a). Longer storage periods may create conditions more conducive to the proliferation of *Lm,* which could account for the observed differences between experiments.

Although some bacteria produce specific VOCs that can indicate their presence, no specific VOC for *Lm* has been identified for this purpose (Cox and Parker, 1979; Kai *et al.*, 2009). The complexity of VOC profiles in food samples suggests that detecting bacteria through the analysis of a set of VOCs may be more effective than relying on single markers (Tait *et al.*, 2014b). For a VOC panel to be practical for detecting *Lm* contamination in rocket, these VOCs must be consistently present across different batches. Despite variability in total VOC profiles, 25 compounds were common to all experiments, suggesting their potential association with *Lm* presence (VOCs highlighted in bold in Table 5.2). Using this reduced panel, CAP successfully discriminated between inoculated and uninoculated leaves for each incubation period,

except in Exp. 4 (Figure 5.6). Furthermore, PerMANOVA revealed a significant effect of inoculation on VOC profiles in Exp. 1 and 3, unlike total VOC profiles (Table 5.7). These results indicate that this panel of VOCs was more sensitive to detecting differences between inoculated and uninoculated leaves than the total VOC profiles. Interestingly, none of the 25 VOCs identified in this study overlapped with those used by Spadafora *et al.* (2016b) to differentiate between inoculated and uninoculated melon. This highlights the substrate specific nature of VOC production by *Lm*, with different produce types likely influencing the VOCs emitted by the bacteria. The variability in VOC profiles from food inoculated with *Lm* underscores the challenges in identifying robust VOC markers for detecting *Lm*. While combining VOCs across studies may help develop a more sensitive VOC panel, the lack of differentiation in Exp. 4 suggests that various conditions should be explored to assess the efficacy of such panels.

Lm and *L. innocua* share the same ecological niches and have both been isolated from the same food processing environments (Carlin *et al.*, 2022). Additionally, *L. innocua* is often isolated from the same foods as *Lm,* and overgrowth of *L. innocua* during enrichment can lead to false-negative results in standard detection methods (Zitz *et al.*, 2011; Milillo *et al.*, 2012). To determine whether the two species could be differentiated using VOCs, VOCs released from rocket inoculated with *L. innocua* were analysed, using the same batch of rocket that was used for *Lm* inoculation.

VOC profiles from *L. innocua* and *Lm* inoculated leaves were distinguishable after 3 h of incubation using CAP, with both profiles distinct from the VOC profile of uninoculated leaves (Figure 5.7). PerMANOVA confirmed a significant effect of inoculation on VOC profiles, although pairwise comparisons did not reveal significant differences between the VOC profiles of *L. innocua* and *Lm* inoculated leaves (Table 5.8; Table 5.9). This highlights that CAP is more sensitive to subtle differences in VOC profiles (Anderson *et al.*, 2008). However, these distinctions may diminish over time. Indeed, after 6 h of incubation, *Lm* and *L. innocua* inoculated leaves could not be differentiated by CAP, indicating that the longer incubation period resulted in fewer discernible differences in VOC profiles (Figure 5.7). Given their ecological co-habitation and physiological and genetic similarity, *Lm* and *L. innocua* may possess similar metabolic pathways and thus produce comparable VOC profiles (Milillo *et al.*, 2012). Upon introduction to a new

growth substrate, bacteria undergo metabolic changes as they adapt to environmental conditions (Rolfe *et al.*, 2012). The adaptation rate of *Lm* and *L. innocua* to the rocket leaf surface may differ, potentially contributing to distinct VOC profiles after 3 h of incubation. Nevertheless, if both bacteria are introduced to rocket leaves early in the supply chain (i.e. during cultivation), allowing time for adaptation to the leaf surface, this could result in more similar VOC profiles that are harder to differentiate. Overall, these results suggest that VOC profiles may not reliably differentiate *Lm* from *L. innocua*. Identifying VOCs specifically associated with each species could improve differentiation between *Lm* and *L. innocua* when analysing VOC profiles. In total, three VOCs in the *L. innocua* samples fell below the baseline value used for filtering compounds in the dataset. Further repetitions using *L. innocua* are needed, and if this trend persists, these compounds could be useful for more effectively differentiating the VOC profiles of *Lm* from *L. innocua*.

5.3.1 Conclusion

This study demonstrates that VOC profiles can differentiate between *Lm*-inoculated and uninoculated rocket leaves. A brief incubation period at 37 °C was used to stimulate *Lm* metabolism and improve detection. The optimal incubation period varied across experiments, likely due to batch-to-batch variability in factors influencing VOC production by both rocket and *Lm*. Across experiments, *Lm* was present on the leaves for only a brief period, providing limited time for adaptation. Despite this, the ability to distinguish *Lm*-inoculated samples in most experiments shows that VOC analysis can be a sensitive and rapid detection method.

For a VOC detection method to be applicable in industry, it must be sensitive and reliable enough to detect contaminants despite seasonal and annual variability in rocket leaf composition and the impact of pre- and post-harvest stresses. In one experiment, VOC profiles from inoculated and uninoculated leaves could not be differentiated. However, the VOCs detected suggested notable differences in the prior storage conditions of the rocket compared to the other experiments. This finding suggests that some product deterioration may be necessary to detect differences between inoculated and uninoculated leaves. Future work should focus on investigating

VOC profiles from rocket inoculated immediately post-harvest and refining the incubation period to improve sensitivity and consistency.

While differences in VOC profiles were observed between *Lm* and *L. innocua*, the two species could not be reliably distinguished after longer incubation periods. This indicates that further research is needed to identify VOCs specific to *Lm*, which could enhance the specificity of this detection method. A set of 25 compounds was identified across all experiments and may serve as potential markers for *Lm* contamination, as they improved the sensitivity in detecting differences between inoculated and uninoculated leaves. Overall, the findings suggest that VOC analysis has the potential to serve as a tool for detecting *Lm* contamination in rocket, but further investigation is needed to optimise the methodology and account for batch variability.

Chapter 6 – General discussion

Foodborne bacteria are the leading cause of mortality among foodborne diseases and are an ongoing food safety concern. Among foodborne bacteria, *L. monocytogenes* (*Lm*) is considered a high-risk pathogen due to its high mortality rate. RTE salads are at high risk for the transmission of *Lm* due to its widespread presence in production environments and the minimal processing RTE salads undergo before consumption. Additionally, *Lm*'s ability to grow under conditions that typically inhibit microbial growth, along with challenges in the timely detection of *Lm* in salads, further compounds the risk. While *Lm* is increasingly linked to RTE salads, limited research exists on the factors influencing its association with leafy vegetables. This study aims to investigate these factors by examining the genotypic and phenotypic characteristics of various *Lm* strains isolated from the fresh produce supply chain and exploring the variability in attachment between different plant surfaces and strains. Additionally, the potential for VOC-based detection of *Lm* in rocket leaves is assessed to determine its applicability for contamination detection and how the method may be refined to improve its efficacy.

6.1 Gene regulation and sequence variation, rather than specific genes, determine contamination potential of leaf vegetables in *L. monocytogenes*

The four strains examined for attachment to spinach and rocket encoded homologs of a cell surface protein (LCP) reported by Bae *et al.* (2013) to be involved in the attachment of *Lm* to salad leaves (Table 3.2). Bae *et al.* (2013) identified a cellulose-binding domain (CBD) within the LCP, suggesting that this domain contributes to the protein's role in attachment to plant surfaces, as cellulose is a major component of the plant cell wall. NLmo8 and NLmo9 both encoded identical CBD domains in the LCP homologs identified (Table 3.2). In contrast, the LCP homolog of EGD-e and NLmo15 exhibited 88.8% and 90.4% amino acid sequence homology with the CBD domain, respectively (Table 3.2). Only a significant difference in attachment between NLmo8 and EGD-e was observed on rocket and spinach (Figure 4.4). This may be because the LCP variant encoded by EGD-e was less effective at binding cellulose than the LCP of NLmo8. In fact, both NLmo8 (1.8×10^3 CFU/cm^3) and NLmo9 (1.4×10^3 CFU/cm^2) had higher

average attachment than NLmo15 (1.2 x 10^3 CFU/cm^2) and EGD-e (1 x 10^3 CFU/cm^2). It may be that differences in the LCP gene sequence contributed to this trend. Unfortunately, efforts to replicate the *in vitro* cellulose adhesion assay described by Bae *et al.* (2013) were unsuccessful, preventing further investigation into whether the observed differences in attachment to leaf surfaces between NLmo8 and EGD-e could be attributed to variations in the LCP gene.

To my knowledge, very few genes have been characterised that mediate *Lm* attachment to plant surfaces. A search in Web of Science and Scopus using the terms "*Listeria monocytogenes*" OR "*Listeria*", "plant" OR "plant surface", and "adhesion" OR "attachment" found only one relevant paper. This study characterised the Crp/Fnr family transcription factor Lmo0753, which was highly conserved (96.9-100%) across the four strains examined for attachment to leaf surfaces (Salazar *et al.*, 2013). Notably, this gene does not directly encode a cell surface component that interacts with the leaf surface but instead influences attachment indirectly by regulating genes involved in biofilm formation and environmental persistence mechanisms. Additionally, previous efforts to identify specific genetic components involved in leaf attachment have been unsuccessful (Palumbo *et al.*, 2005).

Genes implicated in mediating attachment to salad leaves, such as those encoding the LCP and Lmo0753, seem to be conserved across the *Lm* species (Figure 3.5) (Bae *et al.*, 2013; Salazar *et al.*, 2013). Maury *et al.* (2017) report that some strains with specific mutations in the *hly* gene, a highly conserved gene among *Lm* that encodes the pore-forming virulence factor listeriolysin O, exhibited attenuated virulence in mice. Similarly, sequence variation in the genes encoding LCP or Lmo0753 may contribute to strain-specific differences in leaf attachment and colonisation. Additionally, previous research has demonstrated that *Lm* strains with premature stop codons in the virulence gene *inlA*, resulting in reduced virulence, are more prevalent among food isolates than clinical isolates (Nightingale *et al.*, 2008; Van Stelten *et al.*, 2010). Greater variability in the LCP gene sequence was observed in lineage II strains of the *Lm* collection, with these strains (EGD-e and NLmo15) displaying lower average attachment to rocket (Table 3.2**;** Figure 3.5**;** Figure 4.4). Thus, it may be possible to associate specific gene variants with colonisation potential, isolation source and genetic subtypes. However, further

research is needed to identify the genes or genetic pathways involved in plant contamination and understand how these vary across strains and impact plant colonisation in *Lm*.

One limitation of this study is the relatively small number of *Lm* strains examined for their genetic characteristics. While 13 strains were isolated from leaf surfaces (Table 2.1), only a small number of strains from other sources were included in the analysis. Future research should expand the sample set to include more strains isolated from salad leaves and compare them with strains from other food sources, such as meat, fish, or dairy. This could provide insights into whether certain *Lm* subtypes and specific genes are correlated with contamination of salad leaves. These genes may serve as potential targets for further investigation.

In addition to genetic factors, *Lm* possesses inherent characteristics, including flagella and exopolysaccharides, which have been shown to facilitate attachment to plant surfaces (Gorski *et al.*, 2009; Fulano *et al.*, 2023). Therefore, differences in attachment between strains may not solely be attributed to variations in genetic content. Instead, these differences may arise from variations in the regulation of mechanisms facilitating attachment. In fact, Hafner *et al.* (2024) demonstrated that the regulation of virulence genes, rather than their presence or absence, causes differences in virulence between strains, even among closely related strains. This suggests that a strain's capacity to attach is governed by whether the mechanisms facilitating attachment are actively expressed upon encountering the leaf surface.

6.2 *Lm* phenotypes that facilitate attachment to leaf vegetables are context dependent

Numerous genes in *Lm* are regulated in a temperature dependent manner, including motility (Leimeister-Wächter *et al.*, 1992; Cho *et al.*, 2022). Differences in the regulation of motility between EGD-e and NLmo8 may contribute to the variation in attachment observed between the two strains (Figure 3.6**;** Figure 4.1**;** Figure 4.4). *Lm* is motile due to the presence of flagella, which have been shown to facilitate attachment to plant surfaces, with expression typically repressed at 37 °C (Gorski *et al.*, 2009; Cho *et al.*, 2022). Notably, at 30 °C, both NLmo8 and EGD-e exhibited similar motility. However, at

37 °C, NLmo8 displayed significantly higher motility compared to EGD-e. In fact, NLmo8's motility at 37 °C was comparable to that at 30 °C, suggesting continued flagella expression at the higher temperature (Figure 3.6). In the leaf disc assay, a significant difference in attachment to spinach was observed between EGD-e and NLmo8 (Figure 4.1). However, when attachment to spinach was assessed using the whole leaf assay, no significant difference was observed between the strains (Figure 4.3). A key distinction between these assays lies in the incubation temperature of the inoculum: 37 °C for the leaf disc assay and 30 °C for the whole leaf assay. Thus, the continued flagellar expression of NLmo8 at 37 °C may account for the observed difference in attachment between the strains in the leaf disc assay. Overall, 37 °C is not a typical temperature in either salad leaf cultivation or processing environments. The Food Standards Agency in the UK recommends that foods capable of supporting microbial growth should be processed and stored at temperatures below 8 °C (Food Standards Agency, 2016). The regulation of flagella expression in *Lm* at temperatures below 8 °C has not been well investigated. Further research is required to understand how flagella expression is regulated at these lower temperatures and its impact on salad leaf attachment.

Overall, environmental conditions may influence a strain's capacity to attach to leaf surfaces. The inoculum for the leaf attachment assays was not prepared under conditions typical of salad leaf cultivation or processing environments. Future research should explore how attachment varies when inocula are prepared under conditions that reflect those in cultivation and processing, such as low temperatures or the presence of sanitising agents. This could help identify environmental factors and phenotypic characteristics that promote *Lm* attachment to salad leaves.

No significant difference was observed when the attachment of NLmo8 or EGD-e to rocket was compared to that of NLmo9 or NLmo15 (Figure 4.4). Although the attachment of EGD-e was statistically significantly lower than that of NLmo8, the magnitude of the difference is relatively minor when considering the attachment behaviour of all *Lm* strains tested. In fact, the attachment levels of *Lm* compared to those observed for other foodborne pathogens to similar surfaces was relatively low (Berger *et al.*, 2009a; Berger *et al.*, 2009b). For instance, Berger *et al.* (2009b) report that

attachment levels of eight *E. coli* strains to cultivated rocket ranged from 1.5 x 10^3 to 1 x 10^5 CFU/mm^2. In contrast, attachment of *Lm,* when examined with the whole leaf assay, ranged 1 x 10^3 to 1.8 x 10^3 CFU/cm^2 for rocket and 1.05 x 10^3 to 5.41 x 10^3 CFU/cm^2 for spinach (Figure 4.3**;** Figure 4.4**;** Figure 4.5). These results suggest that *E. coli* and *Salmonella* may attach more readily to plant surfaces, which could explain why these pathogens are more frequently implicated in foodborne outbreaks associated with salads compared to *Lm* (EFSA, 2023). Nevertheless, NLmo8 exhibited two-fold higher attachment on rocket and 20-fold higher attachment on spinach in the leaf disc assay, relative to EGD-e, indicating strain-specific differences in attachment to the same leaf surface (Figure 4.1**;** Figure 4.4). Only a limited number of strains and plant surfaces were examined in this study. Future research should investigate the attachment of a wider selection of *Lm* strains to the same leaf surface or the attachment of a single strain across a greater variety of salad leaves. This could provide insights into how *Lm* attachment varies between strains and across different salad varieties, helping to determine if certain varieties are at higher risk of contamination. Additionally, it could identify strains for further examination to uncover characteristics that contribute to enhanced attachment.

6.3 *L. monocytogenes* attaches primarily to areas on the leaf that are damaged

All four *Lm* strains attached to the rocket leaf surface, albeit at varying levels (Figure 4.4). To determine if differences in attachment between strains were due to variations in preferential attachment sites, inoculated rocket and spinach leaves were examined by microscopy and a novel overlay assay (Figure 4.6**;** Figure 4.7**;** Figure 4.9). Unfortunately, due to complications in observing different *Lm* strains on the leaf surface, no strain-specific differences in preferential attachment sites could be determined. Nevertheless, microscopy observations of EGD-e on rocket and the results of the overlay assay indicated that *Lm* preferentially attaches to areas of the leaf where the cuticle may be compromised (Figure 4.6). This observation aligns with those reported by previous studies (Takeuchi *et al.*, 2000; Ells and Truelstrup Hansen, 2006). The leaf surface is oligotrophic, and attachment to damaged areas would be advantageous for *Lm* as it provides access to nutrients from plant cells. Foodborne bacteria such as *E.*

coli and *Salmonella* have been reported to translocate into the internal tissues of leaves through stomata to gain access to nutrients (Saldaña *et al.*, 2011; Schikora *et al.*, 2012). In fact, *Salmonella* has been suggested to actively move towards the stomata following attachment to internalise in plant tissues (Kroupitski *et al.*, 2009). While *Lm* has been observed in and around stomata on leaf surfaces, it remains unclear whether this is due to active tropism or passive entrapment (Ells and Truelstrup Hansen, 2006; Guan *et al.*, 2023). Nevertheless, previous research has shown that *Lm* internalises and colonises lettuce leaves through wound sites (Guan *et al.*, 2023). Whether *Lm* is able to internalise and colonise leaves through other pathways, such as through stomata, remains to be investigated.

Overall, the examination of *Lm* on the leaf surface of rocket and spinach via microscopy proved challenging due to low bacterial counts and fixation issues. Extended exposure of spinach leaves to the inoculum resulted in increased bacterial attachment (Figure 4.3). Future work should involve longer exposure of leaves to the bacterial inoculum, thereby increasing the bacterial load on the leaf surface. Additionally, examination without fixatives mitigates potential fluorescence loss and may enable the observation of leaf tissue at various time points post-inoculation, potentially providing insights into how *Lm* colonises leaf tissues.

6.4 VOC-based detection of *L. monocytogenes* is influenced by leaf condition

Attachment of *Lm* to damaged leaf areas and colonisation at these sites may explain the differences in VOC-based discrimination between *Lm*-inoculated and uninoculated leaves across experiments. Overall, *Lm*-inoculated rocket leaves were successfully differentiated from uninoculated leaves in 3 out of 4 experiments (Figure 5.2**;** Figure 5.3**;** Figure 5.4). VOC profiles in Exp. 1, 2, and 3 could be effectively differentiated, with the most effective incubation period at 37 °C varying between experiments (Figure 5.3**;** Figure 5.4). Among the VOCs detected in Exp. 1 was 3-hexen-1-ol, (Z), a VOC emitted by leaves in response to mechanical damage (Ruther and Kleier, 2005) (Table 5.2). Furthermore, dimethyl disulphide was only detected in Exp. 1, 2 and 3 (Table 5.2), and has been shown to have a direct relationship with microbial counts and storage time in

rocket leaves (Spadafora *et al.*, 2016a; Spadafora *et al.*, 2018). In contrast, the compounds 2-hexenal and 3-hexenal were only detected in Exp. 4 (Table 5.2). These compounds have been shown to have an inverse relationship with storage time and product quality in rocket leaves (Spadafora *et al.*, 2016a; Spadafora *et al.*, 2018). Additionally, both 2-hexenal and 3-hexenal have been shown to have antimicrobial activity against foodborne bacteria such as *S. enteritidis, E. coli* and *Lm* (Nakamura and Hatanaka, 2002; Lanciotti *et al.*, 2003). Thus, the leaves used in Exp. 1, 2 and 3 may have been more deteriorated, allowing better *Lm* attachment and a more favourable environment for colonisation compared to those in Exp. 4. Additionally, proliferation of *Lm* during incubation may have been repressed by the volatiles produced by rocket leaves in Exp. 4. In fact, the relative abundance of hexenal-2 and hexenal-3 was higher in samples inoculated with *Lm* than uninoculated samples (data not shown). Subsequently, *Lm* may have produced more VOCs in Exp. 1, 2 and 3, relative to Exp. 4 resulting in more distinctive VOC profiles between inoculated and uninoculated leaves, enabling their discrimination. Bacterial numbers were not enumerated after VOC sampling, which may have revealed whether fewer *Lm* cells were present on the leaves in Exp. 4 compared to the other experiments. This should be considered in future studies using the same VOC analysis methods, particularly when investigating how the condition of leaves influences VOC profiles.

Salad leaves can become contaminated at any stage of the fresh produce supply chain. Consequently, food safety testing is conducted at various stages to identify contamination risks, including post-harvest, during processing, prior to packaging and at retail (Pinto *et al.*, 2025). In this study, the leaves were inoculated at the retail stage to simulate contamination occurring at a late stage in the supply chain. Contamination can also occur early in the supply chain, as previous research has shown *Lm* contamination in vegetables tested before entering processing facilities (Magdovitz *et al.*, 2021). Bell *et al.* (2017) report that the phytochemical composition and bacterial load of wild and cultivated rocket changes as the leaves progress through the food supply chain. These changes, along with exposure to varying conditions at different stages of the supply chain, may influence the VOCs produced by *Lm* and rocket. In fact, Spadafora *et al.* (2020) demonstrated that VOC profiles from the same rocket variety

differs at various points post-harvest. Future studies should explore whether VOC-based analysis can detect *Lm* at typical testing points used for microbial safety monitoring, following contamination at various stages of the food supply chain. This would help assess the efficacy of VOC-based detection of *Lm* in salad leaves under contamination scenarios that are realistic for the fresh produce supply chain.

6.5 Variation in metabolic capacity drives differences in VOC profiles between *L. monocytogenes* strains

A considerable limitation of this study was that only one strain (NLmo8) was investigated for VOC analysis. While NLmo8 was selected due to its enhanced attachment capacity to rocket leaves compared to other strains, all strains demonstrated potential for contaminating rocket (Figure 4.4). Growth in complex media revealed substantial variability in growth capacity across the *Lm* collection, with strain differences not being consistent across the different media tested (Figure 3.7**;** Figure 3.9). Furthermore, Lepe-Balsalobre *et al.* (2022) identified eight VOCs specifically produced by seven different *Lm* strains during cultivation in thioglycolate broth medium, along with one VOC unique to a single strain. The researchers also demonstrated significant differences between strains in the quantities of these eight VOCs produced. These results highlight that *Lm* strains exhibit varying metabolic capacities and may produce distinct VOC profiles, even on the same leaf surface. Therefore, future research should examine additional strains to determine whether VOC-based analysis can detect differences between inoculated and uninoculated leaves for other strains. Examining more strains could also help determine if the 25 VOCs consistently detected across the 4 experiments can be associated with other *Lm* strains.

6.6 The sensitivity of VOC-based detection of *L. monocytogenes* may depend on contamination levels

Culliney and Schmalenberger (2020) demonstrated that rocket inoculated with 100 CFU/g of *Lm*, reached median cell counts of 3 $\log_{10}$ CFU/g after 7 days of storage at 8 °C. The inoculation levels used in this study (10^4 to 10^6 CFU/g of *Lm*) thus represented

a high level of contamination. Rosberg *et al.* (2021) reported that rocket leaves harboured between 4.2 and 7.7 $\log_{10}$ CFU/g of aerobic bacteria and observed significant variability in bacterial diversity between different harvesting seasons. The natural microbiota of rocket may produce VOCs similar to those emitted by *Lm*. At lower inoculation levels, the VOC profiles of *Lm* and the resident microbiota may overlap, hindering the discrimination between inoculated and uninoculated leaves. In fact, *L. innocua* is often isolated from the same foods as *Lm*, and the VOC profiles of *L. innocua* and *Lm* after 6 h of incubation could not be differentiated (Figure 5.7). This highlights that bacteria co-existing in the same ecological niches as *Lm* may produce similar VOC profiles. Therefore, future studies should investigate lower inoculum levels to evaluate the sensitivity of the VOC-based analysis method used here in detecting *Lm*.

6.7 Genetic differences between *L. monocytogenes* and *L. innocua* may be used to develop a more sensitive VOC based detection method.

A VOC based detection method for *Lm* in salad should be specific enough to account for seasonal variability in leaf composition, metabolic variability among *Lm* strains, and VOC signals from resident microbiota and closely related species. To enhance *Lm* detection through VOC analysis, it may be possible to stimulate metabolic pathways that produce VOCs unique to this organism. WGS analysis revealed that the core-genome of *L. innocua* and the *Lm* collection constituted 2,442 genes, whereas the core-genome of the *Lm* collection alone included 2,541 genes (Figure 3.1). The 99 genes unique to the *Lm* collection may encode enzymes that could be used to develop substrates that stimulate the release of *Lm*-specific VOCs, enabling *Lm* detection in contaminated food. Tait *et al.* (2014a) reported using enzyme-generated VOCs for *Lm* detection, employing two substrates specific to the β-glucosidase and hippuricase enzymes of *Lm*. When these substrates were added to cultures of *Lm*, the VOCs 2-nitrophenol and 3-fluoroaniline were generated and detectable using SPME-GC-MS. However, the method was not entirely specific, as four other *Listeria* spp. and three other bacterial species also produced these same VOCs, indicating that the method requires further refinement for practical applications. Further work is needed to identify

substrates which stimulate the production of VOCs unique to *Lm*. These substrates may improve the sensitivity and reliability of *Lm* detection in food through VOC analysis.

6.8 Conclusion

This study attempted to address the hypotheses regarding the genetic, phenotypic, and leaf surface characteristics influencing *Lm* contamination of leafy salad vegetables, as well as the potential for VOC analysis to detect such contamination.

Genetic variations in the LCP gene were linked to attachment levels in *Lm* strains. However, no clear associations were found between other genetic features and contamination potential in leafy vegetables. The observed differences in attachment to leaf surfaces between strains are likely due to variations in gene regulation rather than gene content. Phenotypic characteristics, such as motility, may account for strain-specific differences in attachment in certain contexts. Ultimately, environmental conditions appear to determine whether *Lm* expresses phenotypes that promote attachment, although the specific conditions that facilitate attachment remain to be clarified. Differences in leaf surface characteristics between plant varieties and species may also play a role in attachment.

While no distinct structural features of the leaf surface were identified as contributing to strain-specific attachment, microscopy and overlay assays indicated that *Lm* preferentially attaches to areas with compromised cuticles. This preference for damaged leaf areas may explain why differentiation of *Lm* inoculated rocket leaves from uninoculated controls was more effective when VOCs produced in response to damage or extended storage were detected. Although VOC analysis demonstrated potential for distinguishing *Lm* inoculated leaves, further refinement is needed to improve sensitivity, specificity, and reliability, particularly given the metabolic variability between strains and the potential overlap with VOC profiles from other microbes. Additionally, the detection method should be evaluated under conditions more representative of the fresh produce supply chain.

This study showed that leaf attachment varies between *Lm* strains, is dependent on environmental conditions, and that leaf damage may be a key factor influencing attachment. VOC-based analysis shows promise for detecting *Lm* contamination in

rocket leaves. Further research is needed to develop VOC-based methods for detecting *Lm* contamination in leafy vegetables, as well as to better understand the *Lm*, plant, and environmental factors that contribute to salad leaf contamination, in order to improve the food safety of RTE salads.

Bibliography

Ahmed, W. M. *et al.* (2018). Methodological considerations for large-scale breath analysis studies: lessons from the U-BIOPRED severe asthma project. *Journal of Breath Research* 13(1), p. 016001. doi: 10.1088/1752-7163/aae557

Aké, F. M. D., Joyet, P., Deutscher, J. and Milohanic, E. (2011). Mutational analysis of glucose transport regulation and glucose-mediated virulence gene repression in *Listeria monocytogenes*. *Molecular Microbiology* 81(1), pp. 274-293. doi: https://doi.org/10.1111/j.1365-2958.2011.07692.x

Alegbeleye, O. and Sant'Ana, A. S. (2022). Survival and growth behaviour of *Listeria monocytogenes* in ready-to-eat vegetable salads. *Food Control* 138, p. 109023. doi: https://doi.org/10.1016/j.foodcont.2022.109023

Alves, Â., Magalhães, R., Brandão, T. R. S., Pimentel, L., Rodríguez-Alcalá, L. M., Teixeira, P. and Ferreira, V. (2020). Impact of exposure to cold and cold-osmotic stresses on virulence-associated characteristics of *Listeria monocytogenes* strains. *Food Microbiology* 87, p. 103351. doi: https://doi.org/10.1016/j.fm.2019.103351

Anderson, M. J. (2001). A new method for non-parametric multivariate analysis of variance. *Austral Ecology* 26(1), pp. 32-46. doi: 10.1111/j.1442-9993.2001.01070.pp.x

Anderson, M. J., Gorley, R. N. and Clarke, K. S. (2008). *PERMANOVA+ for PRIMER. Guide to software and statistical methods*. Plymouth, UK: PRIMER-E Ltd.

Anderson, M. J. and Willis, T. (2003). Canonical Analysis of Principal Coordinates: A Useful Method of Constrained Ordination for Ecology. *Ecological Society of America* 84(2), pp. 511-525.

Andrews, S. (2010). FastQC: A Quality Control Tool for High Throughput Sequence Data. Available at: http://www.bioinformatics.babraham.ac.uk/projects/fastqc/ [Accessed: 8 May 2022].

Angelo, K. M., Jackson, K. A., Wong, K. K., Hoekstra, R. M. and Jackson, B. R. (2016). Assessment of the Incubation Period for Invasive Listeriosis. *Clinical Infectious Diseases* 63(11), pp. 1487-1489. doi: 10.1093/cid/ciw569

Arienzo, A., Murgia, L., Fraudentali, I., Gallo, V., Angelini, R. and Antonini, G. (2020). Microbiological Quality of Ready-to-Eat Leafy Green Salads during Shelf-Life and Home-Refrigeration. *Foods* 9(10), p. 1421. doi: 10.3390/foods9101421

Ayrapetyan, M. and Oliver, J. D. (2016). The viable but non-culturable state and its relevance in food safety. *Current Opinion in Food Science* 8, pp. 127-133. doi: 10.1016/j.cofs.2016.04.010

Aytac, S. A., Ben, U., Cengiz, C. and Taban, B. M. (2010). Evaluation of *Salmonella* and *Listeria monocytogenes* contamination on leafy green vegetables. *Journal of Food Agriculture and Environment* 8(2), pp. 275-279.

Bae, D., Seo, K. S., Zhang, T. and Wang, C. (2013). Characterization of a Potential *Listeria monocytogenes* Virulence Factor Associated with Attachment to Fresh Produce. *Applied and Environmental Microbiology* 79(22), pp. 6855-6861. doi: 10.1128/aem.01006-13

Balestrino, D. *et al*. (2010). Single-Cell Techniques Using Chromosomally Tagged Fluorescent Bacteria To Study *Listeria monocytogenes* Infection Processes. *Applied and Environmental Microbiology* 76(11), pp. 3625-3636. doi: 10.1128/aem.02612-09

Bankevich, A. *et al*. (2012). SPAdes: A New Genome Assembly Algorithm and Its Applications to Single-Cell Sequencing. *Journal of Computational Biology* 19(5), pp. 455-477. doi: 10.1089/cmb.2012.0021

Bastounis, E. E., Yeh, Y.-T. and Theriot, J. A. (2018). Matrix stiffness modulates infection of endothelial cells by *Listeria monocytogenes* via expression of cell surface vimentin. *Molecular Biology of the Cell* 29(13), pp. 1571-1589. doi: 10.1091/mbc.e18-04-0228

Beattie, G. A. and Lindow, S. E. (1999). Bacterial colonization of leaves: a spectrum of strategies. *Phytopathology* 89 5, pp. 353-359.

Beaulieu, J. C. and Grimm, C. C. (2001). Identification of Volatile Compounds in Cantaloupe at Various Developmental Stages Using Solid Phase Microextraction. *Journal of Agricultural and Food Chemistry* 49(3), pp. 1345-1352. doi: 10.1021/jf0005768

Bécavin, C. *et al*. (2014). Comparison of Widely Used *Listeria monocytogenes* Strains EGD, 10403S, and EGD-e Highlights Genomic Differences Underlying Variations in Pathogenicity. *mBio* 5(2), pp. e00969-00914. doi: 10.1128/mbio.00969-14

Behrends, V., Tredwell, G. D. and Bundy, J. G. (2011). A software complement to AMDIS for processing GC-MS metabolomic data. *Analytical Biochemistry* 415(2), pp. 206-208. doi: 10.1016/j.ab.2011.04.009

Bell, L., Lignou, S. and Wagstaff, C. (2020). High Glucosinolate Content in Rocket Leaves (*Diplotaxis tenuifolia* and *Eruca sativa*) after Multiple Harvests Is Associated with

Increased Bitterness, Pungency, and Reduced Consumer Liking. *Foods* 9(12), p. 1799. doi: 10.3390/foods9121799

Bell, L., Spadafora, N. D., Müller, C. T., Wagstaff, C. and Rogers, H. J. (2016). Use of TD-GC–TOF-MS to assess volatile composition during post-harvest storage in seven accessions of rocket salad (*Eruca sativa*). *Food Chemistry* 194, pp. 626-636. doi: https://doi.org/10.1016/j.foodchem.2015.08.043

Bell, L., Yahya, H. N., Oloyede, O. O., Methven, L. and Wagstaff, C. (2017). Changes in rocket salad phytochemicals within the commercial supply chain: Glucosinolates, isothiocyanates, amino acids and bacterial load increase significantly after processing. *Food Chemistry* 221, pp. 521-534. doi: https://doi.org/10.1016/j.foodchem.2016.11.154

Berger, C. N. *et al.* (2009a). Interaction of *Salmonella enterica* with basil and other salad leaves. *The ISME Journal* 3(2), pp. 261-265. doi: 10.1038/ismej.2008.95

Berger, C. N., Shaw, R. K., Ruiz-Perez, F., Nataro, J. P., Henderson, I. R., Pallen, M. J. and Frankel, G. (2009b). Interaction of enteroaggregative *Escherichia coli* with salad leaves. *Environmental Microbiology Reports* 1(4), pp. 234-239. doi: https://doi.org/10.1111/j.1758-2229.2009.00037.x

Bergholz, T. M., den Bakker, H. C., Fortes, E. D., Boor, K. J. and Wiedmann, M. (2010). Salt stress phenotypes in *Listeria monocytogenes* vary by genetic lineage and temperature. *Foodborne Pathogens and Disease* 7(12), pp. 1537-1549. doi: 10.1089/fpd.2010.0624

Bianchi, F. *et al.* (2009). Differentiation of the volatile profile of microbiologically contaminated canned tomatoes by dynamic headspace extraction followed by gas chromatography–mass spectrometry analysis. *Talanta* 77(3), pp. 962-970. doi: doi.org/10.1016/j.talanta.2008.07.061

Bolger, A. M., Lohse, M. and Usadel, B. (2014). Trimmomatic: a flexible trimmer for Illumina sequence data. *Bioinformatics* 30(15), pp. 2114-2120. doi: 10.1093/bioinformatics/btu170

Bonah, E., Huang, X., Aheto, J. H. and Osae, R. (2020). Application of electronic nose as a non-invasive technique for odor fingerprinting and detection of bacterial foodborne pathogens: a review. *Journal of Food Science and Technology* 57(6), pp. 1977-1990. doi: 10.1007/s13197-019-04143-4

Brandl, M. T. and Mandrell, R. E. (2002). Fitness of *Salmonella enterica* serovar Thompson in the Cilantro Phyllosphere. *Applied and Environmental Microbiology* 68(7), pp. 3614-3621. doi: 10.1128/aem.68.7.3614-3621.2002

Cai, S., Worobo, R. W. and Snyder, A. B. (2019). Combined Effect of Storage Condition, Surface Integrity, and Length of Shelf Life on the Growth of *Listeria monocytogenes* and Spoilage Microbiota on Refrigerated Ready-to-Eat Products. *Journal of Food Protection* 82(8), pp. 1423-1432. doi: https://doi.org/10.4315/0362-028X.JFP-18-576

Camacho, C., Coulouris, G., Avagyan, V., Ma, N., Papadopoulos, J., Bealer, K. and Madden, T. L. (2009). BLAST+: architecture and applications. *BMC Bioinformatics* 10(1), p. 421. doi: 10.1186/1471-2105-10-421

Cardenas-Alvarez, M. X., Restrepo-Montoya, D. and Bergholz, T. M. (2022). Genome-Wide Association Study of *Listeria monocytogenes* Isolates Causing Three Different Clinical Outcomes. *Microorganisms* 10(10), p. 1934. doi: 10.3390/microorganisms10101934

Carlin, C. R., Roof, S. and Wiedmann, M. (2022). Assessment of Reference Method Selective Broth and Plating Media with 19 *Listeria* Species Highlights the Importance of Including Diverse Species in *Listeria* Method Evaluations. *Journal of Food Protection* 85(3), pp. 494-510. doi: https://doi.org/10.4315/JFP-21-293

Carpentier, B. and Cerf, O. (2011). Review — Persistence of *Listeria monocytogenes* in food industry equipment and premises. *International Journal of Food Microbiology* 145(1), pp. 1-8. doi: https://doi.org/10.1016/j.ijfoodmicro.2011.01.005

CDC. (2015). *2014 Outbreak of Listeria Infections Linked to Wholesome Soy Products, Inc. Sprouts*. Centers for Disease Control and Prevention. Available at: https://archive.cdc.gov/#/details?url=https://www.cdc.gov/listeria/outbreaks/bean-sprouts-11-14/index.html [Accessed: 09-09-2024].

Chan, Y. C. and Wiedmann, M. (2008). Physiology and Genetics of *Listeria Monocytogenes* Survival and Growth at Cold Temperatures. *Critical Reviews in Food Science and Nutrition* 49(3), pp. 237-253. doi: 10.1080/10408390701856272

Chapin, T. K., Nightingale, K. K., Worobo, R. W., Wiedmann, M. and Strawn, L. K. (2014). Geographical and Meteorological Factors Associated with Isolation of *Listeria* Species in New York State Produce Production and Natural Environments. *Journal of Food Protection* 77(11), pp. 1919-1928. doi: https://doi.org/10.4315/0362-028X.JFP-14-132

Chen, Y. *et al.* (2020). Genetic diversity and profiles of genes associated with virulence and stress resistance among isolates from the 2010-2013 interagency *Listeria monocytogenes* market basket survey. *PLoS ONE* 15(4), p. e0231393. doi: 10.1371/journal.pone.0231393

Chen, Y., Gonzalez-Escalona, N., Hammack, T. S., Allard, M. W., Strain, E. A. and Brown, E. W. (2016). Core Genome Multilocus Sequence Typing for Identification of Globally Distributed Clonal Groups and Differentiation of Outbreak Strains of *Listeria monocytogenes*. *Applied and Environmental Microbiology* 82(20), pp. 6258-6272. doi: 10.1128/aem.01532-16

Chen, Y. *et al*. (2017). Singleton Sequence Type 382, an Emerging Clonal Group of *Listeria monocytogenes* Associated with Three Multistate Outbreaks Linked to Contaminated Stone Fruit, Caramel Apples, and Leafy Green Salad. *Journal of Clinical Microbiology* 55(3), pp. 931-941. doi: 10.1128/jcm.02140-16

Chenal-Francisque, V. *et al*. (2011). Worldwide Distribution of Major Clones of *Listeria monocytogenes*. *Emerging Infectious Diseases* 17(6), pp. 1110-1112. doi: 10.3201/eid1706.101778

Chikhi, L., Mancier, M., Brugère, H., Lombard, B., Faouzi, L., Guillier, L. and Gnanou Besse, N. (2024). Comparison of *Listeria monocytogenes* alternative detection methods for food microbiology official controls in Europe. *International Journal of Food Microbiology* 408, p. 110448. doi: https://doi.org/10.1016/j.ijfoodmicro.2023.110448

Cho, S. Y. *et al*. (2022). Structural basis of flagellar motility regulation by the MogR repressor and the GmaR antirepressor in *Listeria monocytogenes*. *Nucleic Acids Research* 50(19), pp. 11315-11330. doi: 10.1093/nar/gkac815

Connor, T. R. *et al*. (2016). CLIMB (the Cloud Infrastructure for Microbial Bioinformatics): an online resource for the medical microbiology community. *Microbial Genomics* 2(9), doi: 10.1099/mgen.0.000086

Cooper, A. L., Carrillo, C. D., DeschêNes, M. and Blais, B. W. (2021). Genomic Markers for Quaternary Ammonium Compound Resistance as a Persistence Indicator for *Listeria monocytogenes* Contamination in Food Manufacturing Environments. *Journal of Food Protection* 84(3), pp. 389-398. doi: https://doi.org/10.4315/JFP-20-328

Cooper, S. (1991). 1 - Bacterial Growth. In: Cooper, S. ed. *Bacterial Growth and Division*. San Diego: Academic Press, pp. 7-17.

Cormack, B. P., Valdivia, R. H. and Falkow, S. (1996). FACS-optimized mutants of the green fluorescent protein (GFP). *Gene* 173(1), pp. 33-38. doi: https://doi.org/10.1016/0378-1119(95)00685-0

Cox, C. D. and Parker, J. (1979). Use of 2-aminoacetophenone production in identification of Pseudomonas aeruginosa. *Journal of Clinical Microbiology* 9(4), pp. 479-484.

Culliney, P. and Schmalenberger, A. (2020). Growth Potential of *Listeria monocytogenes* on Refrigerated Spinach and Rocket Leaves in Modified Atmosphere Packaging. *Foods* 9(9), p. 1211. doi: 10.3390/foods9091211

Culliney, P. and Schmalenberger, A. (2022). Cultivation Conditions of Spinach and Rocket Influence Epiphytic Growth of *Listeria monocytogenes*. *Foods* 11(19), p. 3056. doi: 10.3390/foods11193056

Dabrowski, W., Iwanski, R., Czeszejko, K. and Medrala, D. (2001). The influence of culture conditions on adhesion of *Listeria monocytogenes* to hexadecane. *Electronic Journal of Polish Agricultural Universities. Series Food Science and Technology* 2(04),

den Bakker, H. C. *et al*. (2013). Evolutionary dynamics of the accessory genome of *Listeria monocytogenes*. *PLoS ONE* 8(6), p. e67511. doi: 10.1371/journal.pone.0067511

den Bakker, H. C., Didelot, X., Fortes, E. D., Nightingale, K. K. and Wiedmann, M. (2008). Lineage specific recombination rates and microevolution in *Listeria monocytogenes*. *BMC Evolutionary Biology* 8(1), p. 277. doi: 10.1186/1471-2148-8-277

Denis, M. *et al*. (2022). Occurrence and Diversity of *Listeria monocytogenes* Isolated from Two Pig Manure Treatment Plants in France. *Microbes and Environments* 37(4), p. n/a. doi: 10.1264/jsme2.me22019

Domínguez, E., Heredia-Guerrero, J. A. and Heredia, A. (2011). The biophysical design of plant cuticles: an overview. *New Phytologist* 189(4), pp. 938-949. doi: 10.1111/j.1469-8137.2010.03553.x

Dong, M., Holle, M. J., Miller, M. J., Banerjee, P. and Feng, H. (2024). Fates of attached *E. coli* O157:H7 on intact leaf surfaces revealed leafy green susceptibility. *Food Microbiology* 119, p. 104432. doi: https://doi.org/10.1016/j.fm.2023.104432

Doumith, M., Buchrieser, C., Glaser, P., Jacquet, C. and Martin, P. (2004a). Differentiation of the Major *Listeria monocytogenes* Serovars by Multiplex PCR. *Journal of Clinical Microbiology* 42(8), pp. 3819-3822. doi: 10.1128/jcm.42.8.3819-3822.2004

Doumith, M. *et al*. (2004b). New aspects regarding evolution and virulence of *Listeria monocytogenes* revealed by comparative genomics and DNA arrays. *Infection and Immunity* 72(2), pp. 1072-1083. doi: 10.1128/iai.72.2.1072-1083.2004

Doyle, E. M. (2007). Microbial Food Spoilage: Losses and Control Strategies A Brief Review of the Literature. Food Research Institute, University of Wisconsin. doi: https://www.wisc.edu/fri/

Edwards, M. (2001). Microscopy Methods for Micro-Organisms on Plant Surfaces. *Microscopy and Analysis*, pp. 9-12.

EFSA. (2018). The European Union summary report on trends and sources of zoonoses, zoonotic agents and food-borne outbreaks in 2017. *EFSA Journal* 16(12), doi: 10.2903/j.efsa.2018.5500

EFSA. (2019). The European Union One Health 2018 Zoonoses Report. *EFSA Journal* 17(12), p. e05926. doi: https://doi.org/10.2903/j.efsa.2019.5926

EFSA. (2021a). The European Union One Health 2019 Zoonoses Report. *EFSA Journal* 19(2), doi: 10.2903/j.efsa.2021.6406

EFSA. (2021b). The European Union One Health 2020 Zoonoses Report. *EFSA Journal* 19(12), p. e06971. doi: https://doi.org/10.2903/j.efsa.2021.6971

EFSA. (2022). The European Union One Health 2021 Zoonoses Report. *EFSA Journal* 20(12), p. e07666. doi: https://doi.org/10.2903/j.efsa.2022.7666

EFSA. (2023). The European Union One Health 2022 Zoonoses Report. *EFSA Journal* 21(12), doi: 10.2903/j.efsa.2023.8442

EFSA *et al*. (2020). The public health risk posed by *Listeria monocytogenes* in frozen fruit and vegetables including herbs, blanched during processing. *EFSA Journal* 18(4), p. e06092. doi: https://doi.org/10.2903/j.efsa.2020.6092

Ells, T. C. and Truelstrup Hansen, L. (2006). Strain and growth temperature influence *Listeria* spp. attachment to intact and cut cabbage. *International Journal of Food Microbiology* 111(1), pp. 34-42. doi: https://doi.org/10.1016/j.ijfoodmicro.2006.04.033

Esmael, A. *et al*. (2023). Fresh Produce as a Potential Vector and Reservoir for Human Bacterial Pathogens: Revealing the Ambiguity of Interaction and Transmission. *Microorganisms* 11(3), doi: 10.3390/microorganisms11030753

European Commission. (2021). *Guidance document on Listeria monocytogenes shelf-life studies for ready-to-eat foods*. Available at:

https://food.ec.europa.eu/system/files/2021-07/biosafety_fh_mc_tech-guide-doc_listeria-in-rte-foods_en_0.pdf [Accessed: 12-09-2024].

Fan, M., Rakotondrabe, T. F., Chen, G. and Guo, M. (2023). Advances in microbial analysis: Based on volatile organic compounds of microorganisms in food. *Food Chemistry* 418, p. 135950. doi: https://doi.org/10.1016/j.foodchem.2023.135950

Farber, J. M. and Peterkin, P. I. (1991). *Listeria monocytogenes*, a food-borne pathogen. *Microbiological Reviews* 55(3), pp. 476-511. doi: 10.1128/mr.55.3.476-511.1991

FDA. (2021). *Outbreak Investigation of Listeria monocytogenes: Dole Packaged Salad*. U.S. Food and Drug Administration. Available at: https://www.fda.gov/food/outbreaks-foodborne-illness/outbreak-investigation-listeria-monocytogenes-dole-packaged-salad-december-2021 [Accessed: 09-09-2024].

FDA. (2023). *Outbreak Investigation of Listeria monocytogenes: Peaches, Plums, & Nectarines*. U.S. Food and Drug Administration. Available at: https://www.fda.gov/food/outbreaks-foodborne-illness/outbreak-investigation-listeria-monocytogenes-peaches-plums-nectarines-november-2023 [Accessed: 09-09-2024].

Félix, B. *et al*. (2022). A European-wide dataset to uncover adaptive traits of *Listeria monocytogenes* to diverse ecological niches. *Scientific Data* 9(1), doi: 10.1038/s41597-022-01278-6

Feng, Y., Yao, H., Chen, S., Sun, X., Yin, Y. and Jiao, X. A. (2020). Rapid Detection of Hypervirulent Serovar 4h *Listeria monocytogenes* by Multiplex PCR. *Frontiers in Microbiology* 11, doi: 10.3389/fmicb.2020.01309

Food Standards Agency. (2016). *Guidance on Temperature Control Legislation in the United Kingdom*. UK: Food Standards Agency. Available at: https://www.foodstandards.gov.scot/downloads/Guidance_on_temperature_control_legislation.pdf [Accessed: 13 February 2025].

Fox, E. M., Allnutt, T., Bradbury, M. I., Fanning, S. and Chandry, P. S. (2016). Comparative Genomics of the *Listeria monocytogenes* ST204 Subgroup. *Frontiers in Microbiology* 7, doi: 10.3389/fmicb.2016.02057

Francis, G. A., Gallone, A., Nychas, G. J., Sofos, J. N., Colelli, G., Amodio, M. L. and Spano, G. (2012). Factors Affecting Quality and Safety of Fresh-Cut Produce. *Critical Reviews in Food Science and Nutrition* 52(7), pp. 595-610. doi: 10.1080/10408398.2010.503685

Fuchs, F., Petruschke, C. and Schreiber, L. (2020). Interaction of Epiphyllic Bacteria with Plant Cuticles. Springer International Publishing, pp. 1-12.

Fulano, A. M., Elbakush, A. M., Chen, L.-H. and Gomelsky, M. (2023). The *Listeria monocytogenes* exopolysaccharide significantly enhances colonization and survival on fresh produce. *Frontiers in Microbiology* 14, doi: 10.3389/fmicb.2023.1126940

Gahan, C. G. M. and Hill, C. (2014). *Listeria monocytogenes*: survival and adaptation in the gastrointestinal tract. *Frontiers in Cellular and Infection Microbiology* 4, doi: 10.3389/fcimb.2014.00009

Gartley, S., Anderson-Coughlin, B., Sharma, M. and Kniel, K. E. (2022). *Listeria monocytogenes* in Irrigation Water: An Assessment of Outbreaks, Sources, Prevalence, and Persistence. *Microorganisms* 10(7), p. 1319. doi: 10.3390/microorganisms10071319

Gasanov, U., Hughes, D. and Hansbro, P. M. (2005). Methods for the isolation and identification of *Listeria* spp. and *Listeria monocytogenes*: a review. *FEMS Microbiology Reviews* 29(5), pp. 851-875. doi: 10.1016/j.femsre.2004.12.002

Gaul, L. K., Farag, N. H., Shim, T., Kingsley, M. A., Silk, B. J. and Hyytia-Trees, E. (2013). Hospital-Acquired Listeriosis Outbreak Caused by Contaminated Diced Celery—Texas, 2010. *Clinical Infectious Diseases* 56(1), pp. 20-26. doi: 10.1093/cid/cis817

Gibbons, N. E. (1972). *Listeria* Pirie—Whom Does It Honor? *International Journal of Systematic and Evolutionary Microbiology* 22(1), pp. 1-3. doi: https://doi.org/10.1099/00207713-22-1-1

Gil, M. I., Truchado, P., Tudela, J. A. and Allende, A. (2024). Environmental monitoring of three fresh-cut processing facilities reveals harborage sites for *Listeria monocytogenes*. *Food Control* 155, p. 110093. doi: https://doi.org/10.1016/j.foodcont.2023.110093

Gil, R. R., Ruiz, B., Lozano, M. S., Martín, M. J. and Fuente, E. (2014). VOCs removal by adsorption onto activated carbons from biocollagenic wastes of vegetable tanning. *Chemical Engineering Journal* 245, pp. 80-88. doi: https://doi.org/10.1016/j.cej.2014.02.012

Giotis, E. S., Muthaiyan, A., Blair, I. S., Wilkinson, B. J. and McDowell, D. A. (2008). Genomic and proteomic analysis of the Alkali-Tolerance Response (AlTR) in *Listeria monocytogenes* 10403S. *BMC Microbiology* 8(1), p. 102. doi: 10.1186/1471-2180-8-102

Glaser, P. *et al.* (2001). Comparative Genomics of *Listeria* Species. *Science* 294(5543), pp. 849-852. doi: doi:10.1126/science.1063447

Gnanou Besse, N. *et al.* (2019). Validation of standard method EN ISO 11290 - Part 1 - Detection of *Listeria monocytogenes* in food. *International Journal of Food Microbiology* 288, pp. 13-21. doi: https://doi.org/10.1016/j.ijfoodmicro.2018.03.024

Gómez, I., Janardhanan, R., Ibañez, F. C. and Beriain, M. J. (2020). The Effects of Processing and Preservation Technologies on Meat Quality: Sensory and Nutritional Aspects. *Foods* 9(10), p. 1416. doi: 10.3390/foods9101416

Gorski, L., Duhé, J. M. and Flaherty, D. (2009). The Use of Flagella and Motility for Plant Colonization and Fitness by Different Strains of the Foodborne Pathogen *Listeria monocytogenes*. *PLoS ONE* 4(4), p. e5142. doi: 10.1371/journal.pone.0005142

Gorski, L., Walker, S., Romanolo, K. F. and Kathariou, S. (2021). Growth and Survival of Attached *Listeria* on Lettuce and Stainless Steel Varies by Strain and Surface Type. *Journal of Food Protection*, doi: https://doi.org/10.4315/JFP-20-434

Goulet, V., King, L. A., Vaillant, V. and De Valk, H. (2013). What is the incubation period for Listeriosis? *BMC Infectious Diseases* 13(1), p. 11. doi: 10.1186/1471-2334-13-11

Guan, H. *et al.* (2023). Infection behavior of *Listeria monocytogenes* on iceberg lettuce (*Lactuca sativa* var. *capitata*). *Food Research International* 165, p. 112487. doi: https://doi.org/10.1016/j.foodres.2023.112487

Guillet, C. *et al.* (2010). Human Listeriosis Caused by *Listeria ivanovii*. *Emerging Infectious Diseases* 16(1), pp. 136-138. doi: 10.3201/eid1601.091155

Gullino, M. L., Gilardi, G. and Garibaldi, A. (2019). Ready-to-Eat Salad Crops: A Plant Pathogen's Heaven. *Plant Disease* 103(9), pp. 2153-2170. doi: 10.1094/pdis-03-19-0472-fe

Gupta, P. and Adhikari, A. (2022). Novel Approaches to Environmental Monitoring and Control of *Listeria monocytogenes* in Food Production Facilities. *Foods* 11(12), doi: 10.3390/foods11121760

Gurevich, A., Saveliev, V., Vyahhi, N. and Tesler, G. (2013). QUAST: quality assessment tool for genome assemblies. *Bioinformatics* 29(8), pp. 1072-1075. doi: 10.1093/bioinformatics/btt086

Haase, J. K., Didelot, X., Lecuit, M., Korkeala, H. and Achtman, M. (2014). The ubiquitous nature of *Listeria monocytogenes* clones: a large-scale Multilocus Sequence Typing study. *Environmental Microbiology* 16(2), pp. 405-416. doi: 10.1111/1462-2920.12342

Hafner, L. *et al.* (2024). Differential stress responsiveness determines intraspecies virulence heterogeneity and host adaptation in *Listeria monocytogenes*. *Nature Microbiology* 9(12), pp. 3345-3361. doi: 10.1038/s41564-024-01859-8

Hammerbacher, A., Coutinho, T. A. and Gershenzon, J. (2019). Roles of plant volatiles in defence against microbial pathogens and microbial exploitation of volatiles. *Plant, Cell & Environment* 42(10), pp. 2827-2843. doi: https://doi.org/10.1111/pce.13602

Havelaar, A. H. *et al.* (2015). World Health Organization Global Estimates and Regional Comparisons of the Burden of Foodborne Disease in 2010. *PLOS Medicine* 12(12), p. e1001923. doi: 10.1371/journal.pmed.1001923

Hellström, S., Kervinen, R., Lyly, M., Ahvenainen-Rantala, R. and Korkeala, H. (2006). Efficacy of Disinfectants To Reduce *Listeria monocytogenes* on Precut Iceberg Lettuce. *Journal of Food Protection* 69(7), pp. 1565-1570. doi: https://doi.org/10.4315/0362-028X-69.7.1565

Hingston, P. *et al.* (2017). Genotypes Associated with *Listeria monocytogenes* Isolates Displaying Impaired or Enhanced Tolerances to Cold, Salt, Acid, or Desiccation Stress. *Frontiers in Microbiology* 8, doi: 10.3389/fmicb.2017.00369

Honjoh, K.-I., Lin, Y., Jo, K., Iwaizako, Y., Maeda, M., Kijima, N. and Miyamoto, T. (2018). Possible Contamination Routes of *Listeria monocytogenes* in Leaf Lettuce during Cultivation. *Food Science and Technology Research* 24(5), pp. 911-920. doi: 10.3136/fstr.24.911

Hunter, P. J., Shaw, R. K., Berger, C. N., Frankel, G., Pink, D. and Hand, P. (2015). Older leaves of lettuce (*Lactuca* spp.) support higher levels of *Salmonella enterica* ser. Senftenberg attachment and show greater variation between plant accessions than do younger leaves. *FEMS Microbiology Letters* 362(11), pp. fnv077-fnv077. doi: 10.1093/femsle/fnv077

Hurtado, A., Ocejo, M. and Oporto, B. (2017). *Salmonella* spp. and *Listeria monocytogenes* shedding in domestic ruminants and characterization of potentially pathogenic strains. *Veterinary Microbiology* 210, pp. 71-76. doi: https://doi.org/10.1016/j.vetmic.2017.09.003

Jablasone, J., Warriner, K. and Griffiths, M. (2005). Interactions of *Escherichia coli* O157:H7, *Salmonella typhimurium* and *Listeria monocytogenes* plants cultivated in a gnotobiotic system. *International Journal of Food Microbiology* 99(1), pp. 7-18. doi: https://doi.org/10.1016/j.ijfoodmicro.2004.06.011

Jackson, B. R. *et al*. (2015). Listeriosis Associated with Stone Fruit-United States, 2014. *Morbidity and Mortality Weekly Report* 64(10), pp. 282-283.

Jackson, B. R. *et al*. (2016). Implementation of Nationwide Real-time Whole-genome Sequencing to Enhance Listeriosis Outbreak Detection and Investigation. *Clinical Infectious Diseases* 63(3), pp. 380-386. doi: 10.1093/cid/ciw242

Jacob, C. and Melotto, M. (2020). Human Pathogen Colonization of Lettuce Dependent Upon Plant Genotype and Defense Response Activation. *Frontiers in Plant Science* 10(1769), doi: 10.3389/fpls.2019.01769

Jordan, K., Hunt, K., Lourenco, A. and Pennone, V. (2018). *Listeria monocytogenes* in the Food Processing Environment. *Current Clinical Microbiology Reports* 5(2), pp. 106-119. doi: 10.1007/s40588-018-0090-1

Kai, M., Haustein, M., Molina, F., Petri, A., Scholz, B. and Piechulla, B. (2009). Bacterial volatiles and their action potential. *Applied Microbiology and Biotechnology* 81(6), pp. 1001-1012. doi: 10.1007/s00253-008-1760-3

Kanchiswamy, C. N., Malnoy, M. and Maffei, M. E. (2015). Chemical diversity of microbial volatiles and their potential for plant growth and productivity. *Frontiers in Plant Science* 6, doi: 10.3389/fpls.2015.00151

Kathariou, S., Kanenaka, R., Allen, R. D., Fok, A. K. and Mizumoto, C. (1995). Repression of motility and flagellin production at 37 degrees C is stronger in *Listeria monocytogenes* than in the nonpathogenic species *Listeria innocua*. *Canadian Journal of Microbiology* 41(7), pp. 572-577. doi: 10.1139/m95-076

Katoh, K. and Standley, D. M. (2013). MAFFT Multiple Sequence Alignment Software Version 7: Improvements in Performance and Usability. *Molecular Biology and Evolution* 30(4), pp. 772-780. doi: 10.1093/molbev/mst010

Koopmans, M. M., Brouwer, M. C., Bijlsma, M. W., Bovenkerk, S., Keijzers, W., Van Der Ende, A. and Van De Beek, D. (2013). *Listeria monocytogenes* Sequence Type 6 and Increased Rate of Unfavorable Outcome in Meningitis: Epidemiologic Cohort Study. *Clinical Infectious Diseases* 57(2), pp. 247-253. doi: 10.1093/cid/cit250

Koukounaras, A., Siomos, A. S. and Sfakiotakis, E. (2007). Postharvest CO2 and ethylene production and quality of rocket (*Eruca sativa* Mill.) leaves as affected by leaf age and storage temperature. *Postharvest Biology and Technology* 46(2), pp. 167-173. doi: https://doi.org/10.1016/j.postharvbio.2007.04.007

Kozlov, A. M., Darriba, D., Flouri, T., Morel, B. and Stamatakis, A. (2019). RAxML-NG: a fast, scalable and user-friendly tool for maximum likelihood phylogenetic inference. *Bioinformatics* 35(21), pp. 4453-4455. doi: 10.1093/bioinformatics/btz305

Kroupitski, Y., Golberg, D., Belausov, E., Pinto, R., Swartzberg, D., Granot, D. and Sela, S. (2009). Internalization of *Salmonella enterica* in leaves is induced by light and involves chemotaxis and penetration through open stomata. *Applied and Environmental Microbiology* 75(19), pp. 6076-6086. doi: 10.1128/aem.01084-09

Kroupitski, Y., Pinto, R., Belausov, E. and Sela, S. (2011). Distribution of *Salmonella typhimurium* in romaine lettuce leaves. *Food Microbiology* 28(5), pp. 990-997. doi: https://doi.org/10.1016/j.fm.2011.01.007

Krueger, F. *et al.* (2023). FelixKrueger/TrimGalore: v0.6.10. Available at: https://github.com/FelixKrueger/TrimGalore [Accessed: 8 May 2022].

Kumar, S., Stecher, G., Li, M., Knyaz, C. and Tamura, K. (2018). MEGA X: Molecular Evolutionary Genetics Analysis across Computing Platforms. *Molecular Biology and Evolution* 35(6), pp. 1547-1549. doi: 10.1093/molbev/msy096

Kurtz, S., Phillippy, A., Delcher, A. L., Smoot, M., Shumway, M., Antonescu, C. and Salzberg, S. L. (2004). Versatile and open software for comparing large genomes. *Genome Biology* 5(2), p. R12. doi: 10.1186/gb-2004-5-2-r12

Kwong, J. C. *et al.* (2016). Prospective Whole-Genome Sequencing Enhances National Surveillance of *Listeria monocytogenes*. *Journal of Clinical Microbiology* 54(2), pp. 333-342. doi: 10.1128/jcm.02344-15

Kyere, E. O., Foong, G., Palmer, J., Wargent, J. J., Fletcher, G. C. and Flint, S. (2019a). Rapid attachment of *Listeria monocytogenes* to hydroponic and soil grown lettuce leaves. *Food Control* 101, pp. 77-80. doi: https://doi.org/10.1016/j.foodcont.2019.02.015

Kyere, E. O., Palmer, J., Wargent, J. J., Fletcher, G. C. and Flint, S. (2019b). Colonisation of lettuce by *Listeria monocytogenes*. *International Journal of Food Science & Technology* 54(1), pp. 14-24. doi: 10.1111/ijfs.13905

Lakicevic, B. Z., Den Besten, H. M. W. and De Biase, D. (2022). Landscape of Stress Response and Virulence Genes Among *Listeria monocytogenes* Strains. *Frontiers in Microbiology* 12, doi: 10.3389/fmicb.2021.738470

Lanciotti, R., Belletti, N., Patrignani, F., Gianotti, A., Gardini, F. and Guerzoni, M. E. (2003). Application of Hexanal, (E)-2-Hexenal, and Hexyl Acetate To Improve the Safety of Fresh-Sliced Apples. *Journal of Agricultural and Food Chemistry* 51(10), pp. 2958-2963. doi: 10.1021/jf026143h

Law, J. W.-F., Ab Mutalib, N.-S., Chan, K.-G. and Lee, L.-H. (2015). An insight into the isolation, enumeration, and molecular detection of *Listeria monocytogenes* in food. *Frontiers in Microbiology* 6, doi: 10.3389/fmicb.2015.01227

Lee, B.-H., Hébraud, M. and Bernardi, T. (2017). Increased Adhesion of *Listeria monocytogenes* Strains to Abiotic Surfaces under Cold Stress. *Frontiers in Microbiology* 8, doi: 10.3389/fmicb.2017.02221

Leimeister-Wächter, M., Domann, E. and Chakraborty, T. (1992). The expression of virulence genes in *Listeria monocytogenes* is thermoregulated. *Journal of Bacteriology* 174(3), pp. 947-952. doi: 10.1128/jb.174.3.947-952.1992

Lepe-Balsalobre, E., Rubio-Sánchez, R., Ubeda, C. and Lepe, J. A. (2022). Volatile compounds from in vitro metabolism of seven *Listeria monocytogenes* isolates belonging to different clonal complexes. *Journal of Medical Microbiology* 71(6), doi: https://doi.org/10.1099/jmm.0.001553

Leveau, J. H. J. (2019). A brief from the leaf: latest research to inform our understanding of the phyllosphere microbiome. *Current Opinion in Microbiology* 49, pp. 41-49. doi: https://doi.org/10.1016/j.mib.2019.10.002

Levin-Reisman, I., Ronin, I., Gefen, O., Braniss, I., Shoresh, N. and Balaban, N. Q. (2017). Antibiotic tolerance facilitates the evolution of resistance. *Science* 355(6327), pp. 826-830. doi: 10.1126/science.aaj2191

Lima, P. M., São José, J. F. B., Andrade, N. J., Pires, A. C. S. and Ferreira, S. O. (2013). Interaction between natural microbiota and physicochemical characteristics of lettuce surfaces can influence the attachment of Salmonella Enteritidis. *Food Control* 30(1), pp. 157-161. doi: 10.1016/j.foodcont.2012.06.039

Linnan, M. J. *et al*. (1988). Epidemic Listeriosis Associated with Mexican-Style Cheese. *New England Journal of Medicine* 319(13), pp. 823-828. doi: 10.1056/nejm198809293191303

Liu, D. (2006). Identification, subtyping and virulence determination of *Listeria monocytogenes*, an important foodborne pathogen. *Journal of Medical Microbiology* 55(6), pp. 645-659. doi: https://doi.org/10.1099/jmm.0.46495-0

Locatelli, A., Depret, G., Jolivet, C., Henry, S., Dequiedt, S., Piveteau, P. and Hartmann, A. (2013). Nation-wide study of the occurrence of *Listeria monocytogenes* in French soils using culture-based and molecular detection methods. *Journal of Microbiological Methods* 93(3), pp. 242-250. doi: https://doi.org/10.1016/j.mimet.2013.03.017

Lopez-Velasco, G., Welbaum, G. E., Falkinham Iii, J. O. and Ponder, M. A. (2011). Phyllopshere Bacterial Community Structure of Spinach (*Spinacia oleracea*) as Affected by Cultivar and Environmental Conditions at Time of Harvest. *Diversity* 3(4), pp. 721-738. doi: 10.3390/d3040721

Lou, Y. and Yousef, A. E. (1997). Adaptation to sublethal environmental stresses protects *Listeria monocytogenes* against lethal preservation factors. *Applied and Environmental Microbiology* 63(4), pp. 1252-1255. doi: 10.1128/aem.63.4.1252-1255.1997

Luca, A., Kjær, A. and Edelenbos, M. (2017). Volatile organic compounds as markers of quality changes during the storage of wild rocket. *Food Chemistry* 232, pp. 579-586. doi: https://doi.org/10.1016/j.foodchem.2017.04.035

Lyautey, E. *et al.* (2007). Characteristics and frequency of detection of fecal *Listeria monocytogenes* shed by livestock, wildlife, and humans. *Canadian Journal of Microbiology* 53(10), pp. 1158-1167. doi: 10.1139/W07-084

Macarisin, D., Patel, J., Bauchan, G., Giron, J. A. and Ravishankar, S. (2013). Effect of Spinach Cultivar and Bacterial Adherence Factors on Survival of *Escherichia coli* O157:H7 on Spinach Leaves. *Journal of Food Protection* 76(11), pp. 1829-1837. doi: 10.4315/0362-028x.jfp-12-556

Madeira, F. *et al.* (2024). The EMBL-EBI Job Dispatcher sequence analysis tools framework in 2024. *Nucleic Acids Research* 52(W1), pp. W521-W525. doi: 10.1093/nar/gkae241

Magdovitz, B. F., Gummalla, S., Garren, D., Thippareddi, H., Berrang, M. E. and Harrison, M. A. (2021). Prevalence of *Listeria* Species and *Listeria* monocytogenes on Raw Produce Arriving at Frozen Food Manufacturing Facilities. *Journal of Food Protection* 84(11), pp. 1898-1903. doi: https://doi.org/10.4315/JFP-21-064

Mahenthiralingam, E. *et al.* (2011). Enacyloxins Are Products of an Unusual Hybrid Modular Polyketide Synthase Encoded by a Cryptic *Burkholderia ambifaria* Genomic Island. *Chemistry & Biology* 18(5), pp. 665-677. doi: https://doi.org/10.1016/j.chembiol.2011.01.020

Maiden, M. C. (2006). Multilocus sequence typing of bacteria. *Annual Review of Microbiology* 60(0066-4227 (Print)), pp. 561–588.

Marik, C. M., Zuchel, J., Schaffner, D. W. and Strawn, L. K. (2020). Growth and Survival of *Listeria monocytogenes* on Intact Fruit and Vegetable Surfaces During Postharvest Handling: A Systematic Literature Review. *Journal of Food Protection* 83(1), pp. 108-128. doi: https://doi.org/10.4315/0362-028X.JFP-19-283

Martin, M. (2011). Cutadapt removes adapter sequences from high-throughput sequencing reads. *EMBnet.journal* 17(1), p. 10. doi: 10.14806/ej.17.1.200

Martínez-Sánchez, A., Allende, A., Cortes-Galera, Y. and Gil, M. I. (2008). Respiration rate response of four baby leaf *Brassica* species to cutting at harvest and fresh-cut washing. *Postharvest Biology and Technology* 47(3), pp. 382-388. doi: https://doi.org/10.1016/j.postharvbio.2007.07.010

Martinez, M. R., Osborne, J., Jayeola, V. O., Katic, V. and Kathariou, S. (2016). Capacity of *Listeria monocytogenes* Strains from the 2011 Cantaloupe Outbreak To Adhere, Survive, and Grow on Cantaloupe. *Journal of Food Protection* 79(5), pp. 757-763. doi: 10.4315/0362-028x.Jfp-15-498

Matereke, L. T. and Okoh, A. I. (2020). *Listeria monocytogenes* Virulence, Antimicrobial Resistance and Environmental Persistence: A Review. *Pathogens* 9(7), p. 528. doi: 10.3390/pathogens9070528

Maury, M. M. *et al*. (2019). Hypervirulent *Listeria monocytogenes* clones' adaption to mammalian gut accounts for their association with dairy products. *Nature Communications* 10(1), p. 2488. doi: 10.1038/s41467-019-10380-0

Maury, M. M. *et al*. (2017). Spontaneous Loss of Virulence in Natural Populations of *Listeria monocytogenes*. *Infection and Immunity* 85(11), pp. 10-1128. doi: 10.1128/iai.00541-17

Maury, M. M. *et al*. (2016). Uncovering *Listeria monocytogenes* hypervirulence by harnessing its biodiversity. *Nature Genetics* 48(3), pp. 308-313. doi: 10.1038/ng.3501

Mcardle, B. H. and Anderson, M. J. (2001). Fitting Multivariate Models to Community Data: A Comment on Distance-Based Redundancy Analysis. *Ecology* 82(1), p. 290. doi: 10.2307/2680104

McCollum, J. T. *et al.* (2013). Multistate Outbreak of Listeriosis Associated with Cantaloupe. *New England Journal of Medicine* 369(10), pp. 944-953. doi: 10.1056/nejmoa1215837

Mensi, I., Daugrois, J.-H. and Rott, P. (2017). Bioassay of *Xanthomonas albilineans* Attachment on Sugarcane Leaves. *BIO-PROTOCOL* 7(2), p. e2111. doi: 10.21769/BioProtoc.2111

Milillo, S. R., Badamo, J. M., Boor, K. J. and Wiedmann, M. (2008). Growth and persistence of *Listeria monocytogenes* isolates on the plant model *Arabidopsis thaliana*. *Food Microbiology* 25(5), pp. 698-704. doi: https://doi.org/10.1016/j.fm.2008.03.003

Milillo, S. R. *et al.* (2012). A Review of the Ecology, Genomics, and Stress Response of *Listeria innocua* and *Listeria monocytogenes*. *Critical Reviews in Food Science and Nutrition* 52(8), pp. 712-725. doi: 10.1080/10408398.2010.507909

Moura, A. *et al.* (2016). Whole genome-based population biology and epidemiological surveillance of *Listeria monocytogenes*. *Nature Microbiology* 2(2), p. 16185. doi: 10.1038/nmicrobiol.2016.185

Moura, A. *et al.* (2017). Real-Time Whole-Genome Sequencing for Surveillance of *Listeria monocytogenes*, France. *Emerging Infectious Diseases* 23(9), pp. 1462-1470. doi: 10.3201/eid2309.170336

Müller, A. *et al.* (2013). Tn6188 - A Novel Transposon in *Listeria monocytogenes* Responsible for Tolerance to Benzalkonium Chloride. *PLoS ONE* 8(10), p. e76835. doi: 10.1371/journal.pone.0076835

Murray, E. G. D., Webb, R. A. and Swann, M. B. R. (1926). A disease of rabbits characterised by a large mononuclear leucocytosis, caused by a hitherto undescribed bacillus *Bacterium monocytogenes* (n.sp.). *The Journal of Pathology and Bacteriology* 29(4), pp. 407-439. doi: https://doi.org/10.1002/path.1700290409

Nakamura, S. and Hatanaka, A. (2002). Green-Leaf-Derived C6-Aroma Compounds with Potent Antibacterial Action That Act on Both Gram-Negative and Gram-Positive Bacteria. *Journal of Agricultural and Food Chemistry* 50(26), pp. 7639-7644. doi: 10.1021/jf025808c

Nelson, K. E. *et al.* (2004). Whole genome comparisons of serotype 4b and 1/2a strains of the food-borne pathogen *Listeria monocytogenes* reveal new insights into the core genome components of this species. *Nucleic Acids Research* 32(8), pp. 2386-2395. doi: 10.1093/nar/gkh562

Nielsen, T., Bergström, B. and Borch, E. (2008). The origin of off-odours in packaged rucola (*Eruca sativa*). *Food Chemistry* 110(1), pp. 96-105. doi: https://doi.org/10.1016/j.foodchem.2008.01.063

Nightingale, K. K., Ivy, R. A., Ho, A. J., Fortes, E. D., Njaa, B. L., Peters, R. M. and Wiedmann, M. (2008). *inlA* premature stop codons are common among *Listeria monocytogenes* isolates from foods and yield virulence-attenuated strains that confer protection against fully virulent strains. *Applied and Environmental Microbiology* 74(21), pp. 6570-6583. doi: 10.1128/aem.00997-08

Nightingale, K. K., Windham, K. and Wiedmann, M. (2005). Evolution and Molecular Phylogeny of *Listeria monocytogenes* Isolated from Human and Animal Listeriosis Cases and Foods. *Journal of Bacteriology* 187(16), pp. 5537-5551. doi: 10.1128/jb.187.16.5537-5551.2005

Noonan, M. J., Tinnesand, H. V. and Buesching, C. D. (2018). Normalizing Gas-Chromatography-Mass Spectrometry Data: Method Choice can Alter Biological Inference. *BioEssays* 40(6), p. 1700210. doi: 10.1002/bies.201700210

NSW Food Authority. (2018). *Listeria Outbreak Investigation*. NSW Government Department of Primary Industries. Available at: https://www.foodauthority.nsw.gov.au/sites/default/files/_Documents/foodsafetyandyou/listeria_outbreak_investigation.pdf [Accessed: 09-09-2024].

Nüesch-Inderbinen, M., Bloemberg, G. V., Müller, A., Stevens, M. J. A., Cernela, N., Kollöffel, B. and Stephan, R. (2021). Listeriosis Caused by Persistence of *Listeria monocytogenes* Serotype 4b Sequence Type 6 in Cheese Production Environment. *Emerging Infectious Diseases* 27(1), pp. 284-288. doi: 10.3201/eid2701.203266

Nyfeldt, A. (1929). Etiologie de la mononucleose infectieuse. *C. R. Soc. Biol* 101, p. 590.

Oksanen, J. (2011). vegan: Community Ecology Package. R package version 1.17-9. *http://cran. r-project. org/package= vegan*,

Olanya, O. M., Hoshide, A. K., Ijabadeniyi, O. A., Ukuku, D. O., Mukhopadhyay, S., Niemira, B. A. and Ayeni, O. (2019). Cost estimation of Listeriosis (*Listeria monocytogenes*) occurrence in South Africa in 2017 and its food safety implications. *Food Control* 102, pp. 231-239. doi: 10.1016/j.foodcont.2019.02.007

Orsi, R. H., Bakker, H. C. d. and Wiedmann, M. (2011). *Listeria monocytogenes* lineages: Genomics, evolution, ecology, and phenotypic characteristics. *International Journal of Medical Microbiology* 301(2), pp. 79-96. doi: https://doi.org/10.1016/j.ijmm.2010.05.002

Orsi, R. H., Jagadeesan, B., Baert, L. and Wiedmann, M. (2021). Identification of Closely Related *Listeria monocytogenes* Isolates with No Apparent Evidence for a Common Source or Location: A Retrospective Whole Genome Sequencing Analysis. *Journal of Food Protection* 84(7), pp. 1104-1113. doi: https://doi.org/10.4315/JFP-20-417

Orsi, R. H., Liao, J., Carlin, C. R. and Wiedmann, M. (2024). Taxonomy, ecology, and relevance to food safety of the genus *Listeria* with a particular consideration of new *Listeria* species described between 2010 and 2022. *mBio* 15(2), doi: 10.1128/mbio.00938-23

Orsi, R. H. and Wiedmann, M. (2016). Characteristics and distribution of *Listeria* spp., including *Listeria* species newly described since 2009. *Applied Microbiology and Biotechnology* 100(12), pp. 5273-5287. doi: 10.1007/s00253-016-7552-2

Painset, A. *et al.* (2019). LiSEQ – whole-genome sequencing of a cross-sectional survey of *Listeria monocytogenes* in ready-to-eat foods and human clinical cases in Europe. *Microbial Genomics* 5(2), doi: https://doi.org/10.1099/mgen.0.000257

Palumbo, J. D., Kaneko, A., Nguyen, K. D. and Gorski, L. (2005). Identification of Genes Induced in *Listeria monocytogenes* during Growth and Attachment to Cut Cabbage, Using Differential Display. *Applied and Environmental Microbiology* 71(9), pp. 5236-5243. doi: 10.1128/aem.71.9.5236-5243.2005

Paramithiotis, S., Spadafora, N., Muller, C., Drosinos, E. H. and Rogers, H. (2018). Sniffing out contaminants. *Food Science and Technology* 32(4), pp. 46-49. doi: 10.1002/fsat.3204_13.x

Partridge, J. D. and Harshey, R. M. (2020). Investigating Flagella-Driven Motility in *Escherichia coli* by Applying Three Established Techniques in a Series. *Journal of Visualized Experiments* (159), doi: 10.3791/61364

Patel, J. and Sharma, M. (2010). Differences in attachment of *Salmonella enterica* serovars to cabbage and lettuce leaves. *International Journal of Food Microbiology* 139(1), pp. 41-47. doi: https://doi.org/10.1016/j.ijfoodmicro.2010.02.005

Paterson, J. S. (1940). The antigenic structure of organisms of the genus *Listerella*. *The Journal of Pathology and Bacteriology* 51(3), pp. 427-436. doi: https://doi.org/10.1002/path.1700510310

Peel, M., Donachie, W. and Shaw, A. (1988). Temperature-dependent Expression of Flagella of *Listeria monocytogenes* Studied by Electron Microscopy, SDS-PAGE and Western Blotting. *Microbiology* 134(8), pp. 2171-2178. doi: 10.1099/00221287-134-8-2171

Perillo, P. M. and Rodríguez, D. F. (2016). Low temperature trimethylamine flexible gas sensor based on TiO2 membrane nanotubes. *Journal of Alloys and Compounds* 657, pp. 765-769. doi: https://doi.org/10.1016/j.jallcom.2015.10.167

Perrin, M., Bemer, M. and Delamare, C. (2003). Fatal Case of *Listeria innocua* Bacteremia. *Journal of Clinical Microbiology* 41(11), pp. 5308-5309. doi: 10.1128/jcm.41.11.5308-5309.2003

Piffaretti, J. C. *et al.* (1989). Genetic characterization of clones of the bacterium *Listeria monocytogenes* causing epidemic disease. *Proceedings of the National Academy of Sciences* 86(10), pp. 3818-3822. doi: 10.1073/pnas.86.10.3818

Pinto, G., Reyes, G. A., Barnett-Neefs, C., Jung, Y., Qian, C., Wiedmann, M. and Stasiewicz, M. J. (2025). Development of a Flexible Produce Supply Chain Food Safety Risk Model: Comparing Tradeoffs Between Improved Process Controls and Additional Product Testing for Leafy Greens as a Test Case. *Journal of Food Protection* 88(1), p. 100393. doi: https://doi.org/10.1016/j.jfp.2024.100393

Pirie, J. H. H. (1927). THE PLAGUE PROBLEM IN SOUTH AFRICA. *The Lancet* 210(5419), pp. 76-77. doi: https://doi.org/10.1016/S0140-6736(01)30683-9

Pirie, J. H. H. (1940). *Listeria*: Change of Name for a Genus Bacteria. *Nature* 145(3668), pp. 264-264. doi: 10.1038/145264a0

Posit team. (2024). RStudio: Integrated Development Environment for R. Boston, MA: Posit Software, PBC.

Pritchard, L., Glover, R. H., Humphris, S., Elphinstone, J. G. and Toth, I. K. (2016). Genomics and taxonomy in diagnostics for food security: soft-rotting enterobacterial plant pathogens. *Analytical Methods* 8(1), pp. 12-24. doi: 10.1039/c5ay02550h

Quereda, J. J., Morón-García, A., Palacios-Gorba, C., Dessaux, C., García-Del Portillo, F., Pucciarelli, M. G. and Ortega, A. D. (2021). Pathogenicity and virulence of *Listeria monocytogenes*: A trip from environmental to medical microbiology. *Virulence* 12(1), pp. 2509-2545. doi: 10.1080/21505594.2021.1975526

R Core Team. (2024). R: A Language and Environment for Statistical Computing. Vienna, Austria: R Foundation for Statistical Computing.

Ragon, M., Wirth, T., Hollandt, F., Lavenir, R., Lecuit, M., Le Monnier, A. and Brisse, S. (2008). A New Perspective on *Listeria monocytogenes* Evolution. *PLOS Pathogens* 4(9), p. e1000146. doi: 10.1371/journal.ppat.1000146

Rapose, A., Lick, S. D. and Ismail, N. (2008). *Listeria grayi* bacteremia in a heart transplant recipient. *Transplant Infectious Disease* 10(6), pp. 434-436. doi: 10.1111/j.1399-3062.2008.00333.x

Rasmussen, O. F., Skouboe, P., Dons, L., Rossen, L. and Olsen, J. E. (1995). *Listeria monocytogenes* exists in at least three evolutionary lines: evidence from flagellin, invasive associated protein and listeriolysin O genes. *Microbiology* 141(9), pp. 2053-2061. doi: https://doi.org/10.1099/13500872-141-9-2053

Ricci, A. *et al.* (2018). *Listeria monocytogenes* contamination of ready-to-eat foods and the risk for human health in the EU. *EFSA Journal* 16(1), doi: 10.2903/j.efsa.2018.5134

Roberts, A., Nightingale, K., Jeffers, G., Fortes, E., Kongo, J. M. and Wiedmann, M. (2006). Genetic and Phenotypic Characterization of *Listeria monocytogenes* Lineage III. *Microbiology* 152(3), pp. 685-693. doi: https://doi.org/10.1099/mic.0.28503-0

Rocourt, J., Hof, H., Schrettenbrunner, A., Malinverni, R. and Bille, J. (1986). [Acute purulent *Listeria seeligeri* meningitis in an immunocompetent adult]. *Schweizerische Medizinische Wochenschrift* 116(8), pp. 248-251.

Rohde, A. *et al.* (2017). Overview of validated alternative methods for the detection of foodborne bacterial pathogens. *Trends in Food Science & Technology* 62, pp. 113-118. doi: https://doi.org/10.1016/j.tifs.2017.02.006

Rolfe, M. D. *et al.* (2012). Lag Phase Is a Distinct Growth Phase That Prepares Bacteria for Exponential Growth and Involves Transient Metal Accumulation. *Journal of Bacteriology* 194(3), pp. 686-701. doi: 10.1128/jb.06112-11

Romantschuk, M. (1992). Attachment of Plant Pathogenic Bacteria to Plant Surfaces. *Annual Review of Phytopathology* 30(Volume 30, 1992), pp. 225-243. doi: https://doi.org/10.1146/annurev.py.30.090192.001301

Rosberg, A. K., Darlison, J., Mogren, L. and Alsanius, B. W. (2021). Commercial wash of leafy vegetables do not significantly decrease bacterial load but leads to shifts in

bacterial species composition. *Food Microbiology* 94, p. 103667. doi: https://doi.org/10.1016/j.fm.2020.103667

Ruppitsch, W. *et al.* (2015). Defining and Evaluating a Core Genome Multilocus Sequence Typing Scheme for Whole-Genome Sequence-Based Typing of *Listeria monocytogenes*. *Journal of Clinical Microbiology* 53(9), pp. 2869-2876. doi: 10.1128/jcm.01193-15

Ruther, J. and Kleier, S. (2005). Plant–Plant Signaling: Ethylene Synergizes Volatile Emission In *Zea mays* Induced by Exposure to (Z)-3-Hexen-1-ol. *Journal of Chemical Ecology* 31(9), pp. 2217-2222. doi: 10.1007/s10886-005-6413-8

Salazar, J. K., Wu, Z., Yang, W., Freitag, N. E., Tortorello, M. L., Wang, H. and Zhang, W. (2013). Roles of a Novel Crp/Fnr Family Transcription Factor Lmo0753 in Soil Survival, Biofilm Production and Surface Attachment to Fresh Produce of *Listeria monocytogenes*. *PLoS ONE* 8(9), p. e75736. doi: 10.1371/journal.pone.0075736

Salcedo, C., Arreaza, L., Alcalá, B., De La Fuente, L. and Vázquez, J. A. (2003). Development of a Multilocus Sequence Typing Method for Analysis of *Listeria monocytogenes* Clones. *Journal of Clinical Microbiology* 41(2), pp. 757-762. doi: 10.1128/jcm.41.2.757-762.2003

Saldaña, Z., Sánchez, E., Xicohtencatl-Cortes, J., Puente, J. L. and Giron, J. A. (2011). Surface Structures Involved in Plant Stomata and Leaf Colonization by Shiga-Toxigenic *Escherichia Coli* O157:H7. *Frontiers in Microbiology* 2, p. 119. doi: 10.3389/fmicb.2011.00119

Saldierna Guzmán, J. P., Nguyen, K. and Hart, S. C. (2020). Simple methods to remove microbes from leaf surfaces. *Journal of Basic Microbiology* 60(8), pp. 730-734. doi: https://doi.org/10.1002/jobm.202000035

Saldivar, J. C., Davis, M. L., Johnson, M. G. and Ricke, S. C. (2018). *Listeria monocytogenes* Adaptation and Growth at Low Temperatures: Mechanisms and Implications for Foodborne Disease. In: Ricke, S.C., Atungulu, G.G., Rainwater, C.E. and Park, S.H. eds. *Food and Feed Safety Systems and Analysis*. Academic Press, pp. 227-248.

Sauders, B. D. *et al.* (2006). Molecular Characterization of *Listeria monocytogenes* from Natural and Urban Environments. *Journal of Food Protection* 69(1), pp. 93-105. doi: https://doi.org/10.4315/0362-028X-69.1.93

Scallan, E. *et al.* (2011). Foodborne Illness Acquired in the United States—Major Pathogens. *Emerging Infectious Diseases* 17(1), pp. 7-15. doi: 10.3201/eid1701.p11101

Scallan Walter, E. J. *et al.* (2025). Foodborne Illness Acquired in the United States—Major Pathogens, 2019. *Emerging Infectious Diseases* 31(4), doi: 10.3201/eid3104.240913

Schikora, A., Garcia, A. V. and Hirt, H. (2012). Plants as alternative hosts for *Salmonella*. *Trends in Plant Science* 17(5), pp. 245-249. doi: 10.1016/j.tplants.2012.03.007

Schindelin, J. *et al.* (2012). Fiji: an open-source platform for biological-image analysis. *Nature Methods* 9(7), pp. 676-682. doi: 10.1038/nmeth.2019

Schirm, M., Kalmokoff, M., Aubry, A., Thibault, P., Sandoz, M. and Logan, S. M. (2004). Flagellin from *Listeria monocytogenes* Is Glycosylated with β-O-Linked N-Acetylglucosamine. *Journal of Bacteriology* 186(20), pp. 6721-6727. doi: 10.1128/jb.186.20.6721-6727.2004

Schlech, W. F., 3rd *et al.* (1983). Epidemic Listeriosis--evidence for transmission by food. *New England Journal of Medicine* 308(4), pp. 203-206. doi: 10.1056/nejm198301273080407

Seeliger, H. P. R. and Höhne, K. (1979). Serotyping of *Listeria monocytogenes* and Related Species. *Methods in Microbiology* 13(C), pp. 31-49. doi: 10.1016/S0580-9517(08)70372-6

Seeliger, H. P. R. and Jones, D. (1986). *Listeria*. *In Bergey's Manual of Systematic Bacteriology*. Baltimore: Williams and Wilkins.

Seemann, T. (2014). Prokka: rapid prokaryotic genome annotation. *Bioinformatics* 30(14), pp. 2068-2069. doi: 10.1093/bioinformatics/btu153

Seemann, T. (2020). mlst. Available at: https://github.com/tseemann/mlst [Accessed: 21 July 2024].

Segado, P., Domínguez, E. and Heredia, A. (2016). Ultrastructure of the Epidermal Cell Wall and Cuticle of Tomato Fruit (*Solanum lycopersicum L.*) during Development. *Plant Physiology* 170(2), pp. 935-946. doi: 10.1104/pp.15.01725

Sévellec, Y. *et al.* (2022). *Listeria monocytogenes*: Investigation of Fitness in Soil Does Not Support the Relevance of Ecotypes. *Frontiers in Microbiology* 13, doi: 10.3389/fmicb.2022.917588

Shen, A. and Higgins, D. E. (2005). The 5' Untranslated Region-Mediated Enhancement of Intracellular Listeriolysin O Production is Required for *Listeria monocytogenes*

Pathogenicity. *Molecular Microbiology* 57(5), pp. 1460-1473. doi: 10.1111/j.1365-2958.2005.04780.x

Shenoy, A. G., Oliver, H. F. and Deering, A. J. (2017). *Listeria monocytogenes* Internalizes in Romaine Lettuce Grown in Greenhouse Conditions. *Journal of Food Protection* 80(4), pp. 573-581. doi: https://doi.org/10.4315/0362-028X.JFP-16-095

Smith, A., Hearn, J., Taylor, C., Wheelhouse, N., Kaczmarek, M., Moorhouse, E. and Singleton, I. (2019a). *Listeria monocytogenes* isolates from ready to eat plant produce are diverse and have virulence potential. *International Journal of Food Microbiology* 299, pp. 23-32. doi: 10.1016/j.ijfoodmicro.2019.03.013

Smith, A., Moorhouse, E., Monaghan, J., Taylor, C. and Singleton, I. (2018). Sources and survival of *Listeria monocytogenes* on fresh, leafy produce. *Journal of Applied Microbiology* 125(4), pp. 930-942. doi: 10.1111/jam.14025

Smith, A. M. *et al.* (2019b). Outbreak of *Listeria monocytogenes* in South Africa, 2017–2018: Laboratory Activities and Experiences Associated with Whole-Genome Sequencing Analysis of Isolates. *Foodborne Pathogens and Disease* 16(7), pp. 524-530. doi: 10.1089/fpd.2018.2586

Spadafora, N. D., Amaro, A. L., Pereira, M. J., Müller, C. T., Pintado, M. and Rogers, H. J. (2016a). Multi-trait analysis of post-harvest storage in rocket salad (*Diplotaxis tenuifolia*) links sensorial, volatile and nutritional data. *Food Chemistry* 211, pp. 114-123. doi: 10.1016/j.foodchem.2016.04.107

Spadafora, N. D., Cammarisano, L., Rogers, H. J. and Müller, C. T. (2018). Using volatile organic compounds to monitor shelf-life in rocket salad. International Society for Horticultural Science (ISHS), Leuven, Belgium, pp. 1299-1306. doi: 10.17660/ActaHortic.2018.1194.183

Spadafora, N. D. *et al.* (2019). A complex interaction between pre-harvest and post-harvest factors determines fresh-cut melon quality and aroma. *Scientific Reports* 9(1), doi: 10.1038/s41598-019-39196-0

Spadafora, N. D. *et al.* (2020). Short-Term Post-Harvest Stress that Affects Profiles of Volatile Organic Compounds and Gene Expression in Rocket Salad during Early Post-Harvest Senescence. *Plants* 9(1), p. 4. doi: 10.3390/plants9010004

Spadafora, N. D., Paramithiotis, S., Drosinos, E. H., Cammarisano, L., Rogers, H. J. and Müller, C. T. (2016b). Detection of *Listeria monocytogenes* in cut melon fruit using

analysis of volatile organic compounds. *Food Microbiology* 54, pp. 52-59. doi: 10.1016/j.fm.2015.10.017

Sprouffske, K. and Wagner, A. (2016). Growthcurver: an R package for obtaining interpretable metrics from microbial growth curves. *BMC Bioinformatics* 17(1), doi: 10.1186/s12859-016-1016-7

Standing, T.-A., du Plessis, E., Duvenage, S. and Korsten, L. (2013). Internalisation potential of *Escherichia coli* O157:H7, *Listeria monocytogenes*, *Salmonella enterica* subsp. enterica serovar Typhimurium and *Staphylococcus aureus* in lettuce seedlings and mature plants. *Journal of Water and Health* 11(2), pp. 210-223. doi: 10.2166/wh.2013.164

Stanly, T. A., Fritzsche, M., Banerji, S., García, E., Bernardino De La Serna, J., Jackson, D. G. and Eggeling, C. (2016). Critical importance of appropriate fixation conditions for faithful imaging of receptor microclusters. *Biology Open* 5(9), pp. 1343-1350. doi: 10.1242/bio.019943

Steele, C. L., Donaldson, J. R., Paul, D., Banes, M. M., Arick, T., Bridges, S. M. and Lawrence, M. L. (2011). Genome Sequence of Lineage III *Listeria monocytogenes* Strain HCC23. *Journal of Bacteriology* 193(14), pp. 3679-3680. doi: 10.1128/jb.05236-11

Stevenson, K., Mcvey, A. F., Clark, I. B. N., Swain, P. S. and Pilizota, T. (2016). General calibration of microbial growth in microplate readers. *Scientific Reports* 6(1), p. 38828. doi: 10.1038/srep38828

Strawn, L. K. *et al.* (2013). Landscape and Meteorological Factors Affecting Prevalence of Three Food-Borne Pathogens in Fruit and Vegetable Farms. *Applied and Environmental Microbiology* 79(2), pp. 588-600. doi: 10.1128/aem.02491-12

Tait, E., Perry, J. D., Stanforth, S. P. and Dean, J. R. (2014a). Bacteria detection based on the evolution of enzyme-generated volatile organic compounds: Determination of *Listeria monocytogenes* in milk samples. *Analytica Chimica Acta* 848, pp. 80-87. doi: https://doi.org/10.1016/j.aca.2014.07.029

Tait, E., Perry, J. D., Stanforth, S. P. and Dean, J. R. (2014b). Use of volatile compounds as a diagnostic tool for the detection of pathogenic bacteria. *TrAC Trends in Analytical Chemistry* 53, pp. 117-125. doi: 10.1016/j.trac.2013.08.011

Takeuchi, K., Matute, C. M., Hassan, A. N. and Frank, J. F. (2000). Comparison of the Attachment of *Escherichia coli* O157:H7, *Listeria monocytogenes*, *Salmonella*

Typhimurium, and *Pseudomonas fluorescens* to Lettuce Leaves. *Journal of Food Protection* 63(10), pp. 1433-1437. doi: https://doi.org/10.4315/0362-028X-63.10.1433

Tan, M. S. F., Rahman, S. and Dykes, G. A. (2016). Pectin and Xyloglucan Influence the Attachment of *Salmonella enterica* and *Listeria monocytogenes* to Bacterial Cellulose-Derived Plant Cell Wall Models. *Applied and Environmental Microbiology* 82(2), pp. 680-688. doi: 10.1128/aem.02609-15

Tange, O. (2018). GNU Parallel 2018. *GNU Parallel*, p. 112. doi: https://doi.org/10.5281/zenodo.1146014

The MathWorks Inc. (2021). MATLAB version: 9.10.0 (R2021a). Natick, Massachusetts, United States: The MathWorks Inc.

Tienungoon, S., Ratkowsky, D. A., McMeekin, T. A. and Ross, T. (2000). Growth Limits of *Listeria monocytogenes* as a Function of Temperature, pH, NaCl, and Lactic Acid. *Applied and Environmental Microbiology* 66(11), pp. 4979-4987. doi: 10.1128/aem.66.11.4979-4987.2000

Tiwari, S. *et al*. (2020). Volatile organic compounds (VOCs): Biomarkers for quality management of horticultural commodities during storage through e-sensing. *Trends in Food Science & Technology* 106, pp. 417-433. doi: https://doi.org/10.1016/j.tifs.2020.10.039

Tompkin, R. B. (2002). Control of *Listeria monocytogenes* in the Food-Processing Environment. *Journal of Food Protection* 65(4), pp. 709-725. doi: https://doi.org/10.4315/0362-028X-65.4.709

Tonkin-Hill, G. *et al*. (2020). Producing polished prokaryotic pangenomes with the Panaroo pipeline. *Genome Biology* 21(1), doi: 10.1186/s13059-020-02090-4

Truong, H. N., Garmyn, D., Gal, L., Fournier, C., Sevellec, Y., Jeandroz, S. and Piveteau, P. (2021). Plants as a realized niche for *Listeria monocytogenes*. *MicrobiologyOpen* 10(6), doi: 10.1002/mbo3.1255

Tsai, Y.-H. L., Maron, S. B., McGann, P., Nightingale, K. K., Wiedmann, M. and Orsi, R. H. (2011). Recombination and positive selection contributed to the evolution of *Listeria monocytogenes* lineages III and IV, two distinct and well supported uncommon *L. monocytogenes* lineages. *Infection, Genetics and Evolution* 11(8), pp. 1881-1890. doi: 10.1016/j.meegid.2011.08.001

Ukuku, D. O. and Fett, W. F. (2002). Relationship of Cell Surface Charge and Hydrophobicity to Strength of Attachment of Bacteria to Cantaloupe Rind. *Journal of Food Protection* 65(7), pp. 1093-1099. doi: https://doi.org/10.4315/0362-028X-65.7.1093

Van Stelten, A., Simpson, J. M., Ward, T. J. and Nightingale, K. K. (2010). Revelation by Single-Nucleotide Polymorphism Genotyping That Mutations Leading to a Premature Stop Codon in inlA Are Common among *Listeria monocytogenes* Isolates from Ready-To-Eat Foods but Not Human Listeriosis Cases. *Applied and Environmental Microbiology* 76(9), pp. 2783-2790. doi: 10.1128/AEM.02651-09

Vázquez-Boland, J. A. *et al*. (2001). *Listeria* Pathogenesis and Molecular Virulence Determinants. *Clinical Microbiology Reviews* 14(3), pp. 584-640. doi: 10.1128/cmr.14.3.584-640.2001

Verhertbruggen, Y., Marcus, S. E., Haeger, A., Ordaz-Ortiz, J. J. and Knox, J. P. (2009). An extended set of monoclonal antibodies to pectic homogalacturonan. *Carbohydrate Research* 344(14), pp. 1858-1862. doi: 10.1016/j.carres.2008.11.010

Vidovic, S., Paturi, G., Gupta, S. and Fletcher, G. C. (2024). Lifestyle of *Listeria monocytogenes* and food safety: Emerging listericidal technologies in the food industry. *Critical Reviews in Food Science and Nutrition* 64(7), pp. 1817-1835. doi: 10.1080/10408398.2022.2119205

Vivant, A.-L., Garmyn, D. and Piveteau, P. (2013). *Listeria monocytogenes*, a down-to-earth pathogen. *Frontiers in Cellular and Infection Microbiology* 3, doi: 10.3389/fcimb.2013.00087

Voronina, O. L. *et al*. (2023). *Listeria monocytogenes* ST37 Distribution in the Moscow Region and Properties of Clinical and Foodborne Isolates. *Life* 13(11), doi: 10.3390/life13112167

Wagner, M. and McLauchlin, J. (2008). Handbook of *Listeria monocytogenes*. In: Liu, D. ed. *Handbook of Listeria monocytogenes*. CRC press.

Wang, Y., Li, Y., Yang, J., Ruan, J. and Sun, C. (2016). Microbial volatile organic compounds and their application in microorganism identification in foodstuff. *TrAC Trends in Analytical Chemistry* 78, pp. 1-16. doi: https://doi.org/10.1016/j.trac.2015.08.010

Wang, Y. *et al*. (2019). Genomic dissection of the most prevalent *Listeria monocytogenes* clone, sequence type ST87, in China. *BMC Genomics* 20(1), p. 1014. doi: 10.1186/s12864-019-6399-1

Ward, T. J., Ducey, T. F., Usgaard, T., Dunn, K. A. and Bielawski, J. P. (2008). Multilocus Genotyping Assays for Single Nucleotide Polymorphism-Based Subtyping of *Listeria monocytogenes* Isolates. *Applied and Environmental Microbiology* 74(24), pp. 7629-7642. doi: 10.1128/aem.01127-08

Way, S. S., Thompson, L. J., Lopes, J. E., Hajjar, A. M., Kollmann, T. R., Freitag, N. E. and Wilson, C. B. (2004). Characterization of flagellin expression and its role in *Listeria monocytogenes* infection and immunity. *Cellular Microbiology* 6(3), pp. 235-242. doi: https://doi.org/10.1046/j.1462-5822.2004.00360.x

Weis, J. and Seeliger, H. P. R. (1975). Incidence of *Listeria monocytogenes* in Nature. *Applied Microbiology* 30(1), pp. 29-32. doi: 10.1128/am.30.1.29-32.1975

Weller, D., Wiedmann, M. and Strawn, L. K. (2015). Spatial and Temporal Factors Associated with an Increased Prevalence of *Listeria monocytogenes* in Spinach Fields in New York State. *Applied and Environmental Microbiology* 81(17), pp. 6059-6069. doi: 10.1128/aem.01286-15

WHO. (2015). *WHO estimates of the global burden of foodborne diseases: foodborne disease burden epidemiology reference group 2007-2015*. Geneva, Switzerland: World Health Organization.

Wick, R. R., Judd, L. M., Gorrie, C. L. and Holt, K. E. (2017). Unicycler: Resolving bacterial genome assemblies from short and long sequencing reads. *PLOS Computational Biology* 13(6), p. e1005595. doi: 10.1371/journal.pcbi.1005595

Wickham, H. (2007). Reshaping Data with the reshape Package. *Journal of Statistical Software* 21(12), pp. 1-20.

Wickham, H. (2016). *Ggplot2: Elegant graphics for data analysis*. 2 ed. Cham, Switzerland: Springer International Publishing.

Wiktorczyk-Kapischke, N., Skowron, K., Grudlewska-Buda, K., Wałecka-Zacharska, E., Korkus, J. and Gospodarek-Komkowska, E. (2021). Adaptive Response of *Listeria monocytogenes* to the Stress Factors in the Food Processing Environment. *Frontiers in Microbiology* 12, doi: 10.3389/fmicb.2021.710085

Willis, C. *et al.* (2020). Occurrence of *Listeria* and *Escherichia coli* in frozen fruit and vegetables collected from retail and catering premises in England 2018–2019. *International Journal of Food Microbiology* 334, p. 108849. doi: https://doi.org/10.1016/j.ijfoodmicro.2020.108849

Wilson, S. M. and Bacic, A. (2012). Preparation of plant cells for transmission electron microscopy to optimize immunogold labeling of carbohydrate and protein epitopes. *Nature Protocols* 7(9), pp. 1716-1727. doi: 10.1038/nprot.2012.096

Wong, C. W. Y., Wang, S., Lévesque, R. C., Goodridge, L. and Delaquis, P. (2019). Fate of 43 *Salmonella* Strains on Lettuce and Tomato Seedlings. *Journal of Food Protection* 82(6), pp. 1045-1051. doi: https://doi.org/10.4315/0362-028X.JFP-18-435

Wright, E., Neethirajan, S., Warriner, K., Retterer, S. and Srijanto, B. (2014). Single cell swimming dynamics of *Listeria monocytogenes* using a nanoporous microfluidic platform. *Lab on a Chip* 14(5), p. 938. doi: 10.1039/c3lc51138c

Zamudio, R. *et al*. (2020). Lineage-specific evolution and gene flow in *Listeria monocytogenes* are independent of bacteriophages. *Environmental Microbiology* 22(12), pp. 5058-5072. doi: 10.1111/1462-2920.15111

Zhou, B., Luo, Y., Huang, L., Fonseca, J. M., Yan, H. and Huang, J. (2022). Determining effects of temperature abuse timing on shelf life of RTE baby spinach through microbial growth models and its association with sensory quality. *Food Control* 133, p. 108639. doi: https://doi.org/10.1016/j.foodcont.2021.108639

Zhu, Q., Gooneratne, R. and Hussain, M. (2017). *Listeria monocytogenes* in Fresh Produce: Outbreaks, Prevalence and Contamination Levels. *Foods* 6(3), p. 21. doi: 10.3390/foods6030021

Zitz, U., Zunabovic, M., Domig, K. J., Wilrich, P.-T. and Kneifel, W. (2011). Reduced Detectability of *Listeria monocytogenes* in the Presence of *Listeria innocua*. *Journal of Food Protection* 74(8), pp. 1282-1287. doi: 10.4315/0362-028x.jfp-11-045

Żuchowska, K. and Filipiak, W. (2024). Modern approaches for detection of volatile organic compounds in metabolic studies focusing on pathogenic bacteria: Current state of the art. *Journal of Pharmaceutical Analysis* 14(4), p. 100898. doi: https://doi.org/10.1016/j.jpha.2023.11.005